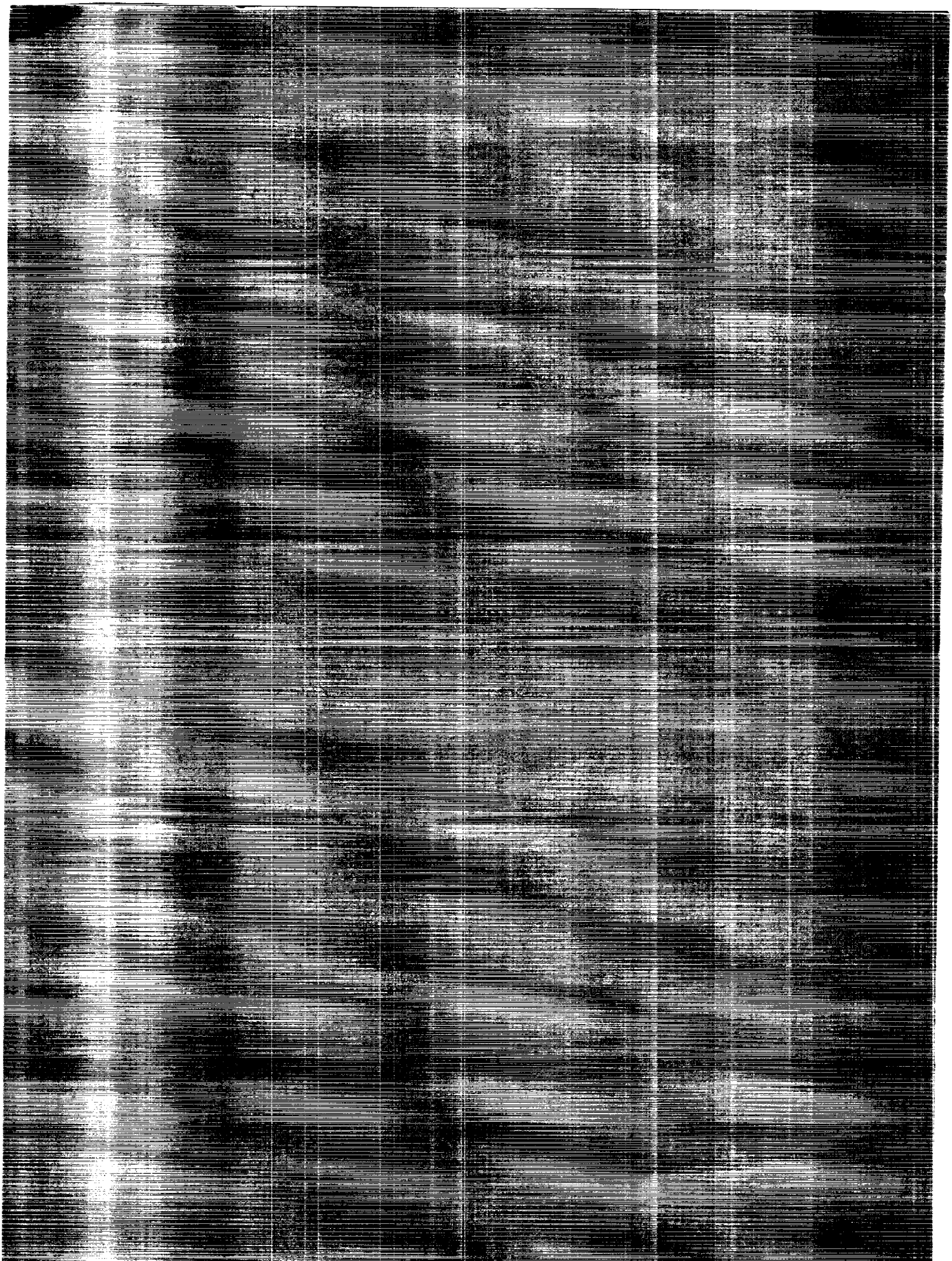

NASA Conference Publication 3111

Nineteenth NASTRAN® Users' Colloquium

Computer Software Management and Information Center
University of Georgia
Athens, Georgia

Proceedings of a colloquium held in
Williamsburg, Virginia
April 22–26, 1991

NASA
National Aeronautics and
Space Administration
Office of Management
Scientific and Technical
Information Division
1991

FOREWORD

NASTRAN® (NASA STRUCTURAL ANALYSIS) is a large, comprehensive, nonproprietary, general purpose finite element computer code for structural analysis which was developed under NASA sponsorship and became available to the public in late 1970. It can be obtained through COSMIC® (Computer Software Management and Information Center), Athens, Georgia, and is widely used by NASA, other government agencies, and industry.

NASA currently provides continuing maintenance of NASTRAN through COSMIC. Because of the widespread interest in NASTRAN, and finite element methods in general, the Nineteenth NASTRAN Users' Colloquium was organized and held at the Fort Magruder Inn and Conference Center, Williamsburg, Virginia on April 22-26, 1991. (Papers from previous colloquia held in 1971, 1972, 1973, 1975, 1976, 1977, 1978, 1979, 1980, 1982, 1983, 1984, 1985, 1986, 1987, 1988, 1989 and 1990 are published in NASA Technical Memorandums X-2378, X-2637, X-2893, X-3278, X-3428, and NASA Conference Publications 2018, 2062, 2131, 2151, 2249, 2284, 2328, 2373, 2419, 2481, 2505, 3029 and 3069.) The Nineteenth Colloquium provides some comprehensive general papers on the application of finite element methods in engineering, comparisons with other approaches, unique applications, pre- and post-processing or auxiliary programs, and new methods of analysis with NASTRAN.

Individuals actively engaged in the use of finite elements or NASTRAN were invited to prepare papers for presentation at the Colloquium. These papers are included in this volume. No editorial review was provided by NASA or COSMIC; however, detailed instructions were provided each author to achieve reasonably consistent paper format and content. The opinions and data presented are the sole responsibility of the authors and their respective organizations.

CONTENTS

CONTENTS
(Continued)

94

N91-20507

IMPROVED NASTRAN PLOTTING

53260
9P

by

Gordon C. Chan
Unisys Corporation
Huntsville, Alabama

INTRODUCTION

The graphic department of NASTRAN has received few changes since Level 17.5 (1980). Only hidden line and shrink plots were added in 1983 and 1985 respectively. An attempt to straighten up the FIND and NOFIND options in 1985 was not very successful. Color was also added about the same time. However, the basic plotting mechanism and the structure of the plot file remain unchanged, and they are biased towards CDC and UNIVAC machines. The plot commands were built on the technology of six bits per byte that make the 8-bit/byte machine very awkward to use. The new 1991 COSMIC/NASTRAN version, downward compatible with the older versions, tries to remove some of the old constraints, and make it easier to extract information from the plot file. It also includes some useful improvements and new enhancements. The new features available in the 1991 version include:

1. New PLT1 tape with simplified ASCII plot commands and short records.
2. Combined hidden and shrunk plot.
3. An x-y-z coordinate system on all structural plots.
4. Element offset plot.
5. Improved character size control.
6. Improved FIND and NOFIND logic.
7. A new NASTPLOT post-processor to perform screen plotting or generate PostScript files.
8. A BASIC/NASTPLOT program for PC.

PLT1/PLT2 FILE

Since Level 17.5 through the 1990 version, all the plotting goes to a PLT2 file which is described as the "general plotter tape". The structure of the plot commands in the PLT2 file is fully described in the user's and programmer's manuals. The commands, originally designed to be used for all machines with 32-, 36- or 60-bit computer words, were constructed based on 6 bits per byte structure. However, for IBM, VAX, and others, which are using 8-bits/byte word architecture, the 6 bits per byte technology has long been abandoned, leaving the manuals inaccurate and misleading. To use the PLT2 file for graphic plotting, a user needs to write an external program to interpret those NASTRAN generated plot commands, and to drive his particular plotter, if such a program is not already available. Normally this involves heavy bit and byte manipulation and data reconstruction. A disadvantage to the user is that the original bit and byte data on the PLT2 file cannot be printed to assist in debugging of his program.

In the 1991 NASTRAN version, the PLT2 file is left alone as it is. A PLT1 file is re-activated. (Before Level 17.5, PLT1 was used for 7-track plot tape). The PLT1 file contains the same plot commands in ASCII format and in 130 column short records. Therefore, the plot command data can be printed, and can be transported from one machine to another through normal channels. When this file is read by an external program, no data reconstruction from bits and bytes is required. The following table compares the two plot files:

	PLT2 file	PLT1 file
File type - sequential, formatted	No carriage ctrl	Carriage ctrl
Record type	ASCII/Binary*	ASCII
Record length	3000 bytes	130 columns
FORTRAN format	(10(180A4))*	(5(2I3,4I5))
Plot commands per physical record	100	5
Data type per plot command	30 Bytes	26 Decimals
No. of computer words per plot command	7.5	6
Edit, print, or terminal viewing of data	No	Yes
Disc space usage, referenced to PLT2	-	30% less
If tape is used - track and parity	9,Odd	9,Odd
File transmission through 'PROCOMM/KERMIT'	*	No problem

* 1. ASCII record, but data stored in binary bytes.
2. Since the record length is 3000 bytes, a format of (750A4) is sufficient.
3. Data transmission of the PLT2 file using standard PROCOMM/KERMIT software is difficult, if not impossible.

Two samples of NASTRAN plot commands are presented in Appendix A. The sample from PLT1 file is clearly readable, and provides meaningful information to any user who wants to use the data. The sample from PLT2 file cannot be fully printed, nor edited, because the record is too long. Both samples were taken from a test problem running on a VAX machine.

HIDDEN-LINE AND SHRINK PLOTS

The hidden-line plot and the 2-D and 3-D element shrink plots were added to NASTRAN in 1983 and 1985. They work very well alone, and work well together with other plot options such as label and color. However, the hidden-line plot and the element shrink plot are exclusive to one another. A modification of the plotting source code now allows the merging of the two plot options in the 1991 NASTRAN version.

X-Y-Z COORDINATE SYSTEM

In all previous NASTRAN structural plots, there is no information about how the model structure is oriented in space with respect to the basic rectangular system. A user can specify the viewing angle, vantage point, origin, and scale, and yet the actual plots contain no such information. In the 1991 version, a small x-y-z coordinate is always plotted at the lower right corner of each structural plot frame. This coordinate is rotated exactly

the same way the structural model is when subjected to different view angle, vantage point, and origin. Therefore, it gives the user instant information about the orientation of his structure in space. Of course, the x-y-z coordinate should not be present in all x-y table plots.

Normally there are four lines of labels and sub-labels at the bottom of each plot. The new x-y-z coordinate is placed at the right end of these four lines. Since the character size of the labels and sub-labels can be altered by the CSCALE option, the actual x-y-z coordinate size therefore varies accordingly.

OFFSET PLOT

In NASTRAN element repertoire, three elements, CBAR, CTRIA3 and CQUAD4, have grid point offset capability. In previous NASTRAN structural plots, all elements were treated equally, and they were always connected from grid points to grid points. Offsets were not considered. The argument for this practice is that since the offsets are usually very small, they will have no effect on the overall plot whether the offsets are considered or not. On the other hand, some users want the actual offset to be plotted such that the plots can help to detect any input card error. They argue that if the unintentional error is big enough, it will show on the plot, and corrective action can be taken immediately. The 1991 NASTRAN will satisfy both arguments.

The 1991 version shows the offsets two ways.

1. In an overall structure plot that includes all elements, and the offsets are always included in the plot. The offset absolute distances are computed, but the true offset directions are not. If the offsets are small, they will hardly show on the plot. If an offset is unintentionally large, a line may fly off in an uncontrolled direction.

2. A new 'OFFSET n' option is added to the 1991 NASTRAN PLOT command. If this option is exercised, only the elements with offsets will be plotted. The offset distances are magnified n times each to help bring out the offset magnitudes in plotting. The true offset directions are also computed and applied. If color plot is requested, the offset legs are plotted in different color than the color of the elements. Element label and other plot parameters can be requested simultaneously with the 'OFFSET n' option.

In both (1) and (2), the grid points with offsets are marked by asterisks. For example, a CBAR element with offsets in (2) with large n value will look like a staple, with asterisks at the corners

The "OFFSET n" option is only available for undeformed plot. Default value of n is 1.

CHARACTER SIZE CONTROL

The NASTRAN User's Manual indicates that the character size control, CSCALE n, is used only for the x-y plot. As mentioned above in the x-y-z coordinate discussion,

CSCALE controls also the character size of the labels and sub-labels of the structural plot. The factor 'n' was used to be an integer input. When n was set to 2, the character size on the labels and sub-labels was 4 times larger than normal size. Any increase of n may result in the labels and sub-labels exceeding the plot frame size. In the 1991 NASTRAN, the factor 'n' is changed to real number input with default value of 1.0. When n is set to 1.1, the character size is increased by 10 percent. The character size is double (not four times larger) for n equals 2.0

FIND/NOFIND

The descriptions of FIND, NOFIND, PLOT and ORIGIN in NASTRAN plotting commands are not easily understood. They can be plot commands by themselves, or they (except PLOT) can be options (or parameters) of another plot commnad. Confusion and misuse of these commands or options are quite common.

The FIND command (not used as an option in PLOT command) uses five parameters: SCALE, ORIGIN, VANTAGE POINT, REGION and SET. The PLOT command covers as many as 35 options or parameters, including ORIGIN and NOFIND. NOFIND, used only as an option in PLOT command, has no associated parameter. ORIGIN can be a plot command by itself, or a parameter to FIND, or an option to PLOT. Many of the parameters to FIND, ORIGIN and PLOT are optional and they may or may not have associated default values. The commands FIND and ORIGIN (not used as options) are optional, and need not be present in a series of plot commands. Some of the PLOT options or parameters are themselves linked to other options or other plot commands, which may or may not appear in a series of plot commands. For example, the SCALE and REGION parameters are linked to SCALE (plot size control), CSCALE (character size control), CAMERA, VIEW, and VANTAGE POINTS, any of which may or may nor appear as plot commands.

The FIND-NOFIND-ORIGIN-PLOT picture above seems very complicated and confusing. To make the matter worse, some of the missing plot commands or options have default values, while others have none. However, the following observations, derived from the NASTRAN User's Manual and from actual experimental testing, can be very helpful:

1. If ORIGIN is not defined in a FIND card, ORIGIN ID of zero is used by NASTRAN. It is not a good practice to force NASTRAN to select a zero ORIGIN ID.
2. No matter what ORIGIN ID's the user used in multiple FIND cards, the first ORIGIN ID is the origin no. 1. The second ORIGIN ID, only if it is different from the first, is origin no. 2, and so on. A maximum of ten ORIGIN ID's can be used. If more then ten ORIGIN ID's are used, all the remaining ID's go to the eleventh.
3. ORIGIN ID can be re-used in a sequence of plots. In this case, the plot parameters and controls, such as scale, view, frame size etc., associating to the previous ORIGIN of the same ID, are completely replaced by those of the new ORIGIN data.
4. The ORIGIN ID, requested on a FIND card, defines a number of plotting parameters associating with the current structure orientation in space (such as left, right, upper and bottom plot frame limits, view angle, vantage point, plot scale etc.). These data are saved, and can be recalled by the ORIGIN ID on the PLOT command. Note - if the current PLOT command does not specify this

ORIGIN ID, the data saved are not used in the current plot.

5. Therefore, the ORIGIN ID requested in a FIND command, and the ORIGIN ID used by a PLOT card, are unrelated; unless the same ID is specified by both FIND and PLOT. If the PLOT command does not specify any ORIGIN ID, observation (1) above applies. The following example shows that ORIGIN 0 is used by PLOT, not 50:

```
FIND  SCALE, ORIGIN 50, SET 1
PLOT
```

6. NOFIND causes all plotting parameters, including ORIGIN ID, to be the same as the previous plot in a series of plot sequences. The NOFIND option is actually a special case of the PLOT-ORIGIN arrangement. The following examples give identical results in $PLOT 2:

```
$PLOT 1                          $PLOT 1
FIND SCALE, ORIGIN 50, SET 2     FIND SCALE, ORIGIN 50, SET 2
PLOT ORIGIN 50                   PLOT ORIGIN 50

$PLOT 2                          $PLOT 2
PLOT NOFIND                      PLOT ORIGIN 50
```

NOFIND did not work in 1990 and earlier NASTRAN releases as advertised in the user's manual. It always reverted to the first defined ORIGIN ID. Also, each time a FIND card was used, a new AXIS line, plus any old axes previous saved, were printed on the engineering data echo for the current plot. No additional information was printed to indicate which AXIS (or ORIGIN) is being used. The 1991 NASTRAN will print only one AXIS data line, which is the current ORIGIN being used for the current plot.

PROGRAM NASTPLOT
for main-frame, mini, micro and workstation

As mentioned in the PLT1/PLT2 FILE section above, a user needs an external program to read the NASTRAN general plotter tape, interpret the plot commands, and produce the NASTRAN graphic plots. Such a program is usually called a NASTRAN post-processer. Some of the NASTRAN post-processers may be very sophisticated and expensive, and capable of doing many additional things. Some may be relatively simple and cheap, and dedicated only to processing NASTRAN plot file. NASTPLOT is one of the better known products that perform this dedicated task. In fact, there are many versions of NASTPLOT written by various people for different combinations of computer-and-plotter. One common factor of the NASTPLOT programs is that they all use PLT2 file.

A new NASTPLOT program will be included in the 1991 COSMIC/NASTRAN release. This new NASTPLOT program does not necessarily perform better than any existing old ones. However, it has its own virtues:

1. It is FORTRAN written in simple and straightforward program logic.
2. It handles PLT1 or PLT2 tape.
3. It produces Tektronix screen plots, or PostScript files that can be sent to a PostScript printer, or a LaserJet printer (equipped with a PostScript cartridge) for hard-copies.

4. All supporting routines can be easily identified. All Tektronix routines are prefixed by "TX", and all PostScript routines by "PS", (User can easily swap these routines for other plotter requirements).
5. This program was written on a VAX, but the source code is almost machine independent.

BASIC/NASTPLOT
for PC, with MS-DOS and graphic capability

Since the PC is almost a household product nowadays, many offices have a few available already, most PC's come with graphic capability and BASIC language, and since the NASTRAN PLT1 file can be transported easily from one computer system to another, it becomes logical to tap into this vast resource for NASTRAN advantage. To move the plotting to a PC is almost an instant bonus to enhance NASTRAN capability. And it can be done very economically.

A new MS-DOS BASIC/NASTPLOT program was written and tested successfully on a VAX-PC (UNISYS/8080 chip, BASIC 3.2) combination. (Also 286 and 386 PC's.) This BASIC/NASTPLOT program, requiring no special hardware, or software, produces screen plots on a PC just as satisfactory, and just as fast, as any expensive equipment. It even produces color plots if the PC is equipped with a color monitor. 4K byte memory is needed. However, a high resolution monitor is recommended for best results. This program, with complete listing in Appendix B, serves as a demonstration of tapping into the PC world. It can be easily converted to other non MS-DOS systems, such as the Apple and Macintosh.

APPENDIX A

TWO SAMPLES OF NASTRAN PLOT COMMANDS

Sample Plot Commands from a PLT2 file:

```
(3000 bytes/record)
¯a¯a¯a¯a¯a¯a¯a¯a¯A¯a¯a¯a¯F¯a¯a¯a¯a¯a¯a¯a¯a¯a¯a¯a¯a¯C¯a¯a¯a¯a¯a¯a¯a¯a¯a¯a¯a¯F¯a¯a¯a¯a¯a¯a¯a¯a¯a¯a¯a¯a¯a¯a¯a¯a¯a¯a¯a¯a¯a¯a¯a¯a¯a¯a
¯a¯a¯a¯a¯a¯C¯a¯a¯a¯a¯a¯a¯a¯F¯a¯a  ¯a¯a¯a¯a¯a¯a¯a¯a¯a¯a¯a¯a¯a¯a¯a¯a    ¯a¯D¯a¯a¯a¯a¯a¯a¯a¯a¯a¯a¯a¯a¯a¯a¯a¯a¯a¯a¯a¯a¯a¯a¯a¯a¯a¯a¯a
¯a¯a¯a¯a¯a¯a¯a¯a¯a¯a¯a¯a¯a¯a¯a¯a¯a¯A¯a¯a¯a¯a¯a¯a¯a¯a¯a¯a¯F¯a¯a¯a¯a¯a¯a¯a¯a¯a¯a¯a¯a¯a¯a¯a¯a¯a¯a¯a¯a¯a¯a¯a¯a¯a¯a¯a¯a¯a¯a¯a¯a¯a¯a¯a
¯a¯a¯a¯a¯a¯a¯A¯F¯a¯a¯a¯a¯a¯K¯a¯a¯a¯a¯F¯a¯a¯a¯a¯a¯a  ¯a¯a¯a¯a¯a¯a¯a¯a¯a¯C¯a¯a¯a¯a¯a¯a¯a¯a¯a¯a¯a¯a¯a¯a¯a¯a¯a¯a¯a¯a¯a¯a¯a¯a¯a¯a¯a¯a
¯a¯a¯C¯a¯a¯a¯a¯D¯a¯D¯a¯a¯a¯C¯a¯a¯a¯a¯a¯a¯a¯a¯a¯a¯a¯a¯a¯a¯a¯a¯a¯a¯a¯a¯a¯a¯a¯a¯a¯a¯a¯a¯a¯a¯a¯a¯a¯a¯a¯a¯a¯a¯a¯a¯a¯a¯a¯a¯a¯a
¯a¯a¯a¯a¯a¯a¯a¯a¯a    ¯a¯a¯a¯A¯a¯a¯a¯a¯a¯a¯a¯a¯a¯F¯F¯a¯a¯a¯a¯a¯a¯a¯C¯a¯a¯a  ¯a¯a¯a¯a¯a¯a¯a¯a¯a¯a¯a¯a¯a¯a¯a¯a¯a¯a¯a¯a¯a¯a¯a¯a¯a¯a
  :
```

Sample Plot Commands from a PLT1 file:

```
(130 columns/record)
 1  1    1 1023 1023    0  2  2    0    0    0    0  3  2    0    0    0    0 16  1    0 1015 1019 1015  6  1    0 1012 1019 1012
 6  1    0 1009 1019 1009  6  1    0 1006 1019 1006  6  1    0 1003 1019 1003  6  1    0 1000 1019 1000  6  1    0  997 1019  997
 6  1    0  994 1019  994  6  1    0  991 1019  991  6  1    0  988 1019  988  6  1    0  985 1019  985  6  1    0  982 1019  982
 6  1    0  979 1019  979  6  1    0  976 1019  976  6  1    0  973 1019  973  6  1    0  970 1019  970  6  1    0  967 1019  967
 6  1    0  964 1019  964  6  1    0  961 1019  961  6  1    0  958 1019  958  6  1    0  955 1019  955  6  1    0  952 1019  952
   :
 6  1    0  604 1019  604  6  1    0  601 1019  601  6  1    0  598 1019  598  6  1    0  595 1019  595  6  1    0  592 1019  592
 6  1    0  589 1019  589  6  1    0  586 1019  586  6  1    0  583 1019  583  6  1    0  580 1019  580  6  1    0  577 1019  577
 6  1    0  574 1019  574  6  1    0  571 1019  571  6  1    0  568 1019  568 15  1  197  555  199  555  5  1  199  555  198  555
 5  1  198  555  198  550  5  1  198  550  197  549  5  1  197  549  195  549  5  1  195  549  194  550  5  1  202  555  202  550
 5  1  202  550  203  549  5  1  203  549  206  549  5  1  206  549  207  550  5  1  207  550  207  555  5  1  215  554  214  555
 5  1  214  555  211  555  5  1  211  555  210  554  5  1  210  554  210  553  5  1  210  553  211  552  5  1  211  552  214  552
   :
 5  1  287  538  286  539  5  1  286  539  283  539  5  1  283  539  282  538  5  1  282  538  282  534  5  1  282  534  283  533
 5  1  283  533  286  533  5  1  286  533  287  534  5  1  287  534  287  536  5  1  287  536  285  536 16  1    0    0 1019    0
 6  1    0    3 1019    3  6  1    0    6 1019    6  6  1    0    9 1019    9  6  1    0   12 1019   12  6  1    0   15 1019   15
 6  1    0   18 1019   18  6  1    0   21 1019   21  6  1    0   24 1019   24  6  1    0   27 1019   27  6  1    0   30 1019   30
 6  1    0   33 1019   33  6  1    0   36 1019   36  6  1    0   39 1019   39  6  1    0   42 1019   42  6  1    0   45 1019   45
   :
 5  1  121 1012  122 1011  5  1  122 1011  126 1011  5  1  126 1011  127 1012  5  1  127 1012  127 1016  5  1 1017 1016 1018 1017
 5  1 1018 1017 1018 1011  5  1 1018 1011 1017 1011  5  1 1017 1011 1019 1011  0  0    0    0    0    0  0  0    0    0    0    0
15  1    9   59   12   59  5  1   12   59   12   53  5  1   12   53   12   59' 5  1   12   59   15   59  5  1   22   59   17    5
 5  1   17   59   17   56  5  1   17   56   20   56  5  1   20   56   17   56  5  1   17   56   17   53  5  1   17   53   22   53
   :
```

APPENDIX B

BASIC/NASTPLOT PROGRAM LISTING

```
10  'PROGRAM NASTPLOT, MS-DOS PC/BASIC VERSION
20  'BASIC 3.2, WITH EGA OR CGA GRAPHIC CAPABILITY
30  'NO PARTICULAR HARDWARE OR SOFTWARE REQUIRED
40  'INPUT: NASTRAN PLT1 FILE (NOT PLT2 FILE)
50  'WRITTEN BY G.CHAN/UNISYS  11/90
60  'TO RUN THIS PROGRAM     1. BASIC
70  '                        2. LOAD "NASTPLOT
80  '                        3. F2 or RUN "NASTPLOT
90  '                        4. answer all questions asked
100 '             AT END     5. SYSTEM
110 KEY OFF: CLS: PRINT "": PRINT ""
120 ? "                              ****"
130 ? "                            *        *"
140 ? "                           *           *"
150 ? "                           *   N A S T P L O T"
160 ? "                           *           *"
170 ? "                            *        *"
180 ? "                              ****"
190 ? ""
200 ? "        PC/BASIC MS-DOS GRAPHIC          SYSTEM RELEASE - NOV. 1990"
210 ? "
220 ? "        WRITTEN BY UNISYS/               FOR COSMIC"
230 ? "        NASTRAN MAINTENANCE GROUP        UNIVERSITY OF GEORGIA"
240 ? "        HUNTSVILLE, ALABAMA              ATHENS, GEORGIA 30602"
250 ? "                                         PHONE: (404) 542-3265"
260 PRINT "": PRINT ""
270 ? "        *** AT THE END OF EACH PLOT, HIT C/R TO CONTINUE ***"
280 ? "                    ===                  ==="
290 PRINT ""
300 DEFINT I-J,Z
310 OPTION BASE 1
320 DIM Z(30)
330 LET YES$="YES":  LET Y$="Y":  LET YSS$="yes":  LET YS$="y"
340 F =0.30
350 JX=640-480: JY=320  '480 & 320 TO CENTER PLOT,  640 TO REVERSE IMAGE
360 '*** CURRENTLY SET UP FOR EGC WITH HI-RESOLUTION MONITOR - SCREEN 9
370 J12=1
380 INPUT "ENTER PLOT FILE FULL NAME: ",FIL$
390 OPEN "I",1,FIL$
400 INPUT "ENTER PLOT NUMBER, ZERO TO QUIT: ",ID
410 IF ID =0 GOTO 880
420 IF J12=2 GOTO 470
430 INPUT#1, Z(1),Z(2),Z(3),Z(4),Z(5),Z(6),Z(7),Z(8),Z(9),Z(10),Z(11),Z(12),Z(
435 '        Z(1),Z(2),...,Z(30) ALL ON ONE LINE
440 IF EOF(1) GOTO 800
450 IF Z(1) <>1 GOTO 420  'NEW PLOT BEGINS WITH ONE IN Z(1)
460 IF Z(19)=16 GOTO 420  'SKIP FIRST ID PLOT IF IT IS PRESENT
470 I3=Z(3)               'SAVE PLOT NUMBER IN I3
480 PRINT " ...WORKING"
```

```
490 IF I3<>ID GOTO 420     'SEARCH FOR REQUESTED PLOT NUMBER
500 I1=7: IE=0
510 CLS
520 IF J12=2 GOTO 590      'WHEN J12=2, CURRENT RECORD IS ALREADY READ
530  SCREEN 9              'EGC with EGD, Advanced screen A (640X350)
535 'SCREEN 2              'CGA and different valus for F,JX and JY
540 COLOR 6,0              'SET COLOR TO ORANGE AND BLACK
550 GOTO 600
560 INPUT#1, Z(1),Z(2),Z(3),Z(4),Z(5),Z(6),Z(7),Z(8),Z(9),Z(10),Z(11),Z(12),Z(
565 '        Z(1),Z(2),...,Z(30) ALL ON ONE LINE
570 IF EOF(1) GOTO 700
580 I1=1
590 J12=1
600 FOR I=I1 TO 30 STEP 6 'LOOP FOR 5 COMMANDS, 6 WORDS EACH
610 IC=Z(I)                'IC IS PLOT COMMAND
620 IF IC=1  GOTO 710      'A NEW PLOT IF IC IS ONE
630 IF IC>10 THEN IC=IC-10
640 IF IC<>5 AND IC<>6 GOTO 680
650 IP=Z(I+1)              'IP IS PEN CONTROL, SUCH AS COLOR.
660 JR=JX+Z(I+2)*F: JS=JY-Z(I+3)*F: JT=JX+Z(I+4)*F: JU=JY-Z(I+5)*F
670 LINE (JR,JS)-(JT,JU),IP
680 NEXT
690 GOTO 560
700 IE=1                   'EOF ENCOUNTERED AT END OF A PLOT
710 BEEP                   'END OF A PLOT
720 INPUT "",Q$            'C/R TO CONTINUE
730 IF IE=1 GOTO 800
740 CLS                    'CLEAR SCREEN
750 J12=2                  'RESET FLAGS. FIRST RECORD OF NEXT PLOT ALREADY READ
760 GOTO 400               'LOOP BACK FOR NEXT PLOT
800 IF I3=0 THEN PRINT "EOF ENCOUNTERED. THERE IS NO PLOT IN ";FIL$
810 IF I3=1 THEN PRINT "EOF ENCOUNTERED. THERE IS ONLY ONE PLOT IN ";FIL$
820 IF I3>1 THEN PRINT "EOF ENCOUNTERED. THERE ARE ONLY";I3"PLOTS IN ";FIL$
830 INPUT "START ALL OVER AGAIN";Q$
840 IF Q$<>YES$ AND Q$<>Y$ AND Q$<>YSS$ AND Q$<>YS$ GOTO 880
850 CLOSE #1
860 J12=1: I1 =1
870 GOTO 390                'CYCLE BACK FOR MORE PLOT
880 PRINT "END OF JOB"
890 COLOR 7,0:  CLS         'RESET COLORS TO BLACK AND WHITE
900 END
```

N91-20508

ONLINE NASTRAN DOCUMENTATION

by

Horace Q. Turner
David F. Harper
Unisys Corporation
Huntsville, Alabama

SUMMARY

The distribution of NASTRAN User Manual information has been difficult because of the delay in printing and difficulty in identification of all users. This has caused many NASTRAN users not to have the current information for the release of NASTRAN that is available to them. The User Manual updates have been supplied with the NASTRAN Releases, but distribution within organizations was not coordinated with access to releases. The Executive Control, Case Control, and Bulk Data sections are supplied in machine readable format with the 91 Release of NASTRAN. This information is supplied on the release tapes in ASCII format, and a FORTRAN program to access this information is supplied on the release tapes. This will allow each user to have immediate access to User Manual level documentation with the release. The sections on Utilities, Plotting, and Substructures are expected to be prepared for the 92 Release.

INTRODUCTION

The main objective in this effort is to provide machine readable files of the User Manual sections of Executive Control, Case Control, and Bulk Data that can be used for both publication quality updates and online access with any terminal. To meet this object it was necessary to reformat parts of the manual to use only character information and to define a form of storing graphic information.

The process of creating the files and the features for access are discussed in the following sections:

DOCUMENTATION SCAN INTO ASCII FILE
DOCUMENTATION FORMAT FOR STORAGE
REQUIREMENTS FOR PRINTING
METHOD OF ONLINE ACCESS

DOCUMENTATION SCAN INTO ASCII FILE

The first step in preparation of the User Manual sections for online access was to scan the existing manual sections into machine readable format. This was done using a scanner integrated with a PC computer. The output of the scan was an ASCII file containing only character data. The figures and line data were dropped during the scan. The scanner used was a Kurzweil device located at a government facility in Huntsville, Alabama. The scanner software was able to read the reduced pages and different font styles that had been used in preparation of the User Manual over the years. The scanner software was trainable for recognition of overstrike characters as required in the User Manual.

DOCUMENTATION FORMAT FOR STORAGE

To meet the objective of maintaining the User Manual sections in one database format for both publishing quality and online access, the following rules were used for the document storage format:

Stored in page format by card type

All lines reduced to 80 characters

Page length is 82 lines

All graphics removed

All subscripts and superscripts replaced

All equations written in FORTRAN notation

PC box drawing codes are used to represent line data

No embedded codes are used for formatting

No overstrike or underline characters

The document is stored in line per record format with each section of the document in a separate file.

The Executive Control and Case Control sections required the most change in appearance of the pages . Attached is a sample page showing the replacement of the large "{}" by PC box drawing characters. This will allow for substitution of these characters on any terminal.

The Bulk Data section maintains most of its appearance with the lines and figures replaced by PC box drawing characters.

REQUIREMENTS FOR PRINTING

The document can be printed on an HP LaserJet or compatible with legal size paper using 6 lines per inch and the native 10 character per inch Courier font containing PC box drawing characters. This page then has to reduced to 85 percent to produce a standard 8.5 by 11 inch manual update page. To print on other devices the PC box drawing characters can be replaced. This replacement can be done with an editor or a program to translate the file.

METHOD OF ONLINE ACCESS

A FORTRAN program to read and display the pages on the screen is supplied on the 91 Release tapes. This program allows the user to select the section and the key topic for display. The key topic is a Bulk Data, Executive Control, or Case Control card name. This program allows the user to set the number of lines for display on the output device and stops when that number of lines is displayed. At any time, the user can back up or advance a specified number of lines. This program assumes the terminal can only display standard ASCII characters, and therefore converts the PC box drawing characters to +, -, and | for display. The figures that can be stored in this format will be shown on the display.

Case Control Data Card - ACCELERATION - Acceleration Output Request.

Description: Requests form and type of acceleration vector output.

Format and Example(s):

$$\text{ACCELERATION}\left[\begin{array}{l}(\ \text{SORT1}\ ,\ \text{PRINT}\ ,\ \text{REAL}\ \ )\\ \ \ \text{SORT2}\ \ \ \ \text{PUNCH}\ \ \ \text{IMAG}\\ \ \ \ \ \ \ \ \ \ \ \ \ \ \ \ \ \ \text{PHASE}\end{array}\right] = \left[\begin{array}{l}\text{ALL}\\ \text{n}\\ \text{NONE}\end{array}\right]$$

ACCELERATION = 5

ACCELERATION(SORT2, PHASE) = ALL

ACCELERATION(SORT1, PRINT, PUNCH, PHASE) = 17

Option	Meaning
SORT1	Output will be presented as a tabular listing of grid points for each load, frequency, eigenvalue, or time, depending on the rigid format. SORT1 is not available in Transient problems (where the default is SORT2).
SORT2	Output will be presented as a tabular listing of frequency or time for each grid point. SORT2 is available only in Transient and Frequency Response problems.
PRINT	The printer will be the output media.
PUNCH	The card punch will be the output media.
REAL or IMAG	Requests real and imaginary output on Frequency Response problems.
PHASE	Requests magnitude and phase (0.0 <= phase < 360.0 degrees) on Frequency Response problems.
ALL	Accelerations for all points will be output.
n	Set identification of a previously appearing SET card. Only accelerations of points whose identification numbers appear on this SET card will be output (Integer > 0).
NONE	Accelerations for no points will be output.

Remarks: 1. Both PRINT and PUNCH may be requested.

2. An output request for ALL in Transient and Frequency response problems generally produces large amounts of printout. An alternative to this would be to define a SET of interest.

3. Acceleration output is only available for Transient and Frequency Response problems.

4. In a frequency Response problem any request for SORT2 output causes all output to be SORT2.

5. ACCELERATION = NONE allows overriding an overall output request.

N91-20509

Experiences in Porting NASTRAN® to Non-Traditional Platforms

Gregory L. Davis
Robert L. Norton
Jet Propulsion Laboratory

Summary

The 1990 UNIX version of NASTRAN was ported to two new platforms that are not supported by COSMIC: the Sun SPARC workstation and the Apple Macintosh using the A/UX version of UNIX. This paper summarizes the experiences of the authors in porting NASTRAN, and makes suggestions for users who might attempt similar ports.

Introduction

Historically, NASTRAN has been supported on only the largest, most capable mainframe computers. For many years the computers supported by COSMIC were the CDC, IBM, and UNIVAC mainframes. In the late 1970s various manufacturers introduced what became known as minicomputers. These computers offered capable performance at much lower cost than traditional mainframe computers. After the very successful DEC VAX minicomputer was introduced, NASTRAN was ported to it. Over the last ten years the widespread use of VAX minicomputers has extended the use of NASTRAN to many new sites, and VAX leases now amount to over half of all NASTRAN leases. The introduction of small office-environment VAXes has allowed consultants and departments to bring NASTRAN nearly to the engineer's desk.

As the cost of computer hardware has decreased, the workstation market has emerged. Workstations offer the performance of minicomputers at a cost and size that allows single-user computers. The market has seen a variety of proprietary operating systems grow and then falter; the dominant operating system for workstations is now clearly UNIX. For the user this trend has been very helpful, allowing the user to concentrate on the proper hardware solution without having to also select the operating system. One significant advantage for the hardware manufacturer is the ability to concentrate on developing high performance hardware without having to divert resources into operating system development.

As UNIX workstations have become pervasive, COSMIC has released a new version of NASTRAN designed to be portable enough to run on a variety of these workstations. The first release of this version was designed for the DEC ULTRIX operating system and retained many of the non-standard FORTRAN extensions that are used in the VAX version. Later releases have moved closer to standard FORTRAN. Experiences with porting NASTRAN to new UNIX workstations have allowed the removal of certain impediments.

The rapid development of hardware has not been the exclusive province of workstations. Since the early 1980s microcomputers or personal computers have also shown amazing growth in capability. While the early 8-bit microcomputers

were almost useless for finite element analysis, some work could be done on the 16-bit microcomputers of the middle to late 1980s. With the introduction of high speed 32-bit microcomputers, the boundary between workstations and microcomputers has become blurred. The cost of workstations has dropped enough that low-end workstations are cheaper than high-end personal computers, while the performance of high-end personal computers approaches the performance of workstations.

Many people have wrestled with the definitions of workstations and personal computers. Rather than focus on hardware to establish the difference, it makes more sense to look at the differences from the user's point of view. One big appeal of the personal computer has always been the vast array of software available. Few engineers would want to do without the personal productivity software they now routinely use. The vast volume of personal computers along with the relatively small number of display devices allows the development of niche software to go with the high volume software (e.g. word processors, spreadsheets). Probably the strongest feature of workstations is the robustness of UNIX. While it is trivial to write a program to crash a personal computer, it is much more difficult to crash UNIX.

Naturally enough, most engineers don't want to choose only the personal productivity software of the personal computers or only the robustness of UNIX — they want both on their desktop at the same time. Thus hardware manufacturers are producing computers that run both UNIX and traditional personal computer operating systems. There are many computers using Intel architecture that run UNIX and MS-DOS programs. Apple has available A/UX (their version of UNIX), which also runs regular Macintosh software and can even run MS-DOS software in emulation mode. The workstation hardware manufacturers are countering with Reduced Instruction Set Computers (RISC) that also run MS-DOS in emulation. One manufacturer has even announced a laptop RISC machine that runs UNIX, MS-DOS, and Macintosh software.

One clear winner has emerged from the confusion of operating systems and computer architecture — the end user. We now have available an amazing, almost paralyzing set of options. For the NASTRAN community this revolution means that "NASTRAN for the masses" is at hand. We have $10,000 desktop computers that are at least as capable as the multi-million-dollar mainframes that were used at the dawn of NASTRAN twenty years ago. Manufacturers have recently announced portable UNIX computers that are fully capable of running NASTRAN. Now the individual engineer can not only have NASTRAN at the desk, but also can carry NASTRAN to the work!

General Porting Comments

The sheer size of NASTRAN is one of the biggest obstacles to porting. The 1990 VAX version has 84 machine-dependent subroutines (0.3 MBytes) and 1695 machine-independent subroutines (13.3 MBytes), for a total of 1779 subroutines (13.7 MBytes). This size has always created problems for NASTRAN, and it

typically pushes the boundaries of the computer and operating system capabilities.

Although the VAX version has been all FORTRAN, a number of VAX extensions to FORTRAN have been used. UNISYS has been trying to eliminate as many extensions as possible, but a number of extensions to FORTRAN are still used. Following is a summary of the extensions used, along with some suggestions for porting:

1. Some non-standard variable types are used: `REAL*4`, `REAL*8`, `INTEGER*2`, `INTEGER*4`, and `LOGICAL*1`. These extensions are often supported, but if not they can be easily changed.

2. Hexadecimal constants are used, and the required form of the hexadecimal constants may vary from one compiler to another. The hexadecimal edit descriptor `Z` and the octal edit descriptor `O` are used in the `FORMAT` statement.

3. Some non-standard functions are used: `IAND`, `IOR`, `IEOR`, `ISHFT`, `JMOD`, and `NOT`. All of these except `JMOD` are used in bit manipulation.

4. In-line comments are used, with ! signifying the beginning of the comment.

5. Hollerith constants are used in `DATA` statements.

6. The alternate `RETURN` specifier is used with & to indicate the statement label. Change the & to * to meet the standard.

7. `READONLY` is used in a file `OPEN` statement in subroutine `DSXOPN`.

8. File names in `READ` and `WRITE` statements are stored in arrays (using Hollerith constants) rather than using `CHARACTER` variables. These references should be changed to use `CHARACTER` variables.

9. Variable names exceed the 6 characters permitted by the standard.

10. `DISP=` rather than `STATUS=` is used in several `CLOSE` statements.

11. `TYPE=` rather than `STATUS=` is used in an `OPEN` statement.

12. The `%LOC` function is used to return the location in memory where a variable is stored.

13. Lower case source code is used.

14. Subroutines `CPUTIM`, `TDATE`, and `WALTIM` are used to get the cpu time, date, and all clock time from the system. The calls from these subroutines to get the system level information will be different for each new port.

Most of the extensions can be worked around. The truly significant extensions are the use of the %LOC and the non-standard functions. All of the above extensions are located in the machine-dependent subroutines, identified by the .MDS extension on the VAX. All the machine-independent routines, identified by the .MIS extension, compiled on the Sun and the Macintosh with no changes at all.

Sun Porting Experiences

The 1990 UNIX release of NASTRAN was shipped to JPL from UNISYS on a TK50 tape, where it was read onto a VAX ULTRIX machine and copied over to a Sun 4/390 using FTP. The ensuing porting and debugging process fell into three main stages.

Stage 1 consisted of fixing initial, fairly obvious incompatibilities between the Sun and VAX FORTRAN compilers. The machine-dependent subroutines were initially screened for the incompatibilities listed above in General Porting Comments. After all subroutines were compiled, the 15 executable NASTRAN links were generated. Gordon Chan of UNISYS was frequently consulted at this stage of the process and he provided invaluable assistance.

Stage 2 consisted of modifying the ancillary UNIX shell scripts used to drive the executable NASTRAN links. The script problems originally became apparent in trying to run sample problem D01000A.NID, when the proper UNIX links could not be established. XQT and @XQT are well-written UNIX shell scripts to provide a friendly user interface for running the NASTRAN program; however, these had to be modified to properly represent the user directory structure and to properly establish the UNIX links between the rigid format and the alter files.

Stage 3 consisted of debugging the executable links. Problems in execution became immediately apparent when trying to run sample problem D011A.NID. The first problem was eventually traced to bit shifting operations in subroutine KHRFN1: see point 2 under Recommendations to Users for details. A second problem in execution was traced to subroutine INTPK in link 4. This was inadvertently repaired by relinking link 4 with INTPK included twice in the link statement. Link ordering does become crucial! This ad hoc fix was then applied to all NASTRAN links containing INTPK. These repairs finally permitted the successful execution of test problem D01011A.NID on the Sun computer.

Macintosh Porting Experiences

The first major challenge with the Macintosh version was getting the source code downloaded to the Macintosh from the VAX. The only connection was via a 9600-baud local area network. Kermit was used to automatically download all the subroutines, which took about 10 hours. The UNIX versions of the machine-dependent subroutines were obtained via FTP from the Sun computer.

The FORTRAN compiler supplied with A/UX does not have the extensions required to properly compile the machine-dependent subroutines, so a third-party FORTRAN compiler sold by NKR Research, Inc. of San Jose, California was selected. NKR proved to be very helpful during this project, providing useful advice and compiler updates on a timely basis.

The organization of the files on the Macintosh took a couple of tries to get right. A/UX allows the use not only of the usual UNIX editors, `vi` and `ed`, but also of Macintosh graphical user interface editors, such as `TextEditor` (supplied by Apple with A/UX), `QUED/M` (a commercial editor), or `Alpha` (a shareware editor). Unfortunately, since the Macintosh file system does not adequately handle directories with large numbers of files, the source files cannot be stored together in one directory. The UNIX file system does cope with large directories, but the Macintosh editors use the Macintosh file system to open the files. The source files were put into 26 directories corresponding to the first letter of the subroutine name. In this way the largest directory had only 253 files.

The next hurdle was using the UNIX `ar` utility to create the library of object files. The VAX and other UNIX systems put all the object files together in one library. This library is then used as input to the linker to form each of the 15 executable files. The ar utility supplied with A/UX could not load all the object files into the library. After about 1400 files, it produced an error message when additional files were to be added to the library. In addition to the error in creating the library, it took one hour to load the object files into the library. To avoid the library problem all the object files were copied to a single directory. Since no Macintosh programs would be used in this directory, the weakness of the Macintosh file system did not matter. To link the executable files, a list of all the subroutines used in a link was generated on the VAX and used as input to the A/UX linker.

Recommendations to UNISYS

As the current maintenance contractor to COSMIC, UNISYS has done a splendid job in producing the UNIX version of NASTRAN. UNISYS has spent several years reducing the number of non-standard extensions to FORTRAN used in the code and has ported NASTRAN to several UNIX platforms.

There is a fundamental tension between the desire to produce a truly generic version which can be ported to new UNIX platforms relatively easily and the desire to optimize the code for a particular platform. The various proprietary versions of NASTRAN will probably continue to be more efficient than the generic version on any given platform, and some users will always complain. However, it is in the best interests of COSMIC and UNISYS to place the emphasis on portability. As the hardware manufacturers continue their rapid performance improvements, it seems to make more sense to upgrade the hardware than to "tweak" the code for improved performance.

From our experience in these ports of NASTRAN, we have several suggestions for UNISYS:

- NASTRAN is, of course, a rather old code, and FORTRAN has seen many changes since the FORTRAN IV that was used in the beginning. FORTRAN 77 introduced features that could simplify the code and also help the reading and maintainability of the code. The FORTRAN 90 that is currently being reviewed will introduce even more radical changes. UNISYS should move toward the use of structured programing. While it is possible to carry this to extremes with overly deeply nested `IF` clauses, a gradual transition to the use of the `IF - THEN - END IF` rather than repeated `GO TO` statements would help readability. After FORTRAN 90 becomes approved and supported, constructs such as `DO WHILE` and `DO - END DO` would also be helpful. The 1990 NASTRAN release does not use `IF - THEN - END IF` anywhere.

- The bit handling features of the code should be modernized by using character variables. Character variables were not available in the FORTRAN compilers used when these routines were written and the available computer memory was meager, so non-standard bit handling techniques were used. Now that NASTRAN is routinely used on computers with several hundred to several thousand times as much memory as the 16k-word IBM 7094 and since the FORTRAN 77 compilers support character variables, it is time to eliminate the bit manipulation.

- Have a dedicated UNIX machine at UNISYS connected to the Internet, thereby greatly facilitating program development and user/vendor communications. Program fixes and enhancements could then be transmitted using FTP, and user/vendor messages could be transmitted through e-mail.

- Provide the UNIX NASTRAN source codes and related shell scripts on media other than the TK50 tape, which is VAX specific. Other common media on UNIX-based "mainframe" type machines are $1/4$ inch tape cartridges and 8 mm cassette tapes. CD-ROMs would provide a wonderful distribution media, especially when the manuals become available in electronic form.

Recommendations to Users

Porting NASTRAN to other computer platforms is an ambitious undertaking. At the outset the authors counsel patience and perseverance — the very large amount of code will probably stretch the computer's and user's resources to the limit. The following general approach for porting the UNIX version of NASTRAN over to other platforms profits from our own experience and mistakes.

1. Copy the NASTRAN source code over to the host machine, renaming the files as appropriate for the host's FORTRAN compiler. We highly recommend maintaining the `MDS/MIS` distinction in the directory structure — most of the coding incompatibilities will be in the `.MDS` routines. It is also a good idea to make a write-protected copy of *all* subroutines in the `.MDS` directory to preserve the capability to recover from inadvertent or incorrect edits during the debugging process. Develop a bookkeeping system to keep track of the large number of subroutines.

2. Initially screen the .MDS subroutines for coding incompatibilities with the host FORTRAN compiler. Prime candidates for compiler-dependent problems are listed in the above General Porting Comments. Comment any changes made for future reference.

   Bit shifting operations using the subroutine `khrfn1` need to be examined. This may or may not be a problem depending upon the convention for ordering the position in a character variable. Specifically, the character position of the VAX word is numbered left to right; the corresponding Sun and Macintosh word is numbered right to left. The current code assumes the VAX convention. This problem may arise in the `.MIS` subroutines `XSEM01-15`, which are the main drivers for each executable link.

3. Compile the source code. If the compiler has an option to produce a symbol table for a debugger, enabling it will prove very handy later. The `.MIS` subroutines should compile uneventfully; the `.MDS` subroutines may still have additional bugs. Debug any new errors and comment any changes for future reference. *Successful compilation is no guarantee of successful linking or successful execution.*

4. Upon completion of (3), archive the object modules using the supplied shell scripts to form the main library. If building the library exhausts the usable memory, subdivide the libraries into smaller, more manageable units or place all the object modules in one subdirectory and do without a library.

5. Upon completion of (4), build the 15 executable links using the supplied makefiles. Libraries containing certain intrinsic functions, or those supporting the VMS extensions, may have to be explicitly included in the link statement. Any unresolved cross-references among the subroutines will appear as errors here. Debug any new errors and comment the changes for future reference. *Successful compilation and linking are no guarantee of successful execution.*

6. Upon completion of (5), begin running the sample problems using the supplied shell scripts. Sample problems `D01000A.NID` and `D01001A.NID` are tests of LINK1, a good, simple initial test. At this stage, bugs will be more difficult to run down. The system debugging utility could prove invaluable here; however, there is one caveat: NASTRAN is so large that it may overload the symbol tables used by the debugger, giving incorrect error diagnoses. You then must resort to using strategically placed `WRITE` statements to debug.

7. After an error in a particular link is located, the following is a convenient way to test the fix. Initially, it is not necessary to rebuild the library; instead, the subroutine containing the prospective fix can be inserted directly into the link statement. Generate the appropriate makefile for the link being debugged based on the `makelink1` model supplied. Insert the debugged subroutine after `$(BLKDAT)` and before `$(LIB)`. *Linking is order dependent.* Regenerate the new executable link from this makefile. The fix can be tested by either rerunning the NASTRAN program from the beginning (LINK1) or having

saved the FORTRAN I/O files at the successful termination of the previous link, rerunning only the repaired link. If all is well, the library can then be rebuilt and all the links regenerated from the updated library.

Iterate through steps (6) and (7) until all of the sample problems run properly.

Implications for COSMIC

As it becomes easier to port NASTRAN to a wide variety of platforms, COSMIC is forced to deal with several difficult issues. The first of these issues is the question of how many versions of NASTRAN COSMIC should officially support. The present four versions could be drastically multiplied if COSMIC were to provide an official version for each of the hardware manufacturers that desires a port. One proprietary version of NASTRAN supports 15 different manufacturers, and some manufacturers require more than one version. This would be an intolerable burden for COSMIC and UNISYS. COSMIC's position is that only the current four versions will be supported, leaving the users, hardware manufacturers, and third-party software companies responsible for porting NASTRAN to other platforms.

This leads to the second issue. Once these new ports of NASTRAN have been accomplished, how does COSMIC control their quality? No one wants to see a situation where any number of people can make available new ports of NASTRAN and sell them without having some provision for quality control. The suggestion of the NASTRAN Advisory Group has been for COSMIC and UNISYS to work on an expanded suite of demonstration and validation problems. Only after a company certified that their port successfully passes this expanded suite would the company be allowed to advertise their port of NASTRAN. This is probably the best solution for now, but the policy might have to adjust over time.

Conclusions

The development of powerful desktop computers, both workstations and personal computers, combined with the UNIX version of NASTRAN has turned the dream of desktop NASTRAN into a reality. Enterprising users can do the port themselves, and third-party software companies will undoubtedly provide NASTRAN on a wide variety of computers. This development is a tribute to the original designers of NASTRAN, who provided such a robust program structure. This could well be the beginning of a new era of NASTRAN use, with the potential to provide an even better product, arising from the synergies of interaction between COSMIC and the new, expanded user community.

Acknowledgment

This paper presents research results carried out in part at the Jet Propulsion Laboratory, California Institute of Technology, under contract with the National Aeronautics and Space Administration (NASA).

N91-20510

MODELING OF CONNECTIONS BETWEEN SUBSTRUCTURES

Thomas G. Butler
BUTLER ANALYSES

The focus of this paper is on joints that are only partially connected such as slip joints in bridges and in ship superstructures or sliding of a grooved structure onto the rails of a mating structure as shown in the sketch.

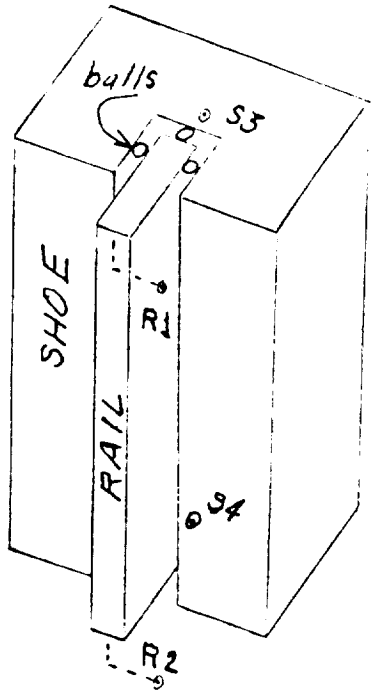

In substructure analysis it is desireable to organize each substructure so as to be self contained for purposes of validity checking. If part of the check is to embrace a connection, then all of the elements of the interface that it sees in

its mate should be included within its model. In the case of the groove/rail structure, shown above, it will enhance the checking if the rail points, to which the shoe points will connect, are duplicated in the substructure with the shoe. Thus a complete job of checking out the shoe substrucure can be done in Phase 1 with statics and eigenvalues and not protract the checking procedure of basic substructures into Phase 2.

To implement such a scheme, referring to the sketch, points R1 & R2 are included in the shoe model. The connection from S3 to R1 and from S4 to R2 are made in Phase 1 and now become available for complete chekout of the shoe substructure, including its mating with the rail. To make this example general, postulate that the planes through the four points are not parallel to the coordinate planes. In effect there are offsets. Generally, one likes to plan to avoid having out-of-plane offsets, butexigencies do crop up which forces the analyst to face up to such realities. Often such interface connections involve MPC's or elastic ties. In any case a requirement of Substructure Analysis is that points that are to be connected in Phase 2 must be available in Phase 2; i.e. they cannot be condensed out or constrained out in Phase 1. Therefore, if an MPC is used, the connecting points must be the independent degrees of freedom in the MPC relationship.

The needs of this joint are that there will be no relative translation in either transverse direction and no relative rotation about the long axis of the rail. In terms of the indicated coordinate system, translations in x and z directions must be constrained together and rotations about y must be constrained together. Just a pair of connecting points will be used herein to carry on the discussion. A sketch will be used to

assist in the discussion of making the connection by means of multi-point constraints.

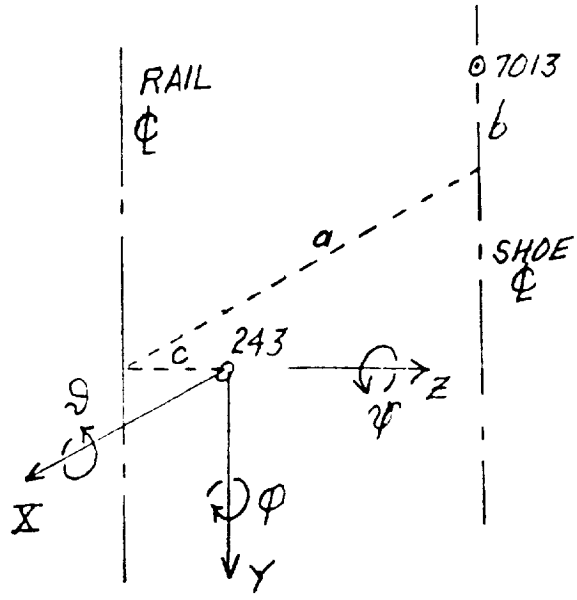

Include rail point 243 in the Shoe Model. When Phase 2 COMBINE operation is invoked, NASTRAN will recognize that rail 243 = shoe 243. As remarked above, since point 243 is going to be commanded to connect in Phase 2, it must therefore be an active available point for joining; and must therefore be an independent point in an MPC relationship. Now following the needs of this joint, constrain point 7013(X,Z,Φ) to 243(X,Z,Φ). The constraint equations for translations in X and Z are:

$$7013(X) = 243(X) - c \times 243(\Phi) + b \times 243(\Psi)$$
$$7013(Z) = 243(Z) + a \times 243(\Phi) - b \times 243(\Theta).$$

But 243(Ψ) and 243(Θ) are rail rotations which are not sensed by the shoe. If 243(4,6) are included in the shoe model they would be independent shoe rotations which will engage in the MPC relationship but would have no elastic path out to other parts of

the shoe. Thus, if nominal mass were added to these rail points to keep the eigenvalue matrix from being singular, an eigenvalue check for rigid body modes would show the shoe model to fail. One might argue, why not leave the rotations in until they are connected during COMBINE, then they are no longer disjoint. I cannot afford to leave the 243(4,6) rotations in the shoe model, because after connecting with the rail these rail rotations must not be transmitted back to the shoe. Moments in the shoe/rail configuration about the two transverse axes are produced only by couples of forces not by local rotational bending. This rules out the use of MPC's during Phase 1 in this case. There are other cases of connections between substructures in which MPC's in Phase 1 would work. The case in which there were no transverse offsets would work. A NASTRAN run of a simple model demonstrates these results in Appendix A.

The alternative is to make a stiff elastic connection, but not so stiff as to cause matrix ill-conditioning. If a bar instead of elastic scalars is used, it will be modeled so as to be fully connected in all 6 degrees of freedom at the shoe end, but only partially connected at the rail end. At the rail end it must allow for sliding along the rail and not transmit rotations to the shoe about the rail transverse axes. This implies that pin flags must be used at the rail and to inhibit these freedoms.

This stiff bar connection can be implemented the wrong way or the right way. One gets trapped into modeling the wrong way by forgetting that pin flags are applied to bar coordinates not to the displacement coordinates. I fell into this trap and will show you what happens. Then I will follow it up with the correct way to model it.

BAR CONNECTION

WRONG WAY

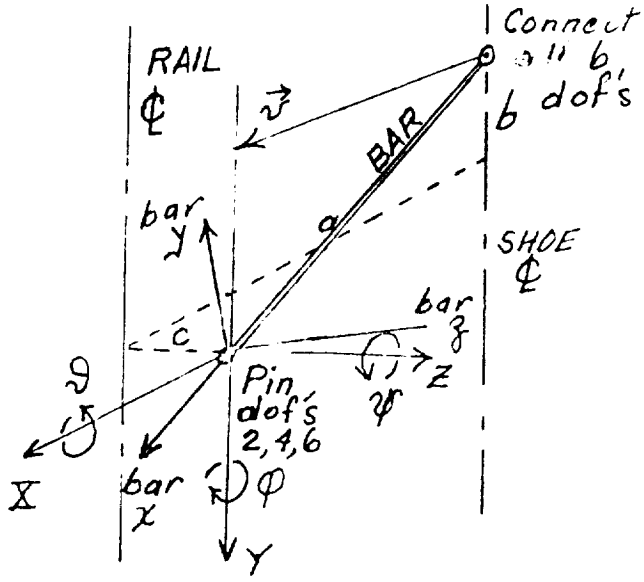

Include the rail grid points in the shoe model and apply SPC's at the GRID level in d.o.f.'s 2,4,6. Connect the shoe point to the rail point with a stiff bar. Note that the connection from shoe GP to rail GP produces bar coordinates that are skewed with respect to the displacement coordinates. Thus when bar element coordinate 2 is pinned, a component of force still develops at the rail end of the bar in the Y displacement coordinate direction, and so the eigenvalue check for rigid body modes fails once again. The listing in Appendix B of a simple model, incorporating this wrong approach, shows the constraint forces in the rigid body modes in freedoms T1, R1, & R3 to be non-negligible. Then the elastic mode shows large constraint forces in these freedoms.

BAR CONNECTION

RIGHT WAY

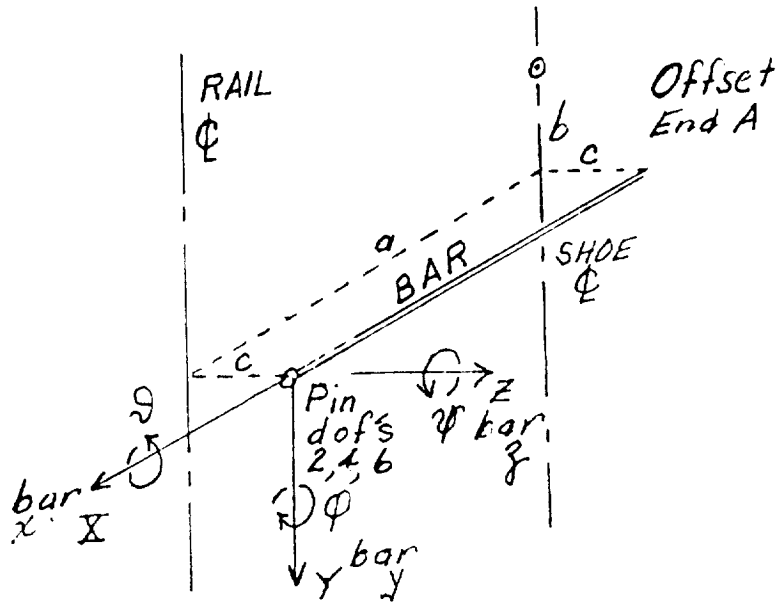

Offset the bar at the shoe end so as to terminate the bar at the rail end so as to be perpendicular to all displacement coordinates at the rail end. This connection passes the eigenvalue check for rigid body modes. Appendix C is a listing of a simple demonstration problem of the joint modeled the right way. Note that the constraint forces in freedoms T2, R1, & R3 are negligible in rigid body modes as well as in elastic modes.

CONCLUSIONS

This paper has demonstrated that complete checkout of a basic substructure can be done under the special circumstances of a sliding connection with offsets. Stiff bar connections make this possible so long as the bar coordinates are aligned with the displacement coordinates at the sliding surface.

APPENDIX A
RUN WITH MPC CONNECTION

```
                ID   OFFSET,CONNECT
                APP  DISP
                SOL  3,0
                DIAG  8,21,22
                TIME  10
                CEND
FREE-BODY MODAL STUDY OF SHOE/RAIL CONNECTIONS WITH MPC'S      JANUARY  30, 1991   UAI/NASTRAN VERSION 11.1A       PAGE     2
ALIGNED WITH OFFSETS. RAIL END INDEPENDENT.
```

C A S E C O N T R O L P A C K E T E C H O

```
TITLE = FREE-BODY MODAL STUDY OF SHOE/RAIL CONNECTIONS WITH MPC'S
SUBTITLE = ALIGNED WITH OFFSETS. RAIL END INDEPENDENT.
OUTPUT
   DISP = ALL
   ELFORCES = ALL
$   SPCFORCES = ALL
SUBCASE 1
   LABEL = ALL 6 DOF'S RETAINED ON BOTH ENDS.
   MPC = 20
   METHOD = 3
BEGIN BULK
```

S O R T E D B U L K D A T A E C H O

SORTED COUNT	....1...	....2...	....3...	....4...	....5...	....6...	....7...	....8...	....9...	...10...
1-	CBAR	1	1	71	72	1.0	1.0	0.0		SHOE
2-	CMASS2	132	0.1	13	2					31Y
3-	CMASS2	142	0.1	14	2					14Y
4-	CMASS2	715	0.1	71	5					71PHI
5-	CMASS2	725	0.1	72	5					72PHI
6-	EIGR	3	INV	0.0	10.0	8	8	6	1.-3	+ALLMODE
7-	+ALLMODE	MAX								
8-	GRID	13	0	3.0	2.0	2.0	0			RAIL1PT
9-	GRID	14	0	3.0	17.0	2.0	0			RAIL2PT
10-	GRID	71	0	0.0	0.0	0.0	0			SHOE1PT
11-	GRID	72	0	0.0	15.0	0.0	0			SHOE2PT
12-	MAT1	1	3.+7		0.28	2.4-4				
13-	MPC	20	71	1	1.0	13	1	-1.0		+UP1BAR
14-	+UP1BAR		13	5	2.0	13	6	-2.0		
15-	MPC	20	71	3	1.0	13	3	-1.0		+UP3BAR
16-	+UP3BAR		13	4	2.0	13	5	-3.0		
17-	MPC	20	71	5	1.0	13	5	-1.0		+UP5BAR
18-	MPC	20	72	1	1.0	14	1	-1.0		+LO1BAR
19-	+LO1BAR		14	5	2.0	14	6	-2.0		
20-	MPC	20	72	3	1.0	14	3	-1.0		+LO3BAR
21-	+LO3BAR		14	4	2.0	14	5	-3.0		
22-	MPC	20	72	5	1.0	14	5	-1.0		+LO5BAR
23-	PARAM	COUPMASS	7							
24-	PBAR	1	1	1.0	1.0	1.0	1.0			
25-	PBAR	2	1	100.0	100.0	100.0	100.0			
	ENDDATA									

R E A L E I G E N V A L U E S

MODE NO.	EXTRACTION ORDER	EIGENVALUE	RADIAN FREQUENCY	CYCLIC FREQUENCY	GENERALIZED MASS	GENERALIZED STIFFNESS
1	3	0.000000E+00	0.000000E+00	0.000000E+00	1.521215E-03	0.000000E+00
2	4	0.000000E+00	0.000000E+00	0.000000E+00	4.247887E-03	0.000000E+00
3	5	0.000000E+00	0.000000E+00	0.000000E+00	1.607912E-03	0.000000E+00
4	6	0.000000E+00	0.000000E+00	0.000000E+00	2.451029E-03	0.000000E+00
5	7	0.000000E+00	0.000000E+00	0.000000E+00	1.061112E-03	0.000000E+00
6	9	0.000000E+00	0.000000E+00	0.000000E+00	1.012346E-01	0.000000E+00
7	1	9.563905E-12	3.092556E-06	4.921956E-07	4.928215E-02	4.713298E-13
8	2	1.161892E-08	1.077911E-04	1.715549E-05	3.912935E-03	4.546408E-11
9	8	1.562500E+07	3.952847E+03	6.291152E+02	2.222214E-02	3.472210E+05

MODE NUMBER = 1 FREQUENCY = 0.000000E+00 HZ. EIGENVALUE = 0.000000E+00

R E A L E I G E N V E C T O R N O . 1

POINT ID.	TYPE	T1	T2	T3	R1	R2	R3
13	GRID	4.885226E-01	-3.069099E-02	1.000000E+00	0.0	2.000755E-02	0.0
14	GRID	-1.334166E-03	-3.410552E-03	-6.272650E-01	0.0	2.000755E-02	0.0
71	GRID	4.485075E-01	1.761184E-01	1.060023E+00	-1.084843E-01	2.000755E-02	3.265712E-02
72	GRID	-4.134927E-02	1.761184E-01	-5.672423E-01	-1.084843E-01	2.000755E-02	3.265712E-02

MODE NUMBER = 2 FREQUENCY = 0.000000E+00 HZ. EIGENVALUE = 0.000000E+00

R E A L E I G E N V E C T O R N O . 2

POINT ID.	TYPE	T1	T2	T3	R1	R2	R3
13	GRID	-6.913960E-02	3.166597E-02	1.000000E+00	0.0	-1.377827E-01	0.0
14	GRID	-3.550368E-01	3.518357E-03	9.440481E-02	0.0	-1.377827E-01	0.0
71	GRID	2.064258E-01	5.781769E-04	5.866519E-01	-6.037301E-02	-1.377827E-01	1.905981E-02
72	GRID	-7.947137E-02	5.781769E-04	-3.189434E-01	-6.037301E-02	-1.377827E-01	1.905981E-02

MODE NUMBER = 3 FREQUENCY = 0.000000E+00 HZ. EIGENVALUE = 0.000000E+00

R E A L E I G E N V E C T O R N O . 3

POINT ID.	TYPE	T1	T2	T3	R1	R2	R3
13	GRID	8.612644E-01	-1.069826E-02	-3.312686E-01	0.0	-2.891179E-03	0.0
14	GRID	-5.001400E-01	-1.188542E-03	1.000000E+00	0.0	-2.891179E-03	0.0
71	GRID	8.670468E-01	4.258756E-03	-3.399421E-01	8.875124E-02	-2.891179E-03	9.076030E-02
72	GRID	-4.943576E-01	4.258756E-03	9.913265E-01	8.875124E-02	-2.891179E-03	9.076030E-02

MODE NUMBER = 4 FREQUENCY = 0.000000E+00 HZ. EIGENVALUE = 0.000000E+00

REAL EIGENVECTOR NO. 4

POINT ID.	TYPE	T1	T2	T3	R1	R2	R3
13	GRID	1.000000E+00	3.279515E-03	-5.439819E-01	0.0	-1.890255E-03	0.0
14	GRID	-6.589970E-02	3.642190E-04	-6.497411E-01	0.0	-1.890255E-03	0.0
71	GRID	1.003780E+00	-1.787680E-03	-5.496526E-01	-7.050612E-03	-1.890255E-03	7.105998E-02
72	GRID	-6.211919E-02	-1.787680E-03	-6.554118E-01	-7.050612E-03	-1.890255E-03	7.105998E-02

MODE NUMBER = 5 FREQUENCY = 0.000000E+00 HZ. EIGENVALUE = 0.000000E+00

REAL EIGENVECTOR NO. 5

POINT ID.	TYPE	T1	T2	T3	R1	R2	R3
13	GRID	-2.679756E-01	-4.753040E-03	-7.319843E-02	0.0	-3.266693E-03	0.0
14	GRID	1.000000E+00	-5.290496E-04	2.902177E-01	0.0	-3.266693E-03	0.0
71	GRID	-2.614422E-01	2.310795E-03	-8.299851E-02	2.422774E-02	-3.266693E-03	-8.453170E-02
72	GRID	1.006533E+00	2.310795E-03	2.804176E-01	2.422774E-02	-3.266693E-03	-8.453170E-02

MODE NUMBER = 6 FREQUENCY = 0.000000E+00 HZ. EIGENVALUE = 0.000000E+00

REAL EIGENVECTOR NO. 6

POINT ID.	TYPE	T1	T2	T3	R1	R2	R3
13	GRID	-1.127395E-05	-1.111122E-01	2.954264E-05	0.0	-8.683184E-07	0.0
14	GRID	9.360020E-05	1.000000E+00	-1.109201E-05	0.0	1.072533E-06	0.0
71	GRID	-9.537311E-06	-4.564906E-07	2.693768E-05	-2.320808E-06	-8.683184E-07	-6.732830E-06
72	GRID	9.145513E-05	-4.564906E-07	-7.874410E-06	-2.320804E-06	1.072533E-06	-6.732828E-06

MODE NUMBER = 7 FREQUENCY = 4.921956E-07 HZ. EIGENVALUE = 9.563905E-12

REAL EIGENVECTOR NO. 7

POINT ID.	TYPE	T1	T2	T3	R1	R2	R3
13	GRID	1.000000E+00	6.632150E-01	7.963101E-01	0.0	1.036273E-01	0.0
14	GRID	2.864973E-01	7.369055E-02	-3.282914E-01	0.0	1.036273E-01	0.0
71	GRID	7.927454E-01	2.984467E-01	1.107192E+00	-7.497343E-02	1.036273E-01	4.756685E-02
72	GRID	7.924265E-02	2.984467E-01	-1.740939E-02	-7.497343E-02	1.036273E-01	4.756685E-02

MODE NUMBER = 8 FREQUENCY = 1.715549E-05 HZ. EIGENVALUE = 1.161892E-08

R E A L E I G E N V E C T O R N O . 8

POINT ID.	TYPE	T1	T2	T3	R1	R2	R3
13	GRID	-2.487581E-01	-1.668238E-03	-4.699167E-01	0.0	-1.139360E-02	0.0
14	GRID	-9.521336E-03	-1.851357E-04	2.772007E-01	0.0	-1.139360E-02	0.0
71	GRID	-2.259709E-01	1.000000E+00	-5.040975E-01	4.980783E-02	-1.139360E-02	-1.594912E-02
72	GRID	1.326586E-02	1.000000E+00	2.430200E-01	4.980783E-02	-1.139360E-02	-1.594912E-02

MODE NUMBER = 9 FREQUENCY = 6.291152E+02 HZ. EIGENVALUE = 1.562500E+07

R E A L E I G E N V E C T O R N O . 9

POINT ID.	TYPE	T1	T2	T3	R1	R2	R3
13	GRID	-6.666663E-01	7.100735E-08	1.000000E+00	0.0	-3.333327E-01	0.0
14	GRID	6.666647E-01	-6.390596E-07	-9.999965E-01	0.0	3.333327E-01	0.0
71	GRID	-7.944661E-07	-1.626112E-10	1.744123E-06	-7.029677E-07	-3.333327E-01	-3.188153E-07
72	GRID	-7.893768E-07	1.631945E-10	1.717579E-06	6.817177E-07	3.333327E-01	3.147009E-07

APPENDIX B
RUN WITH WRONG BAR CONNECTION

G R I D P O I N T S I N G U L A R I T Y T A B L E SPC 0 MPC 0

POINT ID.	SINGULARITY TYPE	LIST OF COORDINATE COMBINATIONS THAT WILL REMOVE SINGULARITY ORDER	STRONGEST COMBINATION	WEAKER COMBINATION	WEAKEST COMBINATIO
71	G	1	5	4	
72	G	1	5	4	

6 ROOTS BELOW 1.973921E+01

E I G E N V A L U E A N A L Y S I S S U M M A R Y (INVERSE POWER METHOD)

NUMBER OF EIGENVALUES EXTRACTED		7
NUMBER OF STARTING POINTS USED		1
NUMBER OF STARTING POINT MOVES		0
NUMBER OF TRIANGULAR DECOMPOSITIONS		1
TOTAL NUMBER OF VECTOR ITERATIONS		34
REASON FOR TERMINATION		7*
LARGEST OFF-DIAGONAL MODAL MASS TERM	0.13E-06	
MODE PAIR		6
		4
NUMBER OF OFF-DIAGONAL MODAL MASS TERMS FAILING CRITERION	0	

(* 1 OR MORE ROOT OUTSIDE FR.RANGE.
SEE NASTRAN U.M. SECTION 2.3.3)

R E A L E I G E N V A L U E S

MODE NO.	EIGENVALUE	CYCLIC FREQUENCY	GENERALIZED MASS	GENERALIZED STIFFNESS

****
*
*
* NASTRAN INFORMATION MESSAGE 3308, LOWEST EIGENVALUE FOUND *
* AS INDICATED BY THE STURM'S SEQUENCE OF THE DYNAMIC MATRIX *
*
* (THIS MESSAGE CAN BE SUPPRESSED BY DIAG 37) *
****

1	-7.963921E-08	4.491420E-05	2.016630E-01	-1.606029E-08
2	2.852769E-08	2.688150E-05	1.250841E-01	3.568360E-09
3	9.751177E-08	4.969911E-05	1.946527E-01	1.898093E-08
4	1.989545E-07	7.098997E-05	1.088651E-01	2.165920E-08
5	2.305249E-07	7.641507E-05	2.362906E-01	5.447087E-08
6	3.321909E-07	9.173054E-05	1.223466E-01	4.064244E-08
7	7.002442E+06	4.211578E+02	1.515952E-01	1.061536E+06

```
    ID   OFFSET,CONNECT
    APP  DISP
    SOL  3,0
    DIAG  8,21,22
    TIME  10
    CEND
FREE-BODY MODAL STUDY OF SHOE/RAIL CONNECTIONS WITH BARS JAN 20,1991 PAGE  2
     WRONG WAY WITH CONNECTOR BAR SKEWED TO RAIL.

C A S E    C O N T R O L    D E C K    E C H O

TITLE = FREE-BODY MODAL STUDY OF SHOE/RAIL CONNECTIONS WITH BARS
SUBTITLE = WRONG WAY WITH CONNECTOR BAR SKEWED TO RAIL.WANT 3 RB MODES.
OUTPUT
DISP = ALL
MPCFORCES = ALL
ELFORCES = ALL
SPCFORCES = ALL
SUBCASE 1
LABEL = BARS PINNED AT RAIL END. NO OFFSETS AT SHOE END.
METHOD = 3
BEGIN BULK
          S O R T E D    B U L K    D A T A    E C H O

---1--- +++2+++ ---3--- +++4+++ ---5--- +++6+++ ---7--- +++8+++ ---9--- +++10+++
CBAR     1        1        71       72       1.0      1.0      0.0               SHOE
CBAR     2        2        71       13       14                                 +TIE UP
+TIE UP          246
CBAR     3        2        72       14       13                                 +TIE DWN
+TIE DWN         246
CMASS2   131      0.1      13       4                                           31THETA
CMASS2   141      0.1      14       4                                           14THETA
CMASS2   711      0.1      71       4                                           71THETA
CMASS2   712      0.1      71       5                                           71PHI
CMASS2   721      0.1      72       4                                           72THETA
CMASS2   722      0.1      72       5                                           72PHI
EIGR     3        INV      0.0      1.0      6        6        3        1.-3     +ALLMODE
+ALLMODEMAX
GRID     13       0        3.0      2.0      2.0      0        246               RAIL1PT
GRID     14       0        3.0      17.0     2.0      0        246               RAIL1PT
GRID     71       0        0.0      0.0      0.0      0                          SHOE1PT
GRID     72       0        0.0      15.0     0.0      0                          SHOE1PT
MAT1     1        3.+7              0.28     2.4-4
PARAM    COUPMASS7
PBAR     1        1        1.0      1.0      1.0      1.0
PBAR     2        1        100.0    100.0    100.0    100.0
ENDDATA
```

SUBCASE 1 EIGENVALUE = -7.963921E-08

R E A L E I G E N V E C T O R N O . 1

PT	ID.	T1	T2	T3	R1	R2	R3
13		3.308091E-01	0.0	5.615981E-01	0.0	9.189782E-02	0.0
14		-6.346744E-01	0.0	-9.552183E-01	0.0	9.189782E-02	0.0
71		3.910763E-01	-5.288029E-01	1.000000E+00	-1.011211E-01	6.503133E-02	6.436E-2
72		-5.744071E-01	-5.288029E-01	-5.168163E-01	-1.011211E-01	6.503133E-02	6.436E-2

EIGENVALUE = 2.852769E-08 R E A L E I G E N V E C T O R N O . 2

PT	ID.	T1	T2	T3	R1	R2	R3
1		-1.806720E-01	0.0	3.554041E-01	0.0	-1.205854E-01	0.0
14		-7.829153E-01	0.0	1.000000E+00	0.0	-1.205854E-01	0.0
71		1.403818E-01	-1.730800E-01	4.690333E-02	4.297306E-02	-8.839797E-02	4.015E-2
72		-4.618614E-01	-1.730800E-01	6.914992E-01	4.297306E-02	-8.839797E-02	4.015E-2

EIGENVALUE = 9.751177E-08 R E A L E I G E N V E C T O R N O . 3

PT	ID.	T1	T2	T3	R1	R2	R3
13		-7.289532E-01	0.0	2.853720E-01	0.0	-1.817658E-01	0.0
14		3.520157E-01	0.0	2.345846E-01	0.0	-1.817658E-01	0.0
71		-8.096893E-02	-6.163144E-01	-7.029006E-02	-3.385834E-03	-2.055022E-01	-7.2E-3
72		1.000000E+00	-6.163144E-01	-1.210776E-01	-3.385834E-03	-2.055022E-01	-7.2E-3

EIGENVALUE = 1.989545E-07 R E A L E I G E N V E C T O R N O . 4

PT	ID.	T1	T2	T3	R1	R2	R3
13		3.177751E-01	0.0	1.764639E-02	0.0	-3.180602E-01	0.0
14		-4.354112E-01	0.0	3.301453E-01	0.0	-3.180602E-01	0.0
71		1.000000E+00	-9.989289E-02	-9.057981E-01	2.083326E-02	-2.929949E-01	5.02E-2
72		2.468137E-01	-9.989289E-02	-5.932992E-01	2.083326E-02	-2.929949E-01	5.02E-2

EIGENVALUE = 2.305249E-07 R E A L E I G E N V E C T O R N O . 5

PT	ID.	T1	T2	T3	R1	R2	R3
13		9.812109E-01	0.0	1.000000E+00	0.0	-1.272332E-02	0.0
14		8.707730E-01	0.0	5.573768E-01	0.0	-1.272332E-02	0.0
71		7.983168E-01	4.514050E-01	8.229362E-01	-2.950821E-02	-2.407710E-02	7.363E-3
72		6.878789E-01	4.514050E-01	3.803130E-01	-2.950821E-02	-2.407710E-02	7.363E-3

EIGENVALUE = 3.321909E-07 R E A L E I G E N V E C T O R N O . 6

PT	ID.	T1	T2	T3	R1	R2	R3
13		-7.600989E-01	0.0	1.000000E+00	0.0	-3.662173E-01	0.0
14		-3.776701E-01	0.0	3.752712E-01	0.0	-3.662173E-01	0.0
71		-1.461953E-01	2.568173E-01	-1.776728E-01	-4.164859E-02	-3.932845E-01	-2.6E-
72		2.362335E-01	2.568173E-01	-8.024015E-01	-4.164859E-02	-3.932845E-01	-2.6E-

EIGENVALUE = 7.002442E+06 R E A L E I G E N V E C T O R N O . 7

PT	ID.	T1	T2	T3	R1	R2	R3
13		-6.670417E-01	0.0	1.000000E+00	0.0	-6.548009E-01	0.0
14		5.839078E-01	0.0	-8.773038E-01	0.0	5.701413E-01	0.0
71		6.416196E-01	1.446323E-03	-9.644380E-01	2.011386E-01	-5.263158E-01	1.14E-1
72		-5.595077E-01	7.309780E-03	8.305104E-01	5.448166E-02	6.091975E-01	4.62E-2

EIGENVALUE = -7.963921E-08 FORCES OF SINGLE-POINT CONSTRAINT

PT ID.	T1	T2	T3	R1	R2	R3
13	0.0	2.806213E+01	0.0	-2.590351E+01	0.0	-1.726900E+01
14	0.0	-1.530662E+01	0.0	-4.709728E+00	0.0	-3.139819E+00

EIGENVALUE = 2.852769E-08 FORCES OF SINGLE-POINT CONSTRAINT

PT ID.	T1	T2	T3	R1	R2	R3
13	0.0	2.551103E+00	0.0	1.177432E+00	0.0	7.849547E-01
14	0.0	-2.551103E+00	0.0	-1.118560E+01	0.0	-7.457070E+00

EIGENVALUE = 9.751177E-08 FORCES OF SINGLE-POINT CONSTRAINT

PT ID.	T1	T2	T3	R1	R2	R3
13	0.0	-1.275551E+00	0.0	1.876532E+00	0.0	1.251022E+00
14	0.0	5.102206E+00	0.0	1.103843E-01	0.0	7.358950E-02

EIGENVALUE = 1.989545E-07 FORCES OF SINGLE-POINT CONSTRAINT

PT ID.	T1	T2	T3	R1	R2	R3
13	0.0	9.566635E-01	0.0	3.017170E+00	0.0	2.011446E+00
14	0.0	-5.102206E+00	0.0	4.121012E+00	0.0	2.747341E+00

EIGENVALUE = 2.305249E-07 FORCES OF SINGLE-POINT CONSTRAINT

PT ID.	T1	T2	T3	R1	R2	R3
13	0.0	1.020441E+01	0.0	1.964840E+01	0.0	1.309893E+01
14	0.0	2.793968E-09	0.0	-5.077676E+00	0.0	-3.385117E+00

EIGENVALUE = 3.321909E-07 FORCES OF SINGLE-POINT CONSTRAINT

PT ID.	T1	T2	T3	R1	R2	R3
13	0.0	-2.551103E+00	0.0	-3.532296E+01	0.0	-2.354864E+01
14	0.0	-2.551103E+00	0.0	-1.236304E+01	0.0	-8.242024E+00

EIGENVALUE = 7.002442E+06 FORCES OF SINGLE-POINT CONSTRAINT

PT ID.	T1	T2	T3	R1	R2	R3
13	0.0	-3.846585E+01	0.0	-2.479790E+04	0.0	-1.653193E+04
14	0.0	-1.149591E+02	0.0	2.221343E+04	0.0	1.480896E+04

APPENDIX C
RUN WITH RIGHT BAR CONNECTION

```
                    ID   OFFSET,CONNECT
                    APP  DISP
                    SOL  3,0
                    DIAG  8,21,22
                    TIME  10
                    CEND
FREE-BODY MODAL STUDY OF SHOE/RAIL CONNECTIONS WITH BARS       PAGE     2
RIGHT WAY WITH CONNECTOR BAR NORMAL TO RAIL.
```

C A S E C O N T R O L P A C K E T E C H O

```
                    TITLE = FREE-BODY MODAL STUDY OF SHOE/RAIL CONNECTIONS WITH BARS
                    SUBTITLE = RIGHT WAY WITH CONNECTOR BAR NORMAL TO RAIL.
                    OUTPUT
                       DISP = ALL
                       ELFORCES = ALL
                       SPCFORCES = ALL
                    SUBCASE 1
                       LABEL = BARS PINNED AT RAIL END. OFFSETS AT SHOE END.
                       METHOD = 3
                    BEGIN BULK
```

S O R T E D B U L K D A T A E C H O

```
SORTED
COUNT       ....1... ....2... ....3... ....4... ....5... ....6... ....7... ....8... ....9... ...10...
   1-       CBAR     1        1        71       72       1.0      1.0      0.0                SHOE
   2-       CBAR     2        2        71       13       1.0      1.0      0.0                +TIE UP
   3-       +TIE UP           246      0.0      2.0      2.0
   4-       CBAR     3        2        72       14       1.0      1.0      0.0                +TIE DWN
   5-       +TIE DWN          246      0.0      2.0      2.0
   6-       CMASS2   131      0.1      13       4                                            31THETA
   7-       CMASS2   141      0.1      14       4                                            14THETA
   8-       CMASS2   711      0.1      71       4                                            71THETA
   9-       CMASS2   712      0.1      71       5                                            71PHI
  10-       CMASS2   721      0.1      72       4                                            72THETA
  11-       CMASS2   722      0.1      72       5                                            72PHI
  12-       EIGR     3        INV      0.0      10.0     6        6        3        1.-3     +ALLMODE
  13-       +ALLMODE MAX
  14-       GRID     13       0        3.0      2.0      2.0      0        246               RAIL1PT
  15-       GRID     14       0        3.0      17.0     2.0      0        246               RAIL1PT
  16-       GRID     71       0        0.0      0.0      0.0      0                          SHOE1PT
  17-       GRID     72       0        0.0      15.0     0.0      0                          SHOE1PT
  18-       MAT1     1        3.+7              0.28     2.4-4
  19-       PARAM    COUPMASS 7
  20-       PBAR     1        1        1.0      1.0      1.0      1.0
  21-       PBAR     2        1        100.0    100.0    100.0    100.0
            ENDDATA
```

R E A L E I G E N V A L U E S

MODE NO.	EXTRACTION ORDER	EIGENVALUE	RADIAN FREQUENCY	CYCLIC FREQUENCY	GENERALIZED MASS	GENERALIZED STIFFNESS
1	2	-8.597651E-07	9.272352E-04	1.475741E-04	8.360698E-02	-7.188236E-08
2	3	-3.708519E-07	6.089761E-04	9.692155E-05	7.466593E-02	-2.769000E-08
3	1	5.746691E-08	2.397226E-04	3.815303E-05	1.415073E-01	8.131985E-09
4	4	1.050890E-07	3.241743E-04	5.159394E-05	1.495328E-01	1.571424E-08
5	5	1.103310E-07	3.321611E-04	5.286507E-05	2.399001E-01	2.646841E-08
6	6	3.483668E-07	5.902261E-04	9.393740E-05	1.215011E-01	4.232696E-08

MODE NUMBER = 1 FREQUENCY = 1.475741E-04 HZ. EIGENVALUE = -8.597651E-07

R E A L E I G E N V E C T O R N O . 1

POINT ID.	TYPE	T1	T2	T3	R1	R2	R3
13	GRID	-2.433693E-04	0.0	9.871816E-01	0.0	-3.738998E-01	0.0
14	GRID	-4.052280E-01	0.0	1.000000E+00	0.0	-3.738998E-01	0.0
71	GRID	8.015541E-01	4.693623E-03	-1.362268E-01	8.545591E-04	-3.738998E-01	2.699898E-02
72	GRID	3.965695E-01	4.693623E-03	-1.234084E-01	8.545591E-04	-3.738998E-01	2.699898E-02

MODE NUMBER = 2 FREQUENCY = 9.692155E-05 HZ. EIGENVALUE = -3.708519E-07

R E A L E I G E N V E C T O R N O . 2

POINT ID.	TYPE	T1	T2	T3	R1	R2	R3
13	GRID	7.450739E-02	0.0	9.888168E-02	0.0	2.797289E-01	0.0
14	GRID	-5.090036E-01	0.0	-3.656060E-01	0.0	2.797289E-01	0.0
71	GRID	-4.071489E-01	1.079729E-01	1.000000E+00	-3.096585E-02	2.797289E-01	3.890074E-02
72	GRID	-9.906599E-01	1.079729E-01	5.355123E-01	-3.096585E-02	2.797289E-01	3.890074E-02

MODE NUMBER = 3 FREQUENCY = 3.815303E-05 HZ. EIGENVALUE = 5.746691E-08

R E A L E I G E N V E C T O R N O . 3

POINT ID.	TYPE	T1	T2	T3	R1	R2	R3
13	GRID	2.404255E-01	0.0	2.897290E-01	0.0	1.577857E-01	0.0
14	GRID	6.952828E-01	0.0	5.630910E-01	0.0	1.577857E-01	0.0
71	GRID	-1.357936E-01	-3.387907E-01	7.266380E-01	1.822414E-02	1.577857E-01	-3.032382E-02
72	GRID	3.190636E-01	-3.387907E-01	1.000000E+00	1.822414E-02	1.577857E-01	-3.032382E-02

MODE NUMBER = 4 FREQUENCY = 5.159394E-05 HZ. EIGENVALUE = 1.050890E-07

R E A L E I G E N V E C T O R N O . 4

POINT ID.	TYPE	T1	T2	T3	R1	R2	R3
13	GRID	8.741319E-01	0.0	-1.770641E-01	0.0	-3.227559E-02	0.0
14	GRID	4.142550E-01	0.0	3.377019E-01	0.0	-3.227559E-02	0.0
71	GRID	1.000000E+00	7.083516E-01	-3.425264E-01	3.431774E-02	-3.227559E-02	3.065846E-02
72	GRID	5.401231E-01	7.083516E-01	1.722396E-01	3.431774E-02	-3.227559E-02	3.065846E-02

BARS PINNED AT RAIL END. OFFSETS AT SHOE END. SUBCASE 1

MODE NUMBER = 5 FREQUENCY = 5.286507E-05 HZ. EIGENVALUE = 1.103310E-07

R E A L E I G E N V E C T O R N O . 5

POINT ID.	TYPE	T1	T2	T3	R1	R2	R3
13	GRID	-9.356353E-01	0.0	1.000000E+00	0.0	-1.059662E-01	0.0
14	GRID	9.272855E-01	0.0	-2.696967E-01	0.0	-1.059662E-01	0.0
71	GRID	-9.720924E-01	5.534579E-01	8.513944E-01	-8.464644E-02	-1.059662E-01	-1.241947E-01
72	GRID	8.908284E-01	5.534579E-01	-4.183022E-01	-8.464644E-02	-1.059662E-01	-1.241947E-01

MODE NUMBER = 6 FREQUENCY = 9.393740E-05 HZ. EIGENVALUE = 3.483668E-07

R E A L E I G E N V E C T O R N O . 6

POINT ID.	TYPE	T1	T2	T3	R1	R2	R3
13	GRID	7.174048E-01	0.0	6.860800E-01	0.0	-9.937754E-02	0.0
14	GRID	8.860417E-02	0.0	-6.589323E-01	0.0	-9.937754E-02	0.0
71	GRID	1.000000E+00	-4.786835E-01	5.672824E-01	-8.966749E-02	-9.937754E-02	4.192004E-02
72	GRID	3.711993E-01	-4.786835E-01	-7.777300E-01	-8.966749E-02	-9.937754E-02	4.192004E-02

MODE NUMBER = 1 FREQUENCY = 1.475741E-04 HZ. EIGENVALUE = -8.597651E-07

F O R C E S O F S I N G L E - P O I N T C O N S T R A I N T

POINT ID.	TYPE	T1	T2	T3	R1	R2	R3
13	GRID	0.0	-4.023161E-10	0.0	0.0	0.0	2.413897E-09

MODE NUMBER = 2 FREQUENCY = 9.692155E-05 HZ. EIGENVALUE = -3.708519E-07

F O R C E S O F S I N G L E - P O I N T C O N S T R A I N T

POINT ID.	TYPE	T1	T2	T3	R1	R2	R3
13	GRID	0.0	-5.796661E-10	0.0	0.0	0.0	3.477997E-09

MODE NUMBER = 3 FREQUENCY = 3.815303E-05 HZ. EIGENVALUE = 5.746691E-08

F O R C E S O F S I N G L E - P O I N T C O N S T R A I N T

POINT ID.	TYPE	T1	T2	T3	R1	R2	R3
13	GRID	0.0	4.518601E-10	0.0	0.0	0.0	-2.711161E-09

BARS PINNED AT RAIL END. OFFSETS AT SHOE END. SUBCASE 1

MODE NUMBER = 4 FREQUENCY = 5.159394E-05 HZ. EIGENVALUE = 1.050890E-07

F O R C E S O F S I N G L E - P O I N T C O N S T R A I N T

POINT ID.	TYPE	T1	T2	T3	R1	R2	R3
13	GRID	0.0	-4.568466E-10	0.0	0.0	0.0	2.741080E-09

MODE NUMBER = 5 FREQUENCY = 5.286507E-05 HZ. EIGENVALUE = 1.103310E-07

F O R C E S O F S I N G L E - P O I N T C O N S T R A I N T

POINT ID.	TYPE	T1	T2	T3	R1	R2	R3
13	GRID	0.0	1.850646E-09	0.0	0.0	0.0	-1.110387E-08

MODE NUMBER = 6 FREQUENCY = 9.393740E-05 HZ. EIGENVALUE = 3.483668E-07

F O R C E S O F S I N G L E - P O I N T C O N S T R A I N T

POINT ID.	TYPE	T1	T2	T3	R1	R2	R3
13	GRID	0.0	-6.246573E-10	0.0	0.0	0.0	3.747944E-09

N91-20511

MODELING A BALL SCREW/BALL NUT IN SUBSTRUCTURING

Thomas G. Butler
BUTLER ANALYSES

INTRODUCTION

A ball screw/ball nut mechanism causes one part to move with respect to another with a minimum of friction. Such a structure is a good candidate for substructuring by assigning the mating parts to two separate substructures. Figure 1 shows a cut-away photograph of an assembled nut and screw. Matching helical grooves in each share a continuous stream of steel balls which are fed by the screw in the direction of travel through the nut to a conduit that returns the balls to the trailing end for continuous, smooth, quiet operation.

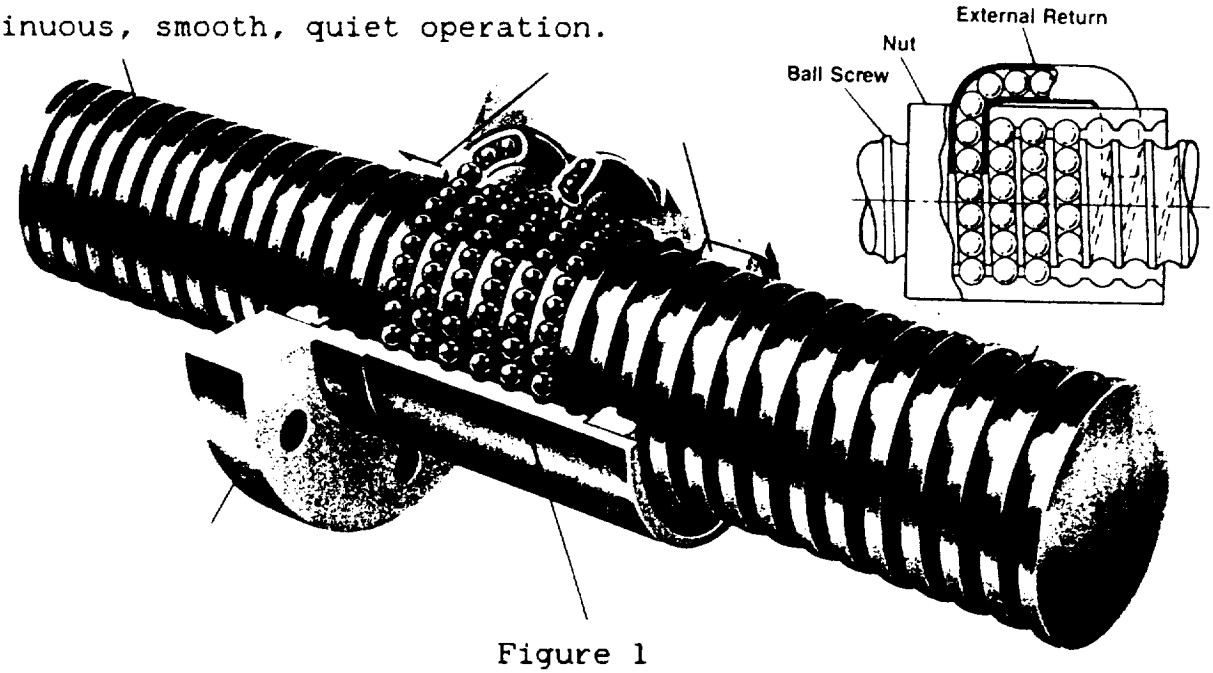

Figure 1

Making a finite element model of this device and coordinating the nut in one substructure with the screw in another substructure is not straightforward. I made several stabs at this before I was satisfied, and decided to share the toils of this challenge at the NASTRAN Colloquium.

BALL SCREW/BALL NUT

PLAN

In the particular application being discussed here, the screw was attached to the moving structure and the nut was attached to the stationery structure. The object of the overall analysis was to determine the vibration characteristics of the whole structure for various configurations; i.e. the evaluation of the mode shapes and frequencies when parts were moved to different mating positions. Therefore, it was necessary to provide for the ball screw to be moved and reconnected to the ball nut at a number of differenct locations along its length. The Substructure capability in NASTRAN makes it possible to prescribe a connection with a COMBINE operation in Phase 2 and perform an eigenvalue analysis for that configuration. Once these results are catalogued, the analyst erases these results and returns to the COMBINE operation for a new set of connections and performs a second eigenvalue analysis. Succeeding runs can be made for as many repositionings as is desired. The challenge is in modeling the nut so as to represent both the rigid body relation of the helix plus the elastic relations of its members. The scheme then is to model the nut and the screw so as to be invariant for any combination of positions, such that repositioning is achieved by specifying that location on the screw that is to be in contact with the nut in the Phase 2 COMBINE step.

MODEL

The first step is to represent the elastic parts in a simple arrangement. The NUT will consist of two yokes at either end of the nut and an axial tie between the two yokes. The yoke models the nut housing that connects the ball interface to the stationary structure (P). The yoke consistS of two bars extending on either side of the screw (S) centroid to the bolts in P. The sketch shows this simple arrangement.

BALL SCREW/BALL NUT

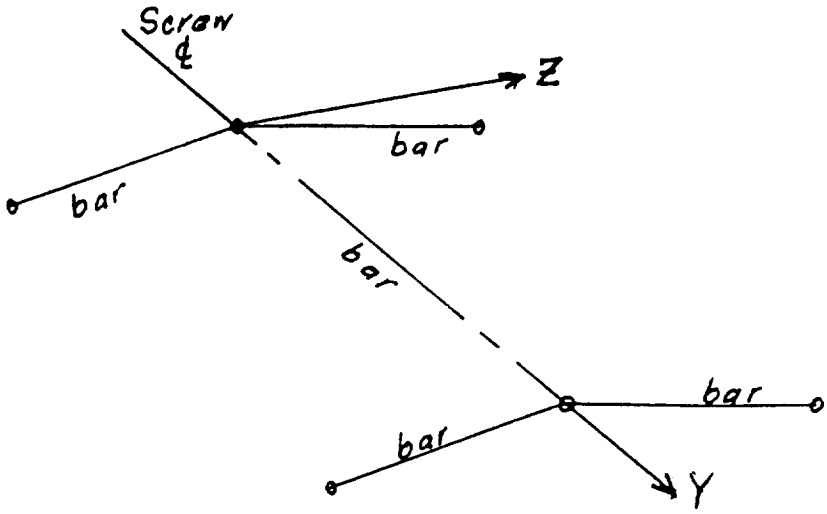

So far this is pretty boring. It will liven things up to introduce the rotation of the screw vs. the translation of the screw. There will be a string of grid points along the screw - available for connecting to the nut. The nut has 2 grid points on line with the screw centroid. But these 2 grid points serve only the elastic function so far. In order to get load into the nut it needs to be endowed with some rather special things.

When the screw turns it will cause the <u>screw</u> to advance axially only as a result of its helix reacting the nut. So a device is used to cause the screw rotation to advance the <u>nut</u> axially. This does not happen in reality, but it is a device to provide a loading rate from screw into the nut. The specifications for the ball nut/screw is one inch of advance for one full rotation of the screw; i.e. one inch per 2π radians. This can be imposed with an MPC (Multi - Point - Constraint). Relating this to the sketch, a unit translation in the Y coordinate direction of the nut is constrained to 2π (6.2832) radians of rotation about the Y axis of the screw. But now that the nut is loaded with this displacement, it must be transformed into an elastic force which will be reacted into structure P and then back into an axial force in the screw. In effect what

needs to be accomplished is to take a rotation of the screw and give it to the nut to intercede then deliver a translation back into the screw. Just saying it, however, doesn't accomplish it, because a number of needs of subsctructure analysis need to be served.

The nut has to be self contained, if it is to be able to be repositioned without having to be remodeled each time. One way is to duplicate a point in the nut to represent the axial rotation of the screw. Then duplicate another point to represent the axial translation of the same point of the screw. Now the helix constraint of the screw via the two special points of the nut can be enacted with the MPC. It operates to connect the translation of the helix elastically into the nut drive point with a spring value equal to the compressibility of the set of balls plus the stiffness of the lands of the helix. This rotation of the screw causes the nut drive point to move axially. Finally, the nut drive point axial translation connects back to the screw axial translation, when the substructures are COMBINE'd.

SUBSTRUCTURE COMMANDS

So far this discussion has been confined to a word description, but more hurdles have to be overcome in finally translating this scheme to problem data. A return to the sketch will be helpful by embellishing it with the screw and assigning numbers to the points. Point 2 of the NUT will connect translational dof's only in to point 10 of the SCREW and similarly point 5 of the NUT will connect translational dof's only to point 11 of the SCREW. However, GP's 2 & 5 will maintain all 6 dof's operational in order to support the link of the yokes to the stationary structure P. As a first step toward incorporating the helical action into the NUT, 2 new pairs of points are introduced.

BALL SCREW/BALL NUT

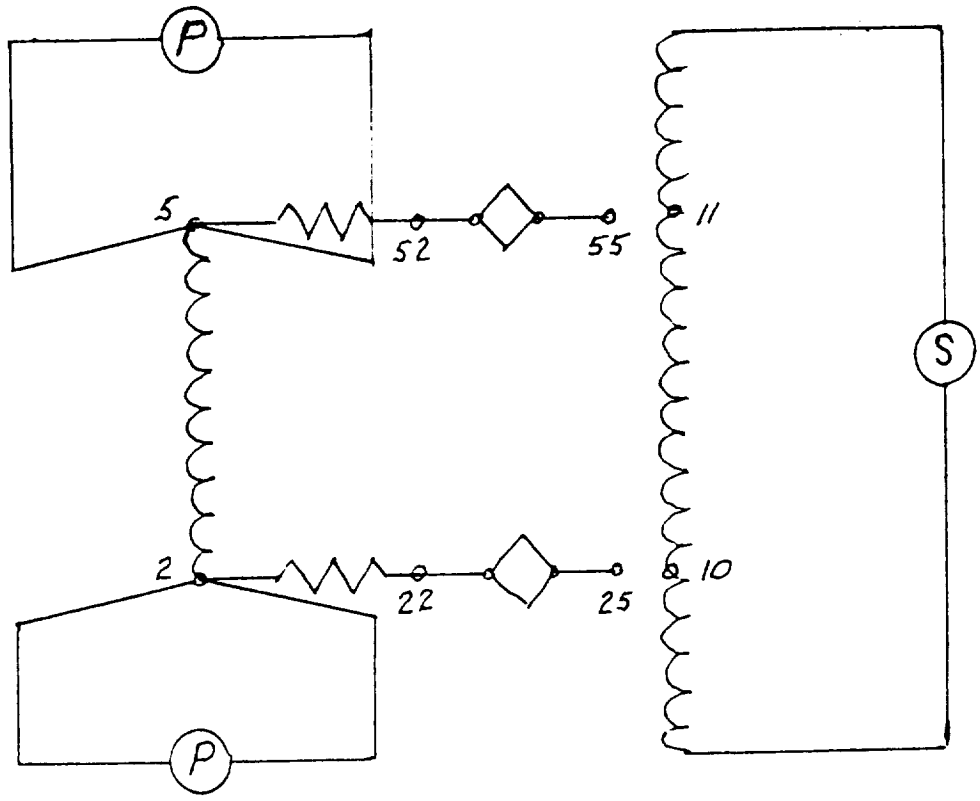

Points 25 & 55 are added to pick up the rotations of SCREW points 10 & 11. Only rotations about the Y axis will be enabled in GP's 25 & 55 by eliminating dof's 1, 2, 3, 4, & 6 on the GRID bulk card. The pair of points 22 & 52 are inserted to have translational freedom in the Y direction only by eliminating dof's 1, 3, 4, 5, & 6 on the GRID bulk card. The helix is put in place with MPC's between 25(5) and 22(2) and between 55(5) and 52(2) by applying a factor of 2π i.e.

MPC	ID#	22	2	-1.0	25	5	6.2832
MPC	ID#	52	2	-1.0	55	5	6.2832.

Note that GP's 25 & 55 are retained as independent. This is done in order for them to be extant when NUT and SCREW are COMBINE'd later.

All is ready for the introduction of scalar springs between GP 22(2) and GP2(2) and between GP52(2) and GP5(2) to

represent the drive resistance between SCREW and NUT which is carried into the stationary structure by the bars connecting 2 & 5 to GP's 1, 2, 4, & 6. The translational response of NUT drive points 2 and 5 are ready for connecting back to the SCREW in a COMBINE operation.

Now a word about Phase 2 COMBINE operations. If the automatic option for COMBINE is chosen, it finds all dof's at the same physical location and ties all like colocated dof's together unless otherwise inhibited. The substructure control packet will command that substructure P be COMBINE'd with substructrure S. In this case the set of GP's 2, 10, 22, & 25 and the set of GP's 5, 11, 52, & 55 are colocated. It is well to pause to tabulate what the requirements are and what action is needed to implement these desires.

1. Requirements

GP 2(1,2,3) should tie to GP 10(1,2,3)

Gp 5(1,2,3) should tie to GP 11(1,2,3).

Remedy

Note is taken that all 6 dof's are active at both points. In order to limit the tie to only translations, the substructure bulk data card called RELES is employed to command the release of dof's 4, 5, & 6 during a COMBINE operation.

2. Requirements

GP 25(5) should tie to GP 10(5).

GP 55(5) should tie to GP 11(5).

Remedy

Since GP's 25 & 55 have only dof 5 active and since the requirement is to tie them to dof 5 of GP's 10 & 11 respectively, there is no need to intercede. Allow the automatic option to proceed unhindered.

3. Requirements

GP 22(2) & 52(2) should not tie to any part of substructure S.

Remedy

Impose a RELES on GP 22(2) & 52(2) to keep them free of any influence from substructure S.

SUMMARY

The action which will ensue from this model is as follows. NUT point GP 25(5) will pick up the rotation from SCREW POINT GP 10(5). The MPC will advance the translation of NUT point GP 22(2) from the rotation of GP 25(5) in the ratio of 1 : 2π. The translation of GP 22(2) will be opposed by the elastic link to the NUT drive point GP 2(2). This helical loading will be carried to the NUT housing bars and reacted into the stationary substructure P. The net translation in all 3 coordinate directions of NUT drive point GP 2 will be tied directly into the 3 translationals of SCREW substructure drive point 10. A parallel set of actions will also take place between GP's SCREW 11 to NUT 55 to 52 to 5 to SCREW 11. This completes the logic.

As a mathematician would say: "This is a pathological case", in that such an elaborate device would not have had to be resorted to for modeling a ball nut, if it were not for the special requirement of having to reposition the NUT with respect to the SCREW. The repositioning requirement demanded that the NUT be self-contained so as to be independent of the relative locations. Thus, in order to be self-contained, the NUT in effect picked up the duties of the helical advancement from the SCREW and carried them out internally in a highly artificial manner in order to transmit the reaction into the parent structure before handing back the results of the helical advancement to the SCREW. As a bonus, this modeling left the analyst free to reposition the NUT at will along the SCREW merely by specifying the coordinate transformation in moving the SCREW to a new position and by specifying new GRID POINT numbers on the RELES cards.

This paper has shown an achievement of a simple set of operating conditions to an otherwise complicated modeling task.

N91-20512

NASTRAN GPWG TABLES FOR COMBINED SUBSTRUCTURES

Tom Allen
McDonnell Douglas Space Systems Co.
Huntsville Alabama

ABSTRACT

A method for computing the mass and center of gravity for basic and combined substructures stored on the NASTRAN Substructure Operating File (SOF) is described. The three step method recovers SOF data blocks for the relevant substructure, processes these data blocks using a specially developed FORTRAN routine, and generates the NASTRAN gridpoint weight generator (GPWG) table for the substructure in a PHASE2 SOF execution using a Direct Matrix Abstraction Program (DMAP) sequence. Verification data for the process is also provided in this report.

1.0 INTRODUCTION

Once a basic substructure has been put on the Substructure Operating File, the ability to obtain the mass and center of gravity (cg) of the basic substructure or any combined substructure of which it is part is lost in a normal NASTRAN execution. The user is unable to verify the mass and cg of the subsequent combined substructures nor is he able to attest to the quality of the PHASE1 reductions performed on his models. The method described here allows the user to obtain the mass and cg of any substructure that is stored on the SOF and to recover them in the form of the customary GPWG tabular format.

The three step method that is used to obtain the mass and cg of the substructures is described in the next section. Verification of the process is provided after the method description.

2.0 METHODOLOGY

The method used to obtain the GPWG table of a substructure is divided into three steps. The first step is the recovery of the SOF data blocks BGSS, EQSS, and CSTM for the substructure of interest. The second step reformats these data blocks into standard NASTRAN input bulk data. During the third step, the user executes a DMAP sequence

that uses the bulk data from the second step to define the geometry, and the stored mass matrix to calculate the GPWG table. Each of these three steps will be described below.

2.1 Step 1 - Data Block Recovery

Step 1 of the process involves obtaining the SOF data blocks BGSS, EQSS, and CSTM for the substructure of interest from the SOF. The PHASE2 substructure control deck required for this operation is shown in Figure 1. The data is taken from the SOF and written to NASTRAN file FORT17. Sample records for each of the three data blocks are provided in Figure 2.

2.2 Step 2 - Defining Input Bulk Data

Step 2 takes the data blocks recovered from Step 1 and converts them into standard NASTRAN Bulk Data that is used to define the geometry of the model. The SOF data blocks will be described below. The bulk data that is created from the data blocks will also be defined.

2.2.1 BGSS Data Block Description

The BGSS data block contains the location in the basic coordinate system of each internal point in the substructure as well as the output coordinate system of the internal point. If the output coordinate system is -1, the internal point is a scalar point rather than a physical gridpoint of the substructure. The BGSS data are converted to GRID or SCALAR bulk data cards that define the substructure geometry.

2.2.2 EQSS Data Block Description

The EQSS data block contains data that describe the degrees of freedom (DOF) that are associated with each internal point of the substructure. The data is binary coded data that is stored in an integer variable. The on/off sequence of the bit sequence tells NASTRAN the DOF that are retained for that point. For example, the integer value 7 has a bit sequence of 111000 which indicates that DOF 123 were retained and DOF 456 were removed during the PHASE1 execution. The EQSS data are converted to DMI bulk data cards that are used to merge the reduced mass matrix stored on the SOF to a full sized mass matrix in the DMAP sequence.

2.2.3 CSTM Data Block Description

The CSTM data block contains the transformation matrix for each of the output coordinate systems in the substructure. These data are used to make CORD2R bulk data cards so that the correct coordinate transformations are performed inside the GPWG Module.

At the end of Step 2, the user has created a set of NASTRAN bulk data. A sample set of input bulk data is shown in Figure 3.

2.3 Step 3 - Calculate Mass and CG

Step 3 of the process uses a DMAP sequence in conjunction with the bulk data that was created in Step 2 to obtain the GPWG table. The DMAP sequence that is used to calculate the GPWG table is shown in Figure 4. Verification of the method is provided in the next section.

3.0 VERIFICATION

Three test cases were executed to verify the method. The first case uses a simple beam element model that contains no MPC, SPC, or OMIT cards. The second case is a complex combined substructure that comprises 16 basic substructures. The third case uses a Craig-Bampton modally reduced model of the second case. The data provided for these cases demonstrate the validity of the method. Each of the example problems will be discussed below.

Figure 5 shows the simple beam element model that was used for the first test case. The GPWG table from the 'straight' execution (non-substructuring) is shown in Table 1. Table 2 is the GPWG table of the substructure model. The data contained in these tables are identical.

The second case used a combined substructure (pseudo-structure in NASTRAN parlance) made up of 16 basic substructures. The mass and cg of the combined substructure calculated using PHASE1 GPWG data taken from each of the basic substructures is provided in Table 3. The GPWG table of the combined pseudostructure is provided in Table 4. Any discrepancies between these data can be attributed to changes introduced by the SPC, MPC, and Guyan reductions performed during the PHASE1 executions of the individual basic substructures.

The final test case used a Craig-Bampton modally reduced model of the second test case. The GPWG table for this execution is provided in Table 5. A comparison of the data in this table with that in Table 4 shows good agreement between the two models, the only large discrepancy being in the x direction. The discrepancy in the x direction can be attributed to the addition of extra x mass to the Craig-Bampton model. Discrepancies in the y and z directions can be attributed to the Craig-Bampton modal reduction.

The three test cases discussed above show good agreement with expected results. Hence, the method is considered verified.

4.0 CONCLUSION

A method for obtaining PHASE2 Grid Point Weight Generator tables of substructures stored on the Substructure Operating File has been described. Data from several test executions were provided. These data verify the method.

ACRONYMS AND ABBREVIATIONS

cg	Center of gravity
DMAP	Direct Matrix Abstraction Program
DOF	Degree(s) of freedom
GPWG	Gridpoint Weight Generator
SOF	Substructure Operating File
NASTRAN	NASA Structural Analysis program

```
SUBSTRUCTURE PHASE2
PASSWORD = password
SOF(1) = FTxx
SOFOUT(EXTERNAL) FORT17, DISK
  POSITION = REWIND
     NAMES = model id
     ITEMS = BGSS
SOFOUT(EXTERNAL) FORT17, DISK
  POSITION = NOREWIND
     NAMES = model id
     ITEMS = EQSS
SOFOUT(EXTERNAL) FORT17, DISK
  POSITION = NOREWIND
     NAMES = model id
     ITEMS = CSTM
```

FIGURE 1. NASTRAN PHASE2 DECK FOR RECOVERY OF SOF DATA BLOCKS

```
DIT                2       2       1       2
FULL
MDI                10      6       1       3
      0       0       0       0       0       0
FULL    BGSS       3       3       1       2
FULL          5
FULL    BGSS       6      20       1       3
      10 0.000000E+00 0.000000E+00 0.000000E+00      10 1.000000E+01 0.000000E+00 0.000000E+00
      10 2.000000E+01 0.000000E+00 0.000000E+00      10 5.000000E+00 1.000000E+01 0.000000E+00
      10 1.500000E+01 1.000000E+01 0.000000E+00
DIT                2       2       1       2
FULL
MDI                10      6       1       3
      0       0       0       0       0       0
FULL    EQSS       3       6       1       2
FULL          1       5FULL
FULL    EQSS       10      15      1       2
      1       1      63       2       2      63       3       3      63       4       4      63       5       5      63
FULL    EQSS       10      10      1       3
      1      63       7      63      13      63      19      63      25      63
DIT                2       2       1       2
FULL
MDI                10      6       1       3
      0       0       0       0       0       0
FULL    CSTM       3       2       1       2
FULL
FULL    CSTM       8       4       1       1
     10       1 0.000000E+00 0.000000E+00
FULL    CSTM       9      10       1       1
 0.000000E+00 1.000000E+00 0.000000E+00 0.000000E+00 0.000000E+00 1.000000E+00 0.000000E+00 0.000000E+00 0.000000E+00 1.000000E+00
FULL    CSTM       9       0       1       2
FULL    CSTM       0       0       1       3
&EOF
&EOF
```

FIGURE 2. DATA BLOCKS BGSS, EQSS, AND CSTM FOR TEST CASE 1

S O R T E D   B U L K   D A T A   E C H O

```
CARD
COUNT       .   1  ..   2  ..   3  ..   4  ..   5  ..   6  ..   7  ..   8  ..   9  ..  10  .

   1-       DMI     CP      0       2       1       1               30      1
   2-       DMI     CP      1       1       1.0     1.0     1.0     1.0     1.0
   3-       +DMI    11.0    1.0     1.0     1.0     1.0     1.0     1.0     1.0     +DMI    1
   4-       +DMI    21.0    1.0     1.0     1.0     1.0     1.0     1.0     1.0     +DMI    2
   5-       +DMI    31.0    1.0     1.0     1.0     1.0     1.0     1.0     1.0     +DMI    3
   6-       +DMI    41.0                                                            +DMI    4
   7-       GRID    *1                              .00000          .00000          +DMI    5
   8-       *GRD    1        0.00000        0                                       *GRD    1
   9-       GRID    *2                              10.00000        .00000
  10-       *GRD    2        0.00000        0                                       *GRD    2
  11-       GRID    *3                              20.00000        .00000
  12-       *GRD    3        0.00000        0                                       *GRD    3
  13-       GRID    *4                              5.00000         10.00000
  14-       *GRD    4        0.00000        0                                       *GRD    4
  15-       GRID    *5                              15.00000        10.00000
  16-       *GRD    5        Q.00000        0                                       *GRD    5
            ENDDATA
```

FIGURE 3. SAMPLE INPUT BULK DATA

```
BEGIN     $
PARAM     //*ADD*/DRY/1/0  $
SOFI      /M1,,,,/DRY/*model id*/*MMTX*/  $
MERGE,    ,,,M1,CP,/MGG////  $
GP1       GEOM1,GEOM2,/GPL,EQEXIN,GPDT,CSTM,BGPDT,SIL/S,N,LUSET/
          NOGPDT/ALWAYS=-1  $
GPWG      BGPDT,CSTM,EQEXIN,MGG/OGPWG/V,Y,GRDPNT=0/C,Y,WTMASS  $
OFP       OGPWG,,,,//S,N,CARDNO  $
END       $
```

FIGURE 4. NASTRAN DMAP SEQUENCE

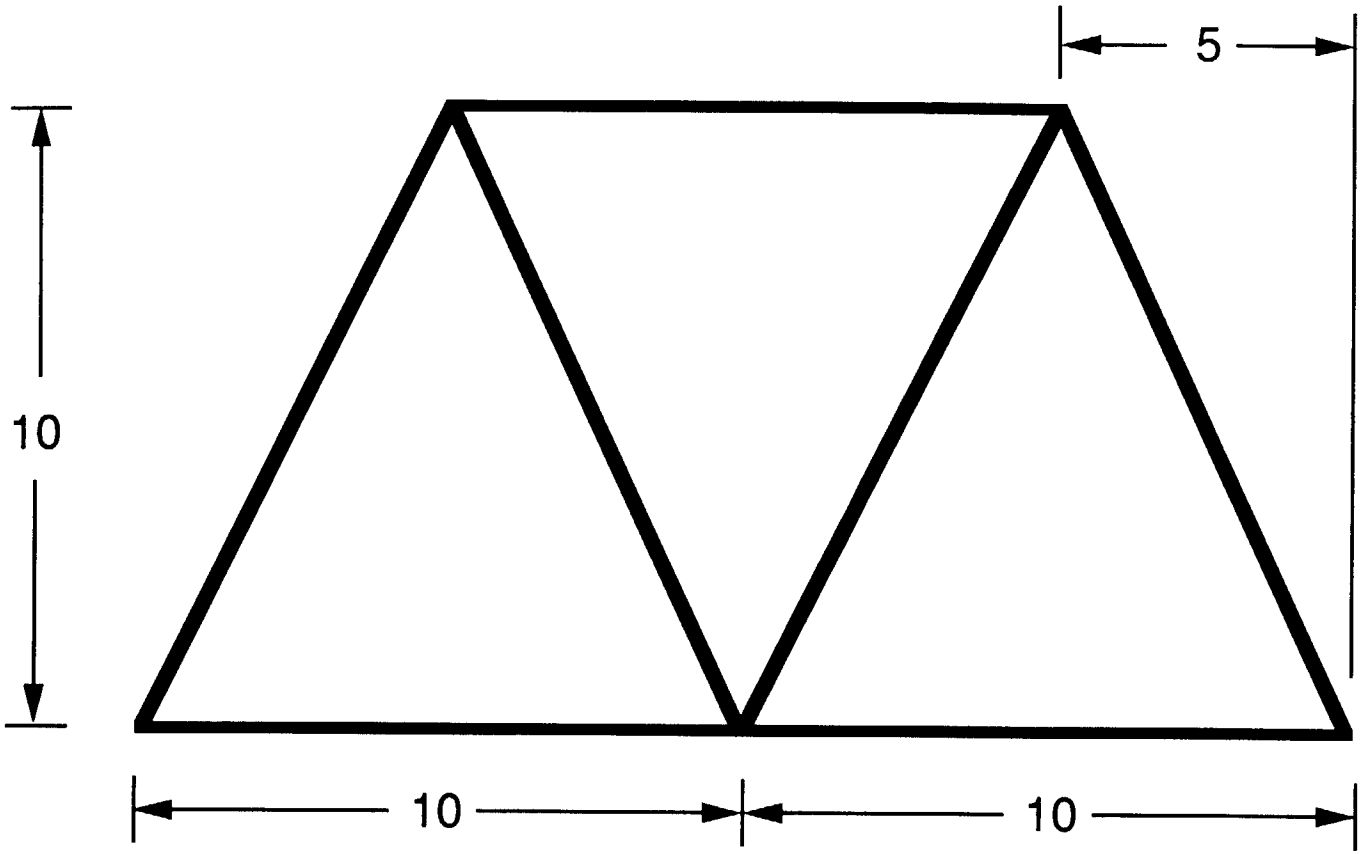

A = 1.0

ρ = 0.00259

FIGURE 5. SIMPLE BEAM MODEL FOR TEST CASE 1

TABLE 1. GPWG TABLE FOR TEST CASE 1 - STRAIGHT EXECUTION

O U T P U T F R O M G R I D P O I N T W E I G H T G E N E R A T O R

REFERENCE POINT = 0

MO - RIGID BODY MASS MATRIX IN BASIC COORDINATE SYSTEM

1.93528321E-01	0.00000000E+00	0.00000000E+00	0.00000000E+00	0.00000000E+00	-8.38141606E-01
0.00000000E+00	1.93528321E-01	0.00000000E+00	0.00000000E+00	0.00000000E+00	-1.93528321E+00
0.00000000E+00	0.00000000E+00	1.93528321E-01	8.38141606E-01	-1.93528321E+00	0.00000000E+00
0.00000000E+00	0.00000000E+00	8.38141606E-01	8.38141606E+00	-8.38141606E+00	0.00000000E+00
0.00000000E+00	0.00000000E+00	-1.93528321E+00	-8.38141606E+00	2.69338942E+01	0.00000000E+00
-8.38141606E-01	1.93528321E+00	0.00000000E+00	0.00000000E+00	0.00000000E+00	3.53153102E+01

S - TRANSFORMATION MATRIX FOR SCALAR MASS PARTITION

1.00000000E+00	0.00000000E+00	0.00000000E+00
0.00000000E+00	1.00000000E+00	0.00000000E+00
0.00000000E+00	0.00000000E+00	1.00000000E+00

DIRECTION MASS AXIS SYSTEM (S)	MASS	X-C.G.	Y-C.G.	Z-C.G.
X	1.935283212E-01	0.000000000E+00	4.330847293E+00	0.000000000E+00
Y	1.935283212E-01	1.000000000E+01	0.000000000E+00	0.000000000E+00
Z	1.935283212E-01	1.000000000E+01	4.330847293E+00	0.000000000E+00

I(S) - INERTIAS RELATIVE TO C.G.

4.751552755E+00	1.421085472E-14	0.000000000E+00
1.421085472E-14	7.581062046E+00	0.000000000E+00
0.000000000E+00	0.000000000E+00	1.233261480E+01

I(Q) - PRINCIPAL INERTIAS

4.751552755E+00		
	7.581062046E+00	
		1.233261480E+01

Q - TRANSFORMATION MATRIX - I(Q) = QT*I(S)*Q

1.000000000E+00	0.000000000E+00	0.000000000E+00
0.000000000E+00	1.000000000E+00	0.000000000E+00
0.000000000E+00	0.000000000E+00	1.000000000E+00

TABLE 2. GPWG TABLE FOR TEST CASE 1 - SUBSTRUCTURE EXECUTION

O U T P U T F R O M G R I D P O I N T W E I G H T G E N E R A T O R

REFERENCE POINT = 0

MO - RIGID BODY MASS MATRIX IN BASIC COORDINATE SYSTEM

1.93528321E-01	0.00000000E+00	0.00000000E+00	0.00000000E+00	0.00000000E+00	-8.38141606E-01
0.00000000E+00	1.93528321E-01	0.00000000E+00	0.00000000E+00	0.00000000E+00	1.93528321E+00
0.00000000E+00	0.00000000E+00	1.93528321E-01	8.38141606E-01	-1.93528321E+00	0.00000000E+00
0.00000000E+00	0.00000000E+00	8.38141606E-01	8.38141606E+00	-8.38141606E+00	0.00000000E+00
0.00000000E+00	0.00000000E+00	-1.93528321E+00	-8.38141606E+00	2.69338942E+01	0.00000000E+00
-8.38141606E-01	1.93528321E+00	0.00000000E+00	0.00000000E+00	0.00000000E+00	3.53153102E+01

S - TRANSFORMATION MATRIX FOR SCALAR MASS PARTITION

1.00000000E+00	0.00000000E+00	0.00000000E+00
0.00000000E+00	1.00000000E+00	0.00000000E+00
0.00000000E+00	0.00000000E+00	1.00000000E+00

DIRECTION MASS AXIS SYSTEM (S)	MASS	X-C.G.	Y-C.G.	Z-C.G.
X	1.935283212E-01	0.000000000E+00	4.330847293E+00	0.000000000E+00
Y	1.935283212E-01	1.000000000E+01	0.000000000E+00	0.000000000E+00
Z	1.935283212E-01	1.000000000E+01	4.330847293E+00	0.000000000E+00

I(S) - INERTIAS RELATIVE TO C.G.

4.751552755E+00	1.421085472E-14	0.000000000E+00
1.421085472E-14	7.581062046E+00	0.000000000E+00
0.000000000E+00	0.000000000E+00	1.233261480E+01

I(Q) - PRINCIPAL INERTIAS

4.751552755E+00		
	7.581062046E+00	
		1.233261480E+01

Q - TRANSFORMATION MATRIX - I(Q) = QT*I(S)*Q

1.000000000E+00	0.000000000E+00	0.000000000E+00
0.000000000E+00	1.000000000E+00	0.000000000E+00
0.000000000E+00	.0.000000000E+00	1.000000000E+00

TABLE 3. MASS AND SUMMARY FOR TEST CASE 2

Structure	Mass	X-C.G.	Y-C.G.	Z-C.G.
APAL	5.389	1141.125	-1.134	359.726
APLAT	6.728	1158.744	-1.805	410.715
ASTRUT	0.369	1160.547	-0.129	372.939
ATCS	0.886	959.030	-71.278	390.090
CPAC	1.276	1182.138	17.198	354.407
EU	0.562	1207.724	22.010	336.323
FPAL	5.805	1015.142	6.069	361.969
FPLAT	7.137	1047.601	13.446	406.102
FSTRUT	0.351	1042.066	0.142	372.978
IGLOO	3.808	947.519	0.263	358.548
ISOASSY	1.500	1180.181	-57.152	418.016
SPHERE1	0.147	984.000	-58.922	425.189
SPHERE2	0.147	984.000	58.922	425.189
SUSIM	0.751	1209.700	-71.200	391.600
TU	0.964	1208.029	-20.736	337.345
TOTAL	35.820	1085.615	-2.069	382.287

TABLE 4. GPWG TABLE FOR TEST CASE 2

O U T P U T F R O M G R I D P O I N T W E I G H T G E N E R A T O R

REFERENCE POINT = 0

MO - RIGID BODY MASS MATRIX IN BASIC COORDINATE SYSTEM

3.58097988E+01	-1.80881318E-07	2.63223649E-07	6.27762442E-05	1.36892055E+04	7.30915994E+01
-1.80881323E-07	3.58097995E+01	-3.14055231E-07	-1.36892058E+04	2.22413846E-04	3.88794590E+04
2.63223679E-07	-3.14055197E-07	3.56843584E+01	-7.42786562E+01	-3.87534840E+04	-3.20814805E-04
6.27762447E-05	-1.36892058E+04	-7.42786562E+01	5.34050882E+06	9.04648197E+04	-1.48764079E+07
1.36892055E+04	2.22413830E-04	-3.87534840E+04	9.04648197E+04	4.76251078E+07	3.07591410E+04
7.30915994E+01	3.88794590E+04	-3.20814868E-04	-1.48764079E+07	3.07591410E+04	4.25489537E+07

S - TRANSFORMATION MATRIX FOR SCALAR MASS PARTITION

1.00000000E+00	0.00000000E+00	0.00000000E+00
0.00000000E+00	1.00000000E+00	0.00000000E+00
0.00000000E+00	0.00000000E+00	1.00000000E+00

DIRECTION MASS AXIS SYSTEM (S)	MASS	X-C.G.	Y-C.G.	Z-C.G.
X	3.580979878E+01	1.753046550E-06	-2.041106120E+00	3.822754085E+02
Y	3.580979949E+01	1.085721215E+03	6.210977143E-06	3.822754093E+02
Z	3.568435836E+01	1.086007588E+03	-2.081546639E+00	-8.990348149E-06

I(S) - INERTIAS RELATIVE TO C.G.

1.073074696E+05	-9.797635452E+03	1.374675257E+04
-9.797635452E+03	3.054835813E+05	-2.818020008E+03
1.374675257E+04	-2.818020008E+03	3.365510838E+05

I(Q) - PRINCIPAL INERTIAS

1.060227511E+05		
	3.377348479E+05	
		3.055845357E+05

Q - TRANSFORMATION MATRIX - I(Q) = QT*I(S)*Q

-9.971039046E-01	-6.370888760E-02	4.153289213E-02
-4.814661098E-02	1.060602325E-01	-9.931934006E-01
5.887025853E-02	-9.923166857E-01	-1.088204390E-01

TABLE 5. GPWG TABLE FOR TEST CASE 3

OUTPUT FROM GRID POINT WEIGHT GENERATOR

REFERENCE POINT = 0

MO - RIGID BODY MASS MATRIX IN BASIC COORDINATE SYSTEM

3.61827734E+01	3.37269825E-07	7.36971850E-06	-1.24223283E-04	1.38187648E+04	7.30920865E+01
3.37269768E-07	3.58098030E+01	-3.31714290E-07	-1.36892061E+04	6.17809186E-04	3.88794605E+04
7.36971860E-06	-3.31714091E-07	3.56843560E+01	-7.42786658E+01	-3.87534782E+04	-3.08294358E-04
-1.24223268E-04	-1.36892061E+04	-7.42786658E+01	5.34050862E+06	9.04646580E+04	-1.48764072E+07
1.38187648E+04	6.17808982E-04	-3.87534782E+04	9.04646580E+04	4.76711615E+07	3.07595132E+04
7.30920865E+01	3.88794605E+04	-3.08294577E-04	-1.48764072E+07	3.07595132E+04	4.25502349E+07

S - TRANSFORMATION MATRIX FOR SCALAR MASS PARTITION

1.00000000E+00	0.00000000E+00	0.00000000E+00
0.00000000E+00	1.00000000E+00	0.00000000E+00
0.00000000E+00	0.00000000E+00	1.00000000E+00

DIRECTION MASS AXIS SYSTEM (S)	MASS	X-C.G.	Y-C.G.	Z-C.G.
X	3.618277342E+01	-3.433216173E-06	-2.020079712E+00	3.819155764E+02
Y	3.580980296E+01	1.085721151E+03	1.725251566E-05	3.822753812E+02
Z	3.568435601E+01	1.086007499E+03	-2.081547044E+00	-8.639482173E-06

I(S) - INERTIAS RELATIVE TO C.G.

1.073075349E+05	-9.797469966E+03	1.374666989E+04
-9.797469966E+03	3.069920234E+05	-2.844506799E+03
1.374666989E+04	-2.844506799E+03	3.378346633E+05

I(Q) - PRINCIPAL INERTIAS

1.060308852E+05		
	3.390214067E+05	
		3.070819296E+05

Q - TRANSFORMATION MATRIX - I(Q) = QT*I(S)*Q

-9.971403308E-01	-6.340796537E-02	4.111679123E-02
-4.778493476E-02	1.075110325E-01	-9.930548715E-01
5.854708022E-02	-9.921798264E-01	-1.102335320E-01

N91-20513

MODELING AN ELECTRIC MOTOR IN 1-D

Thomas G. Butler
BUTLER ANALYSES

INTRODUCTION

Quite often the dynamicist will be faced with having an electric drive motor as a link in the elastic path of a structure such that the motor's characteristics must be taken into account to properly represent the dynamics of the primary structure. He does not want to model it so accurately that he could get detailed stress and displacements in the motor proper, but just sufficiently to represnt its inertia loading and elastic behavior from its mounting bolts to its drive coupling. This paper describes how the rotor and stator of such a motor can be adequately modeled as a colinear pair of beams.

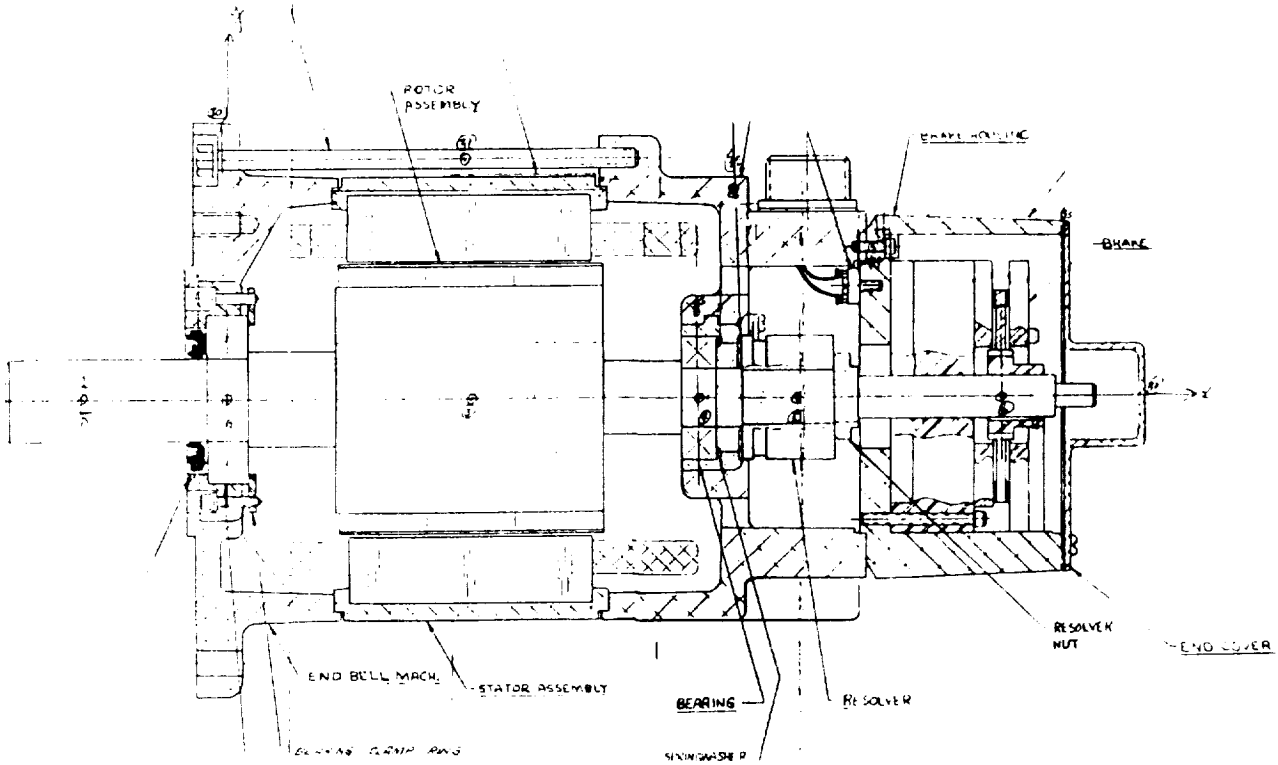

Figure 1

MODELING AN ELECTRIC MOTOR IN 1 - D

PLAN

Figure 1 shows an assembly drawing of a motor equipped with a disk brake. The application in which this motor was incorporated required that the brake be set; consequently, the electric coupling from the armature to the stator field was not modeled. The discussion of the modeling will be taken up in four parts: the rotor, the stator, the brake and the mount.

The overall scheme is to locate grid points at the bearings, at the concentrations of mass, at the brake, and at the mating interfaces. Six (6) grid points were assigned to the rotor and 8 grid points were assigned to the stator. See Table 1. Between the grid points the structure undergoes several changes of section. Each section is considered separately then the stiffness for an equivalent prismatic bar is computed for the sequence of sections between grid points.

One of the intriguing features about finite element analysis is that parts can occupy the same physical location yet can still remain disjoint. That feature will be employed here. The stator is concentric with the rotor so the centroid of the stator is coincident with the centroid of the rotor. Thus their individual beam models will be colinear.

EQUIVALENCE

An example of one equivalent bar will be developed for the rotor and another for the stator. The rotor between the bell housing and the armature center of gravity has 3 separate sections: the bearing journal, intermediate shaft and armature. The three sections are arrayed in line one after the other. This is an elastic series situation so equivalence is found by summing compliances (Z). The formulas for equivalent area and equivalent bending inertia are:

$$\frac{E\,A_{equiv}}{L_{total}} = \left(\sum Z_{area}\right)^{-1} = \left[\frac{L_1}{A_1\,E_1} + \frac{L_2}{A_2\,E_2} + \frac{L_3}{A_3\,E_3}\right]^{-1}.$$

Since the copper windings are surrounded by a preponderance of steel it is permissible to assume that the material in the armature can be represented as steel thus all E's are the same and the equivalent area becomes:

$$A_{equiv} = L_{total}\left[\left(\frac{L}{A}\right)_1 + \left(\frac{L}{A}\right)_2 + \left(\frac{L}{A}\right)_3\right]^{-1}$$

$$= 4.889\left[\frac{1}{\pi/4}\left(\frac{.389}{1.3785^2} + \frac{1.67}{2.25^2} + \frac{2.83}{3.831^2}\right)\right]^{-1} = 5.28$$

Similarly, the computation of the equivalent bending inertias proceeds with

$$\frac{E\,I_{equiv}}{L_{total}} = \left(\sum Z_I\right)^{-1} = \left[\frac{L_1}{E_1\,I_1} + \frac{L_2}{E_2\,I_2} + \frac{L_3}{E_3\,I_3}\right]^{-1}.$$

$$I_{equiv} = L_{total}\left[\left(\frac{L}{I}\right)_1 + \left(\frac{L}{I}\right)_2 + \left(\frac{L}{I}\right)_3\right]^{-1} =$$

$$= 4.889\left[\frac{1}{\pi/64}\left(\frac{.389}{1.3785^4} + \frac{1.670}{2.25^4} + \frac{2.83}{3.831^4}\right)\right]^{-1} = 1.29$$

$$J_{equiv} = 2\,I_{equiv}.$$

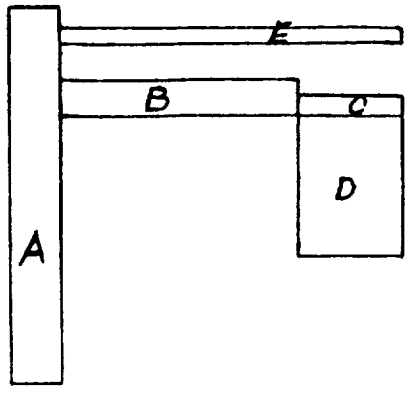

Figure 2

The approach to equivalent properties for the stator is similar to that for the rotor except that the sections are not solid, the array is partially in parallel and partially in series, and it involves distinct materials, as seen in Figure 2. Note that sections C & D act in parallel; therefore the net combined stiffness "K" is $K_{CD} = K_C + K_D$, and the net compliance is $Z_{CD} = 1/K_{CD}$. Section B acts in series with the CD combination, therefore the net combined compliance is $Z_{BCD} = Z_B + Z_{CD}$. Section E acts in parallel with the inner combination of BCD, therefore the net elasticity is obtained by adding stiffnesses. $K_{BCDE} = K_E + K_{BCD} = K_E + Z_{BCD}^{-1}$ and $Z_{BCDE} = 1/K_{BCDE}$. Finally, section A acts in series with the combined sections BCDE; i.e. $Z_{net} = Z_A + Z_{BCDE}$. The equivalent sectional properties can be obtained from Z_{net}. The numerical statistics for the components of this stator bar example are given in Table 3. Use of these data in the combining formulas is carried out just for stator equivalent area as follows.

$$K_{CD}^{area} = \frac{A\,E}{L}\Big)_C + \frac{A\,E}{L}\Big)_D = \frac{\pi/4(7.12^2 - 6.75^2) \times 10^7}{2.689} + \frac{\pi/4(6.75^2 - 4.58^2)\ 3 \times 10^7}{2.689} =$$

$$= \frac{\pi \times 10^7}{4 \times 2.689}\left(5.132 + 3 \times 24.586\right) = 2.304 \times 10^8.$$

$$Z_{CD}^{area} = 4.340 \times 10^{-9}.$$

Combining item B in series with the CD combination gives

$$Z_{BCD}^{area} = Z_B^{area} + Z_{CD}^{area} = \frac{L_B}{A_B E_{al}} + Z_{CD}^{area} =$$

$$= \frac{2.007}{\pi/4(7.38^2 - 6.5^2) \times 10^7} + 4.34 \times 10^{-9} = 2.526 \times 10^{-8}$$

$$K_{BCD}^{area} = \left(Z_{BCD}^{area}\right)^{-1} = 3.95 \times 10^7.$$

Item E combines in parallel with item BCD.

$$K_{BCDE}^{area} = \frac{4(\pi/4)(5/16)^2 \times 3 \times 10^7}{4.53} + 3.958 \times 10^7 = 4.162 \times 10^7.$$

$$Z^{area}_{BCDE} = \left(K^{area}_{BCDE}\right)^{-1} = 2.403 \times 10^{-8}.$$

And now section A can be combined in series with the current result.

$$Z^{area}_{net} = \frac{L_A}{A_A E_{al}} + Z^{area}_{BCDE} = \frac{0.62}{(7.5^2 - \frac{\pi}{4}\, 2/85^2) \times 10^7} + 2.403 \times 10^{-8}$$

$$= 2.567 \times 10^{-8} = \frac{L_{total}}{E_{al} A_{equiv}}.$$

$$A_{equiv} = \frac{E_{al}}{L_{total}\, Z^{area}_{net}} = 19.347.$$

Similar calculations yield equivalent area moment of inertia I_{equiv} as was shown for the rotor bar example.

COLLATERAL

These operations were performed for the rest of the rotor and stator. This completes the complement of properties for equivalent prismatic bars. It will be mentioned, only in passing, that the mass can be well modeled automatically (except for torsional inertias) by calling for COUPMASS. The assignment of torsional mass moment of inertia per grid point must be manually determined and entered as CMASS2 elements. The next topic concerns the mating of the rotor to the stator at the bearings. This motor was designed with ball bearings which can absorb thrust. Therefore, the two bearings link the rotor and stator without connecting any rotations. This was represented as Multi-Point-Constraints (MPC's) in all 3 translations, between the two rotor bearing points, numbers 2 & 4 and the corresponding stator points, numbers 30 & 33.

The topic that needed particular study was the disc brake. The following discussion will refer to Figure 3.

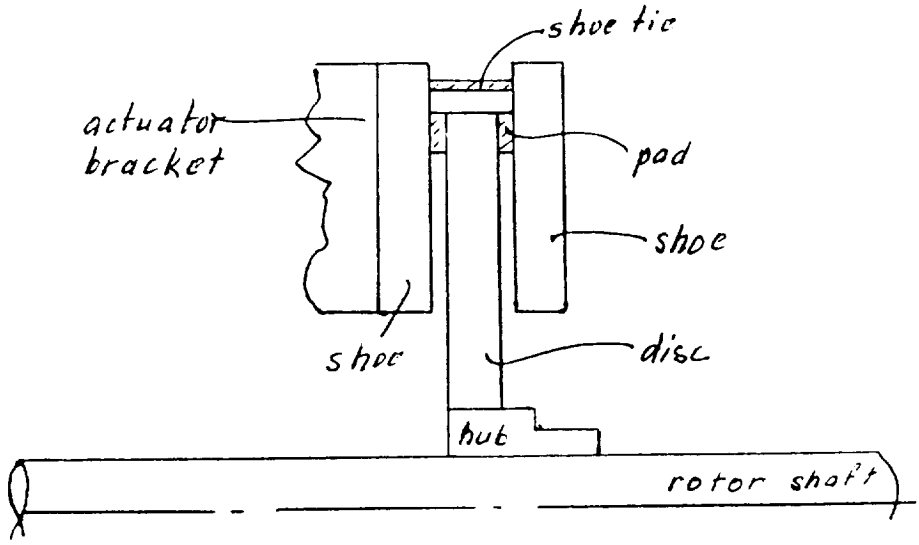

Figure 3

Two shoes bind on the brake disc to hold the rotor shaft. When the brake is actuated, the load path from shaft to stator is all that is of concern. How the brake force is exerted is extraneous to the finite element modeling of the braked condition (if stresses are of no concern). The as-braked load path is from the shaft at the aft end of the brake disc into the hub, into the disc and out of the forward shoe to the brake bracket via the pad then into the resolver bell. Thus there is no contribution to the stiffness of this load path from the after shoe. The modeling starts by incorporating the hub into the bar of the rotor shaft. The stator bar begins with the disc and connects in series with the forward pad. Then the shoe is a series component in the equivalent bar extending from the resolver bell through the actuator bracket and the shoe. It was difficult to get material properties for the asbestos pad so it was assumed that the asbestos could be reasonably represented by limestone.

Finally, consideration must be given to the connection of this one dimensional model to the outside world. The drive shaft will connect throught a keyway into a power shaft of a reduction gear or similar; so this poses no difficulty in linking 1 - D to

1 - D. With the stator bell it is a different matter. The motor casing attaches at either end bell or through feet along its length to a 2 - D or 3 - D parent. In this model it is through the forward bell. If MPC's or rigid elements are chosen to make this connection at the forward bell one must review the MPC used to tie the ball bearings together. The ball bearing MPC must retain the stator degrees of freedom as independent, so that they will be available to be picked up for further tying to the mounting bolts. If instead of constraints, bar connections are used, then consideration must be exercised so as not to short circuit the forward bell elasticity with an overly stiff representation. Nor should the bars be so limber as to introuce wobble into the connnection.

SUMMARY

The statistics for this 1 - D model of an electric motor are:

Grid Points - 6 in the rotor, 8 in the stator = 14.
Bars - 5 in rotor, 8 in stator = 13
MPC - 3
Torsional Mass Elements CMASS2 - 14

An exploded plot of these 2 colinear elements in Figure 4 illustrates the connections at bearings, brake, and externals.

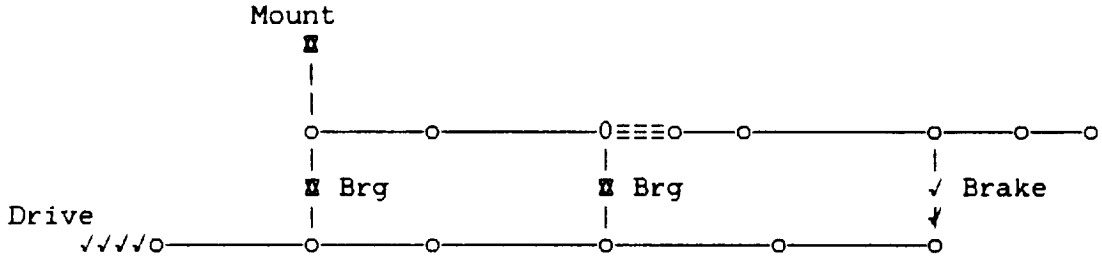

Figure 4

CONCLUSION

It has been shown that the necessary characteristics of an electric motor can be incorporated into a dynamic model by means of a lean bar model without having to resort to a full blown three dimensional model.

MODELING AN ELECTRIC MOTOR IN 1 - D
TABLE OF GRID POINTS

ROTOR

GP	LOCATION
1	Drive Shaft Coupling Keyway
2	Center Line of Bell Housing with Bearings
3	Center of Gravity of Rotor Armature
4	Bearing at Brake End
5	Center of Gravity of Resolver
6	Center Line of Brake Disc

STATOR

30	Center line of Bell Housing with Bearings
31	Center of Gravity of Stator Coil
32	Center Line of Outer Resolver Bell
33	Bearing at Brake End
34	Resolver End Bell
35	Brake Housing
36	End Cover
37	Brake Shoe Plate

Table 1

MODELING AN ELECTRIC MOTOR IN 1 - D
TABLE OF COMPONENT STATISTICS

ROTOR COMPONENT STATISTICS

DESCRIPTION	DIAMETER	LENGTH	MATERIAL
1/2 Bearing Journal	1.3875	0.389	Steel
Intermediate Shaft	2.25	1.670	Steel
1/2 Armature	3.831	2.830	Steel/Copper
Total		4.889	Steel

Table 2

STATOR BAR COMPONENT STATISTICS

ITEM	DESCRIPTION	DIAMETER OD/ID	LENGTH	MATERIAL
A	Bell	7.5 / 2.85 Square Round	0.62	Aluminum
B	Shell	7.38/2.85	2.007	Aluminum
C	Stator Shell	7.12/6.75	2.689	Aluminum
D	Stator	6.75/4.58	2.689	Steel/Copper
E	4 Bolts	$\frac{5}{16}$	4.53	Steel
	Total		4.889	Aluminum

Table 3

COMPUTER ANIMATION OF NASTRAN DISPLACEMENTS ON IRIS 4D-SERIES WORKSTATIONS: CANDI/ANIMATE POSTPROCESSING OF NASHUA RESULTS

Janine L. Fales
Los Alamos National Laboratory
Advanced Engineering Technology (MEE-13)
Los Alamos, New Mexico 87545

SUMMARY

The capabilities of the postprocessing program CANDI (Color Animation of Nastran DIsplacements) [1] have been expanded to accept results from axisymmetric analyses. An auxiliary program, ANIMATE, has been developed to allow color display of CANDI output on the IRIS 4D-series workstations. The user can interactively manipulate the graphics display by three-dimensional rotations, translations, and scaling through the use of the keyboard and/or dials box. The user can also specify what portion of the model is displayed. These developments are limited to the display of complex displacements calculated with the NASHUA/NASTRAN procedure for structural acoustics analyses [2].

INTRODUCTION

Animation of results has become an increasingly popular method of postprocessing because of the wealth of information conveyed to the analyst in a short amount of time. Animation allows the analyst to visualize time-dependent results that previously could only be imagined from a series of static plots. Through animation, the analyst is able to focus on the interpretation of the results, having been freed from the burden of envisioning their time dependency.

The advantages of animation were recognized by Lipman at David Taylor Research Center (DTRC), in the development of the postprocessing computer program, CANDI (Color Animation of Nastran DIsplacements) [1]. CANDI was originally written to

interface with an Evans & Sutherland PS-330 interactive graphics system [3] for the graphics display. Unfortunately, the usefulness of CANDI was limited to those with access to this specific hardware.

A postprocessing tool was required for displaying complex displacements obtained with the NASHUA/NASTRAN procedure (hereafter referred to as NASHUA). NASHUA, developed by Everstine and Quezon at DTRC, is a coupled finite element/boundary element capability built around NASTRAN for calculating the low-frequency, far-field acoustic pressure field radiated or scattered by an arbitrary, submerged, elastic structure subjected to either internal, time-harmonic, mechanical loads or external, time-harmonic, incident loadings [2]. The structure can be axisymmetric or three-dimensional. CANDI was one postprocessing option for three-dimensional NASHUA analyses. An axisymmetric tool was also required.

Rather than replicate the work of Lipman, an auxiliary computer program, ANIMATE, was developed to accept, as input, the output from CANDI and display the results on the IRIS 4D-series workstations, manufactured by Silicon Graphics, Incorporated (SGI). The choice of the IRIS workstation was based on its three-dimensional, graphics display capabilities. CANDI was also expanded to postprocess results from axisymmetric NASHUA analyses.

Because the work described here was done to accomplish specific, programmatic needs, the scope of the computer program developed is limited to the display of complex displacements calculated with NASHUA. Although CANDI is able to postprocess results from other types of analyses, there are no expectations on the part of the author to enable ANIMATE to display these results. It is hoped that the foundations of the program are sound enough to allow enhancements by others, if needed.

THE NASHUA/NASTRAN PROCEDURE (NASHUA)

The NASHUA/NASTRAN procedure, also called the NASHUA capability or NASHUA, is explained, in detail, in Ref. 2. At Los Alamos National Laboratory, NASHUA is executed on a Cray supercomputer running under a CTSS operating system. Table 1 summarizes the steps involved in this type of analysis. Rigid Format 8 (direct frequency response) is used for each NASTRAN execution. All DMAP ALTER sequences are given in Ref. 2. The DMAP ALTER

statements needed for the use of CANDI are the OUTPUT2 statements given in Figure 1. These OUTPUT2 statements produce a binary file, named utl, containing the information needed by CANDI. To avoid the need for a file conversion program to move the utl file (in Cray binary) to another machine for postprocessing, CANDI was ported to the Cray.

TABLE 1
NASHUA/NASTRAN PROCEDURE SUMMARY

STEP	CODE	PURPOSE
1	NASTRAN 1	Define geometry Form structural mass, viscous damping, and stiffness matrices
2	SURF	Form fluid matrices
	NASTRAN 2	Set up coupled system for pressure
	OCSOLVE	Solve coupled system
	NASTRAN 3	Recover velocities
	MERGE	Combine multiple frequencies
3	FAROUT	Calculate far-field quantities
4	NASTRAN 4	Produce deformed structural plots
5,6, ...	IPLOT FAFPLOT CANDI, etc.	Perform additional postprocessing

```
ALTER       1 $ NASHUA STEP 4, COSMIC 1990 RF8
ALTER       8,8 $
ALTER       21,170  $
...
OUTPUT2     CASECC,BGPDT,ECT,FRL,PUPVC1//-1 $
OUTPUT2     ,,,,//-9  $
...
ENDALTER $
```

Figure 1. DMAP ALTER statements required for use of CANDI.

CANDI, THE POSTPROCESSING PROGRAM

CANDI is an interactive program that reads, filters, and outputs results from a variety of NASTRAN analyses, including static, eigenvalue, direct frequency response, direct transient response, and modal frequency response. It reads the binary utl file produced by including DMAP ALTER statements in the NASTRAN executive control deck. (For use with NASHUA, the specific DMAP ALTER statements are given in Figure 1.)

The user is asked a number of interactive questions to determine what output is desired. Figure 2 shows a sample interactive session. Through these questions, the user has control over what is displayed and how it is displayed. For example, portions of the finite element model can be excluded based on a range of XYZ coordinate values, on element type, and/or on element id. Coordinate ranges, element types, and element ids are displayed to assist the user. The user also has control over which results are output - which subcases and which frequencies, in the case of a NASHUA analysis. He also controls how many frames of animation are desired and whether the deformation scale factor computed by CANDI is used. The scale factor is computed so that the magnitude of the displacements will be similar to the dimensions of the finite element model.

Based on the responses, CANDI filters and outputs one or more ASCII files in vector list format. A sample vector list is given in Figure 3. To reduce the computational effort required by the display device,

```
xcandi
   candi - color animation of nastran displacements
   enter file name of the utl file ?
? utl

   coordinate limits of the finite element model
   xmin= 1.0000e-05       ymin= 0.0000e+00       zmin= 0.0000e+00
   ymax= 2.1695e+00       ymax= 3.3930e+01       zmax= 0.0000e+00

   do you want to exclude elements by coordinate ranges (y/n) ?
? n

   3 element type(s) (element type id-element type)
   146-cconeax            287-ctriaax       285-ctrapax

   do you want to exclude elements by element type (y/n) ?
? n

   do you want to exclude elements by element id (y/n) ?
? n

   do you want the vector lists to be
   1 - color coded by element type or  id
   2 - depth cued
? 1

   do you want to color code by element
   1 - type (not user-definable)
   2 - id (user-definable, default=blue)
? 1

   enter file name for the undeformed fem vector list ?
? undef

   do you want to generate any displacement vector lists (y/n) ?
? y

   number of subcases = 2, subcase ids -    1       2
   number of frequencies = 4  (number-frequency)
         1-  60.00      2-  70.00      3-  80.00      4-  90.00

   enter a subcase id and frequency number ?
? 2 3

   enter file name for the displacement vector list ?
? def3

   enter number of frames of animation ?
? 16

   maximum deformation = 2.1680e-03
   computed deformation scale factor (dsf) = 7.8253e+02
   do you want to change the computed dsf (y/n) ?
? n

   do you want to write another displacement vector list (y/n) ?
? n
stop
```

Figure 2. Sample CANDI session of axisymmetric analysis.

CANDI tests whether each side of an element has already been written to the vector list before adding it. The 'p' and 'l' designations are signals to the graphics device. A 'p' indicates 'move to' the given coordinates ; an 'l' indicates 'draw to' the given coordinates. The semicolon signals the end of the vector list. In this way, the undeformed (finite element model) and deformed (results) meshes are drawn efficiently.

```
aaa:=undeformed vec list
p-1.085e+00, 1.696e+01, 0.000e+00
l-9.160e-01, 1.696e+01, 0.000e+00
l-7.486e-01, 1.693e+01, 0.000e+00
l-5.842e-01, 1.690e+01, 0.000e+00
l-4.240e-01, 1.684e+01, 0.000e+00
                . . .
;
```

Figure 3. Portion of vector list for undeformed mesh.

An axisymmetric version of CANDI was required. Structural acoustics problems frequently require fine mesh densities to capture the response of the structure accurately. Three-dimensional models become prohibitive because of computer time required for solution. Hence, axisymmetric analyses, when applicable, become extremely important. CANDI was enhanced to recognize the axisymmetric elements, CCONEAX, CTRIAAX, and CTRAPAX. Other elements could be added, given the knowledge of card type format[1] for each element desired. Additional information about CANDI can be found in Ref. 1.

ANIMATE, THE DISPLAY PROGRAM

ANIMATE was developed on a Personal IRIS®, Model 4D/25TG. It is written in C and uses the Graphics Library (GL) resident on SGI/IRIS workstations. ANIMATE reads the vector lists output by CANDI, calculates, and displays the animation sequence. Control of the display is provided through an extensive user interface. Specific aspects of ANIMATE are discussed in the sections that follow.

---

[1]Card type formats are available in Section 2.3 of the "COSMIC/NASTRAN Programmer's Manual," NASA SP-223(5), August 1987. Header Word 3 is the element id number.

®Personal IRIS is a registered trademark of Silicon Graphics, Incorporated.

HARDWARE / SOFTWARE REQUIREMENTS

The Personal IRIS, Model 4D/25 TG, on which ANIMATE was developed, was originally purchased for its three-dimensional capabilities with PATRAN®. The Personal IRIS (4D/20+) series give favorable price/performance curves. The need to animate complex displacements spearheaded the effort to port CANDI to the IRIS platform. In addition, other postprocessing tools for structural acoustics analyses had been developed for the IRIS 4D-series workstations.

The high-level Graphics Library made the graphics programming relatively easy. However, because the GL was used, ANIMATE is not universally portable. It is only portable to IRIS 4D-series workstations, or to IBM machines on which the GL has been installed. The IRIS Window Manager, based on the NeWS server environment was used to develop the user interface.

ANIMATE was initially developed using the dials box for the three-dimensional rotations, translations, and scaling. While the dial box is an intuitive method to accomplish these transformations, it is an optional peripheral. Therefore, the same functionality was tied to keys found on the standard IRIS keyboard. If available, use of the dial box is preferred.

The minimum hardware requirement to use ANIMATE is an IRIS 4D/20 G workstation. Any graphics workstation of the 4D-series is acceptable. The dial box is useful, but optional.

CALCULATION OF ANIMATION SEQUENCE

Animation of the harmonic time dependence of the complex displacements is accomplished according to the following equation.

$$F_i = V_u + DSF\ [\ V_{Re} \cos\theta_i - V_{Im} \sin\theta_i\ ]$$

where F_i = ith frame of animation,
V_u = undeformed vector list,
V_{Re} = vector list of real components,
V_{Im} = vector list of imaginary components,

®PATRAN is a registered trademark of PDA Engineering.

θ_i = angle for F_i = 360°/(number of frames),

and

DSF = deformation scale factor.

The equation is obtained by multiplying the time invariant result (here given by the complex displacements) by the appropriate time dependency. The simple harmonic variation of the results is given by the real part of this product [4]. For NASHUA, a harmonic time dependency of $e^{i\omega t}$ is assumed. Figure 4 illustrates this product graphically. One complete animation sequence corresponds to a 360° rotation of the complex displacement vector. Each frame of the animation sequence rotates the displacement vector by an angle of θ_i. For smooth animation, the number of frames, i, is normally specified between 12 and 16.

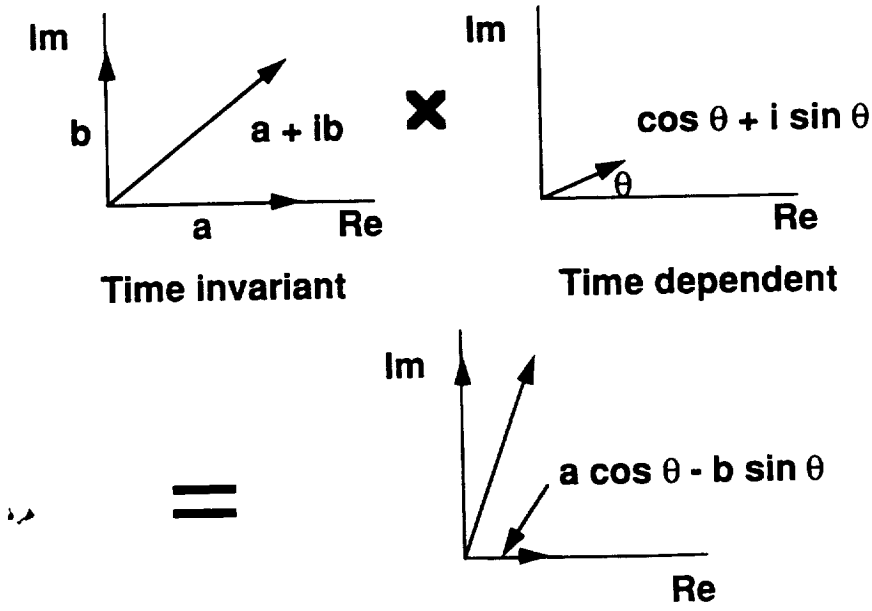

Figure 4. Graphic display of animation concept.

USER INTERFACE

It was important to develop a user interface that helped, not hindered the analyst. Thus, the interface was developed as intuitively as possible, maintaining the function key assignments found in the original CANDI/Evans & Sutherland system. Specific key assignments are listed in Figure 5. Dial assignments and locations are shown in Figure 6. Through this interface, the user has control over the view and scale of the model, the speed of animation, and the display of undeformed mesh and/or the coordinate axes. He can stop and start the animation, or step through it one frame at a time.

Function Key Definitions

FK1	Start animation
FK2	Stop animation
FK3	Step backwards through animation sequence
FK4	Step forwards through animation sequence
FK5	Slow down rate of animation
FK6	Speed up rate of animation
FK7,8	Not assigned
FK9	Reset all rotations and translations
FK10	Toggle on/off undeformed mesh
FK11	Toggle on/off coordinate axes

Other Key Definitions

x/X	Increase/decrease x-rotation
y/Y	Increase/decrease y-rotation
z/Z	Increase/decrease z-rotation
i/I	Left/right x-translation
j/J	Left/right y-translation
k/K	Left/right z-translation
s/S	Increase/decrease scale
ESC	Exit program

Figure 5. Keyboard definitions for user interface.

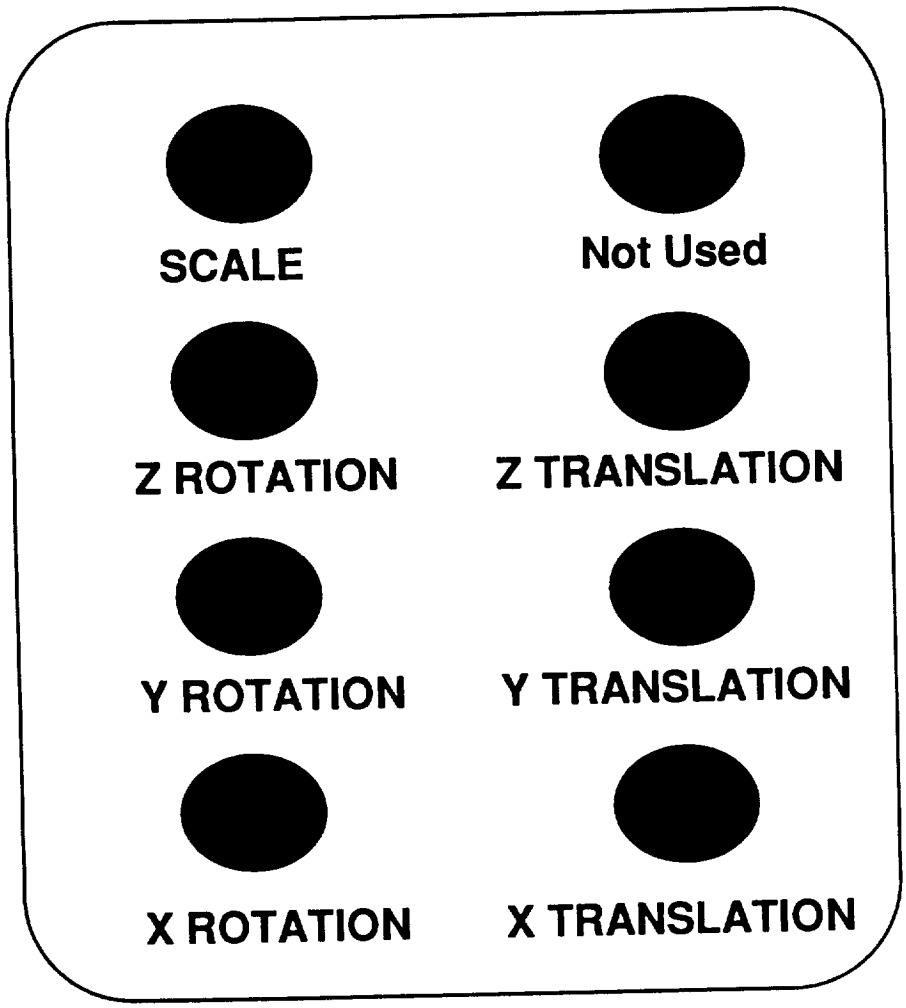

Figure 6. Dial box definitions and dial locations.

REFERENCES

1. R. R. Lipman, "Computer Animation of Modal and Transient Vibrations," Fifteenth NASTRAN Users' Colloquium, NASA CP-2481, National Aeronautics and Space Administration, Washington, D.C., pp 88-97 (May 1987).

2. G. C. Everstine and A. J. Quezon, "User's Guide to the Coupled NASTRAN/Helmholtz Equation Capability (NASHUA) for Acoustic Radiation and Scattering," Third Ed., DTRC report CMLD-88/03 (February 1988).

3. "PS-300 User's Manual," Evans & Sutherland Computer Corporation, Salt Lake City, Utah, 1985.

4. F. Fahy, Sound and Structural Vibration, Radiation, Transmission and Response, Academic Press, 1985.

N91-20515

DISTILLATION TRAY STRUCTURAL PARAMETER STUDY: PHASE I

J. Ronald Winter
Senior Engineering Mechanist
Engineering Division
Tennessee Eastman Company
Kingsport, Tennessee

ABSTRACT

The major purifications process used by the petro/chemical industries is called "distillation." The associated pressure vessels are referred to as distillation columns. These vessels have two basic types of internals: distillation trays and packing. Some special columns have both a packed section and a trayed section. This paper deals with the structural (static and dynamic) analysis of distillation trays within a column. Distillation trays are basically orthogonally stiffened circular plates with perforations in a major portion of the surface. Structural failures of such trays are often attributed to vibration associated with either resonant or forced response. The situations where resonance has been encountered has led to immediate structural failures. These resonant conditions are attributed to the presence of a process pulsation with a frequency within the half-power band width of the first or second major tray structural natural frequency. The other major class of failures are due to fatigue associated with forced response. In addition, occasional tray structural failures have been encountered as a result of sudden large pressure surges usually associated with rapid vaporization of a liquid (flashing), a minor explosion or a sudden loss of vacuum. These latter failures will be briefly discussed in this paper. It should also be noted that corrosion is a common problem that often leads to structural failures and/or a decrease in tray processing efficiency.

The purpose of this study is to identify the structural parameters (plate thickness, liquid level, beam size [moment of inertia], number of beams, tray diameter, etc.) that affect the structural integrity of distillation trays. Once the sensitivity of the trays dynamic response to these parameters has been established, the designer will be able to use this information to prepare more accurate specifications for the construction of new trays. This will result in a reduction in the failure rate which in turn will lead to lower maintenance cost and greater equipment utilization.

LIMITATIONS

This is a report on Phase I of a two phase analysis. It is applicable to trays with diameters ranging from 10 feet to 15 feet and having a single main beam in addition to smaller minor beams. The results are mainly applicable to cross-flow type distillation trays of either the sieve or valve configurations. See Figures 1 and 6, and Appendices I and II. In addition, these results would only apply to trays made of certain metals such as carbon steel, stainless steel, Hastelloys, monels, etc. They would not be applicable to trays made of titanium, copper, aluminum, plastic, etc. Phase II of this study will deal with trays of the same type that have diameters ranging from 3 feet to 10 feet but that do not have a main beam. NOTE: A typical Engineering drawing of a smaller diameter valve tray is shown in Appendix I.

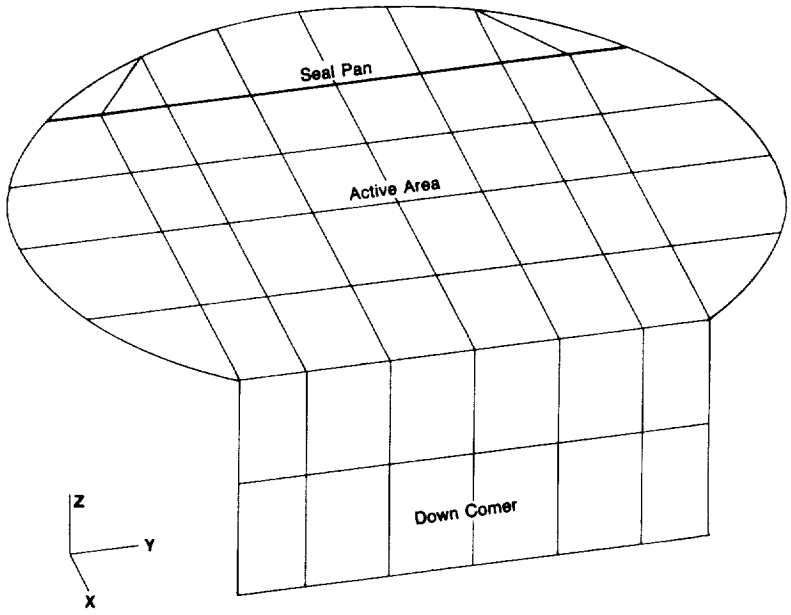

Figure 1: Configuration of a Typical Cross Flow Distillation Tray

ENGLISH TO METRIC CONVERSIONS

All data presented in this report are in English units. Use the table below to convert items to SI (metric) units.

To Convert From	To	Multiply By
Inches	Millimeters	25.4
Square Inches	Square Millimeters	645.2
Inches^4	Centimeters^4	41.62
Feet	Meters	0.3048
Pounds Mass	Kilograms	0.4536
Pounds Force	Newton	4.448
Pounds Per Square Inch	Pascal	6,894.7
Pounds Per Square Foot	Pascal	47.88
Pounds Per Cubic Inch	Kg Per Cubic Meter	2,678

PROCESS OPERATION

The typical geometric layout of trays inside a column is shown in Figure 2. In most situations a pool of liquid chemicals at the bottom of the column is boiled by use of a heat exchanger (reboiler). This is shown in Figure 3. The resulting vapor moves up the column through the perforated plates. At the same time a liquid consisting of two or more chemicals is added at some point around the middle of the column. A relatively pure liquid stream is also added to the top tray of the column. This is referred to as the reflux. The liquid flows across the trays moving down the column, as shown in Figure 4. The resulting heat transfer from tray to tray causes the liquid with the lowest boiling point to vaporize and move up the column while the higher boiling point liquid(s) flows counter current down the column. Purification is thus achieved by the separation of the components with different boiling points.

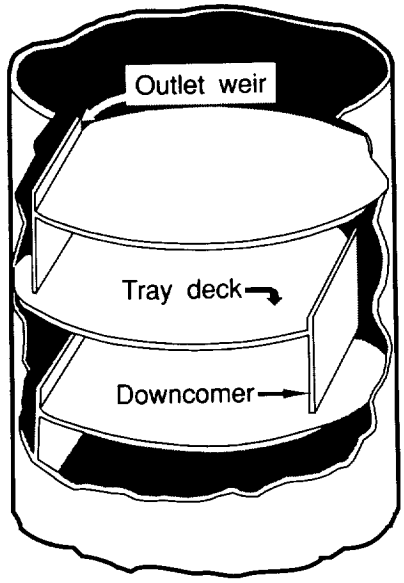

Figure 2: Tray Locations Inside of a Column

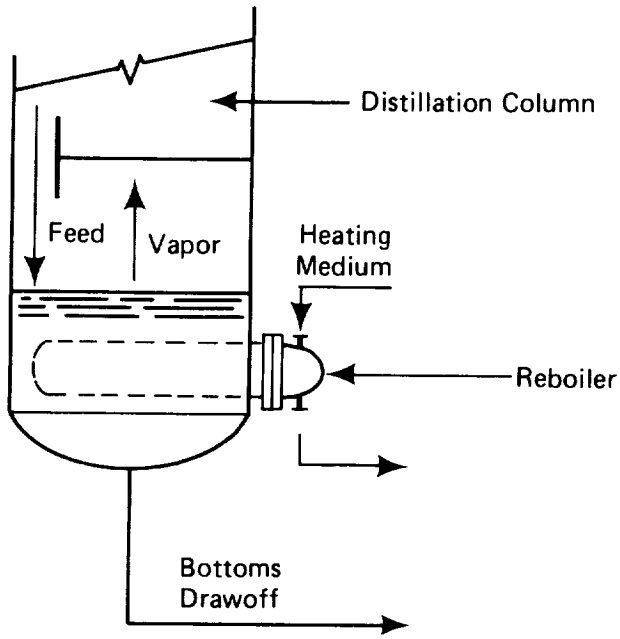

Figure 3: General Configuration of the Bottom Section of a Distillation Column

As shown in Figure 4, the liquid flows diagonally across the tray while the vapor flows through the perforations perpendicular to the liquid flow. As stated previously, the liquid-vapor interactions throughout the column serve to separate the low boiling and high boiling liquids. The result is a vapor flow from the top of the column with a high concentration of the low boiling liquid while the liquid in the base consists of a high concentration of the high boiling liquid(s).

The vapor-liquid interaction in the column can be quite violent depending on the vapor velocity through the tray perforations versus the liquid depth on the tray. This generally produces a liquid froth in a portion of the space between trays. This interaction also produces natural pulsations with the amplitude being sensitive to the ratio of the liquid depth to the vapor velocity. These pulsations are often referred to as auto-pulsations.

Such pulsations (auto-pulsations) produce tray oscillations, the most dangerous of which is a resonant or near resonant condition. This occurs when the auto-pulsation frequency, f_A, is within the half-power bandwidth of the tray first or second natural frequencies, ω_1 and ω_2. This can lead to immediate destruction of the affected trays. One such situation will be discussed in this paper. The other situation involving auto-pulsations produces large fluctuations in pressure across individual trays. This results in forced response which can lead to fatigue failures. Examples of this more prevalent type failure mode will also be discussed.

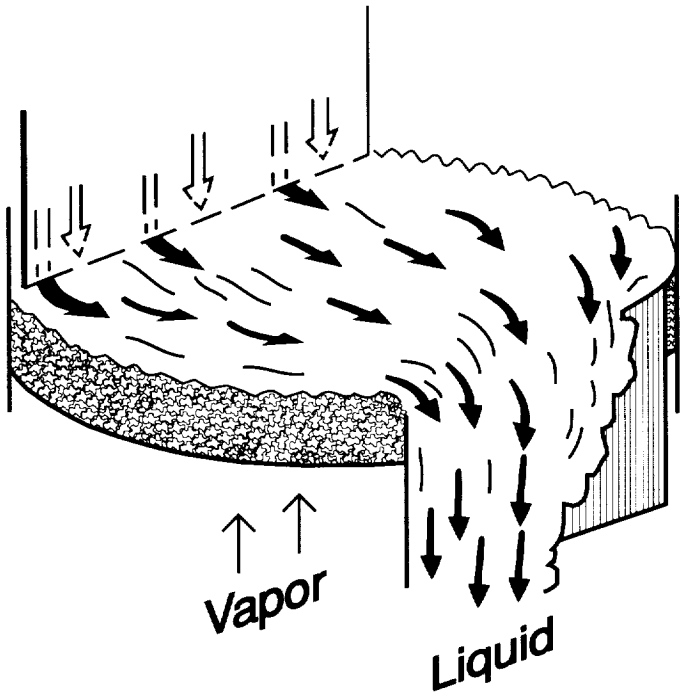

Figure 4: Liquid and Vapor Flow on a Tray

DYNAMIC ANALYSIS

The major emphasis of this study was modal analysis of distillation trays with the major goal to determine the structural parameters that have the most significant effect on the first and second tray structural natural frequencies. This would give the designer the ability to more effectively change the tray design to prevent a resonant, or near resonant condition, or to decrease the amplitude of the trays forced response to auto-pulsation.

STATIC ANALYSIS

The static analyses were limited to determining the maximum deflection of the center portion of the tray due to normal design loads. Large deflections (δ > 0.125") at the center of a tray leads to significant variations in liquid depth across the trays which adversely affects tray performance (efficiency). The design loads for the active tray area vary from 25 psf to 45 psf depending on the tray diameter and the process. A design load of 64 psf is usually used for the seal pan.

One can use a combination of the tray design load and the allowable tray deflection as a means to control a tray's dynamic response. This is often necessary for use in specifications since most tray manufacturers do not have the personnel to perform dynamic finite element analyses.

AUTO-PULSATION

As described previously, auto-pulsation is associated with vapor-liquid interaction on a tray deck as the liquid flows across the tray and the vapor passes through the perforations in the tray deck. As of this date, no one has developed a math model that adequately describes this phenomena. However, some imperical models do exist. Better imperical models could be developed if more data were available for the various combinations of tray diameter, liquid depth, open area (number and size perforations), tray spacing and flow rates. Fortunately, we do have enough data to establish some general trends. Relative to auto-pulsation the "**available**" data "**indicates**" the following trends:

(1) The auto-pulsation frequency, f_A, increases with increasing tray (column) diameter. (See Figure 5)

(2) f_A increases with increasing hole diameter or number of holes; i.e., with increasing open area for vapor flow.

(3) f_A decreases with increased tray spacing; i.e., distance between trays.

(4) f_A increases somewhat as the outlet weir height (liquid depth) increases.

The graph of f_A vs diameter in Figure 5 is shown as a broad band since f_A is also sensitive to the variables discussed in Items 2, 3 and 4 above. In addition f_A is somewhat sensitive to tray performance associated with proper tray installation, operating conditions, stability of the heat exchange system, etc.

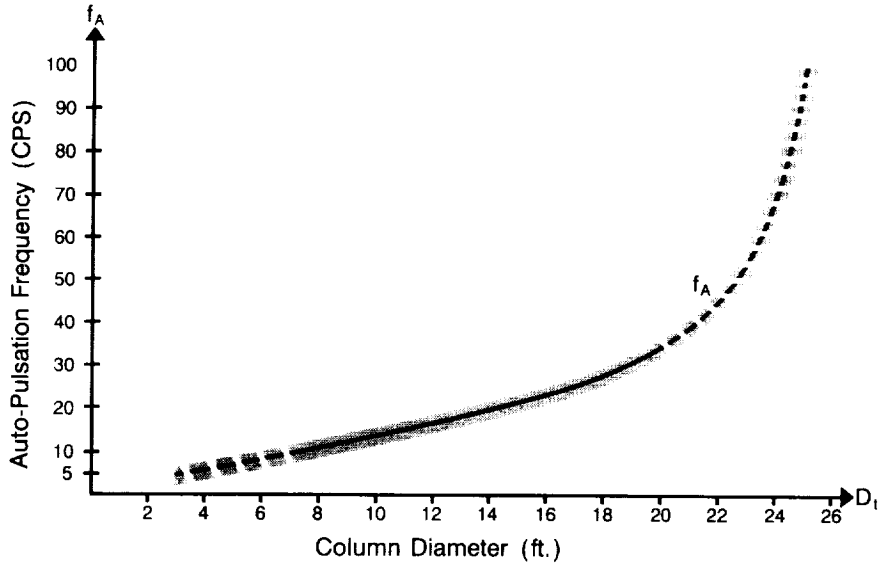

Figure 5: Auto-pulsation Frequency, f_A, Versus Tray/Column Diameter

Tests have also shown that a low frequency pulsation exists that appears to be independent of tray diameter. In some publications this has been referred to as a "swashing" frequency[3,4,5,6]. It involves a wave action across the tray, perpendicular to the liquid flow. In some discussions, engineers refer to it as a standing wave whose frequency is, for the most part, independent of tray diameter. The frequency is generally less than 5 cps.

STRUCTURAL PARAMETER STUDY

The tray structural parameters considered in the static and dynamic analysis of the trays are:

(1) Tray diameter, (D_t): 10 feet to 15 feet.

(2) Tray (plate) thickness, (t_p): 11, 12, 14 gauge.

(3) Minor beams (tray turn downs) moment of inertia, ($I_S = I_{XX}$).

(4) Major beam moment of inertia, ($I_B = I_{YY}$).

(5) Liquid depth on the tray, h_L.

In addition, one must make special corrections to attain the proper mass in the model. First, the thickness of the tray must be reduced to reflect the perforations. If it is a valve tray, then the weight of the valves must be added back into the model as non-structural mass. The effective liquid depth* on the active tray area must be added as non-structural mass. In addition, the higher liquid depth in the seal pan area must be added into the model as non-structural mass.

The number of models developed and the parameters involved are shown in the flow chart on the next page. Each basic model is indicated by a number-letter combination such as 5A. Run 5A involves a 11 ft diameter, 12 gauge tray with minor beam I_{S2} and major beam I_{B2}. This particular model, as well as the other ones, were ran with different liquid depths. In addition to the dynamic (modal) analysis a static analysis was performed on each model. Typical boundary conditions as well as a static load set are presented in Appendix VI.

EXAMPLE ANALYSIS OF A TRAY THAT ENCOUNTERED RESONANCE

This particular column has a diameter of 11 ft. The column contained cross-flow valve trays in the upper half of the vessel and split flow valve trays in the bottom half. Only the more flexible cross flow valve trays as shown in Figure 6 encountered problems. Split flow trays are inherently stiffer than the same diameter cross flow trays provided both are designed for the same loading.

*Due to the vapor liquid interaction the effective liquid depth (liquid mass associated with the tray) will differ from the actual undisturbed liquid depth.

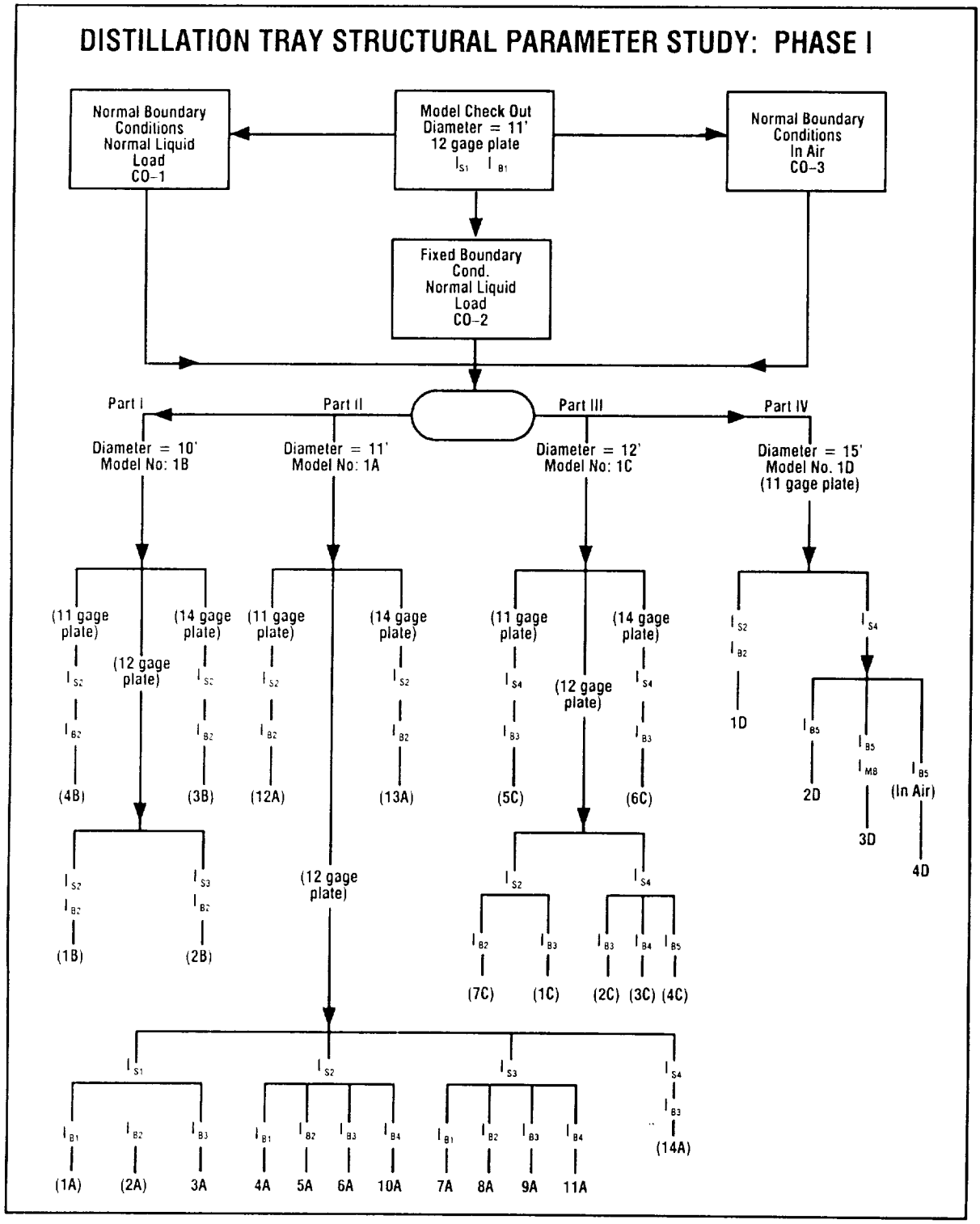
DISTILLATION TRAY STRUCTURAL PARAMETER STUDY: PHASE I
Normal Boundary Conditions Normal Liquid Load CO-1
Model Check Out Diameter = 11' 12 gage plate
Normal Boundary Conditions In Air CO-3
Fixed Boundary Cond. Normal Liquid Load CO-2
Part I
Part II
Part III
Part IV
Diameter = 10' Model No: 1B
Diameter = 11' Model No: 1A
Diameter = 12' Model No: 1C
Diameter = 15' Model No. 1D (11 gage plate)
(11 gage plate)
(12 gage plate)
(14 gage plate)
(4B)
(3B)
(1B)
(2B)
(12A)
(13A)
(5C)
(6C)
(7C)
(1C)
(2C)
(3C)
(4C)
1D
2D
3D
4D
(In Air)
(1A)
(2A)
3A
4A
5A
6A
10A
7A
8A
9A
11A
(14A)

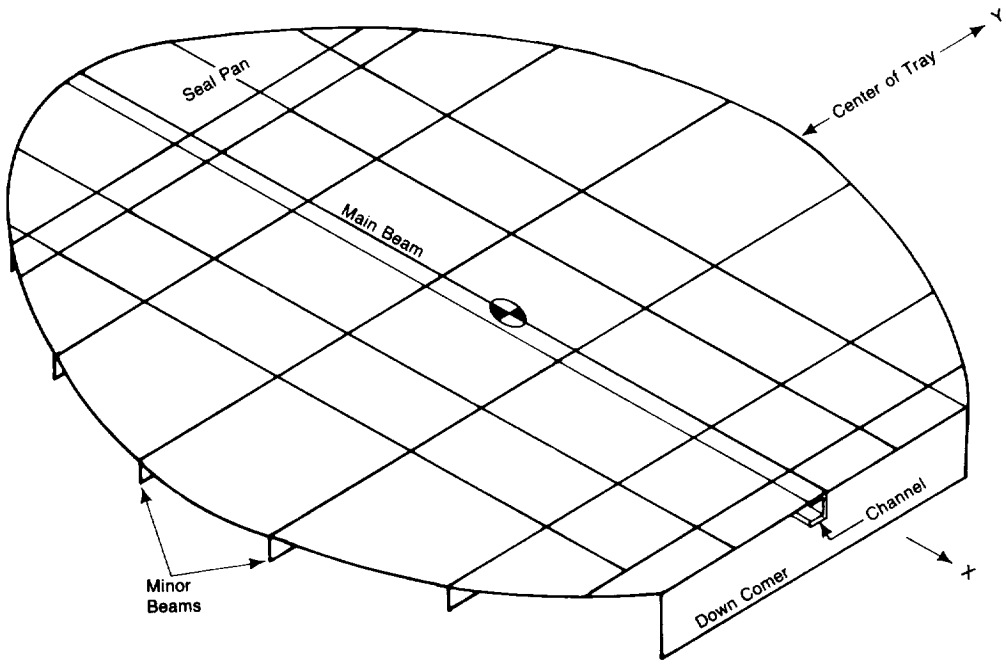

Figure 6: Original Cross Flow Tray

Two finite element codes were used in this analysis:

STRAP3: A code developed by The Eastman Kodak Company for internal use before the release of numerous other finite element codes.

NASTRAN: NASA structural Analysis Code[1,2]. Developed by NASA at Goddard Space Flight Center and released to the general public in 1970. The latest versions are now available for lease from COSMIC at the University of Georgia, Athens, Georgia.

Structural/Model Details

The original tray configuration is shown in Figure 6. There are two structural details that have a significant affect on the tray modal response.

(1) The minor beams are straight; i.e., they are not angles or channels which are more commonly used today.

(2) The main beam is a channel instead of an I-beam. Thus to get the correct first mode shape (modal response) one must correct for the shear center. This was done. The applicable model in the flow chart is 12A. The checkout model also applies.

Tray Failure Details

During initial start-up of the column, all process operations were proceeding normally until the tray operation was at about 25% of its capacity. At this point the overall column efficiency began to drop dramatically as the flow-rates increased. The unit was shut down in an effort to determine the cause of the unexpected loss in capacity. Internal inspection of the column revealed:

(1) Cracks at the turn down (minor beams) on the tray decks. See Figure 7.

(2) Cracks in the main beam (channel). See Figure 8.

(3) Damaged valves and tray hardware. See Figures 9 and 10.

(4) Valves missing on the tray deck on one side of the channel; the side opposite the open U. See Figures 7, 11 and 12.

(5) The vessel wall also cracked where the main beam was attached to the wall.

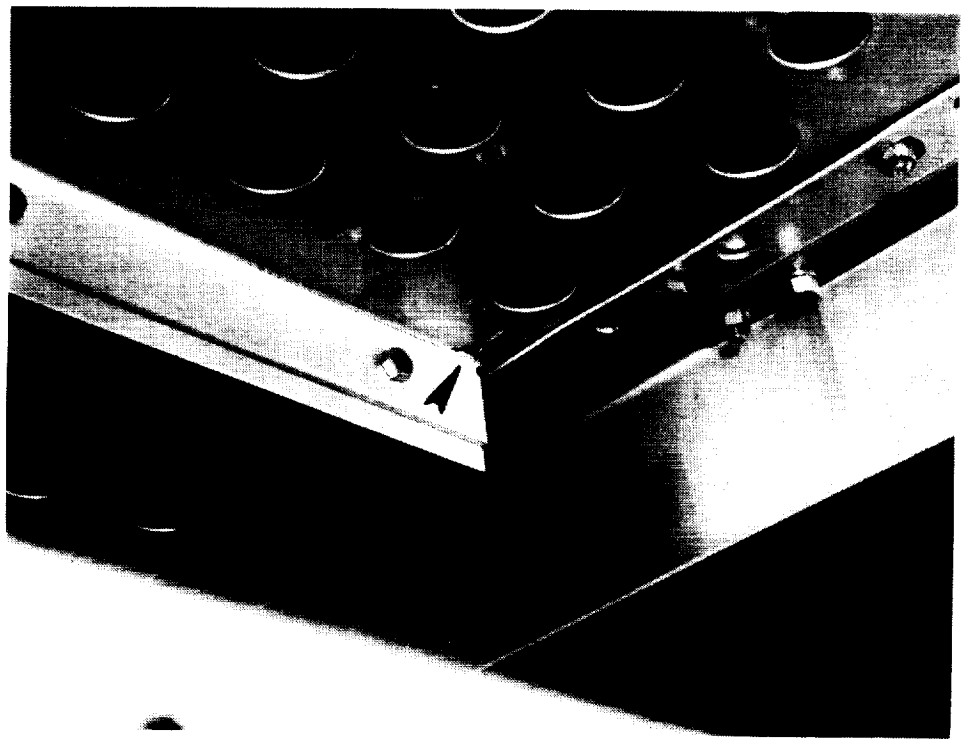

Figure 7: Tray Deck and Minor Beam Cracking

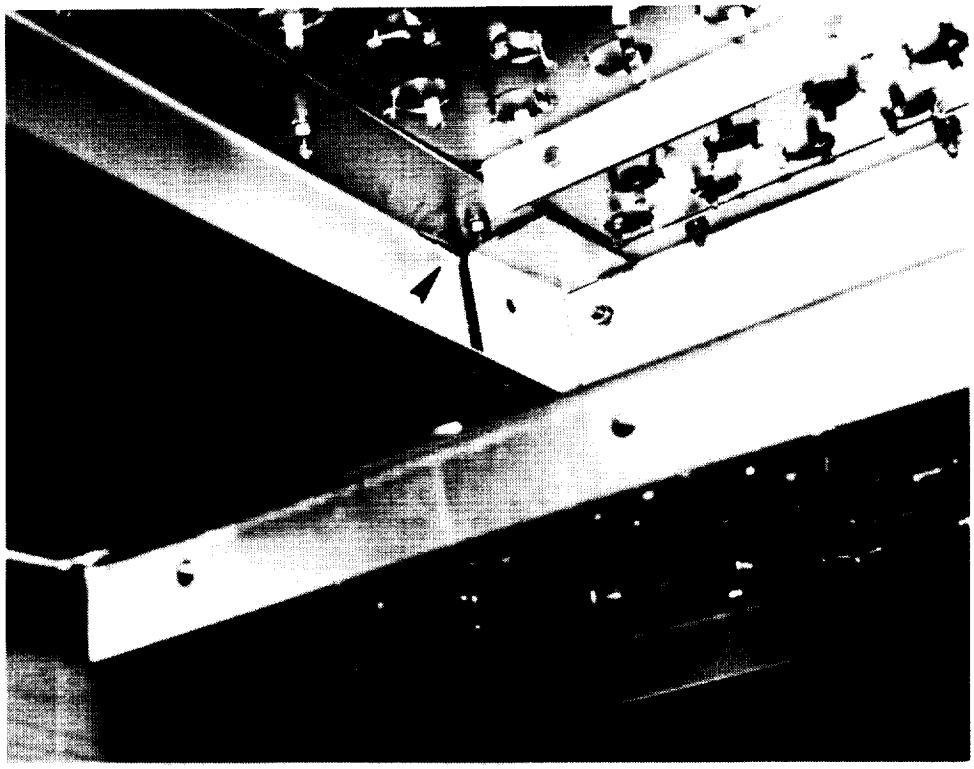

Figure 8: Main Beam Cracking

As shown in Figure 9, some of the legs are broken off the valves due to the dynamic action. Close inspection of the valve legs and the holes in the trays show highly polished or worn surfaces. This is further evidence of high frequency oscillations. Such polished surfaces are not seen in normally operating columns; i.e., columns that operate in a stable, non-resonant condition.

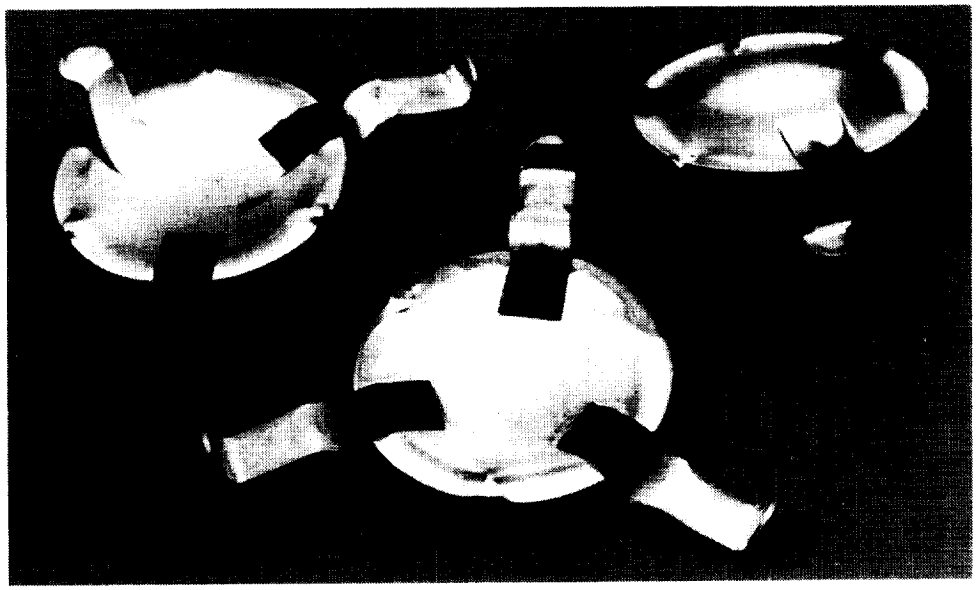

Figure 9: Damaged Valves From the Tray Deck

Damaged tray hardware shown in Figure 10 includes a small section of a tray deck as well as a damaged and a broken tray attachment clip.

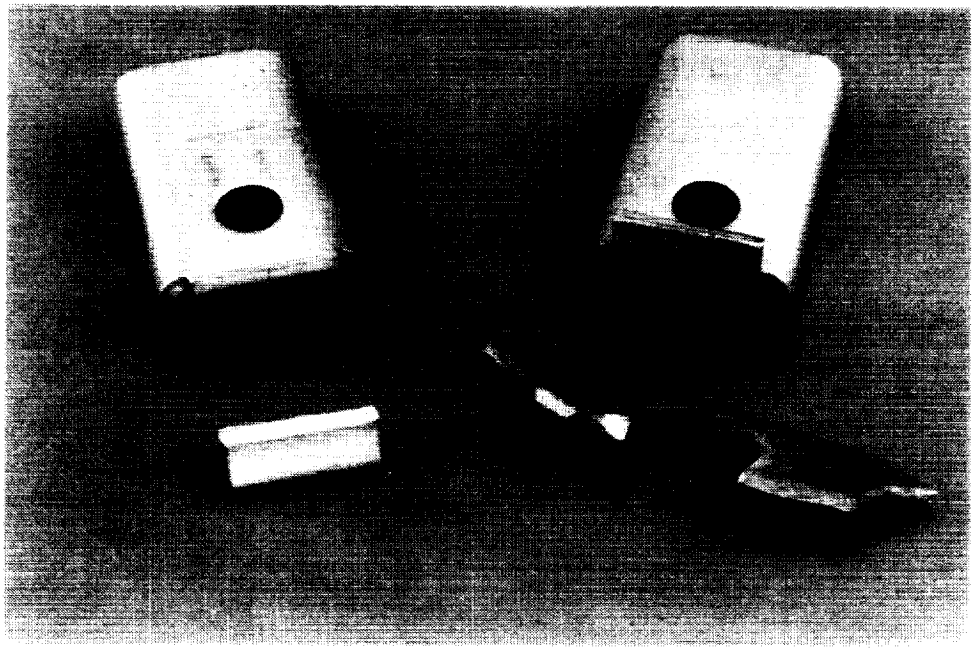

Figure 10: Damaged Tray Hardware

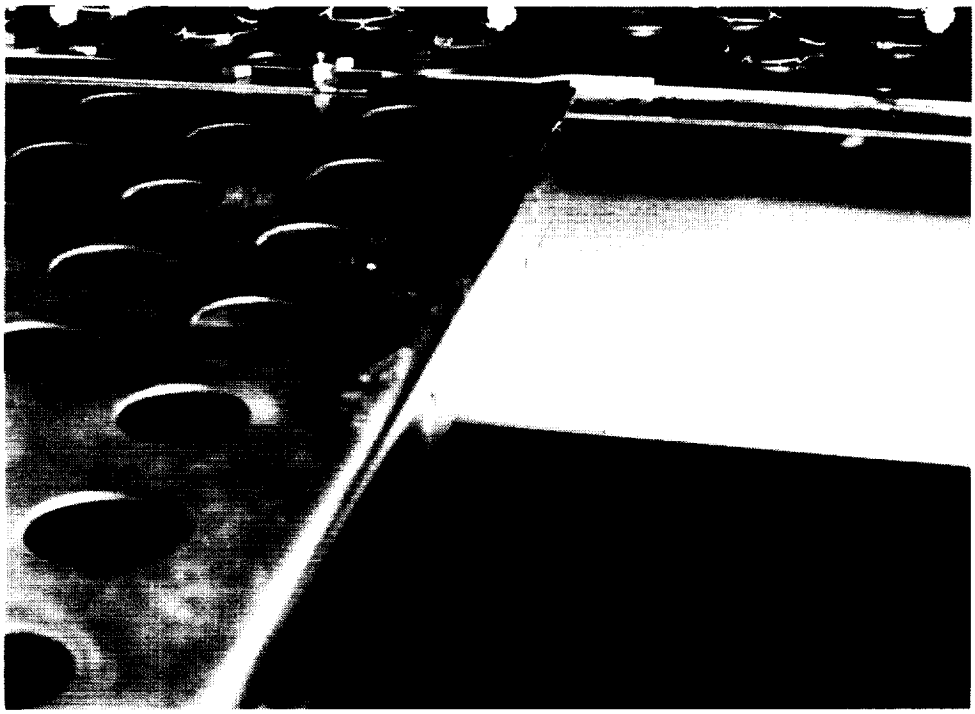

Figure 11: Missing Valves on the Tray Deck

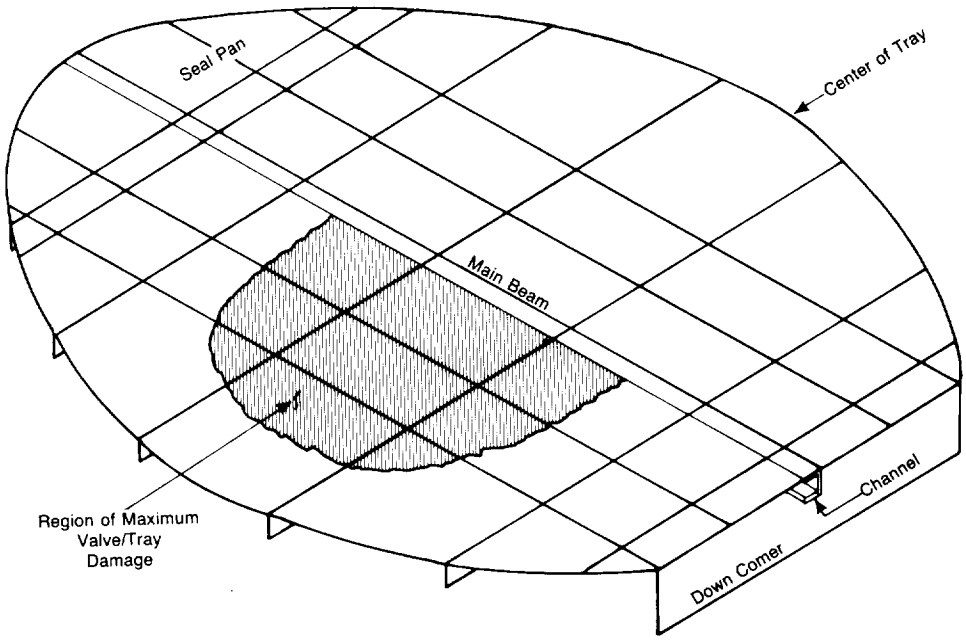

Figure 12: Oblique View of Tray Showing the Region of Maximum Valve Damage

The missing valves as shown in Figure 11 allow vapor to bypass the liquid thus decreasing the vapor-liquid interaction and thus the tray efficiency. This was the first time this type failure had ever been encountered at the Tennessee Eastman Company. This was due to two factors: (1) Nearly all columns up to this time had diameters less than 10 ft., and (2) this tray design was quite flexible compared to most designs. In any event the tray manufacturer was contacted to correct the problem.

The vendor recommended some small changes to the minor beams. Again the cross-flow trays failed during start-up. Subsequently, they recommended using small stiffeners perpendicular to the minor beams. The results were the same. By this time a finite element model had been developed by hand; i.e., hand sketches, keypunch forms and card decks. This model indicated that the above structural modifications changed the tray natural frequency less than 2%. This was definitely not enough to uncouple the system; i.e., to de-tune it. To appreciably change the first natural frequency of such a structure requires either a significant change in stiffness or mass; i.e., a significant change in the stiffness to mass ratio.

The basic philosophy used to substantially increase the first and second natural frequencies was to significantly increase the tray stiffness with only minor increases in mass. By this time it was obvious TEC was on the cutting edge of tray structural design and analysis technology. The vendor did not accept our final recommendations. However, we proceeded with the modifications as described on the subsequent pages.

Analytical Results

The original model was shown in Figure 6. The first mode is shown in Figure 13. The frequency associated with this mode varies from 16 cps to 18 cps depending on the effective liquid depth on the tray. The mode shape shown in Figure 3 actually looks more like a second mode. However, a careful review of the tray support structure explained the skewed (non-symmetric) shape of this mode. It was due to the use of a channel support beam which resulted in a non-symmetric stiffness distribution relative to the central axis of the tray. If a symmetric beam (I-beam, etc.) located at the center line of the tray had been used then the mode shape would have been symmetric relative to the direction of flow; i.e., about the X axis. Of course the mode would obviously not be symmetric relative to the center of the tray along the Y axis since it is neither stiffness symmetric nor mass symmetric relative to the Y axis; i.e., the Y-Z plane. It is also interesting to note that the ratio of the maximum modal displacements from one side of the main beam to the other is 5.6 to 1. The modal acceleration and thus the inertial loads experienced by the valves also varies by a factor of 5.6 from one side of the main beam to the other; i.e., the forces on the valves are 5.6 times as great in the region opposite the open side of the channel. This would mean valve failures and tray deck damage would occur first and be the most severe on this side of the main beam. This is exactly what visual inspection of the damaged trays had revealed. See Figures 7, 11 and 12.

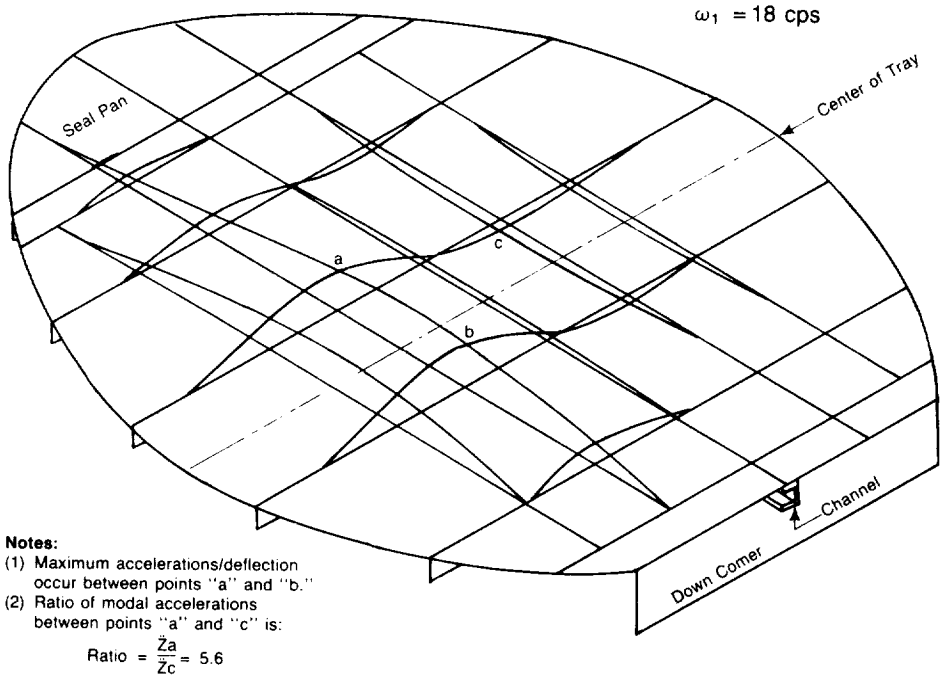

Figure 13: First Mode of the Original Tray Design

Based on these analytical results two structural modifications were investigated. The first consisted of attaching rather large angle stiffeners at two locations perpendicular to the main beam. This increased the first natural frequency substantially; i.e., from 18 cps to 34 cps. This configuration and the first mode shape are shown in Figure 14. As shown in Figure 14, this mode shape is quite symmetric. This is because the combined stiffness of the angles was about the same as that of the channel. However, for process reasons the depth of these angles was such that it would impede the vapor liquid interaction on the tray deck below. Past experience had shown that beams perpendicular to the direction of the liquid flow served to decrease the effective distance between trays (tray spacing) which would decreases the process capacity of the trays.

The next alternative considered involved using smaller angle stiffeners and changing the main beam from a channel to an I-beam. The moment of inertia of the channel was $I_{YY} = 6.29$ in^4 while that of the replacement I-beam was $I_{YY} = 38.25$ in^4. The first natural frequency increased from 16 to 18 cps to 49 cps. The associated mode shape is shown in Figure 15.

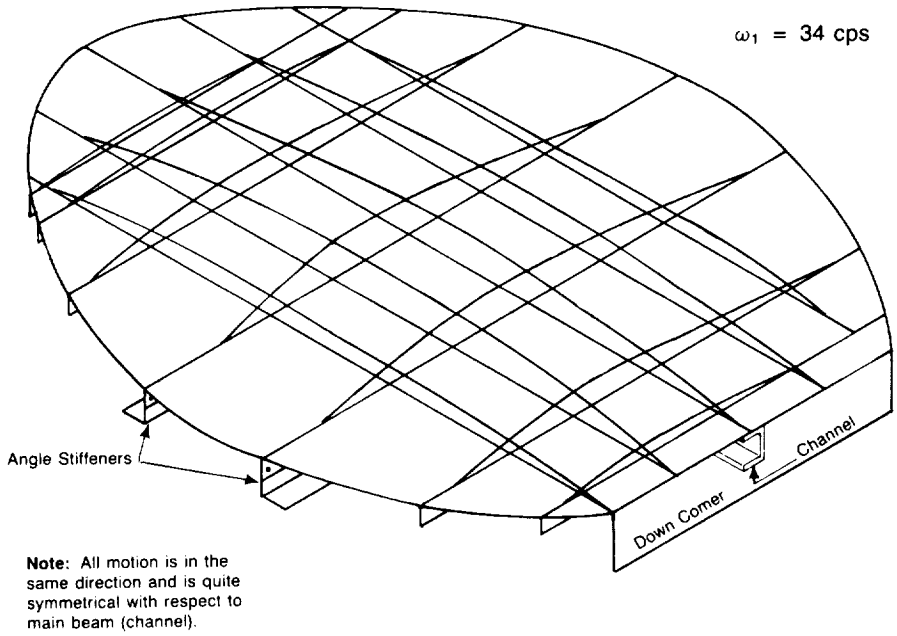

Figure 14: First Mode Shape of Tray Modification A

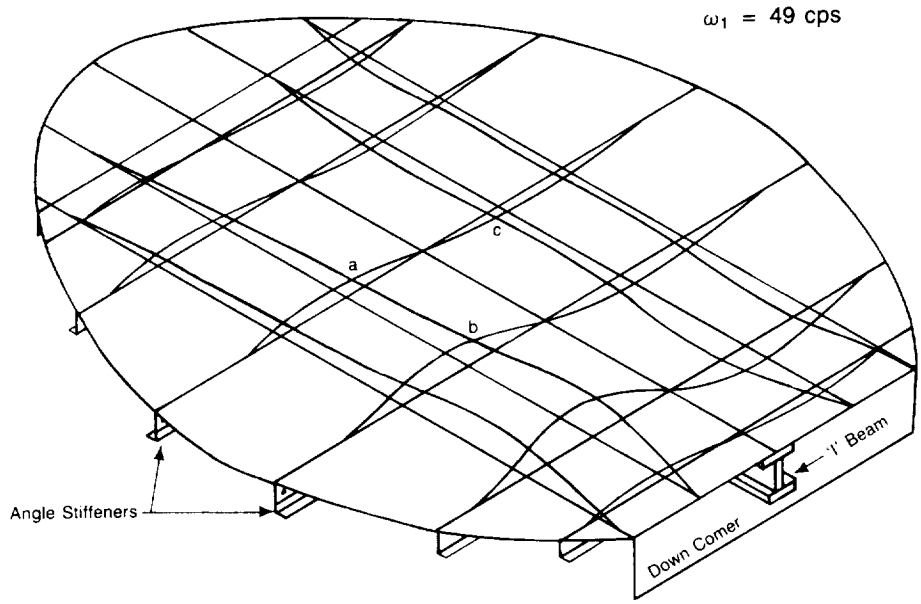

Figure 15: First Mode Shape of the Final Modified Tray

The mode shape shown in Figure 15 is still not symmetric even though a symmetric I-beam was used. Again, it looks like a second mode. The reason the first mode is still not symmetric is because the beam had to be set off-center to match-up with existing fastening points on the tray deck. Thus the tray stiffness relative to the X-axis is still not symmetric. At this time, a larger than needed I-beam was used because we did not know the nature of the forcing functions involved. In any event, this corrected the resonant problem.

At a later date, after the structural modifications had been installed, special instrumentation was installed across several trays to measure pressure fluctuations. Depending on the process conditions; i.e., the liquid and vapor flow-rates; the measured process pulsations varied from 16.75 cps to 17.75 cps. This was within the range of the calculated first structural natural frequency range of 16 to 18 cps. Indeed we had a resonance. It had been reported by several persons working near the column that it sounded like a beehive during attempted start-ups; i.e., a very high frequency chatter. In any event, this problem led to the structural parameter study.

RESULTS OF THE STRUCTURAL PARAMETER STUDY

The dynamic analysis of various diameter distillation trays shows that the first and second structural natural frequencies decrease with increasing diameter. This result is shown in Figure 16 as a scatter band around the mean values. The scatter band indicates that the natural frequencies vary somewhat depending on the liquid depth; i.e., depends on non-structural mass variations. See Appendix V for additional mode shapes associated with the parameter study.

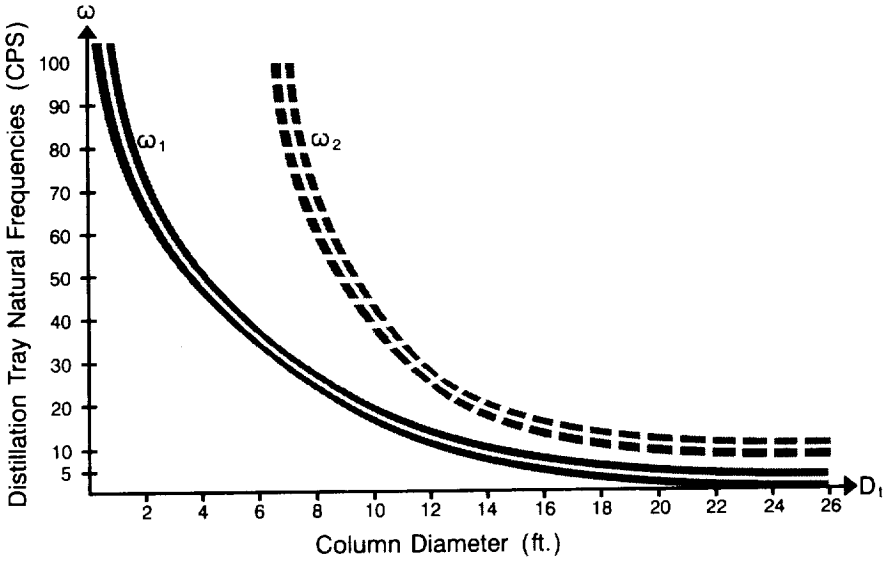

Figure 16: The First and Second Tray Natural Frequencies Versus Tray/Column Diameter

Figures 5 and 16 are combined in Figure 17. It is evident from this figure that at some diameter the frequency of the first or second tray mode has a high probability of coinciding with (being the same as) the auto-pulsation frequency thus producing a resonant condition. Experiences at Tennessee Eastman Company as well as at other petrochemical plants throughout the world agree with this region of maximum incidence of resonance; i.e., at tray diameters between 8 ft. and 16 ft. (2.44 to 4.88 M) for the first mode and 12 ft. to 18 ft. (3.66 to 5.49 M) for the second mode[4]. In-the-field results indicate numerous severe/rapid distillation tray failures have been encountered in this range. However, long term fatigue failures are actually more commonly encountered in this tray diameter range. Fatigue type failures are also very prevalent at tray diameters below and above this diameter range. This is shown in Figure 17. In all diameter ranges corrosion has been a problem which in many cases has been stress corrosion cracking (SCC). One must be aware that SCC failures often mimic fatigue failures. Thus, one should always have a metallurgical analysis performed when tray cracking is observed to determine if the culprit is truly fatigue or stress corrosion cracking or a combination of SCC and fatigue.

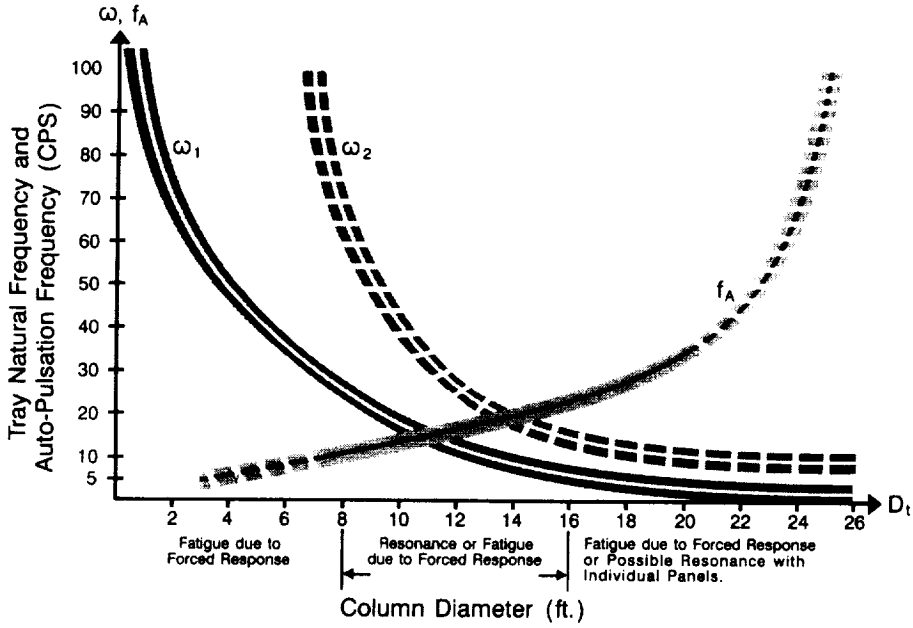

Figure 17: Graphs of the First and Second Tray Natural Frequencies and the Auto-Pulsation Frequency Versus Tray/Column Diameter

In an effort to determine the sensitivity of the distillation tray's dynamic and static response to the various structural parameters studied, a regression analysis using all of the analytical data was performed. The resulting polynomial equations are shown in Appendix IV. These correlations can be used for "**rough**" estimates of a trays first and second natural frequencies and static deflection. They should only be used to determine if a thorough finite element analysis is needed. As a rule of thumb I would recommend that a dynamic analysis be performed or the tray structure changed if the first or second natural frequency predicted by these relationships is within 8 to 10 cps of a <u>suspected</u> process or auto-pulsation frequency.

The first tray natural frequency correlation in the 10 ft. to 12 ft. diameter range shows that diameter has the largest effect with the main beam having the next largest effect. The next most influential parameters are the minor beam with liquid level being the least influential. This simply indicates that the easiest way to substantially change the first tray natural frequency, ω_1, is to modify stiffness of the the main beam. The second would be by changing the stiffness of the the minor beams.

In the same diameter range, the second natural frequency is again most sensitive to tray diameter but the second and third parameters are the minor beams and the liquid depth. The main beam is not a factor because it acts as a nodal line or neutral line for the second mode. Modifying the minor beams is the best way to change the second natural frequency, ω_2.

In the 12 ft. to 15 ft. range, again diameter is the most influential parameter on the first tray natural frequency, ω_1. Next is the main beam. In this diameter range the liquid level has a much greater effect. The minor beam effects are relatively insignificant since this parameter, I_S, does not show up in the relationship. Again, the most effective way to change the first natural frequency is to modify the main beam, I_B.

As in the previous situation, the second natural frequency, ω_2, is most sensitive to diameter with the minor beams and liquid depth being the next most significant parameters. As expected the major beam has very little effect. Thus modifications of the minor beams is the most effective way to change the second tray natural frequency in the 12 ft. to 15 ft. range.

A similar correlation for static deflection in the 10 to 12 feet range shows diameter has the largest affect followed by the main beams and minor beams. Of course, to reduce the tray deflection at any given diameter one would increase the stiffness of either or both the main beam and/or minor beams.

A special correlation indicating the percent of the total tray load carried by the main beam is also presented. As one would expect increasing the stiffness of the minor beams reduces the percent load carried by the main beam since this serves to transmit more of the load to the support ring which is welded to the vessel wall. Thus increasing the stiffness of the minor beams serves to reduce the relatively high loads that exist where the main beam attaches to the vessel wall.

Discussion of Other Type Tray Structural Failures

As indicated previously, longer term fatigue failures are a more common mode of tray failure. This is indicated at the bottom of Figure 17. In many processes the action on the tray decks is quite violent; i.e., there are large pressure variations across the trays. Fortunately this usually does not result in a resonant condition. Instead, the tray is subjected to forced response which leads to long term fatigue failures. Examples of such failures are shown in Figures 18 and 19. An indication of the violent action and resulting large deflections is shown in Figure 20. Note that there are washers in the cracks between tray panels. These washers could not be pulled out. They were wedged in the cracks between tray panels. This indicates the presence of large tray deflections. Of course all of the hardware laying on the tray deck was shaken loose from the above trays by the violent pulsations existing in this particular column. Fortunately, many distillation trays operate in relatively mundane environments and never experience such failures.

In the diameter range greater than 15 feet, trusses are generally used for structural support. See Appendices I, II and III. In the diameter range exceeding 20 feet, two tray decks may be

supported from the same truss or trusses. In this diameter range, a possible resonant condition with a portion of a tray is possible. However, again, the most likely failure mode is fatigue with corrosion often being a problem.

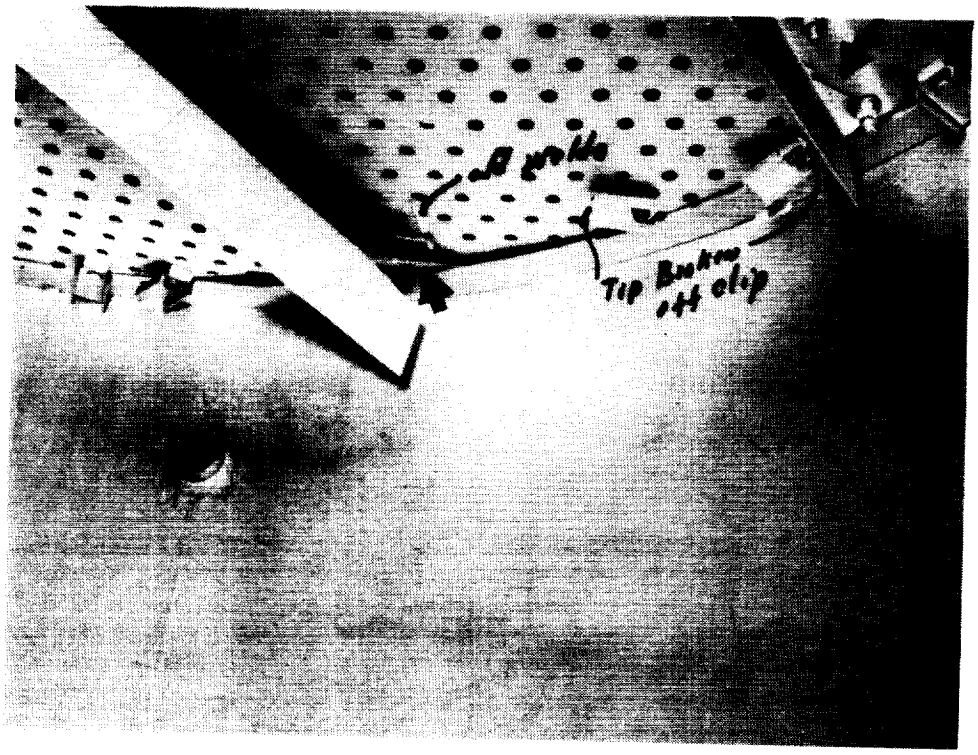

Figure 18: Typical Tray Fatigue Failure (Severe)

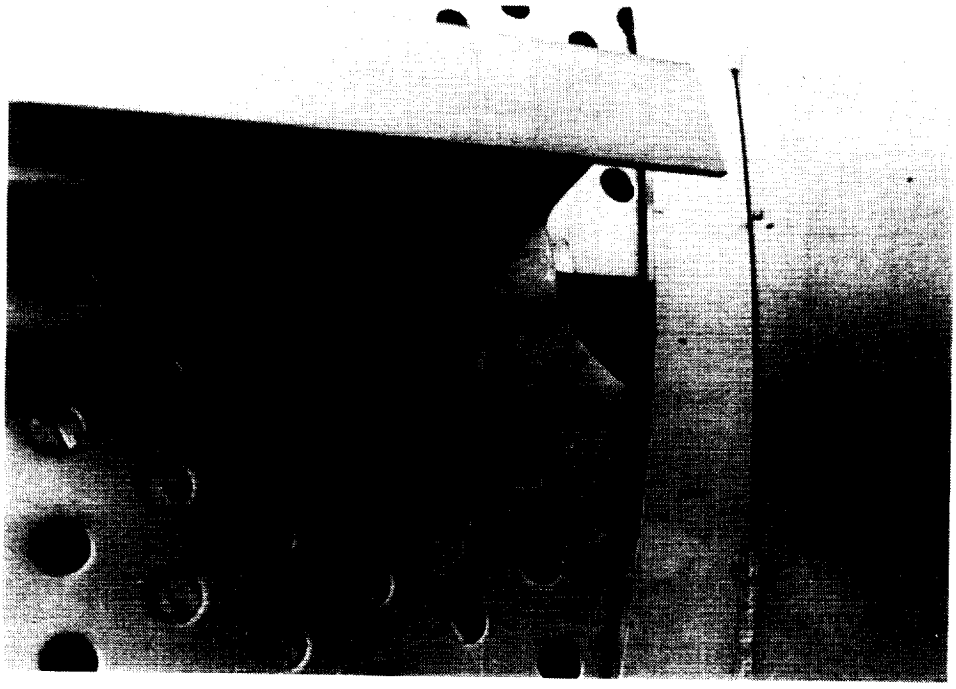

Figure 19: Typical Tray Fatigue Failure (Local)

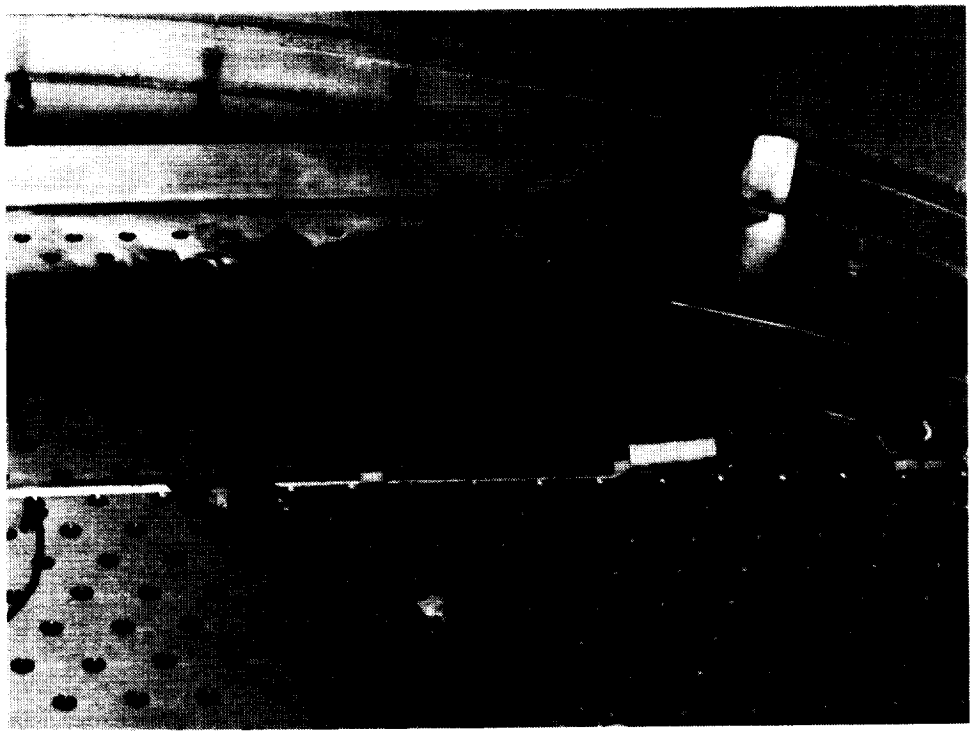

Figure 20: Evidence of Large Tray Deflections

It should be noted that a marginal tray design from a dynamic point of view can encounter a resonant condition after several years of operation if it experiences sufficient corrosion to reduce the first or second natural frequency to the range of the auto-pulsation frequency. This has been encountered at Tennessee Eastman Company. This is another reason you would prefer to have at least a 10 cps difference between the first tray natural frequency, w_1, and any suspected process pulsation or auto-pulsation frequency. This is especially important if you may have corrosion problems; i.e., if you have specified a corrosion allowance.

Another, unfortunately too frequent failure mode is associated with sudden and severe over-pressure of the trays. Since trays are usually designed for a static load (pressure drop) of 25 to 45 psf (0.17 to 0.31 psi) a relatively small pressure pulse can blow the trays out. Such pressure pulses are generally associated with the rapid vaporization or flashing of a pool of liquid at the base of the column or near a process feedstream, a minor internal explosion or a sudden loss of vacuum. Such conditions usually occur during a process upset or during start-up or shut-down of the process. Some typical damage from such situations is shown in Figures 21 and 22.

Figure 21: Tray Damage Due to Flashing in the Base of a Column (10 ft. diameter)

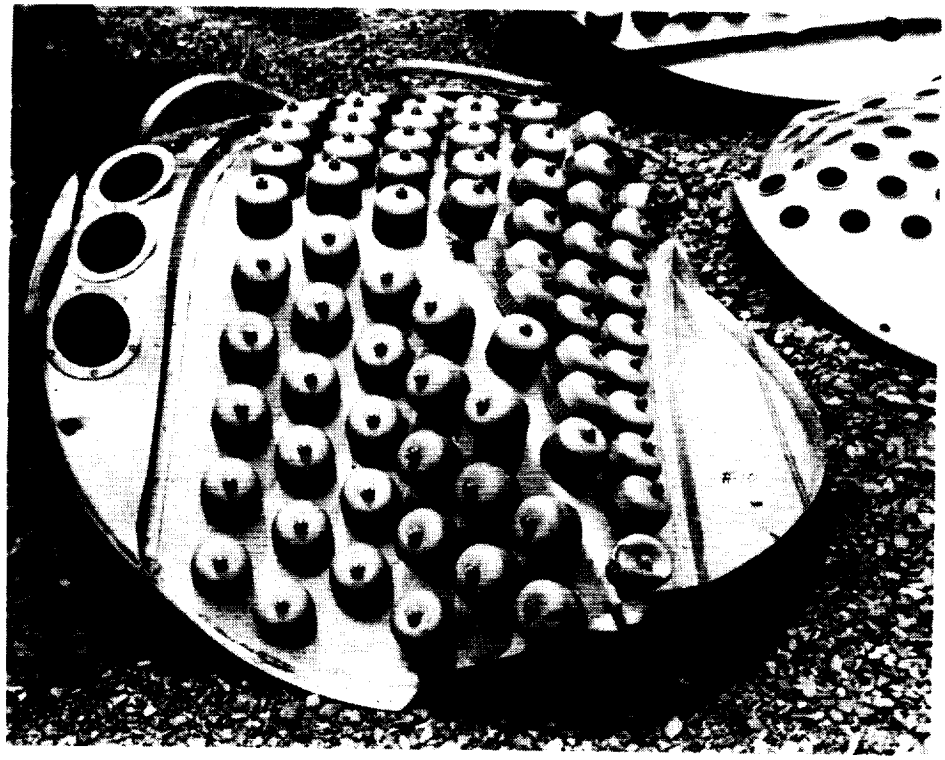

Figure 22: Severe Over-pressure of a Bubble-Cap Tray (5 ft. Diameter)

Certain sections of a column are more susceptible to such damage than others. As a result we generally increase the design load for the trays in these regions; i.e., use a design load of 90 to 130 psf. It is important to realize that the tray panels are designed such that they will come apart when subjected to a large over pressure; i.e., they serve as a pressure relief mechanism. If this was not done, then the over pressure would have to be absorbed by the vessel wall. This would in many cases rip a hole in the vessel wall. To prevent such occurrences would require much thicker vessel walls along with special reenforcements where main beams are attached to the vessel. This would substantially increase the cost of such units and adversely affect product costs. It should also be realized that the tray panels, as designed, are quite flexible and can easily be repositioned. For instance, the seemingly severe damage shown in Figure 21 was repaired within a few weeks; i.e., the trays were reassembled with very few new parts being required.

Conclusions:

This structural parameter study has shown that cross flow distillation trays in the 10 to 15 feet diameter range are susceptible to resonant conditions. It has further identified which structural parameters can be most effectively used to correct a resonant condition and reduce fatigue damage. In addition, these results can be used to prepare static design specifications that reflect dynamic requirements. This is important since many distillation tray vendors at this time do not have the capability to perform the dynamic analysis and thus cannot comply with dynamic specifications.

A future study, Phase II, will extend this cross flow distillation tray structural parameter study to a diameter range of 3 feet to 10 feet.

REFERENCES

(1) NASTRAN Users Manual (NASA SP-222), COSMIC, Barrows Hall, University of Georgia, Athens, Georgia 30601

(2) NASTRAN Programmers Manual (NASA SP-223), COSMIC, Barrows Hall, University of Georgia, Athens, Georgia 30601

(3) Priestman, G. H.; Brown, D. J.: "The Mechanism of Pressure Pulsations in Sieve Tray Columns", Institute of Chemical Engineers, Dept. of Chemical Engineering & Fuel Technology, Sheffield University, England, Trans I ChemE, Vol. 59, 1981.

(4) Priestman, G.H.; Brown, D. J.; Kohler, H. K.; "Pressure Pulsations In Sieve-Tray Columns", ICHEM.E. Symposium Series No. 56.

(5) Biddulph, M. W.; Stephens, D. J.; "Oscillating Behavior on Distillation Trays," Dept. of Chemical Engineering, University of Nottingham, University Park, England.

(6) Brierley, RJP; Whyman, PJM; Erskine, JB; "Flow Induced Vibration of Distillation and Absorption Column Trays", Imperial Chemical Industries Limited, I. Chem. E. Symposium, Series No. 56.

LIST OF APPENDICES

I. Typical Valve Trays

II. Typical Sieve Trays

III. Large Diameter Trays and Other Tray Configurations

IV. Regression Analysis of Analytical Results

V. Some Typical Mode Shapes

VI. Typical Boundary Conditions and an Example Static Load Set

APPENDIX I

TYPICAL VALVE TRAYS

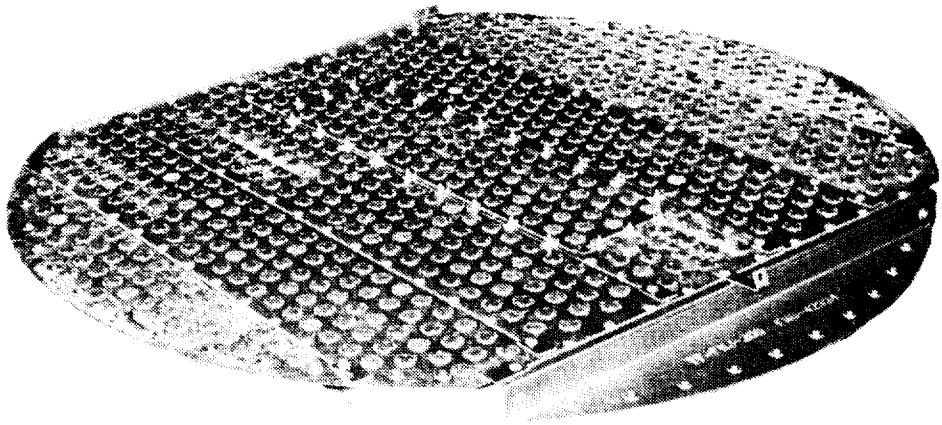

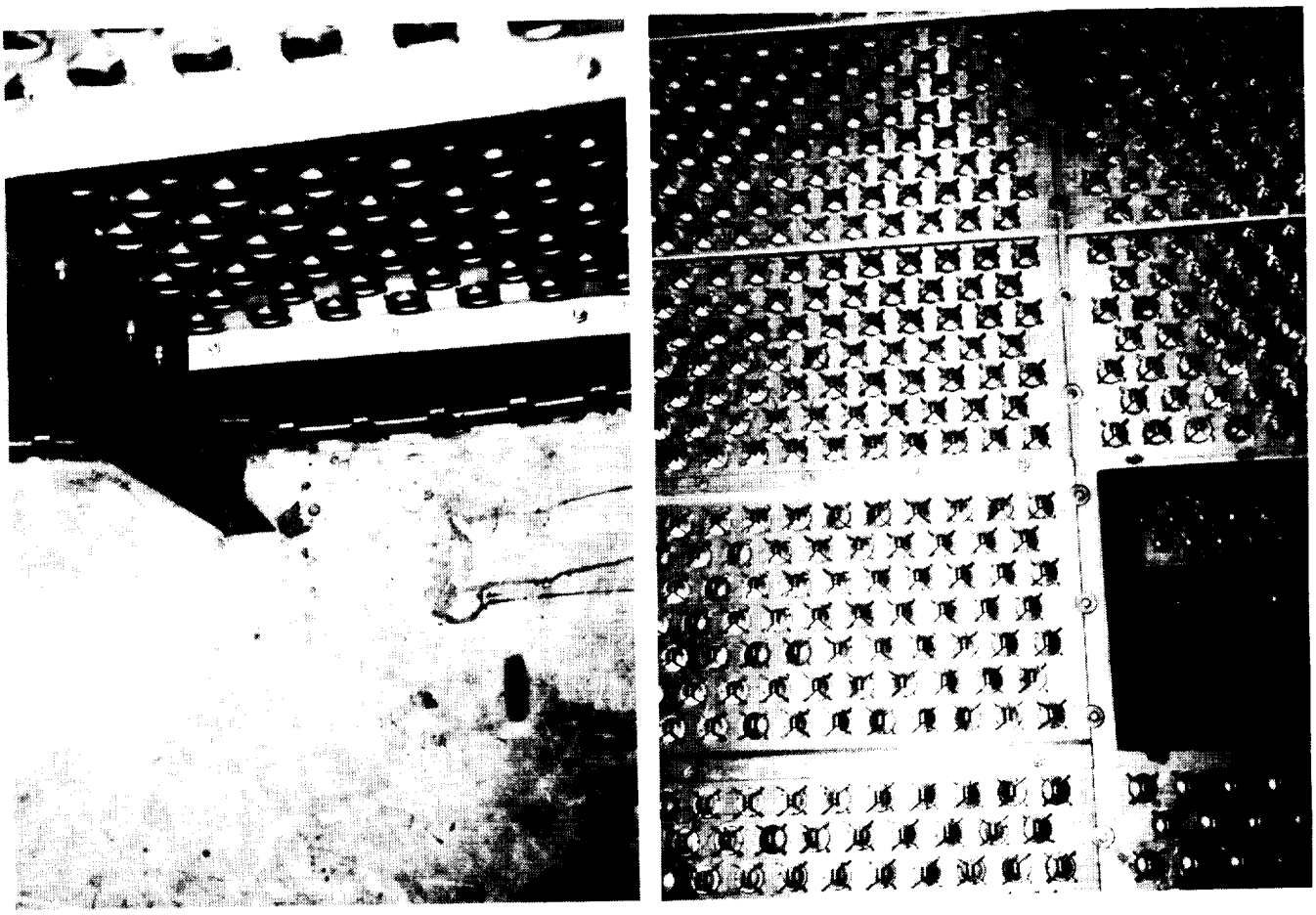

See Appendix III for Large Diameter Distillation Trays.
(D_t > 16 ft.)

ENGINEERING DRAWING OF A TYPICAL VALVE TRAYS

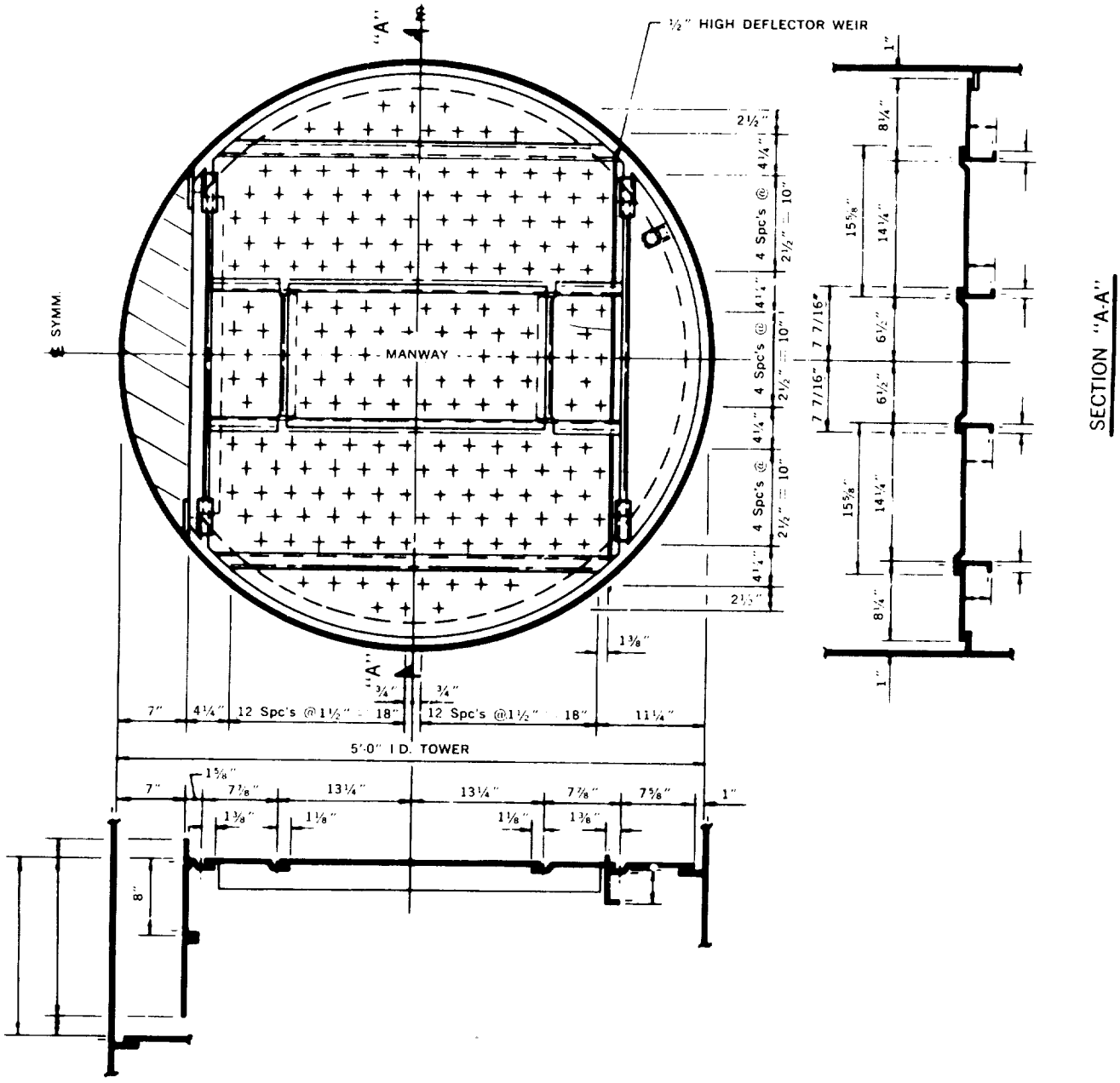

APPENDIX II

TYPICAL SIEVE TRAYS

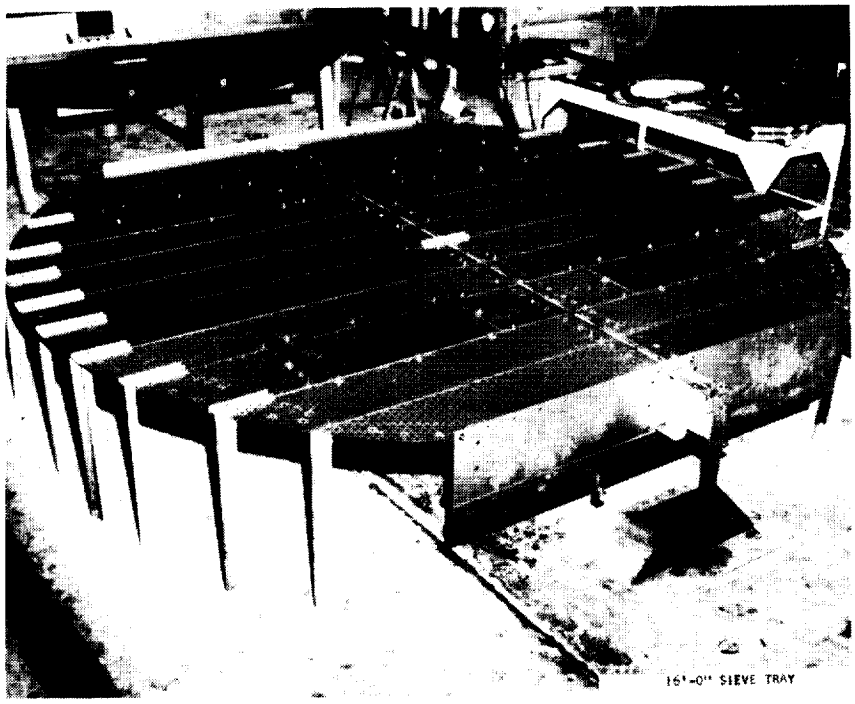

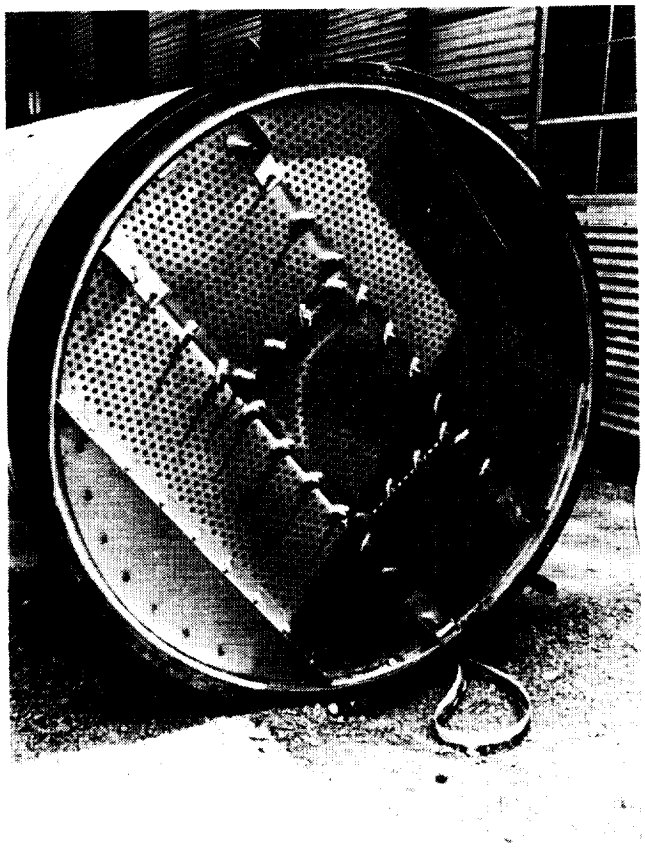

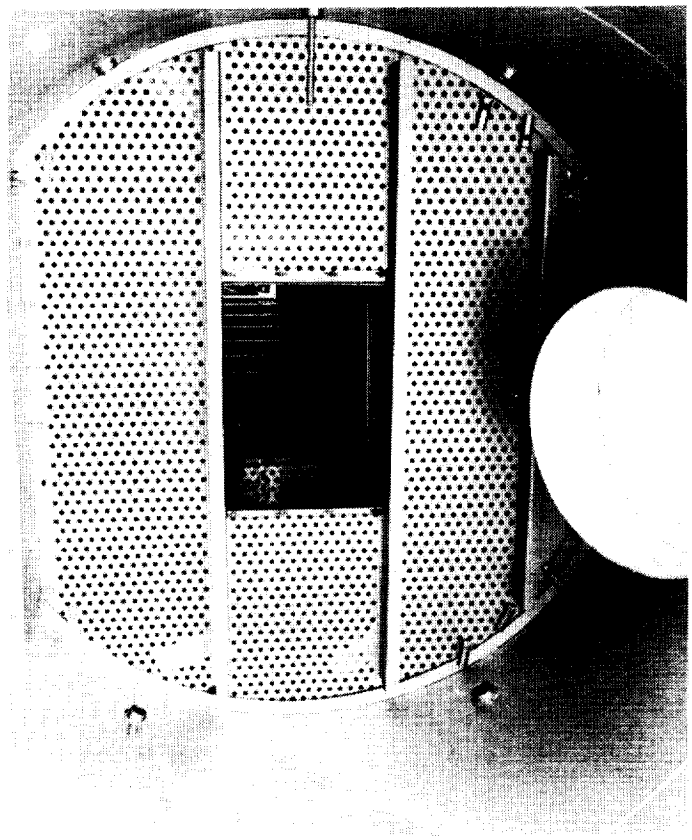

APPENDIX III

LARGE DIAMETER TRAYS AND OTHER TRAY CONFIGURATIONS

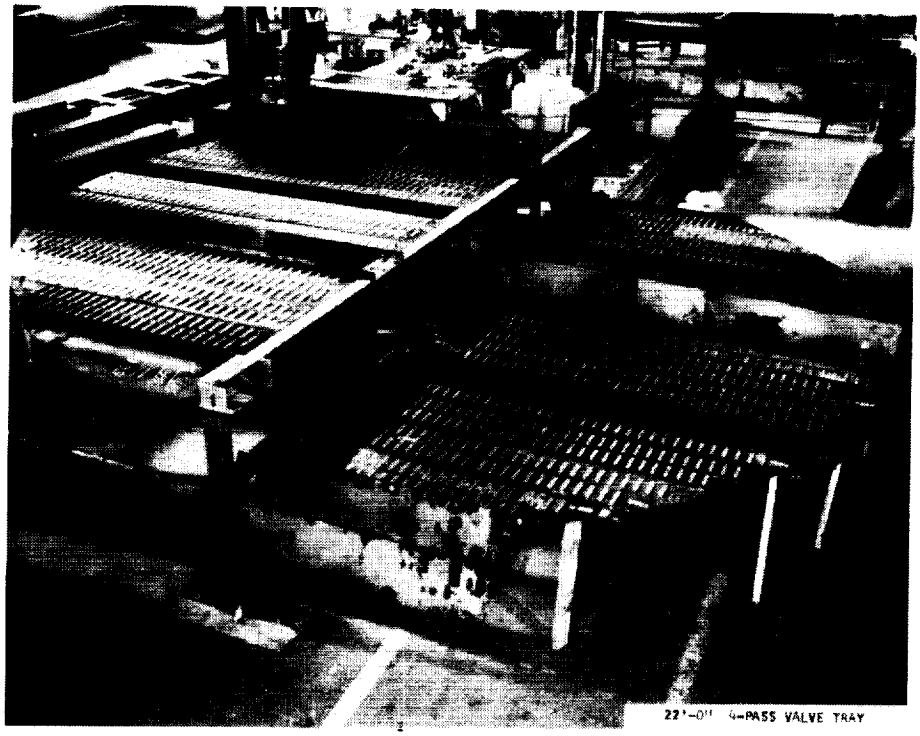

22'-0" 4-PASS VALVE TRAY

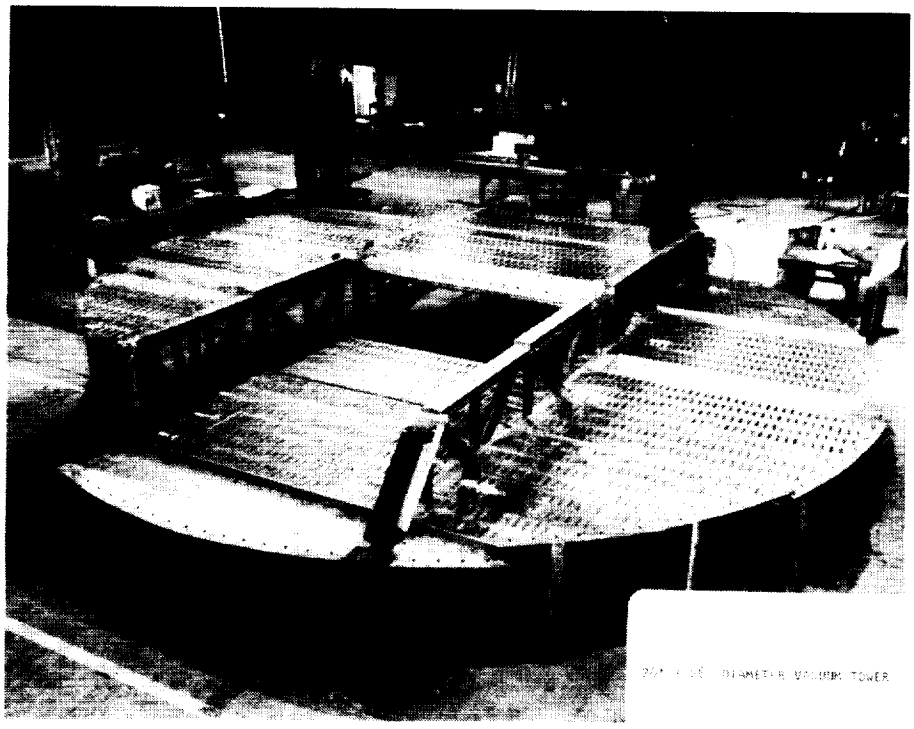

LARGE DIAMETER TRAYS AND OTHER TRAY CONFIGURATIONS

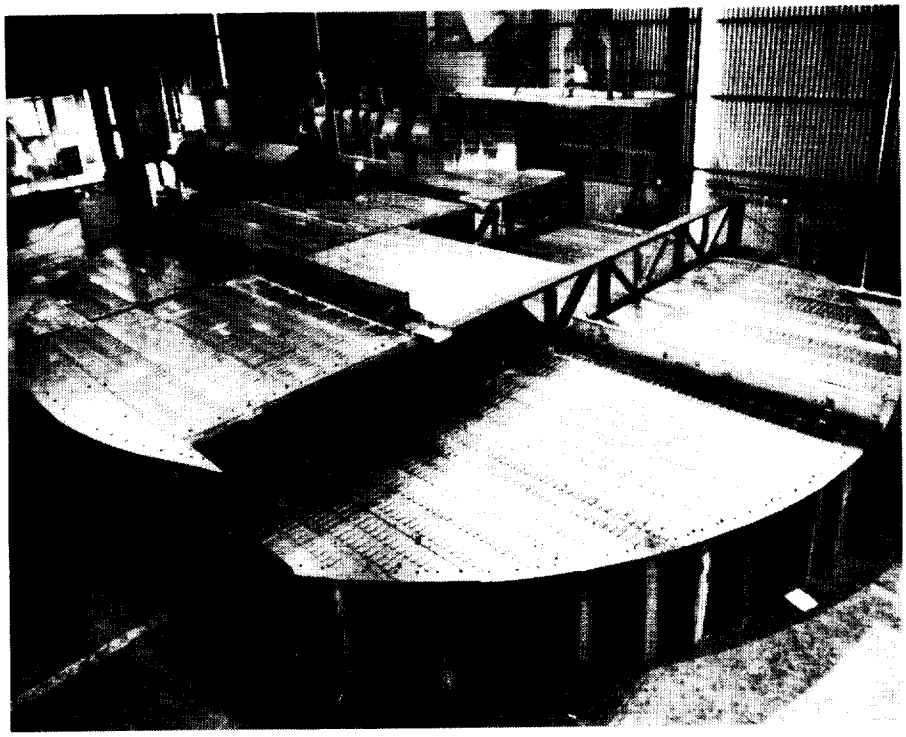

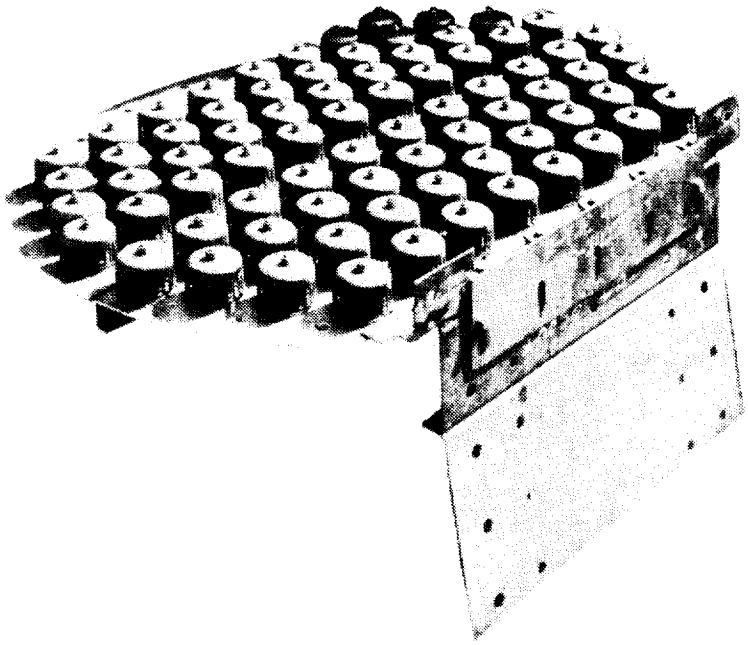

Smaller Diameter Bubble Cap Tray

APPENDIX IV

RESULTS OF THE REGRESSION ANALYSIS OF THE ANALYTICAL RESULTS

NOTE: (1) $I_S = \Sigma I_{Si}$ (In.^{4})

(2) I_{Si} = Moment of Inertia of the Small Beams (In.^{4})

(3) D_t = Tray Diameter in Feet

(4) I_B = Moment of Inertia of Main Beam (In.^{4})

(5) h_L = Liquid Depth in the Active Area (Ins.)

FOR ESTIMATING FIRST AND SECOND NATURAL FREQUENCIES (ω_1, ω_2), [cps]

$12' > D_t > 10'$

$$\omega_1 \simeq 51.6332 - 3.927D_t + .6236\ I_S + 1.6068\ I_B - .0196\ I_S^2 - .512\ I_B h_L$$

$$\omega_2 \simeq 117.416 - 7.334D_t + 3.674\ I_S + 8.733\ h_L - .0847\ I_S^2$$

$15' > D_t > 12'$

$$\omega_1 \simeq 49.947 - 3.0419D_t + .6098\ I_B - 3.3942\ h_L - .0075\ I_B^2$$

$$\omega_2 \simeq 109.26 - 6.656D_t + 3.709\ I_S - 8.386\ h_L - .088\ I_S^2$$

FOR ESTIMATING THE DEFLECTION DUE TO A UNIFORM STATIC LOAD OF 35 PSF/64 PSF (INS.)

$12' > D_t > 10'$

$$\delta_Z \simeq - .1348 + .0327D_t - .0088\ I_S - .0057\ I_B + .00025\ I_S I_B$$

FOR ESTIMATING PERCENT LOAD CARRIED BY THE MAIN BEAM

$12' > D_t > 10'$

$$\%F_B \simeq 51.78 - 2.1162\ I_S + .8379\ I_B - .0199\ I_B^2 + .0512\ I_S I_B$$

APPENDIX V

SOME TYPICAL MODE SHAPES

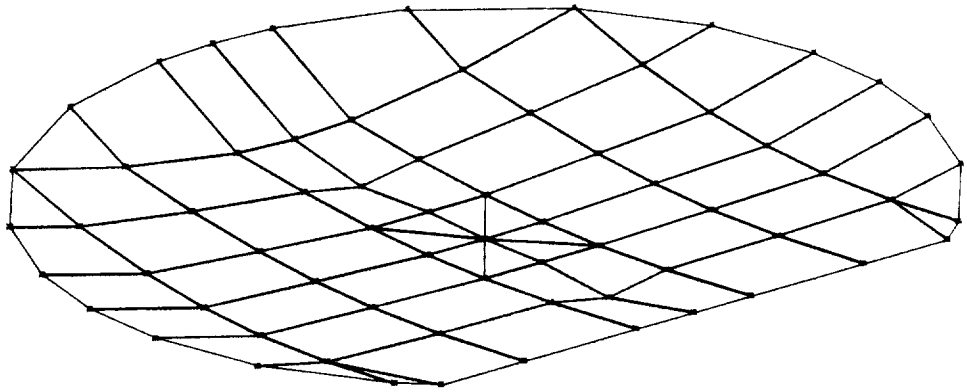

First Mode Shape

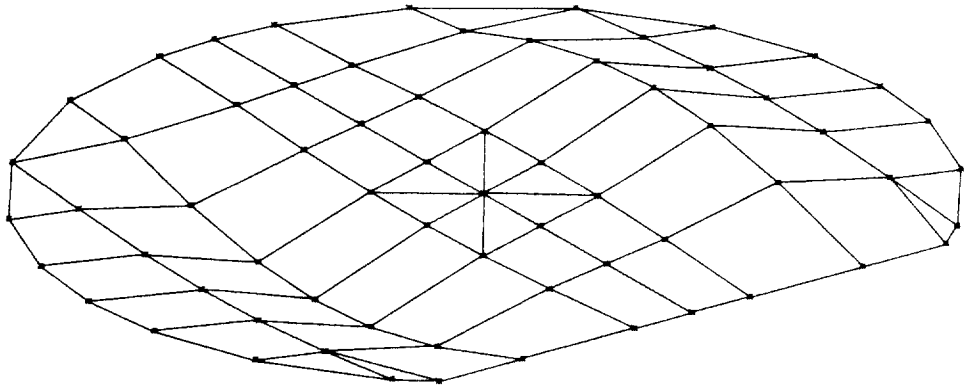

Second Mode Shape

APPENDIX VI

TYPICAL BOUNDARY CONDITIONS

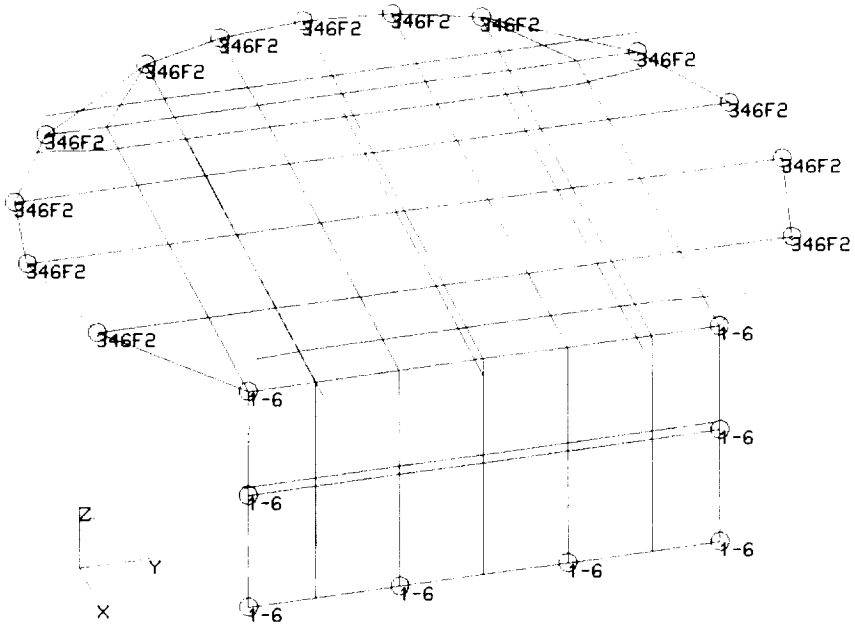

NOTE:

123 456 = XYZ R_X R_Y R_Z or RO R_R R_O R_Z
346F2 means Z R_R R_Z are constrained (Cord. 2)
1-6 means XYZ R_X R_Y R_Z are constrained

EXAMPLE STATIC LOAD SET

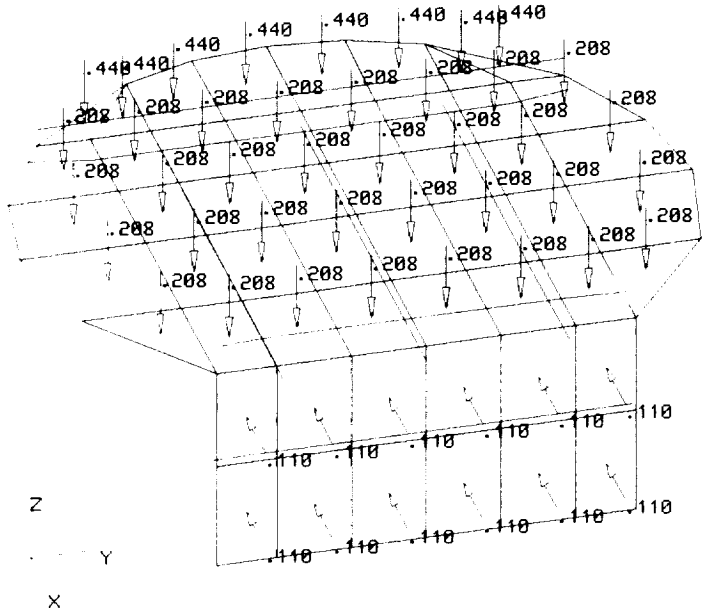

Note: Loads are in psi [0.208 psi = 30 psf, 0.440 psi = 64 psf, 0.110 psi = 16 psf].

N91-20516

EXPERIENCES WITH THE USE OF AXISYMMETRIC ELEMENTS IN COSMIC NASTRAN FOR STATIC ANALYSIS

Michael J. Cooper and William C. Walton
Dynamic Engineering Incorporated

Abstract:

This paper discusses some recent finite element modeling experiences using the axisymmetric elements CONEAX, TRAPAX, and TRIAAX, from the COSMIC NASTRAN element library. These experiences were gained in the practical application of these elements to the static analysis of helicopter rotor force measuring systems (balances) for two design projects for the NASA Ames Research Center. These design projects were the Rotor Test Apparatus, and the Large Rotor Test Apparatus which are dedicated to basic helicopter research. Both analyses involved the successful coupling of an axisymmetric balance model to a non-axisymmetric flexure model.

In this paper a generic axisymmetric model is generated for illustrative purposes. Modeling considerations are discussed, and the advantages and disadvantages of using axisymmetric elements are presented. Asymmetric mechanical and thermal loads are applied to the structure, and single and multi-point constraints are addressed. An example that couples the axisymmetric model to a non-axisymmetric model is demonstrated, complete with DMAP alters. Recommendations for improving the elements and making them easier to use are offered.

1) Introduction:

Recently, there was an opportunity to use the axisymmetric elements CONEAX, TRAPAX,and TRIAAX, from the COSMIC NASTRAN element library for the static analysis of axisymmetric structures. Modeling experience was gained in the practical application of these elements to the static analysis of helicopter rotor force measuring systems (balances). These balances resulted from two design projects for the NASA Ames Research Center. This paper addresses the experiences gained using axisymmetric elements for these programs.

Two large dynamic rotor force measurement systems were designed as part of the Rotor Test Apparatus (RTA) and Large Rotor Test Apparatus (LRTA) programs. All the force generated by the rotor blades passes through four flexure bars that constitute the critical portion of the balance. These flexures rest on a very large axisymmetric base piece and are surmounted by a relatively large axisymmetric ring and axisymmetric mast. Thus, the structure is extensively axisymmetric with a relatively small portion which is not axisymmetric.

The flexures must satisfy strength, sensitivity, fatigue, and frequency constraints. The constraints are severe and contradictory. For example, high strength implies low sensitivity. Moreover, the balance geometry imposes coupling effects that could lead to measurement errors if not properly accounted for in the calibration.

It was necessary to perform a detailed static analysis of these balance systems to demonstrate that:

1) The flexures had sufficient strength.
2) The flexures were sensitive enough to measure small loads.
3) Linear coupling of loads among the flexures were predictable and accountable.

One method of analyzing this type of structure is to generate a conventional three dimensional model using many solid, plate, and bar elements. It is possible to take advantage of symmetry about one plane and thus reduce the number of degrees of freedom. Loads would be applied directly to the mast and reactions forces would be determined at the flexure boundaries.

Some advantages of a traditional type of model are:

- Model generation is straightforward.
- Application of loads and boundary conditions is direct.
- Reactions can be determined easily.
- Force distributions in the structure in the structure are readily determined.

The traditional type of model has several disadvantages:

- Very many elements are needed to represent the structure adequately.
- It is very time consuming to generate a model.
- Incompatible elements must be connected properly (solids have 3 degrees of freedom per node, plates have 5).
- It is time consuming to execute in the computer.

An alternative approach to analyzing this type of structure is to generate an axisymmetric finite element model to represent the relatively extensive axisymmetric parts. Two, three, and four noded elements would be used to model the cross section.

The axisymmetric model has several advantages:

- Fewer number of elements is needed to represent the structure.
- Much less time is required to generate a model.
- Less computer time needed to execute the program.

Some disadvantages of axisymmetric models are:

- Models of axisymmetric and non-axisymmetric portions are not currently compatible in NASTRAN.
- There are restrictions on the element connectivity.
- It is difficult to interpret results.

Since everything about the balances (except the flexures) was axisymmetric, it was decided to take advantage of the symmetry and generate axisymmetric models. The initial approach was to constrain the model at the load points and load the model at the flexure locations, which required only axisymmetric models to be generated. By using the principle of reciprocity, the reactions at the flexure locations (flexure loads) could be determined. The flexure deformations and internal loads were to be computed separately.

This approach was abandoned after it was realized that an axisymmetric model could be combined with a non-axisymmetric model by properly adding the stiffness matrices of each model. This idea was successfully applied to the analysis of each of the balances mentioned above. It is this approach that will be explained later in this paper.

2) Discussion of an axisymmetric finite element model:

A discussion of an axisymmetric finite element model is appropriate before the coupling approach is described. Information concerning axisymmetric element modeling can be found in sections 1.3.6.1 and 1.3.7.1 of the COSMIC NASTRAN User's manual, and sections 4.1, 5.9, and 5.11 of the COSMIC NASTRAN Theoretical manual.

The solution process for axisymmetric models involves expressing the displacements in terms of harmonic (Fourier) coefficients. Axisymmetric finite element models must have the AXIC card in the bulk data to flag NASTRAN that this is an axisymmetric model. The AXIC card specifies the number of harmonics to be used.

Grid points are defined on RINGAX cards which specify the radial (r) and axial (z) coordinates. These are not points in space but circumferential rings. The azimuthal location on the ring is specified by the coordinate θ.

There are three types of axisymmetric elements that can be used with non-axisymmetric loads. These are the two noded conical shell element, CONEAX, the three noded triangular solid element, TRIAAX, and the four noded trapezoidal solid element, TRAPAX. These elements are shown in figures 1a, 1b, and 1c.

The CONEAX element can have five degrees of freedom associated with each ring. These are radial displacement, $u(\theta)$, lateral displacement, $v(\theta)$, axial displacement, $w(\theta)$, rotation about the azimuth, $\Phi(\theta)$, and rotation about the radius, $\Psi(\theta)$. The TRIAAX and TRAPAX elements have three translational degrees of freedom associated with each ring, $u(\theta)$, $v(\theta)$, and $w(\theta)$.

The geometric properties for the conical shell element are defined on a PCONEAX card. These are membrane thickness, transverse shear thickness, and moment of inertia per unit width. There are no geometric properties associated with the triangular and trapezoidal solid elements. The material reference and stress recovery locations are defined on PTRIAAX and PTRAPAX cards.

Material properties are specified on MAT1 cards in the usual way.

Boundary conditions can be specified directly on RINGAX cards or alternatively, on SPCAX cards. Displacements specified on the RINGAX cards are constrained for all harmonics. On SPCAX cards specific harmonics of a displacement are specified to be constrained. RINGAX and SPCAX cards make it possible to constrain entire rings but not to constrain a specific point on the ring. Constraining a single point on a ring can be effected by use of multi-point constraints as will be subsequently discussed.

Multi-point constraints are designated on MPCAX cards. In addition to specifying the degree of freedom and a coefficient, MPCAX cards require the harmonic to be specified. Multi-point constraints are discussed in further detail in the section that addresses mixed models.

Point forces are applied to the model with FORCEAX cards. For harmonic zero loads it is the generalized load that is specified, not the distributed load (i.e. F = 2πRf where R is the radius, and f is the distributed line load.) For higher harmonic loads the generalized load is consistent with the definition of the Fourier coefficients (F = πRf).

Point moments are defined only for conical shell elements and are applied with MOMAX cards. Thermal loads are applied using TEMPAX cards.

POINTAX cards are used to compute the total displacements at various points around the azimuth.

The SPC set, MPC set, and LOAD set are called out as usual in the case control portion of the NASTRAN input file. In addition to these set identifications, the number of harmonics participating in the solution is listed on a HARMONICS card.

For conventional models, the nodal displacements and rotations become the degrees of freedom in the solution. However, for axisymmetric models, the nodal displacements are expanded in terms of Fourier series. The coefficients of the Fourier series are called harmonic coefficients, and it is these coefficients that become the degrees of freedom in the solution.

$$u(\theta) = u_0 + \sum_{n=1}^{N} u_n \cos(n\theta) + \sum_{n=1}^{N} u^*_n \sin(n\theta)$$

$$v(\theta) = v^*_0 + \sum_{n=1}^{N} v_n \sin(n\theta) - \sum_{n=1}^{N} v^*_n \cos(n\theta)$$

$$w(\theta) = w_0 + \sum_{n=1}^{N} w_n \cos(n\theta) + \sum_{n=1}^{N} w^*_n \sin(n\theta)$$

The series are subdivided further into symmetric and anti-symmetric displacements with respect to the $\theta = 0$ plane. The User's Manual refers to the symmetric and anti-symmetric series as the "unstarred" and "starred" series respectively. The "starred" series is indicated by the asterisk in the above equations. A complete solution to an arbitrary problem consists of both "starred" and "unstarred" solutions. The type of solution is specified on an AXISYM card, either "cosine" (unstarred) or "sine" (starred). These cannot be executed at the same time; these must be separate jobs. The results must be combined external to NASTRAN.

The trapezoidal ring element has some limitations in defining its connections. The four corner rings that define the element must be numbered counterclockwise. The bottom and top edges (R1 to R2, and R3 to R4) of the element must be parallel to the radial axis. The triangular ring element must have its corner rings specified counterclockwise. These limitations are not prohibitive, but they must be recognized in the planning stage.

Axisymmetric elements are not compatible with conventional elements in the COSMIC NASTRAN library. All the card images that can be used in an axisymmetric analysis are listed in the User's Manual on the page that describes the AXIC card (page 2.4-12). Nonetheless, the static solution uses rigid format 1 to assemble stiffness and load matrices, apply boundary conditions and multi-point constraints, solve the equations, and compute forces and stresses. This is because the NASTRAN Preface sets up an internally compatible numbering system. BANDIT is not used in this procedure.

The standard displacement output format is available to the user, but, the displacement output consists of the harmonic coefficients. Total displacements can be obtained at selected azimuthal positions specified on POINTAX cards.

Only the bending and shear forces are computed for the conical shell element. These include the bending moment about the azimuthal axis, bending moment about the radial axis, and the twisting moment. Also the radial and hoop shear forces are computed.

The radial, circumferential (hoop), and axial forces are computed at each ring location for the solid axisymmetric elements.

These force quantities are output in harmonic form, that is, they are essentially harmonic coefficients of a Fourier series of the force distribution. The 0^{th} harmonic term has a multiplier of $2\pi R$ and higher harmonics have a multiplier of πR. Additionally, the total force is computed at the locations around the azimuth which were specified on the PCONEAX card, PTRIAAX card, or PTRAPAX card.

The element stresses computed for the conical shell elements are the radial normal stress and the hoop normal stress, which include bending stresses, and in-plane shear stress. The element stresses computed for the solid axisymmetric elements are the three normal stresses, radial, hoop, and axial, and three shear stresses. Like the forces, all these stresses are output in harmonic form, but are summed for locations around the circumference that are specified on the property cards.

3) Discussion of the Finite Element Models:

Several finite element models were generated to illustrate the use of axisymmetric elements.

A simple thin-walled cylinder, shown in figure 2a, was modeled in two ways: first with conical shell elements, and then with two layers of trapezoidal solid elements (figures 2b & 2c). These two models illustrate the representation of a simple axisymmetric structure.

A model of a generic rotor balance was set-up to help explain how an axisymmetric model can be coupled to a non-axisymmetric model. The balance is shown in figure 3. The relatively extensive axisymmetric parts of the structure are the upper balance ring, a conical adaptor piece, and a top plate. Four flexure posts connect the upper balance ring to the grounded base. This flexure arrangement is not axisymmetric. A mast is connected to the top plate.

The flexures and the mast were modeled separately using bar elements as shown in figure 4. The stiffness matrix from this model is combined with the stiffness matrix of the balance model to obtain a unified solution.

3a) Modeling aspects:

Some important modeling aspects need to be considered when generating an axisymmetric finite element model. Some aspects are obvious and pertain to any finite element model. Others are specific to axisymmetric element modeling.

The finite element model should be detailed enough to represent sufficiently the stiffness of the structure. When planning the finite element model keep in mind the limitations of the finite elements. Axisymmetric solid elements need to be generated in a counterclockwise fashion with the upper and lower edges parallel to the radius. Conical shell elements have an extra degree of freedom (rotation) that is not defined in the solid elements. This degree of freedom will have to be accounted for.

The model should not contain so many degrees of freedom as to become excessively time consuming to solve. The total degrees of freedom are the number of degrees of freedom per ring, times the number of rings, times the number of harmonics. So even a simple finite element model can have very many degrees of freedom if the number of harmonics is large. Currently in NASTRAN, the user is compelled to include in the solution degrees of freedom corresponding to all harmonic numbers, up to and including the highest harmonic number specified. This means that the solution may involve lower harmonics that do not participate in the response.

There should be rings positioned at key locations on the model. These locations might be places where loads are applied or the model is bounded. Rings will be needed at levels where an axisymmetric portion of the structure is joined with a non-axisymmetric part. Still other points might be locations where displacements, loads, stresses, or some other computed output is desired.

3b) Simple cylinder model:

The two thin-walled cylinder models used to illustrate an axisymmetric finite element model are briefly described here (figures 2b and 2c). The cylinder has a 86.614 mm (22 inch) radius and is 0.984 mm (0.25 inches) thick and 1.575 mm (4.0 inches) high. It is made from steel with a modulus of elasticity of 196.5 GPa (28.5×10^6 psi), and a coefficient of thermal expansion of 10.8×10^{-6} m/m°C (6.0×10^{-6} in/in-°F). The cylinder is restrained from axial growth, but not from radial growth. Two loading conditions were applied to this structure, a uniform radial pressure of 172.37×10^3 Pa (25 psi), and a uniform temperature change of 55.6°C (100 °F).

The first model of the cylinder uses 20 conical shell elements to represent the structure. The second model uses 16 trapezoidal solid elements. Five harmonics (0 through 4) were specified for both analyses (though it was known that the structure would respond to these loads in the 0^{th} harmonic only).

Boundary conditions were specified on the RINGAX cards for both models. Axial displacement "w" was constrained at the mean radius for $z = 0$.

The pressure load was applied using FORCEAX point load cards. The generalized force on one element is the pressure times the element surface area: $F = (p)(2\pi R)(\Delta z)$. Half of this total element force is distributed at the nodes. For the shell model, the mean radius, 22 inches, was used in the analysis, and for the solid model, the inside radius, 21.875 inches, was used.

The temperature load was applied using TEMPAX cards. A reference temperature of 23.9°C (75°F) was specified on the MAT1 card. A uniform temperature of 79.5°C (175°F) was specified for each ring.

3c) Results from the cylinder models:

The theoretical radial displacement and hoop stress due to pressure is computed from reference 1.

$$\Delta R = pR^2/Et = 0.006688 \text{ mm} \quad (0.001698 \text{ inches})$$

$$\sigma_{hoop} = pR/t = 15.172 \times 10^6 \text{ Pa} \quad (2200 \text{ psi})$$

where p is the applied pressure, 172.37×10^3 Pa (25 psi)
R is the mean radius, 86.614 mm (22 inches)
t is the thickness, 0.984 mm (0.25 inches)
E is the modulus of elasticity, 196.5 GPa (28.5×10^6 psi)
ΔR is the radial displacement, inches
σ_{hoop} is the hoop stress, psi

The radial displacement due to temperature load is:

$$\Delta R = R\alpha\Delta T = 0.052 \text{ mm} \quad (0.0132 \text{ inches})$$

where α is the coefficient of thermal expansion, 10.8×10^{-6} m/m°C (6.0×10^{-6} in/in-°F)
ΔT is the temperature change, 55.6°C (100 °F.)

The results are summarized in the following table where it is seen that the outcomes of finite element calculations are in precise agreement with the theory. This is certainly expected for such simple hoop like responses.

	Theoretical	Shell Model	Solid Model
ΔR,mm (in) σ_{hoop},MPa (psi) (pressure)	.006688 (.001698) 15.17 (2200)	.006681 (.001697) 15.29 (2218)	.006657(.001691) 15.12 (2193)
ΔR,mm (in) (temp)	.052 (.0132)	.052 (.0132)	.052 (.0132)

3d) Balance axisymmetric finite element model:

The upper balance ring is a five inch high, two inch thick cylinder with a mean radius of 39.37 mm (10 inches). The 1.476 mm (0.375 inch) conical adaptor section connects the balance ring to the 1.476 mm (0.375 inch) top plate, which has a hole in its center. The balance material is stainless steel.

There are 10 TRAPAX elements representing the upper balance ring, 8 CONEAX elements that model the conical adaptor piece, and 8 elements (5 TRAPAX and 3 TRIAAX) that make up the top plate. There are 39 rings and 4 harmonics specified (starting with harmonic zero). This makes a total of 591 unconstrained degrees of freedom. There are multi-point constraints between balance ring and cone, and between cone and top plate to relate the rotational degree of freedom of the conical shell elements to displacement degrees of freedom of the solid elements. Because the loads are symmetric with respect to the $\theta = 0$ plane, the cosine solution (unstarred series) is sufficient to solve the problem.

4) Mixed model procedure:

The overall approach to combining axisymmetric models with non-axisymmetric models is to compute the separate stiffness matrices, then combine them to solve the coupled problem. For this example two finite element models were generated, the axisymmetric balance model, (figure 3), and the cartesian mast/flexure model, (figure 4).

There are four steps to the procedure. DMAP alter sequences are listed in the appendix.

1) Assemble the axisymmetric balance model global stiffness matrix and output it to a file. Stop the solution process of this model at this point.

2) Specify external loads applied to the mast/flexure model and obtain the global load and stiffness matrices for both the mast and balance flexures.

3) Read the previously stored balance stiffness matrix into the mast/flexure model. Combine the stiffness matrices from both models using multi-point constraint equations to express compatibility, and solve the problem. Compute displacements and forces, and output the solution vector(s) to a file.

4) Read the solution vector(s) into the balance model. Continue the problem and compute the axisymmetric element forces and stresses.

The key to combining models is to create an array space in the cartesian model that corresponds to the size of the stiffness matrix of the axisymmetric model. This is done by adding phantom grid points to the cartesian model. (Phantom grid points are not connected to any structure; they just provide for space in the stiffness matrix.) Grid points that correspond to the non-axisymmetric structure should be removed from the solution set by OMIT cards. Grid points common to both structures are connected with MPC relations. The remaining degrees of freedom in the cartesian model should correspond exactly to those of the axisymmetric model.

For example, consider an axisymmetric problem with five harmonics specified in the solution (0 through 4) coupled to a non-axisymmetric model in cartesian space. Corresponding to a particular ring in the axisymmetric model, for instance ring number 4, there would be a set of phantom grid points in the cartesian model. These grid points would be numbered, 10004, 11004, 12004, 13004, 14004 in the cartesian model to represent the degrees of freedom of the five harmonics. Rotational degrees of freedom 4, 5, and 6 would be eliminated for all five "phantom" grid points, because axisymmetric solid elements do not have rotational degrees of freedom. Additionally, degree of freedom 2 for grid point 10004 is eliminated since it is not defined for the 0^{th} harmonic in the unstarred solution set. The remaining phantom degrees of freedom have no elements attached to them and are flagged as singularities in the solution. This is allowed because the solution process is modified by adding the stiffness matrix from the axisymmetric model. Stiffness becomes associated with each of these degrees of freedom.

This procedure is straightforward, but it has the disadvantage that file space for two very large matrices must be allocated.

Alternative approaches to combining axisymmetric and non-axisymmetric models were considered. These made use of partitioning routines to extract and combine the necessary information from the stiffness matrices. While these had the advantage of being able to choose the stiffness terms associated with specific harmonics (and thus store smaller matrices), these procedures were not as direct as the one outlined above.

4a) Multi-point constraints:

Two types of multi-point constraints are addressed here, MPC's at specific points around the azimuth, and MPC's at every point around the azimuth.

A) Specific points around the azimuth:

For example, a typical constraint equation relating a radial displacement, "u" of cartesian structure "c" to that of axisymmetric structure "a" at 33.75° around the azimuth might be, for four harmonics, as follows. (The superscript denotes the harmonic coefficient.)

$$u_c = u_a(\theta = 33.75^\circ)$$

but $$u_a(\theta) = u_a^{(0)} + u_a^{(1)}\cos(\theta) + u_a^{(2)}\cos(2\theta) + u_a^{(3)}\cos(3\theta) + u_a^{(4)}\cos(4\theta)$$

so

$$-u_c + u_a^{(0)} + .83147\, u_a^{(1)} + .38268\, u_a^{(2)} - .19509\, u_a^{(3)} - .70711\, u_a^{(4)} = 0.$$

Similar constraints are developed for each point in common.

Each flexure has all six degrees of freedom, three translations and three rotations, that must be attached to the upper balance ring. The flexures are located at convenient positions: θ = 0, 90, 180, and 270 degrees. Many coefficients are zero or unity. From basic elasticity theory, (ref 2), the cone rotations are defined as follows:

- rotation about the radial axis:

$$\omega_r = \theta_4 = \frac{1}{2}\left(\frac{1}{R}\frac{\partial w}{\partial \theta} - \frac{\partial v}{\partial z}\right)$$

- rotation about the azimuthal axis:

$$\omega_\theta = \theta_5 = \frac{1}{2}\left(\frac{\partial u}{\partial z} - \frac{\partial w}{\partial r}\right)$$

- rotation about the vertical axis:

$$\omega_z = \theta_6 = \frac{1}{2}\left(\frac{\partial v}{\partial r} - \frac{1}{R}\frac{\partial u}{\partial \theta} + \frac{v}{R}\right)$$

Derivatives with respect to the azimuthal coordinate, θ, can be carried out explicitly since the displacements are directly dependent on this variable. However, since the axisymmetric solid elements do not have explicit rotational degrees of freedom, derivatives with respect to "r" or "z" must be made numerically.

Due to the symmetric nature of the "unstarred" Fourier expansions, the azimuthal displacement of the 0 and 180 degree flexures is identically zero. Those relations specify the following:

$$v_c = v_a(\theta = 0)$$

but since

$$v_a(\theta) = v_a^{(1)}\sin(\theta) + v_a^{(2)}\sin(2\theta) + v_a^{(3)}\sin(3\theta) + v_a^{(4)}\sin(4\theta)$$

at $\theta = 0$ and 180, each coefficient is identically zero.

B) Every point around the azimuth:

The mast is modeled as a simple beam structure. It could have been modeled as an axisymmetric structure and included with the balance model. Assume for the moment that the mast is not axisymmetric. Then it could have been modeled as a three dimensional plate structure. This model would have definite grid points along the azimuth with which to connect to the axisymmetric model. Then the procedure to relate common points would be as described above.

Since the mast is modeled with bar elements, consider the following situations:

1) A uniform vertical translation of a mast rigidly connected at all locations around the azimuth has no choice but to translate the ring in a harmonic zero fashion.

2) A uniform lateral translation of the mast would cause the ring to translate laterally in a harmonic one mode.

3) A lateral rotation of the mast would cause the ring to translate vertically in a harmonic one manner.

For example, the constraint relations for grid point "c" of the cartesian structure which is rigidly attached to ring "a" of the axisymmetric structure would be:

$$u_c = u_a^{(1)}(1.0)$$

$$w_c = w_a^{(0)}(1.0)$$

$$\theta_c^5 = w_a^{(1)}(1.0)$$

4b) Results of the mixed model analysis:

Results are available to the analyst after the third step in the procedure. Cartesian displacements, forces, and stresses are computed directly in this step. Displacement harmonic coefficients of the axisymmetric model are also available. Axisymmetric model forces and stresses are computed when these coefficients are fed back to the axisymmetric model in the fourth step.

For the example problem discussed here, it is enough to examine the forces in flexures due to the applied loads. These are shown in the forces in the bar elements in output #4 in the Appendix.

5) Conclusions and recommendations:

Several conclusions about the practical use of axisymmetric elements for static analysis are made. Some recommendations for improving the elements and making them easier to use are offered.

1) Axisymmetric elements can be used to solve static problems involving axisymmetric structures with non-axisymmetric loads. Structures modeled with these elements can often be solved a good deal more efficiently than with more common elements.

However, axisymmetric elements can be intimidating to the user. This arises primarily from the (essential) use of Fourier coefficients as the degrees of freedom for axisymmetric elements. At the present level of automation in NASTRAN, skill in executing and interpreting various transformations between Fourier and Cartesian coordinates is required. Many users lack the skill to perform such transformations, and some painful experience may be involved to gain the necessary facility. Examples are lacking.

2) Restrictions on the element connectivity of the solid axisymmetric elements should be eliminated. A paper by Hurwitz, (ref 3), describes how these elements can be updated. Also, the documentation should be improved to make more clear how to prepare the input data, and how to interpret the results.

Other changes might include:

1) The capability to combine results from symmetric (unstarred) solutions with those of unsymmetric (starred) solutions.
2) The capability to specify harmonics to include or drop from the solution set.

The capability to specify harmonics would be very useful indeed. For example, trying to determine the bolt loads in an axisymmetric structure with a bolt pattern having 22 bolts is a practical problem. It is known in advance that the structure will respond in multiples of the 22^{nd} harmonic. Yet, in the analysis, harmonics 0 through 21 must be generated though those harmonic coefficients will be identically zero.

3) There is an error in the code that generates thermal loads for conical shell elements. The results (output #1 in the Appendix, subcase 2) show that for harmonic zero, the computations are correct, but there should be no higher harmonic components. This error should be corrected for the user community to have a high degree of confidence in these elements.

4) Axisymmetric models can be successfully combined with non-axisymmetric models to get unified results. A procedure for doing so is outlined above.

References:

1) Roark and Young, "Formulas for Stress and Strain", 5^{th} edition, 1975 McGraw-Hill, page 448, case 1b.

2) Adel S. Saada, "Elasticity Theory and Applications", 1974, Pergamon Press, page 141.

3) Myles Hurwitz, "Generalizing the TRAPRG and TRAPAX Finite Elements", Eleventh NASTRAN Users' Colloquium, NASA CP 2284, May 2-6, 1983, pages 76-81.

Figure 1a
Conical Shell Element, CONEAX

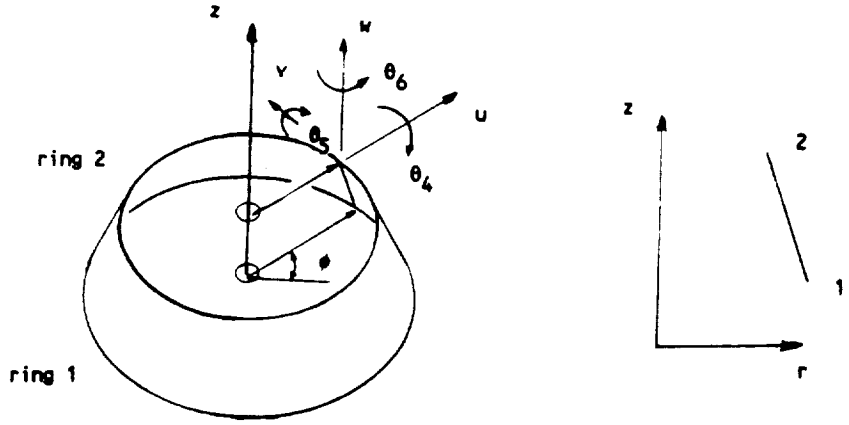

Figure 1b
Axisymmetric Triangular Element, TRIAAX

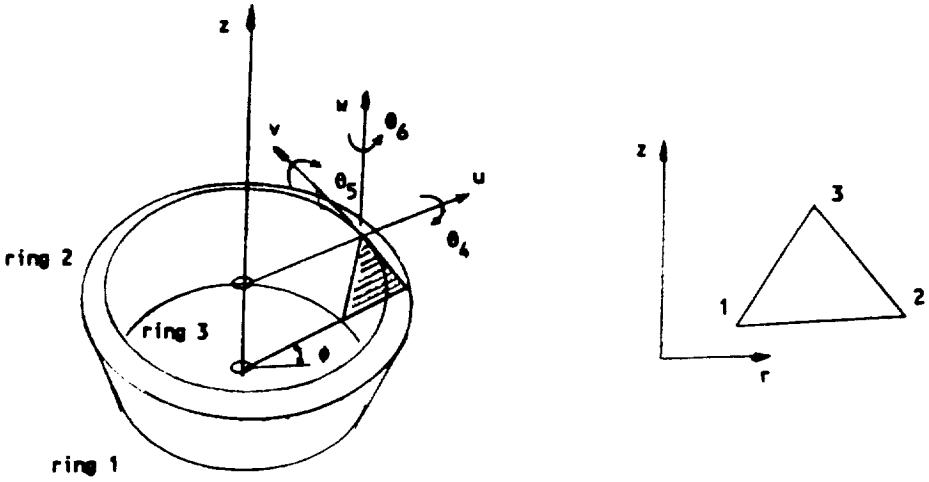

Figure 1c
Axisymmetric Trapezoidal Element, TRAPAX

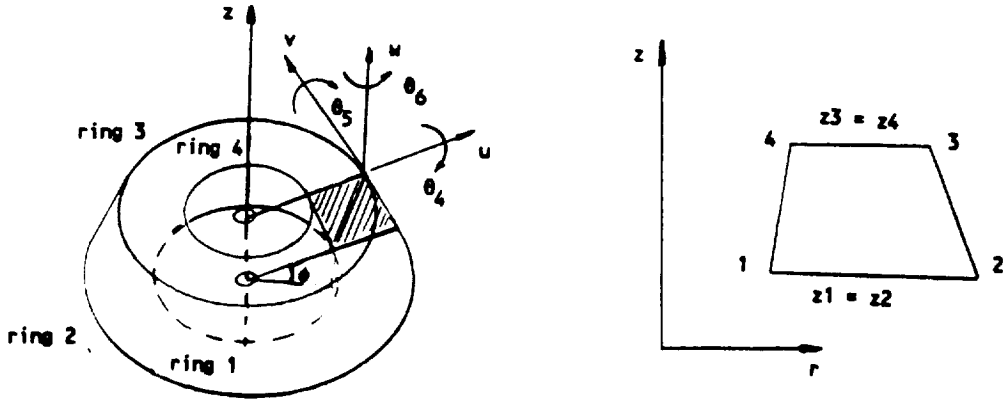

Figure 2a
Thin-walled Cylinder

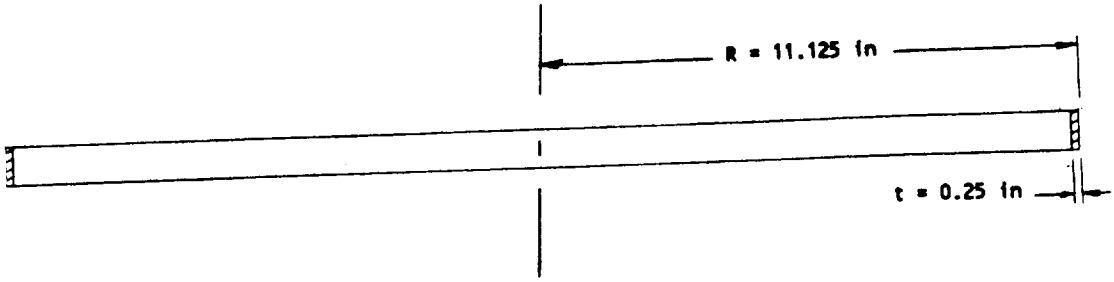

Figure 2b
Conical Shell Finite Element Model
of Thin-Walled Cylinder

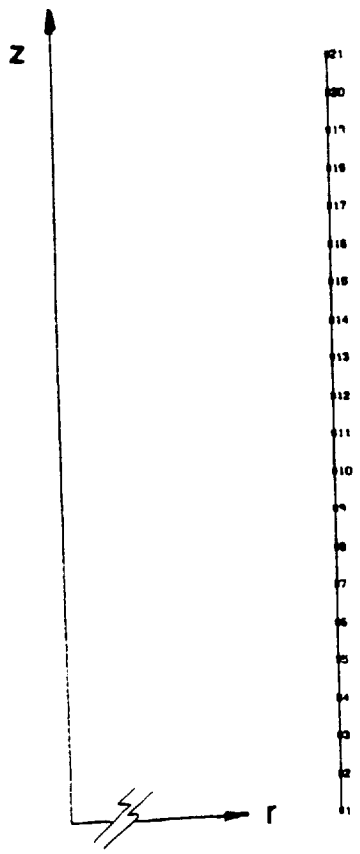

Figure 2c
Trapezoidal Solid Element Model
of Thin-Walled Cylinder

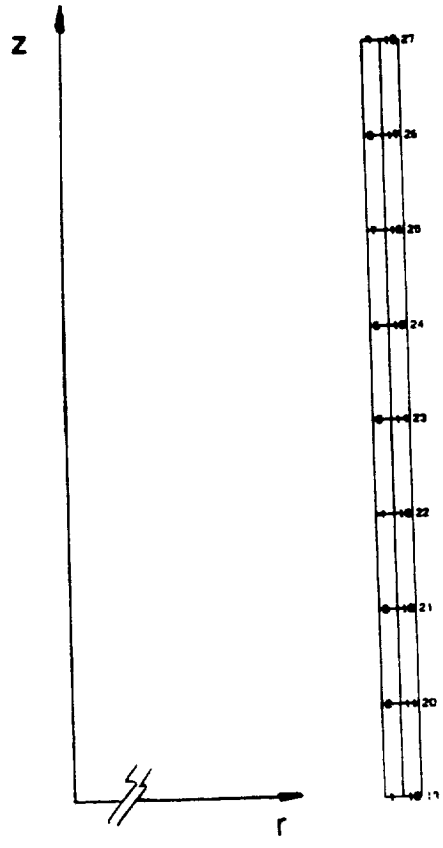

Figure 3
Sketch of Generic Balance and
Axisymmetric part of Finite Element Model

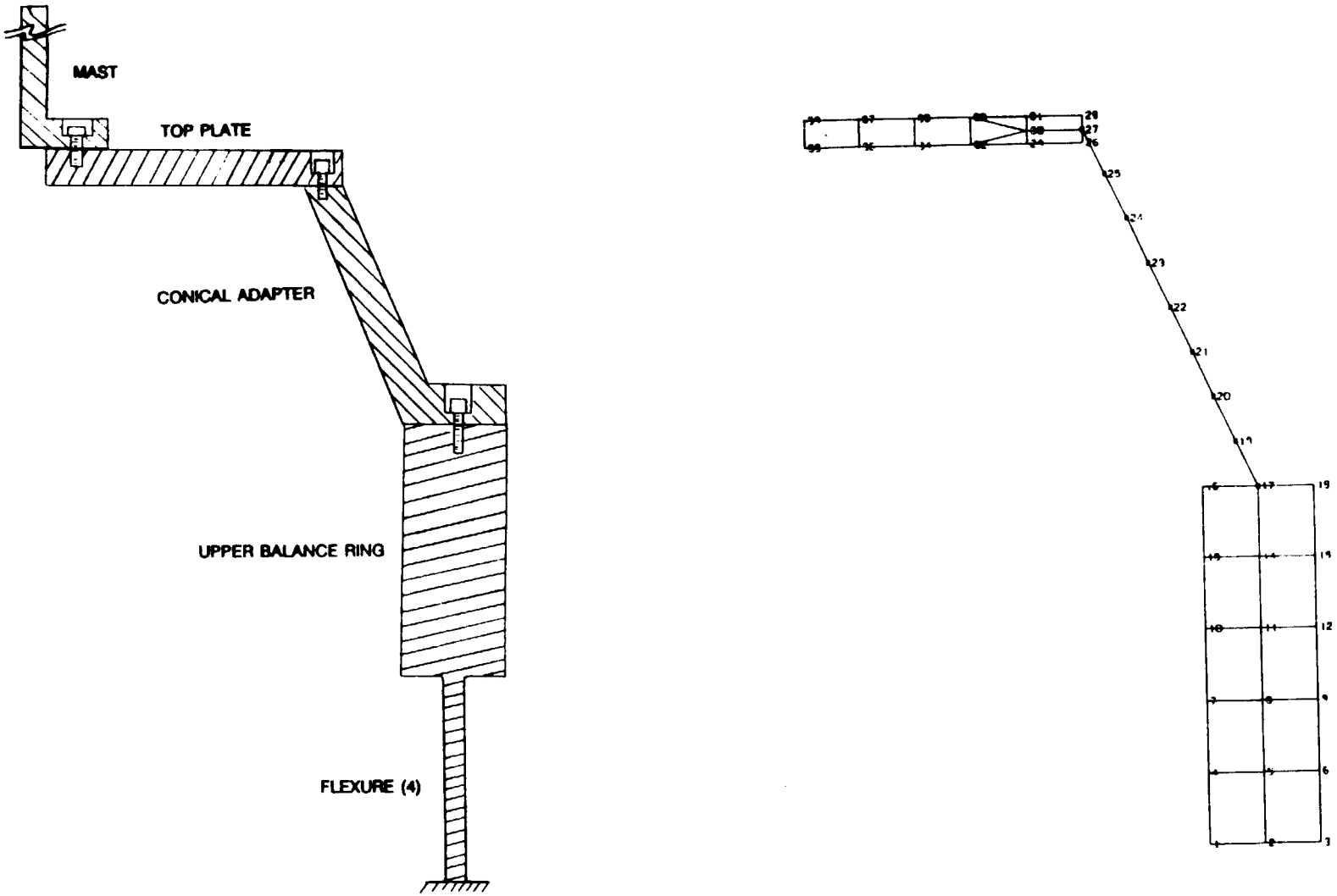

Figure 4
Finite Element Model of Flexures and Mast

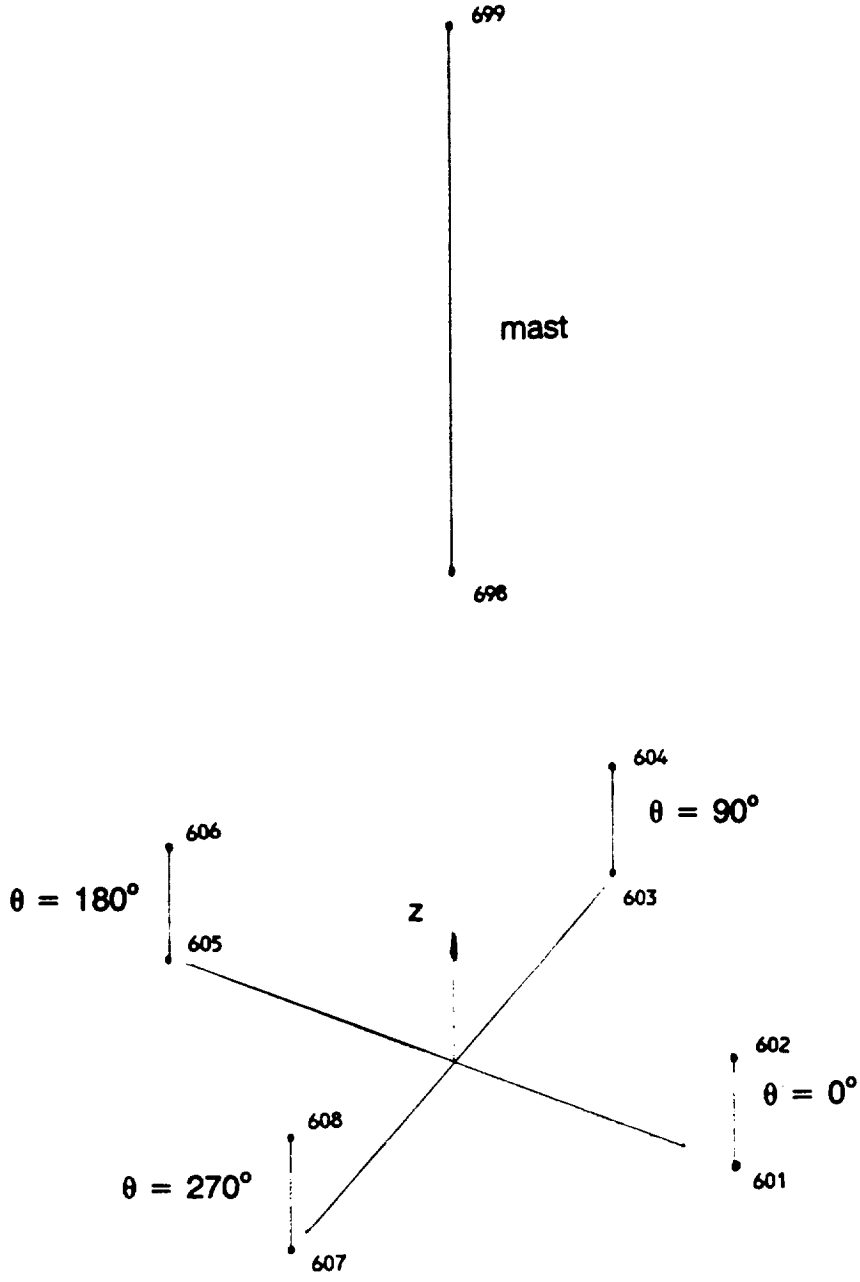

APPENDIX

There are five edited files of NASTRAN output presented here for review. The first two files show the output from the thin-walled cylinder analysis. The last three files show the output, including DMAP Alter sequences for the mixed model analyses.

The output files were modified to save space. The author's comments are enclosed in double angle brackets, << >>.

1) This file contains the results from the thin-walled cylinder analysis using conical shell elements.

```
ID TSTCONE,FEM
APP  DISPLACEMENT
SOL 1,0
TIME 30
CEND
 TEST OF AXISYMM CONE ELEMENTS
                                C A S E    C O N T R O L    D E C K    E C H O
           CARD
           COUNT
            1      $
            2      TITLE = TEST OF AXISYMM CONE ELEMENTS
            3      SUBTITLE = FREE CYLINDER
            4      AXISYM = COSINE
            5      $
            6      OUTPUT
            7       DISP = ALL
            8       SPCFORCE = ALL
            9       HARMONICS = ALL
           10       ELFORCE = ALL
           11       ELSTRESS = ALL
           12      $
           13      SUBCASE 1
           14       LABEL = UNIFORM PRESSURE LOAD
           15       LOAD = 1
           16      SUBCASE 2
           17       LABEL = UNIFORM TEMPERATURE LOAD
           18       TEMP(LOAD) = 2
           19      $
           20      OUTPUT(PLOT)
           21      PLOTTER NASTPLT,D,1
           22      PAPER SIZE 11.0 X 8.5
           23      $
           24       SET 1 ALL
           25      $
           26       AXES X,Y,Z
           27       VIEW 90.,0.,0.
           28       FIND SCALE, ORIGIN 11, SET 1
           29      PLOT SET 1, ORIGIN 11, SYMBOL 2
           30      PLOT STATIC DEFORMATION 0,1 SET 1, ORIGIN 11, PEN 2, SHAPE
           31      $
           32      BEGIN BULK
TEST OF AXISYMM CONE ELEMENTS
                                        S O R T E D    B U L K    D A T A    E C H O
           CARD
           COUNT        ---1--- +++2+++ ---3--- +++4+++ ---5--- +++6+++ ---7--- +++8+++
              1-        AXIC    4
              2-        CCONEAX 1       1       1       2
              3-        CCONEAX 2       1       2       3
              4-        CCONEAX 3       1       3       4
              5-        CCONEAX 4       1       4       5
              6-        CCONEAX 5       1       5       6
              7-        CCONEAX 6       1       6       7
              8-        CCONEAX 7       1       7       8
              9-        CCONEAX 8       1       8       9
             10-        CCONEAX 9       1       9       10
             11-        CCONEAX 10      1       10      11
```

```
12-     CCONEAX 11      1       11      12
13-     CCONEAX 12      1       12      13
14-     CCONEAX 13      1       13      14
15-     CCONEAX 14      1       14      15
16-     CCONEAX 15      1       15      16
17-     CCONEAX 16      1       16      17
18-     CCONEAX 17      1       17      18
19-     CCONEAX 18      1       18      19
20-     CCONEAX 19      1       19      20
21-     CCONEAX 20      1       20      21
22-     FORCEAX 1       1       0       345.575 1.      0.      0.
23-     FORCEAX 1       2       0       691.150 1.      0.      0.
24-     FORCEAX 1       3       0       691.150 1.      0.      0.
25-     FORCEAX 1       4       0       691.150 1.      0.      0.
26-     FORCEAX 1       5       0       691.150 1.      0.      0.
27-     FORCEAX 1       6       0       691.150 1.      0.      0.
28-     FORCEAX 1       7       0       691.150 1.      0.      0.
29-     FORCEAX 1       8       0       691.150 1.      0.      0.
30-     FORCEAX 1       9       0       691.150 1.      0.      0.
31-     FORCEAX 1       10      0       691.150 1.      0.      0.
32-     FORCEAX 1       11      0       691.150 1.      0.      0.
33-     FORCEAX 1       12      0       691.150 1.      0.      0.
34-     FORCEAX 1       13      0       691.150 1.      0.      0.
35-     FORCEAX 1       14      0       691.150 1.      0.      0.
36-     FORCEAX 1       15      0       691.150 1.      0.      0.
37-     FORCEAX 1       16      0       691.150 1.      0.      0.
38-     FORCEAX 1       17      0       691.150 1.      0.      0.
39-     FORCEAX 1       18      0       691.150 1.      0.      0.
40-     FORCEAX 1       19      0       691.150 1.      0.      0.
41-     FORCEAX 1       20      0       691.150 1.      0.      0.
42-     FORCEAX 1       21      0       345.575 1.      0.      0.
43-     MAT1    1       28.5+6          .27     0.285   6.0-6   75.
44-     PCONEAX 1       1       .25     1       1.3021-3                        +PC
45-     +PC     .125    -.125   .0      90.     180.
46-     RINGAX  1               22.     0.                      346
47-     RINGAX  2               22.     0.2                     46
48-     RINGAX  3               22.     0.4                     46
49-     RINGAX  4               22.     0.6                     46
50-     RINGAX  5               22.     0.8                     46
51-     RINGAX  6               22.     1.0                     46
52-     RINGAX  7               22.     1.2                     46
53-     RINGAX  8               22.     1.4                     46
54-     RINGAX  9               22.     1.6                     46
55-     RINGAX  10              22.     1.8                     46
56-     RINGAX  11              22.     2.0                     46
57-     RINGAX  12              22.     2.2                     46
58-     RINGAX  13              22.     2.4                     46
59-     RINGAX  14              22.     2.6                     46
60-     RINGAX  15              22.     2.8                     46
61-     RINGAX  16              22.     3.0                     46
62-     RINGAX  17              22.     3.2                     46
63-     RINGAX  18              22.     3.4                     46
64-     RINGAX  19              22.     3.6                     46
65-     RINGAX  20              22.     3.8                     46
66-     RINGAX  21              22.     4.0                     46
67-     TEMPAX  2       1       0.      175.    2       1       360.    175.
68-     TEMPAX  2       2       0.      175.    2       2       360.    175.
69-     TEMPAX  2       3       0.      175.    2       3       360.    175.
70-     TEMPAX  2       4       0.      175.    2       4       360.    175.
71-     TEMPAX  2       5       0.      175.    2       5       360.    175.
72-     TEMPAX  2       6       0.      175.    2       6       360.    175.
73-     TEMPAX  2       7       0.      175.    2       7       360.    175.
74-     TEMPAX  2       8       0.      175.    2       8       360.    175.
75-     TEMPAX  2       9       0.      175.    2       9       360.    175.
76-     TEMPAX  2       10      0.      175.    2       10      360.    175.
77-     TEMPAX  2       11      0.      175.    2       11      360.    175.
78-     TEMPAX  2       12      0.      175.    2       12      360.    175.
79-     TEMPAX  2       13      0.      175.    2       13      360.    175.
80-     TEMPAX  2       14      0.      175.    2       14      360.    175.
81-     TEMPAX  2       15      0.      175.    2       15      360.    175.
82-     TEMPAX  2       16      0.      175.    2       16      360.    175.
83-     TEMPAX  2       17      0.      175.    2       17      360.    175.
84-     TEMPAX  2       18      0.      175.    2       18      360.    175.
85-     TEMPAX  2       19      0.      175.    2       19      360.    175.
86-     TEMPAX  2       20      0.      175.    2       20      360.    175.
87-     TEMPAX  2       21      0.      175.    2       21      360.    175.
```

ENDDATA

*** USER INFORMATION MESSAGE - GRID-POINT RESEQUENCING PROCESSOR BANDIT IS NOT USED DUE TO THE PRESENCE OF AXISYMMETRIC SOLID DATA

NO ERRORS FOUND - EXECUTE NASTRAN PROGRAM

*** USER INFORMATION MESSAGE 3035
FOR SUBCASE NUMBER 1, EPSILON SUB E = 2.5381723E-13

FOR SUBCASE NUMBER 2, EPSILON SUB E = -2.9740320E-07

UNIFORM PRESSURE LOAD

SUBCASE 1

D I S P L A C E M E N T V E C T O R

SECTOR-ID POINT-ID RING-ID	HARMONIC	T1	T2	T3	R1	R2	R3
1	0	1.700627E-03	0.0	0.0	0.0	-3.704502E-06	0.0
2	0	1.699928E-03	0.0	-4.173392E-06	0.0	-3.289213E-06	0.0
3	0	1.699311E-03	0.0	-8.345169E-06	0.0	-2.879735E-06	0.0
4	0	1.698775E-03	0.0	-1.251553E-05	0.0	-2.480112E-06	0.0
5	0	1.698318E-03	0.0	-1.668468E-05	0.0	-2.092694E-06	0.0
6	0	1.697937E-03	0.0	-2.085279E-05	0.0	-1.718366E-06	0.0
7	0	1.697630E-03	0.0	-2.502007E-05	0.0	-1.356784E-06	0.0
8	0	1.697394E-03	0.0	-2.918667E-05	0.0	-1.006590E-06	0.0
9	0	1.697227E-03	0.0	-3.335278E-05	0.0	-6.656261E-07	0.0
10	0	1.697127E-03	0.0	-3.751857E-05	0.0	-3.311431E-07	0.0
11	0	1.697094E-03	0.0	-4.168419E-05	0.0	3.354394E-12	0.0
12	0	1.697127E-03	0.0	-4.584981E-05	0.0	3.311499E-07	0.0
13	0	1.697227E-03	0.0	-5.001560E-05	0.0	6.656331E-07	0.0
14	0	1.697394E-03	0.0	-5.418171E-05	0.0	1.006594E-06	0.0
15	0	1.697630E-03	0.0	-5.834831E-05	0.0	1.356789E-06	0.0
16	0	1.697937E-03	0.0	-6.251559E-05	0.0	1.718372E-06	0.0
17	0	1.698318E-03	0.0	-6.668371E-05	0.0	2.092700E-06	0.0
18	0	1.698775E-03	0.0	-7.085285E-05	0.0	2.480118E-06	0.0
19	0	1.699311E-03	0.0	-7.502321E-05	0.0	2.879737E-06	0.0
20	0	1.699928E-03	0.0	-7.919499E-05	0.0	3.289214E-06	0.0
21	0	1.700627E-03	0.0	-8.336838E-05	0.0	3.704504E-06	0.0

<< Displacements for higher harmonics were deleted since they were all zero. >>

UNIFORM TEMPERATURE LOAD

SUBCASE 2

D I S P L A C E M E N T V E C T O R

SECTOR-ID POINT-ID RING-ID	HARMONIC	T1	T2	T3	R1	R2	R3
1	0	1.320000E-02	0.0	0.0	0.0	-1.602749E-10	0.0
2	0	1.320000E-02	0.0	1.200000E-04	0.0	-1.635010E-10	0.0
3	0	1.320000E-02	0.0	2.400000E-04	0.0	-1.690184E-10	0.0
4	0	1.320000E-02	0.0	3.600001E-04	0.0	-1.718580E-10	0.0
5	0	1.320000E-02	0.0	4.800000E-04	0.0	-1.713591E-10	0.0
6	0	1.320000E-02	0.0	6.000001E-04	0.0	-1.688681E-10	0.0
7	0	1.320000E-02	0.0	7.200001E-04	0.0	-1.618791E-10	0.0
8	0	1.320000E-02	0.0	8.400001E-04	0.0	-1.552687E-10	0.0
9	0	1.320000E-02	0.0	9.600002E-04	0.0	-1.461382E-10	0.0
10	0	1.320000E-02	0.0	1.080000E-03	0.0	-1.394003E-10	0.0
11	0	1.320000E-02	0.0	1.200000E-03	0.0	-1.319788E-10	0.0
12	0	1.320000E-02	0.0	1.320000E-03	0.0	-1.250832E-10	0.0
13	0	1.320000E-02	0.0	1.440000E-03	0.0	-1.193989E-10	0.0
14	0	1.320000E-02	0.0	1.560000E-03	0.0	-1.190773E-10	0.0
15	0	1.320000E-02	0.0	1.680000E-03	0.0	-1.194626E-10	0.0
16	0	1.320000E-02	0.0	1.800000E-03	0.0	-1.192699E-10	0.0
17	0	1.320000E-02	0.0	1.920000E-03	0.0	-1.188989E-10	0.0
18	0	1.320000E-02	0.0	2.040000E-03	0.0	-1.186790E-10	0.0
19	0	1.320000E-02	0.0	2.160000E-03	0.0	-1.224091E-10	0.0
20	0	1.320000E-02	0.0	2.280000E-03	0.0	-1.250816E-10	0.0
21	0	1.320000E-02	0.0	2.400000E-03	0.0	-1.250580E-10	0.0

<< Displacements for higher harmonics are limited to the first five rings. The point in listing these higher harmonics is that there is an error in the code because these should be identically zero. >>

1	1	3.828026E+01	-3.829019E+01	0.0	0.0	4.608090E-05	0.0
2	1	3.828027E+01	-3.829019E+01	-8.993831E-05	0.0	4.498968E-05	0.0
3	1	3.828028E+01	-3.829019E+01	-1.798967E-04	0.0	4.397644E-05	0.0
4	1	3.828028E+01	-3.829019E+01	-2.698726E-04	0.0	4.309058E-05	0.0
5	1	3.828030E+01	-3.829020E+01	-3.598635E-04	0.0	4.236048E-05	0.0
1	2	3.418656E-03	-6.702370E-03	0.0	0.0	1.411114E-04	0.0
2	2	3.446886E-03	-6.703204E-03	-8.981951E-05	0.0	1.412205E-04	0.0
3	2	3.475164E-03	-6.705698E-03	-1.797000E-04	0.0	1.416164E-04	0.0

4	2	3.503561E-03	-6.709841E-03	-2.696334E-04	0.0	1.424383E-04	0.0
5	2	3.532173E-03	-6.715627E-03	-3.596119E-04	0.0	1.437620E-04	0.0
1	3	9.210605E-04	-3.664352E-03	0.0	0.0	3.069935E-04	0.0
2	3	9.824461E-04	-3.665628E-03	-8.963325E-05	0.0	3.069658E-04	0.0
3	3	1.043900E-03	-3.669423E-03	-1.793976E-04	0.0	3.077363E-04	0.0
4	3	1.105611E-03	-3.675709E-03	-2.692745E-04	0.0	3.095646E-04	0.0
5	3	1.167805E-03	-3.684461E-03	-3.592463E-04	0.0	3.125749E-04	0.0
1	4	-1.470954E-04	-2.502015E-03	0.0	0.0	5.189780E-04	0.0
2	4	-4.339249E-05	-2.503747E-03	-8.941032E-05	0.0	5.183037E-04	0.0
3	4	6.034414E-05	-2.508867E-03	-1.790392E-04	0.0	5.193919E-04	0.0
4	4	1.645048E-04	-2.517312E-03	-2.688528E-04	0.0	5.225801E-04	0.0
5	4	2.695243E-04	-2.529030E-03	-3.588200E-04	0.0	5.279839E-04	0.0

UNIFORM PRESSURE LOAD SUBCASE 1

F O R C E S O F S I N G L E - P O I N T C O N S T R A I N T

SECTOR-ID / POINT-ID / RING-ID	HARMONIC	T1	T2	T3	R1	R2	R3
1	0	0.0	0.0	-3.527417E-11	0.0	0.0	0.0

UNIFORM TEMPERATURE LOAD SUBCASE 2

F O R C E S O F S I N G L E - P O I N T C O N S T R A I N T

SECTOR-ID / POINT-ID / RING-ID	HARMONIC	T1	T2	T3	R1	R2	R3
1	0	0.0	0.0	1.193963E-09	0.0	0.0	0.0
1	1	0.0	0.0	4.233956E-05	0.0	0.0	0.0
1	2	0.0	0.0	-2.195207E+00	0.0	0.0	0.0
1	3	0.0	0.0	-3.430285E+01	0.0	0.0	0.0
1	4	0.0	0.0	-2.067654E+02	0.0	0.0	0.0

UNIFORM PRESSURE LOAD SUBCASE 1

F O R C E S I N A X I S - S Y M M E T R I C C O N I C A L S H E L L E L E M E N T S (CCONEAX)

ELEMENT ID.	HARMONIC NUMBER	POINT ANGLE	BEND-MOMENT V	BEND-MOMENT U	TWIST-MOMENT	SHEAR V	SHEAR U
1	0		-7.521445E-01	-2.030790E-01	0.0	0.0	0.0
1	1		0.0	0.0	0.0	0.0	0.0
1	2		0.0	0.0	0.0	0.0	0.0
1	3		0.0	0.0	0.0	0.0	0.0
1	4		0.0	0.0	0.0	0.0	0.0
1		0.0000	-7.521445E-01	-2.030790E-01	0.0	0.0	0.0
1		90.0000	-7.521445E-01	-2.030790E-01	0.0	0.0	0.0
1		180.0000	-7.521445E-01	-2.030790E-01	0.0	0.0	0.0

UNIFORM TEMPERATURE LOAD SUBCASE 2

F O R C E S I N A X I S - S Y M M E T R I C C O N I C A L S H E L L E L E M E N T S (CCONEAX)

ELEMENT ID.	HARMONIC NUMBER	POINT ANGLE	BEND-MOMENT V	BEND-MOMENT U	TWIST-MOMENT	SHEAR V	SHEAR U
1	0		2.401673E+01	6.484517E+00	0.0	0.0	0.0
1	1		-2.451984E+01	-5.926837E+00	-6.250000E-02	0.0	0.0
1	2		-1.796247E+01	-4.874458E+00	-3.707733E-01	0.0	0.0
1	3		-1.789051E+01	-4.644216E+00	-1.216523E+00	0.0	0.0
1	4		-1.777186E+01	-3.913975E+00	-2.745798E+00	0.0	0.0
1		0.0000	-5.412794E+01	-1.287497E+01	0.0	0.0	0.0
1		90.0000	2.420734E+01	7.445001E+00	1.154023E+00	0.0	0.0
1		180.0000	3.069276E+01	8.267138E+00	-9.905316E-07	0.0	0.0

UNIFORM PRESSURE LOAD SUBCASE 1

S T R E S S E S I N A X I S - S Y M M E T R I C C O N I C A L S H E L L E L E M E N T S (CCONEAX)

ELEMENT ID.	HARMONIC	POINT ANGLE	FIBRE DISTANCE	STRESSES IN ELEMENT COORD SYSTEM NORMAL-V	NORMAL-U	SHEAR-UV	PRINCIPAL STRESSES (ZERO SHEAR) ANGLE	MAJOR	MINOR	MAXIMUM SHEAR
1	0		1.250000E-01	-7.220625E+01	2.183123E+03	0.0				
			-1.250000E-01	7.220363E+01	2.222114E+03	0.0				
1	1		1.250000E-01	0.0	0.0	0.0				
			-1.250000E-01	0.0	0.0	0.0				
1	2		1.250000E-01	0.0	0.0	0.0				
			-1.250000E-01	0.0	0.0	0.0				
1	3		1.250000E-01	0.0	0.0	0.0				
			-1.250000E-01	0.0	0.0	0.0				
1	4		1.250000E-01	0.0	0.0	0.0				
			-1.250000E-01	0.0	0.0	0.0				
1		0.0000	1.250000E-01	-7.220625E+01	2.183123E+03	0.0	90.0000	2.183123E+03	-7.220630E+01	1.127665E+03
			-1.250000E-01	7.220363E+01	2.222114E+03	0.0	90.0000	2.222114E+03	7.220361E+01	1.074955E+03
1		90.0000	1.250000E-01	-7.220625E+01	2.183123E+03	0.0	90.0000	2.183123E+03	-7.220630E+01	1.127665E+03
			-1.250000E-01	7.220363E+01	2.222114E+03	0.0	90.0000	2.222114E+03	7.220361E+01	1.074955E+03
1		180.0000	1.250000E-01	-7.220625E+01	2.183123E+03	0.0	90.0000	2.183123E+03	-7.220630E+01	1.127665E+03

```
                    -1.250000E-01  7.220363E+01  2.222114E+03  0.0          90.0000  2.222114E+03  7.220361E+01  1.074955E+03

     UNIFORM TEMPERATURE LOAD                                                                                          SUBCASE 2
          S T R E S S E S   I N   A X I S - S Y M M E T R I C   C O N I C A L   S H E L L   E L E M E N T S   (CCONEAX)
ELEMENT          POINT     FIBRE          STRESSES IN ELEMENT COORD SYSTEM        PRINCIPAL STRESSES (ZERO SHEAR)          MAXIMUM
  ID.  HARMONIC  ANGLE     DISTANCE       NORMAL-V      NORMAL-U      SHEAR-UV      ANGLE       MAJOR         MINOR          SHEAR
     1    0               1.250000E-01  2.573024E+04  2.404717E+04  0.0
                         -1.250000E-01  2.111908E+04  2.280215E+04  0.0
     1    1               1.250000E-01 -1.992134E+04 -1.816540E+04 -5.999923E+00
                         -1.250000E-01 -1.521359E+04 -1.702747E+04  5.999923E+00
     1    2               1.250000E-01 -1.929260E+04 -1.813068E+04 -3.659378E+01
                         -1.250000E-01 -1.584385E+04 -1.719479E+04  3.459378E+01
     1    3               1.250000E-01 -1.928362E+04 -1.819923E+04 -1.198160E+02
                         -1.250000E-01 -1.584869E+04 -1.730755E+04  1.137535E+02
     1    4               1.250000E-01 -1.926194E+04 -1.820866E+04 -2.695620E+02
                         -1.250000E-01 -1.584978E+04 -1.745718E+04  2.576245E+02
     1         0.0000     1.250000E-01 -5.202926E+04 -4.865680E+04  0.0          90.0000 -4.865680E+04 -5.202926E+04  1.686227E+03
                         -1.250000E-01 -4.163683E+04 -4.618484E+04  0.0           0.0000 -4.163683E+04 -4.618484E+04  2.274008E+03
     1        90.0000     1.250000E-01  2.576090E+04  2.396919E+04  1.138160E+02  3.6202  2.576810E+04  2.396199E+04  9.030555E+02
                         -1.250000E-01  2.111315E+04  2.253977E+04 -1.077535E+02 -85.7049  2.254786E+04  2.110506E+04  7.214023E+02
     1       180.0000     1.250000E-01  2.638067E+04  2.407247E+04 -9.727959E-05  0.0000  2.638067E+04  2.407247E+04  1.154101E+03
                         -1.250000E-01  2.048774E+04  2.248520E+04  9.290005E-05 90.0000  2.248520E+04  2.048774E+04  9.987314E+02

                                    * * * END OF JOB * * *
```

2) This file contains the results of the thin-walled cylinder analysis using the trapezoidal solid elements.

```
ID TSTCYL,FEM
APP  DISPLACEMENT
SOL 1,0
TIME 60
$
CEND
```

C A S E C O N T R O L D E C K E C H O

```
CARD
COUNT
 1      TITLE = TEST CYLINDER
 2      SUBTITLE = UNIFORM PRESSURE
 3      $
 4      AXISYM = COSINE
 5      OUTPUT
 6        DISPLACEMENTS = ALL
 7        SPCFORCES = ALL
 8        ELFORCES = ALL
 9        ELSTRESS = ALL
10        HARMONICS = ALL
11      $
12      SUBCASE 1
13       LABEL = PRESSURE LOAD
14       LOAD = 1
15      SUBCASE 2
16       LABEL = UNIFORM TEMPERATURE LOAD
17       TEMPERATURE(LOAD) = 2
18      $
19      OUTPUT(PLOT)
20      PLOTTER NASTPLT,D,1
21      PAPER SIZE 11.0 X 8.5
22      $
23       SET 1 ALL
24      $
25       AXES X,Y,Z
26       VIEW 90.,90.,0.
27       FIND SCALE, ORIGIN 11, SET 1
28      PLOT SET 1, ORIGIN 11
29      $
30      BEGIN BULK
```

S O R T E D B U L K D A T A E C H O

```
CARD
COUNT        ---1--- +++2+++ ---3--- +++4+++ ---5--- +++6+++ ---7--- +++8+++ ---9--- +++10+++
  1-         AXIC    4
```

```
2-      CTRAPAX 1       1       1       10      11      2
3-      CTRAPAX 2       1       2       11      12      3
4-      CTRAPAX 3       1       3       12      13      4
5-      CTRAPAX 4       1       4       13      14      5
6-      CTRAPAX 5       1       5       14      15      6
7-      CTRAPAX 6       1       6       15      16      7
8-      CTRAPAX 7       1       7       16      17      8
9-      CTRAPAX 8       1       8       17      18      9
10-     CTRAPAX 9       1       10      19      20      11
11-     CTRAPAX 10      1       11      20      21      12
12-     CTRAPAX 11      1       12      21      22      13
13-     CTRAPAX 12      1       13      22      23      14
14-     CTRAPAX 13      1       14      23      24      15
15-     CTRAPAX 14      1       15      24      25      16
16-     CTRAPAX 15      1       16      25      26      17
17-     CTRAPAX 16      1       17      26      27      18
18-     FORCEAX 1       1       0       859.03  1.      0.      0.
19-     FORCEAX 1       2       0       1718.06 1.      0.      0.
20-     FORCEAX 1       3       0       1718.06 1.      0.      0.
21-     FORCEAX 1       4       0       1718.06 1.      0.      0.
22-     FORCEAX 1       5       0       1718.06 1.      0.      0.
23-     FORCEAX 1       6       0       1718.06 1.      0.      0.
24-     FORCEAX 1       7       0       1718.06 1.      0.      0.
25-     FORCEAX 1       8       0       1718.06 1.      0.      0.
26-     FORCEAX 1       9       0       859.03  1.      0.      0.
27-     MAT1    1       28.5+6          .27     0.285   6.0-6   75.
28-     PTRAPAX 1               1
29-     RINGAX  1               21.875  0.                              3456
30-     RINGAX  2               21.875  0.5                             456
31-     RINGAX  3               21.875  1.0                             456
32-     RINGAX  4               21.875  1.5                             456
33-     RINGAX  5               21.875  2.0                             456
34-     RINGAX  6               21.875  2.5                             456
35-     RINGAX  7               21.875  3.0                             456
36-     RINGAX  8               21.875  3.5                             456
37-     RINGAX  9               21.875  4.0                             456
38-     RINGAX  10              22.     0.                              456
39-     RINGAX  11              22.     0.5                             456
40-     RINGAX  12              22.     1.0                             456
41-     RINGAX  13              22.     1.5                             456
42-     RINGAX  14              22.     2.0                             456
43-     RINGAX  15              22.     2.5                             456
44-     RINGAX  16              22.     3.0                             456
45-     RINGAX  17              22.     3.5                             456
46-     RINGAX  18              22.     4.0                             456
47-     RINGAX  19              22.125  0.                              456
48-     RINGAX  20              22.125  0.5                             456
49-     RINGAX  21              22.125  1.0                             456
50-     RINGAX  22              22.125  1.5                             456
51-     RINGAX  23              22.125  2.0                             456
52-     RINGAX  24              22.125  2.5                             456
53-     RINGAX  25              22.125  3.0                             456
54-     RINGAX  26              22.125  3.5                             456
55-     RINGAX  27              22.125  4.0                             456
56-     TEMPAX  2       1       0.      175.    2       1       360.    175.
57-     TEMPAX  2       2       0.      175.    2       2       360.    175.
58-     TEMPAX  2       3       0.      175.    2       3       360.    175.
59-     TEMPAX  2       4       0.      175.    2       4       360.    175.
60-     TEMPAX  2       5       0.      175.    2       5       360.    175.
61-     TEMPAX  2       6       0.      175.    2       6       360.    175.
62-     TEMPAX  2       7       0.      175.    2       7       360.    175.
63-     TEMPAX  2       8       0.      175.    2       8       360.    175.
64-     TEMPAX  2       9       0.      175.    2       9       360.    175.
65-     TEMPAX  2       10      0.      175.    2       10      360.    175.
66-     TEMPAX  2       11      0.      175.    2       11      360.    175.
67-     TEMPAX  2       12      0.      175.    2       12      360.    175.
68-     TEMPAX  2       13      0.      175.    2       13      360.    175.
69-     TEMPAX  2       14      0.      175.    2       14      360.    175.
70-     TEMPAX  2       15      0.      175.    2       15      360.    175.
71-     TEMPAX  2       16      0.      175.    2       16      360.    175.
72-     TEMPAX  2       17      0.      175.    2       17      360.    175.
73-     TEMPAX  2       18      0.      175.    2       18      360.    175.
74-     TEMPAX  2       19      0.      175.    2       19      360.    175.
75-     TEMPAX  2       20      0.      175.    2       20      360.    175.
76-     TEMPAX  2       21      0.      175.    2       21      360.    175.
77-     TEMPAX  2       22      0.      175.    2       22      360.    175.
```

```
78-       TEMPAX  2       23      0.      175.    2       23      360.    175.
79-       TEMPAX  2       24      0.      175.    2       24      360.    175.
80-       TEMPAX  2       25      0.      175.    2       25      360.    175.
81-       TEMPAX  2       26      0.      175.    2       26      360.    175.
82-       TEMPAX  2       27      0.      175.    2       27      360.    175.
          ENDDATA
*** USER INFORMATION MESSAGE - GRID-POINT RESEQUENCING PROCESSOR BANDIT IS NOT USED DUE TO
    THE PRESENCE OF AXISYMMETRIC SOLID DATA
        **NO ERRORS FOUND - EXECUTE NASTRAN PROGRAM**

*** USER INFORMATION MESSAGE 3035
    FOR SUBCASE NUMBER      1, EPSILON SUB E =   1.4020696E-10
    FOR SUBCASE NUMBER      2, EPSILON SUB E =   2.1874433E-11
```

PRESSURE LOAD — SUBCASE 1

D I S P L A C E M E N T V E C T O R

SECTOR-ID / POINT-ID / RING-ID	HARMONIC	T1		T2		T3	R1		R2		R3
1	0	1.693589E-03	0.0		0.0		0.0		0.0		0.0
2	0	1.693747E-03	0.0		-1.031391E-05		0.0		0.0		0.0
3	0	1.693858E-03	0.0		-2.062829E-05		0.0		0.0		0.0
4	0	1.693924E-03	0.0		-3.094285E-05		0.0		0.0		0.0
5	0	1.693946E-03	0.0		-4.125744E-05		0.0		0.0		0.0
6	0	1.693924E-03	0.0		-5.157202E-05		0.0		0.0		0.0
7	0	1.693858E-03	0.0		-6.188658E-05		0.0		0.0		0.0
8	0	1.693747E-03	0.0		-7.220096E-05		0.0		0.0		0.0
9	0	1.693589E-03	0.0		-8.251487E-05		0.0		0.0		0.0
10	0	1.690910E-03	0.0		-4.547979E-08		0.0		0.0		0.0
11	0	1.691068E-03	0.0		-1.034751E-05		0.0		0.0		0.0
12	0	1.691179E-03	0.0		-2.065036E-05		0.0		0.0		0.0
13	0	1.691245E-03	0.0		-3.095377E-05		0.0		0.0		0.0
14	0	1.691267E-03	0.0		-4.125744E-05		0.0		0.0		0.0
15	0	1.691245E-03	0.0		-5.156111E-05		0.0		0.0		0.0
16	0	1.691179E-03	0.0		-6.186451E-05		0.0		0.0		0.0
17	0	1.691068E-03	0.0		-7.216736E-05		0.0		0.0		0.0
18	0	1.690910E-03	0.0		-8.246939E-05		0.0		0.0		0.0
19	0	1.688300E-03	0.0		-9.079706E-08		0.0		0.0		0.0
20	0	1.688458E-03	0.0		-1.038106E-05		0.0		0.0		0.0
21	0	1.688569E-03	0.0		-2.067240E-05		0.0		0.0		0.0
22	0	1.688634E-03	0.0		-3.096467E-05		0.0		0.0		0.0
23	0	1.688656E-03	0.0		-4.125744E-05		0.0		0.0		0.0
24	0	1.688634E-03	0.0		-5.155021E-05		0.0		0.0		0.0
25	0	1.688569E-03	0.0		-6.184247E-05		0.0		0.0		0.0
26	0	1.688458E-03	0.0		-7.213381E-05		0.0		0.0		0.0
27	0	1.688300E-03	0.0		-8.242408E-05		0.0		0.0		0.0

<< Displacements for higher harmonics were deleted since they were all zero. >>

UNIFORM TEMPERATURE LOAD — SUBCASE 2

D I S P L A C E M E N T V E C T O R

SECTOR-ID / POINT-ID / RING-ID	HARMONIC	T1		T2		T3	R1		R2		R3
1	0	1.312525E-02	0.0		0.0		0.0		0.0		0.0
2	0	1.312529E-02	0.0		2.999899E-04		0.0		0.0		0.0
3	0	1.312532E-02	0.0		5.999847E-04		0.0		0.0		0.0
4	0	1.312534E-02	0.0		8.999781E-04		0.0		0.0		0.0
5	0	1.312535E-02	0.0		1.199972E-03		0.0		0.0		0.0
6	0	1.312534E-02	0.0		1.499965E-03		0.0		0.0		0.0
7	0	1.312532E-02	0.0		1.799959E-03		0.0		0.0		0.0
8	0	1.312529E-02	0.0		2.099954E-03		0.0		0.0		0.0
9	0	1.312525E-02	0.0		2.399944E-03		0.0		0.0		0.0
10	0	1.320025E-02	0.0		-1.929753E-08		0.0		0.0		0.0
11	0	1.320029E-02	0.0		2.999818E-04		0.0		0.0		0.0
12	0	1.320032E-02	0.0		5.999781E-04		0.0		0.0		0.0
13	0	1.320034E-02	0.0		8.999750E-04		0.0		0.0		0.0
14	0	1.320035E-02	0.0		1.199972E-03		0.0		0.0		0.0
15	0	1.320034E-02	0.0		1.499968E-03		0.0		0.0		0.0
16	0	1.320032E-02	0.0		1.799965E-03		0.0		0.0		0.0
17	0	1.320029E-02	0.0		2.099962E-03		0.0		0.0		0.0
18	0	1.320025E-02	0.0		2.399963E-03		0.0		0.0		0.0
19	0	1.327525E-02	0.0		-2.548948E-08		0.0		0.0		0.0
20	0	1.327529E-02	0.0		2.999709E-04		0.0		0.0		0.0
21	0	1.327532E-02	0.0		5.999721E-04		0.0		0.0		0.0
22	0	1.327534E-02	0.0		8.999718E-04		0.0		0.0		0.0
23	0	1.327535E-02	0.0		1.199972E-03		0.0		0.0		0.0

24	0	1.327534E-02	0.0	1.499972E-03	0.0	0.0	0.0
25	0	1.327532E-02	0.0	1.799971E-03	0.0	0.0	0.0
26	0	1.327529E-02	0.0	2.099973E-03	0.0	0.0	0.0
27	0	1.327525E-02	0.0	2.399969E-03	0.0	0.0	0.0

<< Displacements for higher harmonics were deleted since they were all zero.>>

PRESSURE LOAD SUBCASE 1

F O R C E S O F S I N G L E - P O I N T C O N S T R A I N T

SECTOR-ID POINT-ID RING-ID	HARMONIC		T1	T2	T3	R1	R2	R3
1	0	0.0	0.0	-3.782911E-07	0.0	0.0	0.0	

UNIFORM TEMPERATURE LOAD SUBCASE 2

F O R C E S O F S I N G L E - P O I N T C O N S T R A I N T

SECTOR-ID POINT-ID RING-ID	HARMONIC		T1	T2	T3	R1	R2	R3
1	0	0.0	0.0	-8.986099E-07	0.0	0.0	0.0	

PRESSURE LOAD SUBCASE 1

F O R C E S I N A X I S - S Y M M E T R I C T R A P E Z O I D A L R I N G E L E M E N T S (CTRAPAX)

ELEMENT ID.	HARMONIC NUMBER	POINT ANGLE	RADIAL (R)	CIRCUMFERENTIAL (THETA-T)	AXIAL (Z)	CHARGE
1	0		8.547845E+02	0.0	5.634766E+00	0.0
			-4.301514E+02	0.0	-1.556641E+00	0.0
			-4.293379E+02	0.0	1.242188E+00	0.0
			8.614746E+02	0.0	-5.189453E+00	0.0
1	1		0.0	0.0	0.0	0.0
			0.0	0.0	0.0	0.0
			0.0	0.0	0.0	0.0
			0.0	0.0	0.0	0.0
1	2		0.0	0.0	0.0	0.0
			0.0	0.0	0.0	0.0
			0.0	0.0	0.0	0.0
			0.0	0.0	0.0	0.0
1	3		0.0	0.0	0.0	0.0
			0.0	0.0	0.0	0.0
			0.0	0.0	0.0	0.0
			0.0	0.0	0.0	0.0
1	4		0.0	0.0	0.0	0.0
			0.0	0.0	0.0	0.0
			0.0	0.0	0.0	0.0
			0.0	0.0	0.0	0.0
1		0.0000	8.547845E+02	0.0	5.634766E+00	0.0
			-4.301514E+02	0.0	-1.556641E+00	0.0
			-4.293379E+02	0.0	1.242188E+00	0.0
			8.614746E+02	0.0	-5.189453E+00	0.0

<< Force output for other elements was deleted. >>

UNIFORM TEMPERATURE LOAD SUBCASE 2

F O R C E S I N A X I S - S Y M M E T R I C T R A P E Z O I D A L R I N G E L E M E N T S (CTRAPAX)

ELEMENT ID.	HARMONIC NUMBER	POINT ANGLE	RADIAL (R)	CIRCUMFERENTIAL (THETA-T)	AXIAL (Z)	CHARGE
1	0		-1.277364E+06	0.0	-3.198784E+05	0.0
			1.284640E+06	0.0	-3.206322E+05	0.0
			1.284622E+06	0.0	3.206169E+05	0.0
			-1.277327E+06	0.0	3.198938E+05	0.0
1	1		0.0	0.0	0.0	0.0
			0.0	0.0	0.0	0.0
			0.0	0.0	0.0	0.0
			0.0	0.0	0.0	0.0
1	2		0.0	0.0	0.0	0.0
			0.0	0.0	0.0	0.0
			0.0	0.0	0.0	0.0
			0.0	0.0	0.0	0.0
1	3		0.0	0.0	0.0	0.0
			0.0	0.0	0.0	0.0
			0.0	0.0	0.0	0.0
			0.0	0.0	0.0	0.0
1	4		0.0	0.0	0.0	0.0
			0.0	0.0	0.0	0.0
			0.0	0.0	0.0	0.0
			0.0	0.0	0.0	0.0
1		0.0000	-1.277364E+06	0.0	-3.198784E+05	0.0
			1.284640E+06	0.0	-3.206322E+05	0.0

1.284622E+06	0.0	3.206169E+05	0.0
1.277327E+06	0.0	3.198938E+05	0.0

<< Force output for other elements was deleted. >>

PRESSURE LOAD

SUBCASE 1

S T R E S S E S   I N   A X I S - S Y M M E T R I C   T R A P E Z O I D A L   R I N G   E L E M E N T S   (CTRAPAX)

ELEMENT ID.	HARMONIC NUMBER	POINT ANGLE	RADIAL (R)	AXIAL (Z)	CIRCUM. (THETA-T)	SHEAR (ZR)	SHEAR (RT)	SHEAR (ZT)	F L U X D E N S I T I E S (R)	(Z)	(T)
1	0		-1.511E+01	2.901E+00	2.203E+03	-5.352E-01	0.000E+00	0.000E+00	0.000E+00	0.000E+00	0.000E+00
			-2.221E+01	-3.674E+00	2.183E+03	-5.430E-01	0.000E+00	0.000E+00	0.000E+00	0.000E+00	0.000E+00
			-2.222E+01	-3.594E+00	2.184E+03	5.237E-01	0.000E+00	0.000E+00	0.000E+00	0.000E+00	0.000E+00
			-1.508E+01	2.963E+00	2.203E+03	5.317E-01	0.000E+00	0.000E+00	0.000E+00	0.000E+00	0.000E+00
			-1.865E+01	-3.777E-01	2.193E+03	-9.552E-03	0.000E+00	0.000E+00	0.000E+00	0.000E+00	0.000E+00
1	1		0.000E+00	0.000E+00	0.000E+00	0.000E+00	0.000E+00	0.000E+00	0.000E+00	0.000E+00	0.000E+00
			0.000E+00	0.000E+00	0.000E+00	0.000E+00	0.000E+00	0.000E+00	0.000E+00	0.000E+00	0.000E+00
			0.000E+00	0.000E+00	0.000E+00	0.000E+00	0.000E+00	0.000E+00	0.000E+00	0.000E+00	0.000E+00
			0.000E+00	0.000E+00	0.000E+00	0.000E+00	0.000E+00	0.000E+00	0.000E+00	0.000E+00	0.000E+00
			0.000E+00	0.000E+00	0.000E+00	0.000E+00	0.000E+00	0.000E+00	0.000E+00	0.000E+00	0.000E+00
1	2		0.000E+00	0.000E+00	0.000E+00	0.000E+00	0.000E+00	0.000E+00	0.000E+00	0.000E+00	0.000E+00
			0.000E+00	0.000E+00	0.000E+00	0.000E+00	0.000E+00	0.000E+00	0.000E+00	0.000E+00	0.000E+00
			0.000E+00	0.000E+00	0.000E+00	0.000E+00	0.000E+00	0.000E+00	0.000E+00	0.000E+00	0.000E+00
			0.000E+00	0.000E+00	0.000E+00	0.000E+00	0.000E+00	0.000E+00	0.000E+00	0.000E+00	0.000E+00
			0.000E+00	0.000E+00	0.000E+00	0.000E+00	0.000E+00	0.000E+00	0.000E+00	0.000E+00	0.000E+00
1	3		0.000E+00	0.000E+00	0.000E+00	0.000E+00	0.000E+00	0.000E+00	0.000E+00	0.000E+00	0.000E+00
			0.000E+00	0.000E+00	0.000E+00	0.000E+00	0.000E+00	0.000E+00	0.000E+00	0.000E+00	0.000E+00
			0.000E+00	0.000E+00	0.000E+00	0.000E+00	0.000E+00	0.000E+00	0.000E+00	0.000E+00	0.000E+00
			0.000E+00	0.000E+00	0.000E+00	0.000E+00	0.000E+00	0.000E+00	0.000E+00	0.000E+00	0.000E+00
			0.000E+00	0.000E+00	0.000E+00	0.000E+00	0.000E+00	0.000E+00	0.000E+00	0.000E+00	0.000E+00
1	4		0.000E+00	0.000E+00	0.000E+00	0.000E+00	0.000E+00	0.000E+00	0.000E+00	0.000E+00	0.000E+00
			0.000E+00	0.000E+00	0.000E+00	0.000E+00	0.000E+00	0.000E+00	0.000E+00	0.000E+00	0.000E+00
			0.000E+00	0.000E+00	0.000E+00	0.000E+00	0.000E+00	0.000E+00	0.000E+00	0.000E+00	0.000E+00
			0.000E+00	0.000E+00	0.000E+00	0.000E+00	0.000E+00	0.000E+00	0.000E+00	0.000E+00	0.000E+00
			0.000E+00	0.000E+00	0.000E+00	0.000E+00	0.000E+00	0.000E+00	0.000E+00	0.000E+00	0.000E+00
1		0.0000	-1.511E+01	2.901E+00	2.203E+03	-5.352E-01	0.000E+00	0.000E+00	0.000E+00	0.000E+00	0.000E+00
			-2.221E+01	-3.674E+00	2.183E+03	-5.430E-01	0.000E+00	0.000E+00	0.000E+00	0.000E+00	0.000E+00
			-2.222E+01	-3.594E+00	2.184E+03	5.237E-01	0.000E+00	0.000E+00	0.000E+00	0.000E+00	0.000E+00
			-1.508E+01	2.963E+00	2.203E+03	5.317E-01	0.000E+00	0.000E+00	0.000E+00	0.000E+00	0.000E+00
			-1.865E+01	-3.777E-01	2.193E+03	-9.552E-03	0.000E+00	0.000E+00	0.000E+00	0.000E+00	0.000E+00

<< Stress output for other elements was deleted. >>

UNIFORM TEMPERATURE LOAD

SUBCASE 2

S T R E S S E S   I N   A X I S - S Y M M E T R I C   T R A P E Z O I D A L   R I N G   E L E M E N T S   (CTRAPAX)

ELEMENT ID.	HARMONIC NUMBER	POINT ANGLE	RADIAL (R)	AXIAL (Z)	CIRCUM. (THETA-T)	SHEAR (ZR)	SHEAR (RT)	SHEAR (ZT)	F L U X D E N S I T I E S (R)	(Z)	(T)
1	0		-6.641E-02	-5.781E-01	1.836E-01	-6.875E-01	0.000E+00	0.000E+00	0.000E+00	0.000E+00	0.000E+00
			2.266E-01	2.188E-01	4.766E-01	-6.875E-01	0.000E+00	0.000E+00	0.000E+00	0.000E+00	0.000E+00
			8.203E-02	2.070E-01	4.570E-01	3.047E-01	0.000E+00	0.000E+00	0.000E+00	0.000E+00	0.000E+00
			-3.164E-01	-5.781E-01	1.836E-01	3.066E-01	0.000E+00	0.000E+00	0.000E+00	0.000E+00	0.000E+00
			2.578E-01	-3.086E-01	7.031E-02	-2.061E-01	0.000E+00	0.000E+00	0.000E+00	0.000E+00	0.000E+00
1	1		0.000E+00	0.000E+00	0.000E+00	0.000E+00	0.000E+00	0.000E+00	0.000E+00	0.000E+00	0.000E+00
			0.000E+00	0.000E+00	0.000E+00	0.000E+00	0.000E+00	0.000E+00	0.000E+00	0.000E+00	0.000E+00
			0.000E+00	0.000E+00	0.000E+00	0.000E+00	0.000E+00	0.000E+00	0.000E+00	0.000E+00	0.000E+00
			0.000E+00	0.000E+00	0.000E+00	0.000E+00	0.000E+00	0.000E+00	0.000E+00	0.000E+00	0.000E+00
			0.000E+00	0.000E+00	0.000E+00	0.000E+00	0.000E+00	0.000E+00	0.000E+00	0.000E+00	0.000E+00
1	2		0.000E+00	0.000E+00	0.000E+00	0.000E+00	0.000E+00	0.000E+00	0.000E+00	0.000E+00	0.000E+00
			0.000E+00	0.000E+00	0.000E+00	0.000E+00	0.000E+00	0.000E+00	0.000E+00	0.000E+00	0.000E+00
			0.000E+00	0.000E+00	0.000E+00	0.000E+00	0.000E+00	0.000E+00	0.000E+00	0.000E+00	0.000E+00
			0.000E+00	0.000E+00	0.000E+00	0.000E+00	0.000E+00	0.000E+00	0.000E+00	0.000E+00	0.000E+00
			0.000E+00	0.000E+00	0.000E+00	0.000E+00	0.000E+00	0.000E+00	0.000E+00	0.000E+00	0.000E+00
1	3		0.000E+00	0.000E+00	0.000E+00	0.000E+00	0.000E+00	0.000E+00	0.000E+00	0.000E+00	0.000E+00
			0.000E+00	0.000E+00	0.000E+00	0.000E+00	0.000E+00	0.000E+00	0.000E+00	0.000E+00	0.000E+00
			0.000E+00	0.000E+00	0.000E+00	0.000E+00	0.000E+00	0.000E+00	0.000E+00	0.000E+00	0.000E+00
			0.000E+00	0.000E+00	0.000E+00	0.000E+00	0.000E+00	0.000E+00	0.000E+00	0.000E+00	0.000E+00
			0.000E+00	0.000E+00	0.000E+00	0.000E+00	0.000E+00	0.000E+00	0.000E+00	0.000E+00	0.000E+00
1	4		0.000E+00	0.000E+00	0.000E+00	0.000E+00	0.000E+00	0.000E+00	0.000E+00	0.000E+00	0.000E+00
			0.000E+00	0.000E+00	0.000E+00	0.000E+00	0.000E+00	0.000E+00	0.000E+00	0.000E+00	0.000E+00
			0.000E+00	0.000E+00	0.000E+00	0.000E+00	0.000E+00	0.000E+00	0.000E+00	0.000E+00	0.000E+00
			0.000E+00	0.000E+00	0.000E+00	0.000E+00	0.000E+00	0.000E+00	0.000E+00	0.000E+00	0.000E+00
			0.000E+00	0.000E+00	0.000E+00	0.000E+00	0.000E+00	0.000E+00	0.000E+00	0.000E+00	0.000E+00
1		0.0000	-6.641E-02	-5.781E-01	1.836E-01	-6.875E-01	0.000E+00	0.000E+00	0.000E+00	0.000E+00	0.000E+00
			2.266E-01	2.188E-01	4.766E-01	-6.875E-01	0.000E+00	0.000E+00	0.000E+00	0.000E+00	0.000E+00
			8.203E-02	2.070E-01	4.570E-01	3.047E-01	0.000E+00	0.000E+00	0.000E+00	0.000E+00	0.000E+00
			-3.164E-01	-5.781E-01	1.836E-01	3.066E-01	0.000E+00	0.000E+00	0.000E+00	0.000E+00	0.000E+00
			2.578E-01	-3.086E-01	7.031E-02	-2.061E-01	0.000E+00	0.000E+00	0.000E+00	0.000E+00	0.000E+00

<< Stress output for other elements was deleted. >>

* * * END OF JOB * * *

3) This file contains data for the axisymmetric finite element model of the generic balance. This is the first step in the mixed model procedure where the stiffness matrix is generated and output to a file.

```
ID BAL1,FEM
APP  DISPLACEMENT
SOL 1,0
$
$ WRITE MATRIX KAA TO FILE 14
$
ALTER 76
OUTPUT2 KAA,,,,//-1/14 $
EXIT
ENDALTER
$
TIME 60
$
CEND
```

C A S E C O N T R O L D E C K E C H O

```
CARD
COUNT
 1      TITLE = EXAMPLE PROBLEM: 20 INCH BALANCE
 2      SUBTITLE = PART 1: OUTPUT STIFFNESS MATRIX
 3      $
 4      AXISYM = COSINE
 5      MPC = 1
 6      OUTPUT
 7        DISPLACEMENTS = ALL
 8        SPCFORCES = ALL
 9        HARMONICS = ALL
10      $
11      SUBCASE 1
12       LABEL = UNIT THRUST LOAD
13       LOAD = 1
14      $
15      OUTPUT(PLOT)
16      PLOTTER NASTPLT,D,1
17      PAPER SIZE 11.0 X 8.5
18      $
19       SET 1 ALL
20      $
21       AXES X,Y,Z
22       VIEW 90.,90.,0.
23       FIND SCALE, ORIGIN 11, SET 1
24      PLOT SET 1, ORIGIN 11
25      $
26      BEGIN BULK
```

S O R T E D B U L K D A T A E C H O

```
CARD
COUNT       ---1--- +++2+++ ---3--- +++4+++ ---5--- +++6+++ ---7--- +++8+++
   1-       AXIC    4
   2-       CCONEAX 11      2       17      19
   3-       CCONEAX 12      2       19      20
   4-       CCONEAX 13      2       20      21
   5-       CCONEAX 14      2       21      22
   6-       CCONEAX 15      2       22      23
   7-       CCONEAX 16      2       23      24
   8-       CCONEAX 17      2       24      25
   9-       CCONEAX 18      2       25      27
  10-       CTRAPAX 1       1       1       2       5       4
  11-       CTRAPAX 2       1       2       3       6       5
  12-       CTRAPAX 3       1       4       5       8       7
  13-       CTRAPAX 4       1       5       6       9       8
  14-       CTRAPAX 5       1       7       8       11      10
  15-       CTRAPAX 6       1       8       9       12      11
  16-       CTRAPAX 7       1       10      11      14      13
  17-       CTRAPAX 8       1       11      12      15      14
  18-       CTRAPAX 9       1       13      14      17      16
  19-       CTRAPAX 10      1       14      15      18      17
  20-       CTRAPAX 19      1       29      26      27      30
  21-       CTRAPAX 20      1       30      27      28      31
  22-       CTRAPAX 24      1       34      32      33      35
  23-       CTRAPAX 25      1       36      34      35      37
  24-       CTRAPAX 26      1       38      36      37      39
```

```
25-       CTRIAAX 21      1       32      29      30
26-       CTRIAAX 22      1       32      30      33
27-       CTRIAAX 23      1       33      30      31
28-       FORCEAX 1       39      0       0.      0.      0.      1.
29-       MAT1    1       30.0+6          .3
30-       MPCAX   1                               17      0       5       -2.     +MP001
31-       +MP001  17      0       1       1.      14      0       1       -1.     +MP002
32-       +MP002  16      0       3       .5      18      0       3       -.5
33-       MPCAX   1                               17      1       5       -2.     +MP101
34-       +MP101  17      1       1       1.      14      1       1       -1.     +MP102
35-       +MP102  16      1       3       .5      18      1       3       -.5
36-       MPCAX   1                               17      3       5       -2.     +MP301
37-       +MP301  17      3       1       1.      14      3       1       -1.     +MP302
38-       +MP302  16      3       3       .5      18      3       3       -.5
39-       MPCAX   1                               17      4       5       -2.     +MP401
40-       +MP401  17      4       1       1.      14      4       1       -1.     +MP402
41-       +MP402  16      4       3       .5      18      4       3       -.5
42-       MPCAX   1                               17      2       5       -2.     +MP201
43-       +MP201  17      2       1       1.      14      2       1       -1.     +MP202
44-       +MP202  16      2       3       .5      18      2       3       -.5
45-       MPCAX   1                               27      2       5       -2.     +MP203
46-       +MP203  28      2       1       2.66667 26      2       1       -2.66667+MP204
47-       +MP204  30      2       3       1.      27      2       3       -1.
48-       MPCAX   1                               27      3       5       -2.     +MP303
49-       +MP303  28      3       1       2.66667 26      3       1       -2.66667+MP304
50-       +MP304  30      3       3       1.      27      3       3       -1.
51-       MPCAX   1                               27      0       5       -2.     +MP003
52-       +MP003  28      0       1       2.66667 26      0       1       -2.66667+MP004
53-       +MP004  30      0       3       1.      27      0       3       -1.
54-       MPCAX   1                               27      1       5       -2.     +MP103
55-       +MP103  28      1       1       2.66667 26      1       1       -2.66667+MP104
56-       +MP104  30      1       3       1.      27      1       3       -1.
57-       MPCAX   1                               27      4       5       -2.     +MP403
58-       +MP403  28      4       1       2.66667 26      4       1       -2.66667+MP404
59-       +MP404  30      4       3       1.      27      4       3       -1.
60-       PCONEAX 2       1       0.375   1       4.3945-3                        +PC1
61-       +PC1    0.1875  -.1875  0.      45.     90.     135.    180.
62-       PTRAPAX 1               1
63-       PTRIAAX 1               1
64-       RINGAX  1               9.      3.                      456
65-       RINGAX  2               10.     3.                      456
66-       RINGAX  3               11.     3.                      456
67-       RINGAX  4               9.      4.                      456
68-       RINGAX  5               10.     4.                      456
69-       RINGAX  6               11.     4.                      456
70-       RINGAX  7               9.      5.                      456
71-       RINGAX  8               10.     5.                      456
72-       RINGAX  9               11.     5.                      456
73-       RINGAX  10              9.      6.                      456
74-       RINGAX  11              10.     6.                      456
75-       RINGAX  12              11.     6.                      456
76-       RINGAX  13              9.      7.                      456
77-       RINGAX  14              10.     7.                      456
78-       RINGAX  15              11.     7.                      456
79-       RINGAX  16              9.      8.                      456
80-       RINGAX  17              10.     8.                      46
81-       RINGAX  18              11.     8.                      456
82-       RINGAX  19              9.625   8.625                   46
83-       RINGAX  20              9.250   9.250                   46
84-       RINGAX  21              8.875   9.875                   46
85-       RINGAX  22              8.500   10.500                  46
86-       RINGAX  23              8.125   11.125                  46
87-       RINGAX  24              7.750   11.750                  46
88-       RINGAX  25              7.375   12.375                  46
89-       RINGAX  26              7.      12.8125                 456
90-       RINGAX  27              7.      13.0                    46
91-       RINGAX  28              7.      13.1875                 456
92-       RINGAX  29              6.      12.8125                 456
93-       RINGAX  30              6.      13.0                    456
94-       RINGAX  31              6.      13.1875                 456
95-       RINGAX  32              5.      12.8125                 456
96-       RINGAX  33              5.      13.1875                 456
97-       RINGAX  34              4.      12.8125                 456
98-       RINGAX  35              4.      13.1875                 456
99-       RINGAX  36              3.      12.8125                 456
100-      RINGAX  37              3.      13.1875                 456
```

```
        101-        RINGAX  38              2.        12.8125                  456
        102-        RINGAX  39              2.        13.1875                  456
                    ENDDATA

USER INFORMATION MESSAGE - GRID-POINT RESEQUENCING PROCESSOR BANDIT IS NOT USED DUE TO THE PRESENCE OF AXISYMMETRIC SOLID DATA
        **NO ERRORS FOUND - EXECUTE NASTRAN PROGRAM**

*** USER INFORMATION MESSAGE 4114

   DATA BLOCK KAA      WRITTEN ON FORTRAN UNIT  14, TRLR  =       581       581        6        2       62       277

                                  * * * END OF JOB * * *
```

4) This file contains the data for the mast/flexure model. The DMAP Alter sequence for reading a matrix, adding it to an existing matrix, and outputing the solution is shown in the executive control.

```
ID BAL2,FEM
APP  DISPLACEMENT
SOL 1,0
DIAG 14
$
$ THIS DATA REPRESENTS FOUR SINGLE ELEMENT FLEXURES IN CYLINDRICAL
$ COORDINATES AND A MAST.  PHANTOM GRID POINTS HAVE BEEN ADDED TO
$ SIMULATE THE SIZE OF A MATRIX THAT COMES FROM AN ASSOCIATED AXISYMMETRIC
$ MODEL.  THE MAST GRIDS ARE OMITTED.
$
$ READ MATRIX KWW FROM TAPE
$ ADD TO MATRIX KAA
$ SOLVE THE PROBLEM
$ OUTPUT TO FILE THE SOLUTION SET VECTOR, ULV
$
ALTER 75
INPUTT2 /KWW,,,,/ -1 / 11 / $
ADD KAA,KWW/KMC/C,Y,ALPHA=(1.0,0.0)/C,Y,BETA=(1.0,0.0)  $
EQUIV  KMC,KAA/ALWAYS  $
ALTER 89
OUTPUT2  ULV,,,,//-1/14 $
ENDALTER
$
TIME 230
CEND
                           C A S E   C O N T R O L   D E C K   E C H O
           CARD
           COUNT
            1       TITLE = FLEXURES AND MAST FOR GENERIC BALANCE MODEL
            2       SUBTITLE = PART 2: ADD STIFFNESS MATRICIES AND SOLVE
            3       $
            4       SPC = 1
            5       MPC = 1
            6       $
            7       SET 1 = 601 THRU 604
            8       $
            9       OUTPUT
           10         DISPLACEMENTS = ALL
           11         SPCFORCES = ALL
           12         FORCES = 1
           13       SUBCASE 1
           14        LABEL = UNIT THRUST LOAD
           15        LOAD = 1
           16       $
           17       SUBCASE 2
           18        LABEL = UNIT PITCH MOMENT LOAD
           19        LOAD = 2
           20       $
           21       SUBCASE 3
           22        LABEL = UNIT AFT FORCE LOAD
           23        LOAD = 3
           24       $
           25       OUTPUT(PLOT)
           26       PLOTTER NASTPLT,D,1
           27       PAPER SIZE 11.0 X 8.5
```

```
28      $
29       SET 1 ALL
30      $
31       AXES X,Y,Z
32       VIEW 60.,30.,0.
33       FIND SCALE, ORIGIN 10, SET 1
34      PLOT SET 1, ORIGIN 10
35      PLOT STATIC DEFORMATION 0,1 SET 1, ORIGIN 10, PEN 2, SHAPE
36      $
37      BEGIN BULK
```

SORTED BULK DATA ECHO

CARD COUNT	---1---	+++2+++	---3---	+++4+++	---5---	+++6+++	---7---	+++8+++	
1-	BAROR					0.	0.	1.	1
2-	CBAR	601	10	601	602	1.	0.	0.	1
3-	CBAR	602	10	603	604	1.	0.	0.	1
4-	CBAR	603	10	605	606	1.	0.	0.	1
5-	CBAR	604	10	607	608	1.	0.	0.	1
6-	CBAR	690	11	698	699	1.	0.	0.	1
7-	CORD2C	1	0	0.	0.	0.	0.	0.	1. +CORD1
8-	+CORD1	1.	0.	1.					
9-	FORCE	1	699		1.0	0.	0.	1.	
10-	FORCE	3	699		1.0	1.	0.	0.	
11-	GRID	601	1	10.0	0.	0.	1		
12-	GRID	602	1	10.0	0.	3.0	1		
13-	GRID	603	1	10.0	90.	0.	1		
14-	GRID	604	1	10.0	90.	3.0	1		
15-	GRID	605	1	10.0	180.	0.	1		
16-	GRID	606	1	10.0	180.	3.0	1		
17-	GRID	607	1	10.0	270.	0.	1		
18-	GRID	608	1	10.0	270.	3.0	1		
19-	GRID	698	1	0.	0.	13.1875	1		
20-	GRID	699	1	0.	0.	28.	1		
21-	GRID	10001		0.	0.	0.			
22-	GRID	10002		0.	0.	0.			
23-	GRID	10003		0.	0.	0.			
24-	GRID	10004		0.	0.	0.			
25-	GRID	10005		0.	0.	0.			
26-	GRID	10006		0.	0.	0.			
27-	GRID	10007		0.	0.	0.			
28-	GRID	10008		0.	0.	0.			
29-	GRID	10009		0.	0.	0.			
30-	GRID	10010		0.	0.	0.			
31-	GRID	10011		0.	0.	0.			
32-	GRID	10012		0.	0.	0.			
33-	GRID	10013		0.	0.	0.			
34-	GRID	10014		0.	0.	0.			
35-	GRID	10015		0.	0.	0.			
36-	GRID	10016		0.	0.	0.			
37-	GRID	10017		0.	0.	0.			
38-	GRID	10018		0.	0.	0.			
39-	GRID	10019		0.	0.	0.			
40-	GRID	10020		0.	0.	0.			
41-	GRID	10021		0.	0.	0.			
42-	GRID	10022		0.	0.	0.			
43-	GRID	10023		0.	0.	0.			
44-	GRID	10024		0.	0.	0.			
45-	GRID	10025		0.	0.	0.			
46-	GRID	10026		0.	0.	0.			
47-	GRID	10027		0.	0.	0.			
48-	GRID	10028		0.	0.	0.			
49-	GRID	10029		0.	0.	0.			
50-	GRID	10030		0.	0.	0.			
51-	GRID	10031		0.	0.	0.			
52-	GRID	10032		0.	0.	0.			
53-	GRID	10033		0.	0.	0.			
54-	GRID	10034		0.	0.	0.			
55-	GRID	10035		0.	0.	0.			
56-	GRID	10036		0.	0.	0.			
57-	GRID	10037		0.	0.	0.			
58-	GRID	10038		0.	0.	0.			
59-	GRID	10039		0.	0.	0.			
60-	GRID	11001		0.	0.	0.			
61-	GRID	11002		0.	0.	0.			
62-	GRID	11003		0.	0.	0.			
63-	GRID	11004		0.	0.	0.			

```
64-     GRID    11005           0.      0.      0.
65-     GRID    11006           0.      0.      0.
66-     GRID    11007           0.      0.      0.
67-     GRID    11008           0.      0.      0.
68-     GRID    11009           0.      0.      0.
69-     GRID    11010           0.      0.      0.
70-     GRID    11011           0.      0.      0.
71-     GRID    11012           0.      0.      0.
72-     GRID    11013           0.      0.      0.
73-     GRID    11014           0.      0.      0.
74-     GRID    11015           0.      0.      0.
75-     GRID    11016           0.      0.      0.
76-     GRID    11017           0.      0.      0.
77-     GRID    11018           0.      0.      0.
78-     GRID    11019           0.      0.      0.
79-     GRID    11020           0.      0.      0.
80-     GRID    11021           0.      0.      0.
81-     GRID    11022           0.      0.      0.
82-     GRID    11023           0.      0.      0.
83-     GRID    11024           0.      0.      0.
84-     GRID    11025           0.      0.      0.
85-     GRID    11026           0.      0.      0.
86-     GRID    11027           0.      0.      0.
87-     GRID    11028           0.      0.      0.
88-     GRID    11029           0.      0.      0.
89-     GRID    11030           0.      0.      0.
90-     GRID    11031           0.      0.      0.
91-     GRID    11032           0.      0.      0.
92-     GRID    11033           0.      0.      0.
93-     GRID    11034           0.      0.      0.
94-     GRID    11035           0.      0.      0.
95-     GRID    11036           0.      0.      0.
96-     GRID    11037           0.      0.      0.
97-     GRID    11038           0.      0.      0.
98-     GRID    11039           0.      0.      0.
99-     GRID    12001           0.      0.      0.
100-    GRID    12002           0.      0.      0.
101-    GRID    12003           0.      0.      0.
102-    GRID    12004           0.      0.      0.
103-    GRID    12005           0.      0.      0.
104-    GRID    12006           0.      0.      0.
105-    GRID    12007           0.      0.      0.
106-    GRID    12008           0.      0.      0.
107-    GRID    12009           0.      0.      0.
108-    GRID    12010           0.      0.      0.
109-    GRID    12011           0.      0.      0.
110-    GRID    12012           0.      0.      0.
111-    GRID    12013           0.      0.      0.
112-    GRID    12014           0.      0.      0.
113-    GRID    12015           0.      0.      0.
114-    GRID    12016           0.      0.      0.
115-    GRID    12017           0.      0.      0.
116-    GRID    12018           0.      0.      0.
117-    GRID    12019           0.      0.      0.
118-    GRID    12020           0.      0.      0.
119-    GRID    12021           0.      0.      0.
120-    GRID    12022           0.      0.      0.
121-    GRID    12023           0.      0.      0.
122-    GRID    12024           0.      0.      0.
123-    GRID    12025           0.      0.      0.
124-    GRID    12026           0.      0.      0.
125-    GRID    12027           0.      0.      0.
126-    GRID    12028           0.      0.      0.
127-    GRID    12029           0.      0.      0.
128-    GRID    12030           0.      0.      0.
129-    GRID    12031           0.      0.      0.
130-    GRID    12032           0.      0.      0.
131-    GRID    12033           0.      0.      0.
132-    GRID    12034           0.      0.      0.
133-    GRID    12035           0.      0.      0.
134-    GRID    12036           0.      0.      0.
135-    GRID    12037           0.      0.      0.
136-    GRID    12038           0.      0.      0.
137-    GRID    12039           0.      0.      0.
138-    GRID    13001           0.      0.      0.
139-    GRID    13002           0.      0.      0.
```

140-	GRID	13003	0.	0.	0.
141-	GRID	13004	0.	0.	0.
142-	GRID	13005	0.	0.	0.
143-	GRID	13006	0.	0.	0.
144-	GRID	13007	0.	0.	0.
145-	GRID	13008	0.	0.	0.
146-	GRID	13009	0.	0.	0.
147-	GRID	13010	0.	0.	0.
148-	GRID	13011	0.	0.	0.
149-	GRID	13012	0.	0.	0.
150-	GRID	13013	0.	0.	0.
151-	GRID	13014	0.	0.	0.
152-	GRID	13015	0.	0.	0.
153-	GRID	13016	0.	0.	0.
154-	GRID	13017	0.	0.	0.
155-	GRID	13018	0.	0.	0.
156-	GRID	13019	0.	0.	0.
157-	GRID	13020	0.	0.	0.
158-	GRID	13021	0.	0.	0.
159-	GRID	13022	0.	0.	0.
160-	GRID	13023	0.	0.	0.
161-	GRID	13024	0.	0.	0.
162-	GRID	13025	0.	0.	0.
163-	GRID	13026	0.	0.	0.
164-	GRID	13027	0.	0.	0.
165-	GRID	13028	0.	0.	0.
166-	GRID	13029	0.	0.	0.
167-	GRID	13030	0.	0.	0.
168-	GRID	13031	0.	0.	0.
169-	GRID	13032	0.	0.	0.
170-	GRID	13033	0.	0.	0.
171-	GRID	13034	0.	0.	0.
172-	GRID	13035	0.	0.	0.
173-	GRID	13036	0.	0.	0.
174-	GRID	13037	0.	0.	0.
175-	GRID	13038	0.	0.	0.
176-	GRID	13039	0.	0.	0.
177-	GRID	14001	0.	0.	0.
178-	GRID	14002	0.	0.	0.
179-	GRID	14003	0.	0.	0.
180-	GRID	14004	0.	0.	0.
181-	GRID	14005	0.	0.	0.
182-	GRID	14006	0.	0.	0.
183-	GRID	14007	0.	0.	0.
184-	GRID	14008	0.	0.	0.
185-	GRID	14009	0.	0.	0.
186-	GRID	14010	0.	0.	0.
187-	GRID	14011	0.	0.	0.
188-	GRID	14012	0.	0.	0.
189-	GRID	14013	0.	0.	0.
190-	GRID	14014	0.	0.	0.
191-	GRID	14015	0.	0.	0.
192-	GRID	14016	0.	0.	0.
193-	GRID	14017	0.	0.	0.
194-	GRID	14018	0.	0.	0.
195-	GRID	14019	0.	0.	0.
196-	GRID	14020	0.	0.	0.
197-	GRID	14021	0.	0.	0.
198-	GRID	14022	0.	0.	0.
199-	GRID	14023	0.	0.	0.
200-	GRID	14024	0.	0.	0.
201-	GRID	14025	0.	0.	0.
202-	GRID	14026	0.	0.	0.
203-	GRID	14027	0.	0.	0.
204-	GRID	14028	0.	0.	0.
205-	GRID	14029	0.	0.	0.
206-	GRID	14030	0.	0.	0.
207-	GRID	14031	0.	0.	0.
208-	GRID	14032	0.	0.	0.
209-	GRID	14033	0.	0.	0.
210-	GRID	14034	0.	0.	0.
211-	GRID	14035	0.	0.	0.
212-	GRID	14036	0.	0.	0.
213-	GRID	14037	0.	0.	0.
214-	GRID	14038	0.	0.	0.
215-	GRID	14039	0.	0.	0.

```
216-    MAT1     1      30.0+6          .3
217-    MOMENT   2      699             1.0     0.      1.      0.
218-    MPC      1      602     3       -1.     10002   3       1.0     +MP1301
219-    +MP1301         11002   3       1.0     12002   3       1.0     +MP1302
220-    +MP1302         13002   3       1.0     14002   3       1.0
221-    MPC      1      602     1       -1.     10002   1       1.0     +MP1101
222-    +MP1101         11002   1       1.0     12002   1       1.0     +MP1102
223-    +MP1102         13002   1       1.0     14002   1       1.0
224-    MPC      1      602     4       -2.     10002   2       0.
225-    MPC      1      602     5       -2.     10005   1       1.0     +MP1501
226-    +MP1501         11005   1       1.0     12005   1       1.0     +MP1502
227-    +MP1502         13005   1       1.0     14005   1       1.0     +MP1503
228-    +MP1503         10002   1       -1.     11002   1       -1.     +MP1504
229-    +MP1504         12002   1       -1.     13002   1       -1.     +MP1505
230-    +MP1505         14002   1       -1.     10003   3       -.5     +MP1506
231-    +MP1506         11003   3       -.5     12003   3       -.5     +MP1507
232-    +MP1507         13003   3       -.5     14003   3       -.5     +MP1508
233-    +MP1508         10001   3       0.5     11001   3       0.5     +MP1509
234-    +MP1509         12001   3       0.5     13001   3       0.5     +MP1510
235-    +MP1510         14001   3       0.5
236-    MPC      1      602     2       -1.     10002   2       0.
237-    MPC      1      602     6       -2.     10002   2       0.
238-    MPC      1      604     1       -1.     10002   1       1.0     +MP2101
239-    +MP2101         12002   1       -1.     14002   1       1.0
240-    MPC      1      604     4       -2.     11002   3       -.1     +MP2401
241-    +MP2401         13002   3       0.3     11005   2       -1.     +MP2402
242-    +MP2402         13005   2       1.0     11002   2       1.0     +MP2403
243-    +MP2403         13002   2       -1.
244-    MPC      1      604     5       -2.     10005   1       1.0     +MP2501
245-    +MP2501         12005   1       -1.     14005   1       1.0     +MP2502
246-    +MP2502         10002   1       -1.     12002   1       1.0     +MP2503
247-    +MP2503         14002   1       -1.     10003   3       -.5     +MP2504
248-    +MP2504         12003   3       0.5     14003   3       -.5     +MP2505
249-    +MP2505         10001   3       0.5     12001   3       -.5     +MP2506
250-    +MP2506         14001   3       0.5
251-    MPC      1      604     2       -1.     11002   2       1.0     +MP2201
252-    +MP2201         13002   2       -1.
253-    MPC      1      604     3       -1.     10002   3       1.0     +MP2301
254-    +MP2301         12002   3       -1.     14002   3       1.0
255-    MPC      1      604     6       -2.     11003   2       0.5     +MP2601
256-    +MP2601         13003   2       -.5     11001   2       -.5     +MP2602
257-    +MP2602         13001   2       0.5     11002   1       0.1     +MP2603
258-    +MP2603         13002   1       -.3     11002   2       0.1     +MP2604
259-    +MP2604         13002   2       -.1
260-    MPC      1      606     4       -2.     11002   2       0.
261-    MPC      1      606     3       -1.     10002   3       1.0     +MP3301
262-    +MP3301         11002   3       -1.     12002   3       1.0     +MP3302
263-    +MP3302         13002   3       -1.     14002   3       1.0
264-    MPC      1      606     2       -1.     11002   2       0.
265-    MPC      1      606     5       -2.     10005   1       1.0     +MP3501
266-    +MP3501         11005   1       -1.     12005   1       1.0     +MP3502
267-    +MP3502         13005   1       -1.     14005   1       1.0     +MP3503
268-    +MP3503         10002   1       -1.     11002   1       1.0     +MP3504
269-    +MP3504         12002   1       -1.     13002   1       1.0     +MP3505
270-    +MP3505         14002   1       -1.     10003   3       -.5     +MP3506
271-    +MP3506         11003   3       0.5     12003   3       -.5     +MP3507
272-    +MP3507         13003   3       0.5     14003   3       -.5     +MP3508
273-    +MP3508         10001   3       0.5     11001   3       -.5     +MP3509
274-    +MP3509         12001   3       0.5     13001   3       -.5     +MP3510
275-    +MP3510         14001   3       0.5
276-    MPC      1      606     6       -2.     11002   2       0.
277-    MPC      1      606     1       -1.     10002   1       1.0     +MP3101
278-    +MP3101         11002   1       -1.     12002   1       1.0     +MP3102
279-    +MP3102         13002   1       -1.     14002   1       1.0
280-    MPC      1      608     6       -2.     11003   2       -.5     +MP4601
281-    +MP4601         13003   2       0.5     11001   2       0.5     +MP4602
282-    +MP4602         13001   2       -.5     11002   1       -.1     +MP4603
283-    +MP4603         13002   1       0.3     11002   2       -.1     +MP4604
284-    +MP4604         13002   2       0.1
285-    MPC      1      608     3       -1.     10002   3       1.0     +MP4301
286-    +MP4301         12002   3       -1.     14002   3       1.0
287-    MPC      1      608     2       -1.     11002   2       -1.0    +MP4201
288-    +MP4201         13002   2       1.0
289-    MPC      1      608     1       -1.     10002   1       1.0     +MP4101
290-    +MP4101         12002   1       -1.     14002   1       1.0
291-    MPC      1      608     4       -2.     11002   3       0.1     +MP4401
```

```
292-        +MP4401         13002   3       -.3     11005   2       1.0             +MP4402
293-        +MP4402         13005   2       -1.     11002   2       -1.             +MP4403
294-        +MP4403         13002   2       1.
295-        MPC     1       608     5       -2.     10005   1       1.0             +MP4501
296-        +MP4501         12005   1       -1.     14005   1       1.0             +MP4502
297-        +MP4502         10002   1       -1.     12002   1       1.0             +MP4503
298-        +MP4503         14002   1       -1.     10003   3       -.5             +MP4504
299-        +MP4504         12003   3       0.5     14003   3       -.5             +MP4505
300-        +MP4505         10001   3       0.5     12001   3       -.5             +MP4506
301-        +MP4506         14001   3       0.5
302-        MPC     1       698     3       -1.     10039   3       1.0
303-        MPC     1       698     1       -1.     11039   1       1.0
304-        MPC     1       698     5       -1.     11039   3       1.0
305-        OMIT    699     123456
306-        PBAR    10      1       0.8480  0.01985 0.18091 0.06283
307-        PBAR    11      1       100.    10.     10.     20.
308-        SPC1    1       46      11019   THRU    11025
309-        SPC1    1       46      12019   THRU    12025
310-        SPC1    1       46      13019   THRU    13025
311-        SPC1    1       46      14019   THRU    14025
312-        SPC1    1       246     698
313-        SPC1    1       246     10019   THRU    10025
314-        SPC1    1       456     11001   THRU    11017
315-        SPC1    1       456     11018
316-        SPC1    1       456     11026
317-        SPC1    1       456     11027   THRU    11039
318-        SPC1    1       456     12001   THRU    12017
319-        SPC1    1       456     12018
320-        SPC1    1       456     12026
321-        SPC1    1       456     12027   THRU    12039
322-        SPC1    1       456     13001   THRU    13017
323-        SPC1    1       456     13018
324-        SPC1    1       456     13026
325-        SPC1    1       456     13027   THRU    13039
326-        SPC1    1       456     14001   THRU    14017
327-        SPC1    1       456     14018
328-        SPC1    1       456     14026
329-        SPC1    1       456     14027   THRU    14039
330-        SPC1    1       2456    10001   THRU    10017
331-        SPC1    1       2456    10018
332-        SPC1    1       2456    10026
333-        SPC1    1       2456    10027   THRU    10039
334-        SPC1    1       123456  601     603     605     607
            ENDDATA

        **NO ERRORS FOUND - EXECUTE NASTRAN PROGRAM**

*** USER WARNING MESSAGE 2015, EITHER NO ELEMENTS CONNECT INTERNAL GRID POINT       11
    OR IT IS CONNECTED TO A RIGID ELEMENT OR A GENERAL ELEMENT.

*** USER WARNING MESSAGE 3017
    ONE OR MORE POTENTIAL SINGULARITIES HAVE NOT BEEN REMOVED BY SINGLE OR MULTI-POINT CONSTRAINTS.
    (USER COULD REQUEST NASTRAN AUTOMATIC SPC GENERATION VIA A 'PARAM AUTOSPC 1' BULK DATA CARD)

          G R I D   P O I N T   S I N G U L A R I T Y   T A B L E      SPC        1  MPC        1
    POINT          SINGULARITY  LIST OF COORDINATE COMBINATIONS THAT WILL REMOVE SINGULARITY
    ID.   TYPE       ORDER       STRONGEST COMBINATION   WEAKER COMBINATION  WEAKEST COMBINATION
    10001   G          2          1       3
    10002   G          2          1       3
    10003   G          2          1       3
    10004   G          2          1       3
    10005   G          2          1       3
    10006   G          2          1       3
    10007   G          2          1       3
    10008   G          2          1       3
    10009   G          2          1       3
    10010   G          2          1       3
<< Output from the singularity table was limited to the first 10 phantom grid points. >>

*** USER INFORMATION MESSAGE 3035
    FOR SUBCASE NUMBER      1, EPSILON SUB E =   5.0293249E-13
*** USER INFORMATION MESSAGE 3035
    FOR SUBCASE NUMBER      2, EPSILON SUB E =   4.4364106E-14
*** USER INFORMATION MESSAGE 3035
    FOR SUBCASE NUMBER      3, EPSILON SUB E =   2.4369392E-14
```

```
*** USER INFORMATION MESSAGE 3035
    FOR SUBCASE NUMBER      1, EPSILON SUB E =   0.0000000E+00
*** USER INFORMATION MESSAGE 3035
    FOR SUBCASE NUMBER      2, EPSILON SUB E =   5.5511151E-17
*** USER INFORMATION MESSAGE 3035
    FOR SUBCASE NUMBER      3, EPSILON SUB E =   5.5511151E-17

*** USER INFORMATION MESSAGE 4114
    DATA BLOCK ULV      WRITTEN ON FORTRAN UNIT  14, TRLR =         3       581         2         2       496      4044
```

UNIT THRUST LOAD

SUBCASE 1

D I S P L A C E M E N T V E C T O R

POINT ID.	TYPE	T1	T2	T3	R1	R2	R3
601	G	0.0	0.0	0.0	0.0	0.0	0.0
602	G	-7.908970E-10	0.0	2.948113E-08	0.0	-1.242338E-09	0.0
603	G	0.0	0.0	0.0	0.0	0.0	0.0
604	G	-7.908970E-10	0.0	2.948113E-08	0.0	-1.242338E-09	0.0
605	G	0.0	0.0	0.0	0.0	0.0	0.0
606	G	-7.908970E-10	0.0	2.948113E-08	0.0	-1.242338E-09	0.0
607	G	0.0	0.0	0.0	0.0	0.0	0.0
608	G	-7.908970E-10	0.0	2.948113E-08	0.0	-1.242338E-09	0.0
698	G	0.0	0.0	3.862959E-06	0.0	0.0	0.0
699	G	0.0	0.0	3.867897E-06	0.0	0.0	0.0
10001	G	2.639826E-09	0.0	3.272975E-08	0.0	0.0	0.0
10002	G	2.598370E-09	0.0	3.418335E-08	0.0	0.0	0.0
10003	G	2.563580E-09	0.0	3.688345E-08	0.0	0.0	0.0
10004	G	7.270202E-10	0.0	3.260277E-08	0.0	0.0	0.0
10005	G	5.405373E-10	0.0	3.464026E-08	0.0	0.0	0.0
11001	G	0.0	0.0	0.0	0.0	0.0	0.0
11002	G	0.0	0.0	0.0	0.0	0.0	0.0
11003	G	0.0	0.0	0.0	0.0	0.0	0.0
11004	G	0.0	0.0	0.0	0.0	0.0	0.0
11005	G	0.0	0.0	0.0	0.0	0.0	0.0
12001	G	0.0	0.0	0.0	0.0	0.0	0.0
12002	G	0.0	0.0	0.0	0.0	0.0	0.0
12003	G	0.0	0.0	0.0	0.0	0.0	0.0
12004	G	0.0	0.0	0.0	0.0	0.0	0.0
12005	G	0.0	0.0	0.0	0.0	0.0	0.0
13001	G	0.0	0.0	0.0	0.0	0.0	0.0
13002	G	0.0	0.0	0.0	0.0	0.0	0.0
13003	G	0.0	0.0	0.0	0.0	0.0	0.0
13004	G	0.0	0.0	0.0	0.0	0.0	0.0
13005	G	0.0	0.0	0.0	0.0	0.0	0.0
14001	G	-3.246454E-09	3.098101E-09	-2.619861E-09	0.0	0.0	0.0
14002	G	-3.389266E-09	2.360525E-09	-4.702220E-09	0.0	0.0	0.0
14003	G	-3.418743E-09	1.552902E-09	-4.313459E-09	0.0	0.0	0.0
14004	G	-2.164515E-09	1.878403E-09	-2.997400E-09	0.0	0.0	0.0
14005	G	-2.586062E-09	1.122367E-09	-3.852546E-09	0.0	0.0	0.0
601	G	0.0	0.0	0.0	0.0	0.0	0.0
602	G	-5.610955E-09	0.0	1.174792E-08	0.0	-1.701747E-09	0.0
603	G	0.0	0.0	0.0	0.0	0.0	0.0
604	G	0.0	2.515618E-09	0.0	-1.900792E-09	0.0	6.087235E-10
605	G	0.0	0.0	0.0	0.0	0.0	0.0
606	G	5.610955E-09	0.0	-1.174792E-08	0.0	1.701747E-09	0.0
607	G	0.0	0.0	0.0	0.0	0.0	0.0
608	G	0.0	-2.515618E-09	0.0	1.900792E-09	0.0	-6.087235E-10
698	G	2.211418E-07	0.0	0.0	0.0	2.801197E-06	0.0
699	G	4.207956E-05	0.0	0.0	0.0	2.850572E-06	0.0
10001	G	0.0	0.0	0.0	0.0	0.0	0.0
10002	G	0.0	0.0	0.0	0.0	0.0	0.0
10003	G	0.0	0.0	0.0	0.0	0.0	0.0
10004	G	0.0	0.0	0.0	0.0	0.0	0.0
10005	G	0.0	0.0	0.0	0.0	0.0	0.0
11001	G	-3.030885E-09	3.937321E-09	1.178935E-08	0.0	0.0	0.0
11002	G	-3.041456E-09	3.963108E-09	1.370397E-08	0.0	0.0	0.0
11003	G	-3.053621E-09	3.963408E-09	1.611813E-08	0.0	0.0	0.0
11004	G	-5.128662E-09	5.348634E-09	1.174310E-08	0.0	0.0	0.0
11005	G	-5.201514E-09	5.350040E-09	1.388887E-08	0.0	0.0	0.0
12001	G	0.0	0.0	0.0	0.0	0.0	0.0
12002	G	0.0	0.0	0.0	0.0	0.0	0.0
12003	G	0.0	0.0	0.0	0.0	0.0	0.0
12004	G	0.0	0.0	0.0	0.0	0.0	0.0
12005	G	0.0	0.0	0.0	0.0	0.0	0.0
13001	G	-2.513659E-09	1.936496E-09	-1.237852E-09	0.0	0.0	0.0
13002	G	-2.569499E-09	1.447490E-09	-1.956046E-09	0.0	0.0	0.0

13003	G	-2.578819E-09	9.642203E-10	-2.183185E-09	0.0	0.0	0.0
13004	G	-2.009346E-09	1.463206E-09	-1.356308E-09	0.0	0.0	0.0
13005	G	-2.121217E-09	9.900493E-10	-1.803383E-09	0.0	0.0	0.0
14001	G	0.0	0.0	0.0	0.0	0.0	0.0
14002	G	0.0	0.0	0.0	0.0	0.0	0.0
14003	G	0.0	0.0	0.0	0.0	0.0	0.0
14004	G	0.0	0.0	0.0	0.0	0.0	0.0
14005	G	0.0	0.0	0.0	0.0	0.0	0.0
601	G	0.0	0.0	0.0	0.0	0.0	0.0
602	G	1.720547E-07	0.0	1.055128E-07	0.0	-1.454852E-08	0.0
603	G	0.0	0.0	0.0	0.0	0.0	0.0
604	G	0.0	-1.707720E-07	0.0	-1.016038E-08	0.0	1.681734E-09
605	G	0.0	0.0	0.0	0.0	0.0	0.0
606	G	-1.720547E-07	0.0	-1.055128E-07	0.0	1.454852E-08	0.0
607	G	0.0	0.0	0.0	0.0	0.0	0.0
608	G	0.0	1.707720E-07	0.0	1.016038E-08	0.0	-1.681734E-09
698	G	3.755716E-06	0.0	0.0	0.0	4.171387E-05	0.0
699	G	6.252536E-04	0.0	0.0	0.0	4.207956E-05	0.0
10001	G	0.0	0.0	0.0	0.0	0.0	0.0
10002	G	0.0	0.0	0.0	0.0	0.0	0.0
10003	G	0.0	0.0	0.0	0.0	0.0	0.0
10004	G	0.0	0.0	0.0	0.0	0.0	0.0
10005	G	0.0	0.0	0.0	0.0	0.0	0.0
11001	G	1.780936E-07	-1.738395E-07	1.002073E-07	0.0	0.0	0.0
11002	G	1.779452E-07	-1.712015E-07	1.147197E-07	0.0	0.0	0.0
11003	G	1.779890E-07	-1.741763E-07	1.338945E-07	0.0	0.0	0.0
11004	G	1.618966E-07	-1.623457E-07	9.972933E-08	0.0	0.0	0.0
11005	G	1.613971E-07	-1.634723E-07	1.165638E-07	0.0	0.0	0.0
12001	G	0.0	0.0	0.0	0.0	0.0	0.0
12002	G	0.0	0.0	0.0	0.0	0.0	0.0
12003	G	0.0	0.0	0.0	0.0	0.0	0.0
12004	G	0.0	0.0	0.0	0.0	0.0	0.0
12005	G	0.0	0.0	0.0	0.0	0.0	0.0
13001	G	-6.107248E-09	3.387790E-09	-5.048370E-09	0.0	0.0	0.0
13002	G	-5.890513E-09	-4.294931E-10	-9.206829E-09	0.0	0.0	0.0
13003	G	-5.440393E-09	1.292965E-09	-9.223636E-09	0.0	0.0	0.0
13004	G	-3.301694E-09	1.366286E-09	-5.586073E-09	0.0	0.0	0.0
13005	G	-3.683499E-09	1.212996E-09	-7.655163E-09	0.0	0.0	0.0
14001	G	0.0	0.0	0.0	0.0	0.0	0.0
14002	G	0.0	0.0	0.0	0.0	0.0	0.0
14003	G	0.0	0.0	0.0	0.0	0.0	0.0
14004	G	0.0	0.0	0.0	0.0	0.0	0.0
14005	G	0.0	0.0	0.0	0.0	0.0	0.0

F O R C E S O F S I N G L E - P O I N T C O N S T R A I N T

POINT ID.	TYPE	T1	T2	T3	R1	R2	R3
601	G	-2.838843E-04	0.0	-2.500000E-01	0.0	-1.792222E-04	0.0
603	G	-2.838843E-04	0.0	-2.500000E-01	0.0	-1.792222E-04	0.0
605	G	-2.838843E-04	0.0	-2.500000E-01	0.0	-1.792222E-04	0.0
607	G	-2.838843E-04	0.0	-2.500000E-01	0.0	-1.792222E-04	0.0

F O R C E S O F S I N G L E - P O I N T C O N S T R A I N T

POINT ID.	TYPE	T1	T2	T3	R1	R2	R3
601	G	8.094393E-04	0.0	-9.962239E-02	0.0	1.551956E-03	0.0
603	G	0.0	8.094393E-04	0.0	2.224564E-03	0.0	-1.471004E-04
605	G	-8.094393E-04	0.0	9.962239E-02	0.0	-1.551956E-03	0.0
607	G	0.0	-8.094393E-04	0.0	-2.224564E-03	0.0	1.471004E-04

F O R C E S O F S I N G L E - P O I N T C O N S T R A I N T

POINT ID.	TYPE	T1	T2	T3	R1	R2	R3
601	G	-5.131291E-02	0.0	-8.947487E-01	0.0	-7.408148E-02	0.0
603	G	0.0	4.486871E-01	0.0	-6.546495E-01	0.0	-4.063975E-04
605	G	5.131291E-02	0.0	8.947487E-01	0.0	7.408148E-02	0.0
607	G	0.0	-4.486871E-01	0.0	6.546495E-01	0.0	4.063975E-04

F O R C E S I N B A R E L E M E N T S (C B A R)

ELEMENT	BEND-MOMENT END-A		BEND-MOMENT END-B		- SHEAR -		AXIAL	
ID.	PLANE 1	PLANE 2	PLANE 1	PLANE 2	PLANE 1	PLANE 2	FORCE	TORQUE
601	1.792222E-04	0.0	-6.724306E-04	0.0	2.838843E-04	0.0	2.500000E-01	0.0
602	1.792222E-04	0.0	-6.724306E-04	0.0	2.838843E-04	0.0	2.500000E-01	0.0
603	1.792222E-04	0.0	-6.724306E-04	0.0	2.838843E-04	0.0	2.500000E-01	0.0
604	1.792222E-04	0.0	-6.724306E-04	0.0	2.838843E-04	0.0	2.500000E-01	0.0

F O R C E S I N B A R E L E M E N T S (C B A R)

ELEMENT	BEND-MOMENT END-A	BEND-MOMENT END-B	- SHEAR -	AXIAL

```
  ID.        PLANE 1        PLANE 2        PLANE 1        PLANE 2        PLANE 1        PLANE 2        FORCE          TORQUE
     601   -1.551956E-03   0.0            8.763619E-04   0.0           -8.094392E-04   0.0             9.962239E-02   0.0
     602    0.0             2.224563E-03  0.0             4.652883E-03   0.0            -8.094398E-04   0.0            1.471004E-04
     603    1.551956E-03   0.0           -8.763619E-04   0.0            8.094392E-04   0.0            -9.962239E-02   0.0
     604    0.0            -2.224563E-03  0.0            -4.652883E-03   0.0             8.094398E-04   0.0           -1.471004E-04

                                F O R C E S   I N   B A R   E L E M E N T S          ( C B A R )
ELEMENT          BEND-MOMENT END-A          BEND-MOMENT END-B          - SHEAR -                      AXIAL
  ID.          PLANE 1        PLANE 2        PLANE 1        PLANE 2        PLANE 1        PLANE 2        FORCE          TORQUE
     601    7.408148E-02   0.0           -7.985723E-02   0.0            5.131290E-02   0.0             8.947487E-01   0.0
     602    0.0            -6.546494E-01   0.0            6.914117E-01   0.0           -4.486870E-01   0.0            4.063975E-04
     603   -7.408148E-02   0.0            7.985723E-02   0.0           -5.131290E-02   0.0            -8.947487E-01   0.0
     604    0.0             6.546494E-01  0.0            -6.914117E-01   0.0            4.486870E-01   0.0           -4.063975E-04
                                                  * * *  END OF JOB  * * *
```

5) This file contains the DMAP alter sequence for the last step in the procedure. The bulk data has been deleted because this model is the same one used in the first step of the procedure.

```
ID BAL3,FEM
APP  DISPLACEMENT
SOL 1,0
DIAG 14
DIAG 36
$
$ READ DISPLACEMENT SET AND COMPUTE ELEMENT FORCES
$
ALTER 75
INPUTT2 /UMC,,,,/ -1 / 11 / $
EQUIV   UMC,ULV/ALWAYS   $
ALTER 88
JUMP    LBL9  $
$ OUTPUT FORCE DATA
ALTER 108
OUTPUT2 OEF1,,,,//-1/12
ENDALTER
$
TIME 160
$
CEND
                                C A S E   C O N T R O L   D E C K   E C H O

          CARD
          COUNT
           1      TITLE = GENERIC BALANCE MODEL
           2      SUBTITLE = PART 3: INPUT DISPLACEMENT SET VECTOR
           3      $
           4      AXISYM = COSINE
           5      $
           6      SET 1 = 2,17
           7      OUTPUT
           8        DISPLACEMENTS = ALL
           9        GPFORCES = 1
          10        ELFORCES = ALL
          11        HARMONICS = ALL
          12      $
          13      SUBCASE 1
          14       LABEL = UNIT THRUST LOAD
          15       LOAD = 1
          16      $
          17      SUBCASE 2
          18       LABEL = UNIT PITCH MOMENT
          19       LOAD = 2
          20      $
          21      SUBCASE 3
          22       LABEL = UNIT AFT LOAD
          23       LOAD = 3
          24      $
          25      OUTPUT(PLOT)
          26      PLOTTER NASTPLT,D,1
          27      PAPER SIZE 11.0 X 8.5
```

```
$
 SET 1 ALL
$
 AXES X,Y,Z
 VIEW 90.,90.,0.
 FIND SCALE, ORIGIN 11, SET 1
PLOT SET 1, ORIGIN 11
$
BEGIN BULK
```

<< The bulk data for this file is exactly the same as file listing #3 in this appendix, because these are the same finite element models. The bulk data has been deleted. >>

```
*** USER INFORMATION MESSAGE - GRID-POINT RESEQUENCING PROCESSOR BANDIT IS NOT USED DUE TO
    THE PRESENCE OF AXISYMMETRIC SOLID DATA

        **NO ERRORS FOUND - EXECUTE NASTRAN PROGRAM**

*** USER INFORMATION MESSAGE 4105, DATA BLOCK UMC      RETRIEVED FROM FORTRAN TAPE 11
    NAME OF DATA BLOCK WHEN PLACED ON FORTRAN TAPE WAS ULV      .
```

UNIT THRUST LOAD   SUBCASE 1

G R I D   P O I N T   F O R C E   B A L A N C E

POINT-ID	ELEMENT-ID	SOURCE	T1	T2	T3	R1	R2	R3
1000002	1001	TRAPAX	-1.962777E-01	0.0	4.697984E-01	0.0	0.0	0.0
1000002	2001	TRAPAX	1.987579E-01	0.0	5.302037E-01	0.0	0.0	0.0
1000002		*TOTALS*	2.480194E-03	0.0	1.000002E+00	0.0	0.0	0.0
1000017	11001	CONEAX	3.862712E+01	0.0	-4.880019E+01	0.0	2.665097E+00	0.0
1000017	9001	TRAPAX	-1.411920E-02	0.0	-4.058314E-01	0.0	0.0	0.0
1000017	10001	TRAPAX	3.094939E+01	0.0	4.290217E+00	0.0	0.0	0.0
1000017		*TOTALS*	6.956239E+01	0.0	-4.491580E+01	0.0	2.665097E+00	0.0
2000002	1002	TRAPAX	0.0	0.0	0.0	0.0	0.0	0.0
2000002	2002	TRAPAX	0.0	0.0	0.0	0.0	0.0	0.0
2000002		*TOTALS*	0.0	0.0	0.0	0.0	0.0	0.0
2000017	11002	CONEAX	0.0	0.0	0.0	0.0	0.0	0.0
2000017	9002	TRAPAX	0.0	0.0	0.0	0.0	0.0	0.0
2000017	10002	TRAPAX	0.0	0.0	0.0	0.0	0.0	0.0
2000017		*TOTALS*	0.0	0.0	0.0	0.0	0.0	0.0
3000002	1003	TRAPAX	0.0	0.0	0.0	0.0	0.0	0.0
3000002	2003	TRAPAX	0.0	0.0	0.0	0.0	0.0	0.0
3000002		*TOTALS*	0.0	0.0	0.0	0.0	0.0	0.0
3000017	11003	CONEAX	0.0	0.0	0.0	0.0	0.0	0.0
3000017	9003	TRAPAX	0.0	0.0	0.0	0.0	0.0	0.0
3000017	10003	TRAPAX	0.0	0.0	0.0	0.0	0.0	0.0
3000017		*TOTALS*	0.0	0.0	0.0	0.0	0.0	0.0
4000002	1004	TRAPAX	0.0	0.0	0.0	0.0	0.0	0.0
4000002	2004	TRAPAX	0.0	0.0	0.0	0.0	0.0	0.0
4000002		*TOTALS*	0.0	0.0	0.0	0.0	0.0	0.0
4000017	11004	CONEAX	0.0	0.0	0.0	0.0	0.0	0.0
4000017	9004	TRAPAX	0.0	0.0	0.0	0.0	0.0	0.0
4000017	10004	TRAPAX	0.0	0.0	0.0	0.0	0.0	0.0
4000017		*TOTALS*	0.0	0.0	0.0	0.0	0.0	0.0
5000002	1005	TRAPAX	-3.393911E-01	-6.053476E-02	-2.903760E-01	0.0	0.0	0.0
5000002	2005	TRAPAX	-1.026829E+00	6.023814E-01	-1.034488E+00	0.0	0.0	0.0
5000002		*TOTALS*	-1.366220E+00	5.418466E-01	-1.324864E+00	0.0	0.0	0.0
5000017	11005	CONEAX	2.364401E-01	-3.854312E-01	-2.812054E-01	0.0	3.798493E-02	0.0
5000017	9005	TRAPAX	-1.272544E+00	-7.269861E-01	-1.453672E+00	0.0	0.0	0.0
5000017	10005	TRAPAX	9.631046E-01	-3.777996E-01	-1.490628E+00	0.0	0.0	0.0
5000017		*TOTALS*	-7.299960E-02	-1.490217E+00	-3.225505E+00	0.0	3.798493E-02	0.0

<< Grid point force balance has been limited to subcase 1 only. >>

```
*** USER INFORMATION MESSAGE 4114

  DATA BLOCK OEF1    WRITTEN ON FORTRAN UNIT  12, TRLR  =     63     1     16     91     6     1
```

<< Displacement output is limited to the first 10 rings. >>

UNIT THRUST LOAD   SUBCASE 1

D I S P L A C E M E N T   V E C T O R

SECTOR-ID POINT-ID RING-ID	HARMONIC	T1	T2	T3	R1	R2	R3
1	0	2.639826E-09	0.0	3.272975E-08	0.0	0.0	0.0
2	0	2.598370E-09	0.0	3.418335E-08	0.0	0.0	0.0
3	0	2.563580E-09	0.0	3.688345E-08	0.0	0.0	0.0
4	0	7.270202E-10	0.0	3.260277E-08	0.0	0.0	0.0
5	0	5.405373E-10	0.0	3.464026E-08	0.0	0.0	0.0
6	0	3.569469E-10	0.0	3.680350E-08	0.0	0.0	0.0
7	0	-1.464268E-09	0.0	3.276735E-08	0.0	0.0	0.0
8	0	-1.509579E-09	0.0	3.495903E-08	0.0	0.0	0.0
9	0	-1.593410E-09	0.0	3.708061E-08	0.0	0.0	0.0
10	0	-3.688067E-09	0.0	3.298806E-08	0.0	0.0	0.0
1	1	0.0	0.0	0.0	0.0	0.0	0.0
2	1	0.0	0.0	0.0	0.0	0.0	0.0
3	1	0.0	0.0	0.0	0.0	0.0	0.0
4	1	0.0	0.0	0.0	0.0	0.0	0.0
5	1	0.0	0.0	0.0	0.0	0.0	0.0
6	1	0.0	0.0	0.0	0.0	0.0	0.0
7	1	0.0	0.0	0.0	0.0	0.0	0.0
8	1	0.0	0.0	0.0	0.0	0.0	0.0

SUBCASE 1

UNIT THRUST LOAD

D I S P L A C E M E N T V E C T O R

SECTOR-ID POINT-ID RING-ID	HARMONIC	T1	T2	T3	R1	R2	R3
9	1	0.0	0.0	0.0	0.0	0.0	0.0
10	1	0.0	0.0	0.0	0.0	0.0	0.0
1	2	0.0	0.0	0.0	0.0	0.0	0.0
2	2	0.0	0.0	0.0	0.0	0.0	0.0
3	2	0.0	0.0	0.0	0.0	0.0	0.0
4	2	0.0	0.0	0.0	0.0	0.0	0.0
5	2	0.0	0.0	0.0	0.0	0.0	0.0
6	2	0.0	0.0	0.0	0.0	0.0	0.0
7	2	0.0	0.0	0.0	0.0	0.0	0.0
8	2	0.0	0.0	0.0	0.0	0.0	0.0
9	2	0.0	0.0	0.0	0.0	0.0	0.0
10	2	0.0	0.0	0.0	0.0	0.0	0.0
1	3	0.0	0.0	0.0	0.0	0.0	0.0
2	3	0.0	0.0	0.0	0.0	0.0	0.0
3	3	0.0	0.0	0.0	0.0	0.0	0.0
4	3	0.0	0.0	0.0	0.0	0.0	0.0
5	3	0.0	0.0	0.0	0.0	0.0	0.0
6	3	0.0	0.0	0.0	0.0	0.0	0.0
7	3	0.0	0.0	0.0	0.0	0.0	0.0
8	3	0.0	0.0	0.0	0.0	0.0	0.0
9	3	0.0	0.0	0.0	0.0	0.0	0.0
10	3	0.0	0.0	0.0	0.0	0.0	0.0
1	4	-4.313459E-09	-2.164515E-09	1.878403E-09	0.0	0.0	0.0
2	4	-2.997400E-09	-2.586062E-09	1.122367E-09	0.0	0.0	0.0
3	4	-3.852546E-09	-2.885780E-09	3.676892E-10	0.0	0.0	0.0
4	4	-4.461612E-09	-1.659919E-09	9.673008E-10	0.0	0.0	0.0
5	4	-2.800361E-09	-1.834405E-09	3.971995E-10	0.0	0.0	0.0
6	4	-3.380789E-09	-1.939248E-09	-2.364189E-10	0.0	0.0	0.0
7	4	-4.078494E-09	-1.117116E-09	3.087811E-10	0.0	0.0	0.0
8	4	-2.572755E-09	-1.178822E-09	-1.237397E-10	0.0	0.0	0.0
9	4	-3.080942E-09	-1.204106E-09	-5.844617E-10	0.0	0.0	0.0
10	4	-3.677761E-09	-6.553869E-10	-2.791431E-10	0.0	0.0	0.0

SUBCASE 2

UNIT PITCH MOMENT

D I S P L A C E M E N T V E C T O R

SECTOR-ID POINT-ID RING-ID	HARMONIC	T1	T2	T3	R1	R2	R3
1	0	0.0	0.0	0.0	0.0	0.0	0.0
2	0	0.0	0.0	0.0	0.0	0.0	0.0
3	0	0.0	0.0	0.0	0.0	0.0	0.0
4	0	0.0	0.0	0.0	0.0	0.0	0.0
5	0	0.0	0.0	0.0	0.0	0.0	0.0
6	0	0.0	0.0	0.0	0.0	0.0	0.0
7	0	0.0	0.0	0.0	0.0	0.0	0.0
8	0	0.0	0.0	0.0	0.0	0.0	0.0
9	0	0.0	0.0	0.0	0.0	0.0	0.0
10	0	0.0	0.0	0.0	0.0	0.0	0.0
1	1	1.178935E-08	-3.041456E-09	3.963108E-09	0.0	0.0	0.0

2	1	1.370397E-08	-3.053621E-09	3.963408E-09	0.0	0.0	0.0
3	1	1.611813E-08	-5.128662E-09	5.348634E-09	0.0	0.0	0.0
4	1	1.174310E-08	-5.201514E-09	5.350040E-09	0.0	0.0	0.0
5	1	1.388887E-08	-5.271955E-09	5.360884E-09	0.0	0.0	0.0
6	1	1.608736E-08	-7.336571E-09	6.839640E-09	0.0	0.0	0.0
7	1	1.180696E-08	-7.354734E-09	6.779539E-09	0.0	0.0	0.0
8	1	1.401556E-08	-7.388014E-09	6.715505E-09	0.0	0.0	0.0
9	1	1.619888E-08	-9.560636E-09	8.350312E-09	0.0	0.0	0.0
10	1	1.188170E-08	-9.552582E-09	8.208898E-09	0.0	0.0	0.0
1	2	0.0	0.0	0.0	0.0	0.0	0.0
2	2	0.0	0.0	0.0	0.0	0.0	0.0
3	2	0.0	0.0	0.0	0.0	0.0	0.0
4	2	0.0	0.0	0.0	0.0	0.0	0.0
5	2	0.0	0.0	0.0	0.0	0.0	0.0
6	2	0.0	0.0	0.0	0.0	0.0	0.0
7	2	0.0	0.0	0.0	0.0	0.0	0.0
8	2	0.0	0.0	0.0	0.0	0.0	0.0
9	2	0.0	0.0	0.0	0.0	0.0	0.0
10	2	0.0	0.0	0.0	0.0	0.0	0.0
1	3	-2.578819E-09	9.642203E-10	-2.183185E-09	0.0	0.0	0.0
2	3	-2.009346E-09	1.463206E-09	-1.356308E-09	0.0	0.0	0.0
3	3	-2.121217E-09	9.900493E-10	-1.803383E-09	0.0	0.0	0.0
4	3	-2.178755E-09	5.026283E-10	-2.206326E-09	0.0	0.0	0.0
5	3	-1.639812E-09	1.025641E-09	-1.347159E-09	0.0	0.0	0.0
6	3	-1.693739E-09	6.213332E-10	-1.718476E-09	0.0	0.0	0.0
7	3	-1.708921E-09	2.049921E-10	-2.120450E-09	0.0	0.0	0.0
8	3	-1.278950E-09	6.394917E-10	-1.320283E-09	0.0	0.0	0.0
9	3	-1.300843E-09	3.035907E-10	-1.657742E-09	0.0	0.0	0.0
10	3	-1.295482E-09	-3.866900E-11	-2.021836E-09	0.0	0.0	0.0
1	4	0.0	0.0	0.0	0.0	0.0	0.0
2	4	0.0	0.0	0.0	0.0	0.0	0.0
3	4	0.0	0.0	0.0	0.0	0.0	0.0
4	4	0.0	0.0	0.0	0.0	0.0	0.0
5	4	0.0	0.0	0.0	0.0	0.0	0.0
6	4	0.0	0.0	0.0	0.0	0.0	0.0
7	4	0.0	0.0	0.0	0.0	0.0	0.0
8	4	0.0	0.0	0.0	0.0	0.0	0.0
9	4	0.0	0.0	0.0	0.0	0.0	0.0
10	4	0.0	0.0	0.0	0.0	0.0	0.0

UNIT AFT LOAD

SUBCASE 3

D I S P L A C E M E N T V E C T O R

SECTOR-ID POINT-ID RING-ID	HARMONIC	T1	T2	T3	R1	R2	R3
1	0	0.0	0.0	0.0	0.0	0.0	0.0
2	0	0.0	0.0	0.0	0.0	0.0	0.0
3	0	0.0	0.0	0.0	0.0	0.0	0.0
4	0	0.0	0.0	0.0	0.0	0.0	0.0
5	0	0.0	0.0	0.0	0.0	0.0	0.0
6	0	0.0	0.0	0.0	0.0	0.0	0.0
7	0	0.0	0.0	0.0	0.0	0.0	0.0
8	0	0.0	0.0	0.0	0.0	0.0	0.0
9	0	0.0	0.0	0.0	0.0	0.0	0.0
10	0	0.0	0.0	0.0	0.0	0.0	0.0
1	1	1.002073E-07	1.779452E-07	-1.712015E-07	0.0	0.0	0.0
2	1	1.147197E-07	1.779890E-07	-1.741763E-07	0.0	0.0	0.0
3	1	1.338945E-07	1.618966E-07	-1.623457E-07	0.0	0.0	0.0
4	1	9.972933E-08	1.613971E-07	-1.634723E-07	0.0	0.0	0.0
5	1	1.165638E-07	1.606930E-07	-1.628763E-07	0.0	0.0	0.0
6	1	1.339398E-07	1.443895E-07	-1.515336E-07	0.0	0.0	0.0
7	1	1.001407E-07	1.443175E-07	-1.523106E-07	0.0	0.0	0.0
8	1	1.179267E-07	1.439687E-07	-1.532900E-07	0.0	0.0	0.0
9	1	1.354955E-07	1.262950E-07	-1.400403E-07	0.0	0.0	0.0
10	1	1.007155E-07	1.264366E-07	-1.416957E-07	0.0	0.0	0.0
1	2	0.0	0.0	0.0	0.0	0.0	0.0
2	2	0.0	0.0	0.0	0.0	0.0	0.0
3	2	0.0	0.0	0.0	0.0	0.0	0.0
4	2	0.0	0.0	0.0	0.0	0.0	0.0
5	2	0.0	0.0	0.0	0.0	0.0	0.0
6	2	0.0	0.0	0.0	0.0	0.0	0.0
7	2	0.0	0.0	0.0	0.0	0.0	0.0
8	2	0.0	0.0	0.0	0.0	0.0	0.0
9	2	0.0	0.0	0.0	0.0	0.0	0.0
10	2	0.0	0.0	0.0	0.0	0.0	0.0
1	3	-5.440393E-09	1.292965E-09	-9.223636E-09	0.0	0.0	0.0

2	3	-3.301694E-09	1.366286E-09	-5.586073E-09	0.0	0.0	0.0
3	3	-3.683499E-09	1.212996E-09	-7.655163E-09	0.0	0.0	0.0
4	3	-4.111131E-09	-5.739011E-10	-9.287293E-09	0.0	0.0	0.0
5	3	-1.839876E-09	4.981898E-10	-5.437970E-09	0.0	0.0	0.0
6	3	-1.950501E-09	-1.892448E-10	-6.959178E-09	0.0	0.0	0.0
7	3	-2.077800E-09	-7.417547E-10	-8.568358E-09	0.0	0.0	0.0
8	3	-4.745768E-10	-7.674623E-10	-5.218832E-09	0.0	0.0	0.0
9	3	-4.650081E-10	-1.047147E-09	-6.521891E-09	0.0	0.0	0.0
10	3	-5.085589E-10	-1.359747E-09	-7.921546E-09	0.0	0.0	0.0
1	4	0.0	0.0	0.0	0.0	0.0	0.0
2	4	0.0	0.0	0.0	0.0	0.0	0.0
3	4	0.0	0.0	0.0	0.0	0.0	0.0
4	4	0.0	0.0	0.0	0.0	0.0	0.0
5	4	0.0	0.0	0.0	0.0	0.0	0.0
6	4	0.0	0.0	0.0	0.0	0.0	0.0
7	4	0.0	0.0	0.0	0.0	0.0	0.0
8	4	0.0	0.0	0.0	0.0	0.0	0.0
9	4	0.0	0.0	0.0	0.0	0.0	0.0
10	4	0.0	0.0	0.0	0.0	0.0	0.0

* * * END OF JOB * * *

N91-20517

Finite Element Solution of Transient Fluid-Structure Interaction Problems

Gordon C. Everstine, Raymond S. Cheng, and Stephen A. Hambric
Computational Mechanics Division (128)
David Taylor Research Center
Bethesda, Maryland 20084

ABSTRACT

A finite element approach using NASTRAN is developed for solving time-dependent fluid-structure interaction problems, with emphasis on the transient scattering of acoustic waves from submerged elastic structures. Finite elements are used for modeling both structure and fluid domains to facilitate the graphical display of the wave motion through both media. For the fluid, the use of velocity potential as the fundamental unknown results in a symmetric matrix equation. The approach is illustrated for the problem of transient scattering from a submerged elastic spherical shell subjected to an incident tone burst. The use of an analogy between the equations of elasticity and the wave equation of acoustics, a necessary ingredient to the procedure, is summarized.

INTRODUCTION

Computational structural acoustics is concerned with the prediction of the acoustic pressure field radiated or scattered by submerged structures subjected to either mechanical or external (fluid) excitation. When the excitation is time-harmonic, the most common numerical approach for solving the interaction problem is to couple a finite element model of the structure with a boundary element model of the surrounding fluid (Ref. 1-8). Other fluid modeling approaches have included finite element (Ref. 9-20), combined finite element/analytical (Ref. 21-23), and T-matrix (Ref. 24-26).

For time domain (transient) analysis, there are several computational approaches which can be used:

- the transformation of frequency domain results to the time domain using the Fourier transform
- the use of a fluid loading approximation such as the doubly asymptotic approximation (DAA) (Ref. 27)
- the time domain boundary element approach, which models the fluid with the retarded potential integral equation (Ref. 28-31)
- the fluid finite element approach, which models the exterior fluid domain with finite elements truncated at a finite distance from the structure and terminated with an approximate radiation boundary condition to absorb outgoing waves (Ref. 9-20)

To our knowledge, the retarded potential integral equation has been used only for special geometries (e.g., axisymmetry) because of the method's relatively high computational cost. The DAA approach, which has been used successfully in underwater shock analysis (Ref. 32-34), may not be adequate for transient acoustics, where the interest is in the response in the fluid as well as in the structure. The principal computational trade-off between the fluid finite element approach and the other three approaches is that the finite element approach yields large, banded matrices, whereas the other three

approaches (which depend on boundary element calculations) yield smaller, densely-populated matrices. This trade-off often favors the finite element approach for long, slender structures like ships which are "naturally banded." In addition, of the four approaches listed, only the fluid finite element approach has directly available an explicit fluid mesh which can be used for graphical display of the wave motion through the fluid. Since a significant part of our interest involves the display of wave propagation through both structure and fluid, we therefore formulate the transient acoustics problem using the fluid finite element approach. The principal drawbacks to a fluid finite element approach are the need for an approximate radiation boundary condition at the outer fluid boundary, the requirements on mesh size and extent (sometimes leading to frequency-dependent fluid meshes (Ref. 17)), and the difficulty of generating the fluid mesh.

Dynamics problems involving the interaction between an elastic structure and an acoustic fluid have been formulated for finite element solution using pressure (Ref. 9,10), fluid particle displacement (Ref. 11-13,15,17), displacement potential (Ref. 16), and velocity potential (Ref. 18,19) as the fundamental unknown in the fluid region. In three dimensions, the pressure and displacement formulations result in, respectively, one and three degrees of freedom per finite element mesh point. Thus the pressure approach has the advantage of fewer unknowns and a smaller overall matrix profile or bandwidth if the grid points are properly sequenced. On the other hand, the displacement approach results in symmetric coefficient matrices (in contrast to the pressure formulation, for which the matrices are nonsymmetric) and a fluid-structure interface condition which is easier to implement with general purpose finite element computer programs. However, the displacement approach also suffers from the presence of spurious resonances (Ref. 15), a situation which can be bothersome in time-harmonic problems, either forced or unforced. The principal disadvantage of the pressure formulation, nonsymmetric coefficient matrices, can be removed merely by reformulating the pressure solution approach so that a velocity potential rather than pressure is used as the fundamental unknown in the fluid region (Ref. 18). For some situations, particularly time-harmonic problems involving damped systems and time-dependent problems, significant computational advantages result.

The principal goal of this paper is to develop in detail the symmetric velocity potential formulation for application to the specific problem of transient acoustic scattering from submerged elastic structures. Previously (Ref. 18), the symmetric potential formulation was described only in general terms for a wide class of fluid-structure interaction problems with no details concerning specific types of applications such as vibrations, shock response, or acoustic scattering.

From an engineering point of view, it is convenient to be able to make use of existing general purpose finite element codes such as NASTRAN, because of their wide availablity, versatility, reliability, consultative support, and abundance of pre- and postprocessors. Thus the next section summarizes an analogy between the equations of elasticity and the wave equation of acoustics. Such an analogy allows the coupled structural acoustic problem to be solved with standard finite element codes.

STRUCTURAL-ACOUSTIC ANALOGY

Since we wish to solve the coupled structural acoustic problem using standard finite element codes, we summarize here the application of such codes to the wave equation of acoustics (Ref. 35,36),

$$\nabla^2 p = \ddot{p}/c^2, \tag{1}$$

where ∇^2 is the Laplacian operator, p is the dynamic fluid pressure, c is the wave speed, and dots denote partial differentiation with respect to time.

On the other hand, the x-component of the Navier equations of elasticity, which are the equations solved by structural analysis computer programs, is

$$\frac{\lambda+2G}{G}u_{,xx} + u_{,yy} + u_{,zz} + \frac{\lambda+G}{G}(v_{,xy} + w_{,xz}) + \frac{1}{G}f_x = \frac{\rho}{G}\ddot{u}, \tag{2}$$

where u, v, and w are the Cartesian components of displacement, λ is a Lame´ elastic constant, G is the shear modulus, f_x is the x-component of body force per unit volume (e.g., gravity), ρ is the mass density, and commas denote partial differentiation.

A comparison of Eqs. 1 and 2 indicates that elastic finite elements can be used to model scalar pressure fields if we let u, the x-component of displacement, represent p, set v = w = 0 everywhere, $f_x = 0$, and $\lambda = -G$. For three-dimensional analysis, the engineering constants consistent with this last requirement are (Ref. 36)

$$E_e = 10^{20}G_e, \qquad \rho_e = G_e/c^2, \tag{3}$$

where the element shear modulus G_e can be selected arbitrarily. The subscript "e" has been added to these constants to emphasize that they are merely numbers assigned to the elements.

A variety of boundary conditions may also be imposed. At a pressure-release boundary, p = 0 is enforced explicitly like other displacement boundary conditions. For gradient conditions, the pressure gradient $\partial p/\partial n$ is enforced at a boundary point by applying a "force" to the unconstrained DOF at that point equal to $G_e A\partial p/\partial n$, where A is the area assigned to the point and n is the outward normal from the fluid region (Ref. 36). For example, the plane wave absorbing boundary condition

$$\frac{\partial p}{\partial n} = -\frac{\dot{p}}{c} \tag{4}$$

is enforced by applying to each point on the outer fluid boundary a "force" given by $-(G_eA/c)\dot{p}$. Since this "force" is proportional to the first time derivative of the fundamental solution variable p, this boundary condition is imposed in the analogy by attaching to the fluid DOF a "dashpot" of constant G_eA/c. The Neumann condition $\partial p/\partial n = 0$ is the natural boundary condition under this analogy. The next higher order local radiation boundary condition, the curved wave absorbing boundary condition (Ref. 20,37)

$$\frac{\partial p}{\partial n} = -\frac{\dot{p}}{c} - \frac{p}{r}, \tag{5}$$

where r is the radius of the boundary, is enforced under the analogy by attaching in parallel both a "dashpot" and a "spring" between each boundary point and ground.

At a fluid-structure interface (an accelerating boundary), momentum and continuity considerations require that

$$\frac{\partial p}{\partial n} = -\rho\ddot{u}_n, \tag{6}$$

where n is the normal at the interface, ρ is the mass density of the fluid, and $\ddot{u}_n$ is the normal component of fluid particle acceleration. Under the analogy, this condition is enforced by applying to the fluid DOF at a fluid-structure interface a "force" given by $-(G_e\rho A)\ddot{u}_n$.

To summarize, the wave equation, Eq. 1, can be solved with elastic finite elements if the three-dimensional region is modeled with 3-D solid finite elements having material properties given by Eq. 3, and only one of the three Cartesian components of displacement is retained to represent the scalar variable p. In Cartesian coordinates, any of the three components can be used. The solution of axisymmetric problems in cylindrical coordinates follows the same approach except that the z-component of displacement is the only one which can be used to represent p (Ref. 36).

SCATTERING FROM ELASTIC STRUCTURES

In the scattering problem, a submerged elastic body is subjected to a plane wave incident loading, as shown in Fig. 1. For the time-harmonic case, the excitation has a single circular frequency ω. For the time-dependent (transient) case of interest here, the prescribed pressure loading is an arbitrary function of time. Without loss of generality, we can assume that the incident wave propagates in the negative z direction. The speed of such propagation is c, the speed of sound in the fluid.

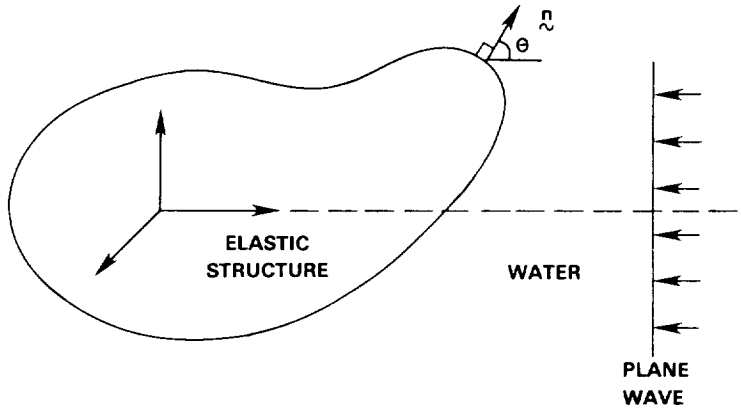

Fig. 1. The scattering problem.

Within the fluid region, the total pressure p satisfies the wave equation, Eq. 1. Since the incident free-field pressure p_i is known, it is convenient to decompose the total pressure p into the sum of incident and scattered pressures

$$p = p_i + p_s, \tag{7}$$

each of which satisfies the wave equation. (By definition, the incident free-field pressure is that pressure which would occur in the fluid in the absence of any scatterer.)

We now formulate the problem for finite element solution. Consider an arbitrary, submerged, three-dimensional elastic structure subjected to either internal time-dependent loads or an external time-dependent incident pressure. If the structure is modeled with finite elements, the resulting matrix equation of motion for the structural degrees of freedom (DOF) is

$$M\ddot{u} + B\dot{u} + Ku = F - GAp, \tag{8}$$

where M, B, and K are the structural mass, viscous damping, and stiffness matrices (dimension s x s), respectively, u is the displacement vector for all structural DOF (wet and dry) in terms of the coordinate systems selected by the user (s x r), F is the vector of applied mechanical forces applied to the structure (s x r), G is the rectangular transformation matrix of direction cosines to transform a vector of outward normal forces at the wet points to a vector of forces at all points in the coordinate systems selected by the user (s x f), A is the diagonal area matrix for the wet surface (f x f), p is the vector of total fluid pressures (incident + scattered) applied at the wet grid points (f x r), and dots denote differentiation with respect to time. The pressure p is assumed positive in compression. In the above dimensions, s denotes the total number of independent structural DOF (wet and dry), f denotes the number of fluid DOF (the number of wet points), and r denotes the number of load cases. If first order finite elements are used for the surface discretization, surface areas, normals, and the transformation matrix G can be obtained from the calculation of the load vector resulting from an outwardly directed static unit pressure load on the structure's wet surface. The matrix

product GA can then be interpreted as the matrix which converts a vector of negative fluid pressures to structural loads in the global coordinate system. The last two equations can be combined to yield

$$M\ddot{u} + B\dot{u} + Ku + GAp_s = F - GAp_i. \tag{9}$$

A finite element model of the fluid region (with scattered pressure p_s as the unknown) results in a matrix equation of the form

$$Q\ddot{p}_s + C\dot{p}_s + Hp_s = F^{(p)}, \tag{10}$$

where p_s is the vector of scattered fluid pressures at the grid points of the fluid region, Q and H are the fluid "inertia" and "stiffness" matrices (analogous to M and K for structures), C is the "damping" matrix arising from the radiation boundary condition (Eq. 4), and $F^{(p)}$ is the "loading" applied to fluid DOF due to the fluid-structure interface condition, Eq. 6. Using the analogy described in the preceding section, structural finite elements can be used to model both structural and fluid regions. Material constants assigned to the elastic elements used to model the fluid are specified according to Eq. 3. In three dimensions, elastic solid elements are used (e.g., isoparametric bricks for general 3-D analysis or solids of revolution for axisymmetric analysis).

At the fluid-structure interface, Eqs. 6 and 7 can be combined to yield

$$\frac{\partial p_s}{\partial n} = \rho(\ddot{u}_{ni} - \ddot{u}_n), \tag{11}$$

where n is the outward unit normal, and $\ddot{u}_{ni}$ and $\ddot{u}_n$ are, respectively, the incident and total outward normal components of fluid particle acceleration at the interface. Thus, from the analogy, we impose the fluid-structure interface condition by applying a "load" to each interface fluid point given by

$$F^{(p)} = -\rho G_e A\,(\ddot{u}_{ni} - \ddot{u}_n), \tag{12}$$

where the first minus sign is introduced since, in the coupled problem, we choose n as the outward normal from the structure into the fluid, making n an inward normal for the fluid region. The normal displacements u_n are related to the total displacements u by the same rectangular transformation matrix G used above:

$$u_n = G^T u, \tag{13}$$

where the superscript T denotes the matrix transpose. Eqs. 10, 12, and 13 can be combined to yield

$$Q\ddot{p}_s + C\dot{p}_s + Hp_s - \rho G_e (GA)^T \ddot{u} = -\rho G_e A \ddot{u}_{ni}. \tag{14}$$

Since the fluid-structure coupling terms in Eqs. 9 and 14 are nonsymmetric, we symmetrize the problem (Ref. 18) by using a new fluid unknown q such that

$$q = \int_0^t p_s\, dt, \qquad \dot{q} = p_s. \tag{15}$$

If Eq. 14 is integrated in time, and the fluid element "shear modulus" G_e is chosen as

$$G_e = -1/\rho, \tag{16}$$

the overall matrix system describing the coupled problem can be written as

$$\begin{bmatrix} M & 0 \\ 0 & Q \end{bmatrix} \begin{Bmatrix} \ddot{u} \\ \ddot{q} \end{Bmatrix} + \begin{bmatrix} B & (GA) \\ (GA)^T & C \end{bmatrix} \begin{Bmatrix} \dot{u} \\ \dot{q} \end{Bmatrix} + \begin{bmatrix} K & 0 \\ 0 & H \end{bmatrix} \begin{Bmatrix} u \\ q \end{Bmatrix} = \begin{Bmatrix} F - (GA)p_i \\ Av_{ni} \end{Bmatrix}, \tag{17}$$

where v_{ni} $(=\dot{u}_{ni})$ is the outward normal component of incident fluid particle velocity.

The new variable q is, except for a multiplicative constant, the velocity potential ϕ, since

$$p = -\rho\dot{\phi}. \tag{18}$$

Eq. 17 could also be recast in terms of ϕ rather than q as the fundamental fluid unknown, but no particular advantage would result. In fact, the use of q rather than ϕ has the practical advantage that the fluid pressure can be recovered directly from the finite element program as the time derivative (velocity) of the unknown q.

To summarize, both structural and fluid regions are modeled with finite elements. For the fluid region, the material constants assigned to the finite elements are

$$E_e = -10^{20}/\rho, \quad G_e = -1/\rho, \quad \nu_e = \text{unspecified}, \quad \rho_e = -1/(\rho c^2), \tag{19}$$

where E_e, G_e, ν_e, and ρ_e are the Young's modulus, shear modulus, Poisson's ratio, and mass density, respectively, assigned to the fluid finite elements. The properties ρ and c above are the actual density and sound speed for the fluid medium. The radiation boundary condition used is the plane wave approximation, Eq. 4, which appears to be adequate if the outer fluid boundary is sufficiently far from the structure (Ref. 17). With this boundary condition, matrix C in Eq. 17 arises from dashpots applied at the outer fluid boundary with damping constant $-A/(\rho c)$ at each grid point to which the area A has been assigned. At the fluid-structure interface, matrix GA is entered using the areas (or areal direction cosines) assigned to each wet degree of freedom. (Recall that GA can be interpreted as the matrix which converts a vector of negative fluid pressures to structural loads in the global coordinate system.)

The right-hand side of Eq. 17 can be simplified further since, for plane waves propagating in the negative z direction at speed c, the incident free-field pressure and incident fluid particle velocity in the z direction are related by (Ref. 38)

$$p_i = -\rho c v_{zi}. \tag{20}$$

Then, like in Fig. 1, if we define θ as the angle between the normal n and the positive z axis,

$$v_{ni} = v_{zi}\cos\theta = -p_i\cos\theta/(\rho c). \tag{21}$$

For plane waves, the z component of the free-field fluid particle velocity v_{zi} is the same at all points in space except for a time delay, which depends only on the z coordinate of the points.

Thus, Eq. 17 can alternatively be written

$$\begin{bmatrix} M & 0 \\ 0 & Q \end{bmatrix} \begin{Bmatrix} \ddot{u} \\ \ddot{q} \end{Bmatrix} + \begin{bmatrix} B & (GA) \\ (GA)^T & C \end{bmatrix} \begin{Bmatrix} \dot{u} \\ \dot{q} \end{Bmatrix} + \begin{bmatrix} K & 0 \\ 0 & H \end{bmatrix} \begin{Bmatrix} u \\ q \end{Bmatrix} = \begin{Bmatrix} F - (GA)p_i \\ -Ap_i \cos\theta/(\rho c) \end{Bmatrix}. \tag{22}$$

This is the form of the equations which we will use to solve the transient scattering problem. The right-hand side, which has nonzero contributions for both structure and fluid interface points, depends only on the incident free-field pressure at the fluid-structure interface. For scattering problems, the mechanical load F is zero. For radiation problems, F is nonzero, and the incident pressure p_i vanishes.

We note that the structural and fluid unknowns are not sequenced as perhaps implied by the partitioned form of Eq. 22. The coupling matrix GA is quite sparse and has nonzeros only for matrix rows associated with the structural DOF at the fluid-structure interface and columns associated with the coincident fluid points. Thus, the grid points should be sequenced for minimum matrix bandwidth or profile as if the structural and fluid meshes comprised a single large mesh. As a result, the structural and fluid grid points will, in general, be interspersed in their numbering, and the system matrices will be sparse and banded.

EXAMPLE: SCATTERING FROM A SUBMERGED SPHERICAL SHELL

The validation of the procedure described above was made by comparing the finite element prediction of the time history of the structural response of a spherical shell subjected to a step incident pressure loading with the series solution (Ref. 28,39). These results will not be presented here. Instead, we will illustrate the approach by calculating the transient response of a submerged, thin-walled, evacuated spherical shell subjected to a brief tone burst, as illustrated in Fig. 2. For convenience, we nondimensionalize lengths to the shell mean radius a, velocities to the fluid sound speed c, and pressures to the fluid bulk modulus ρc^2. Thus, nondimensional time becomes ct/a. The particular problem solved was a 2% thick steel shell immersed in water. Hence, in nondimensional units, the shell properties are thickness = 0.02, Young's modulus = 96.9, Poisson's ratio = 0.3, and density = 7.79.

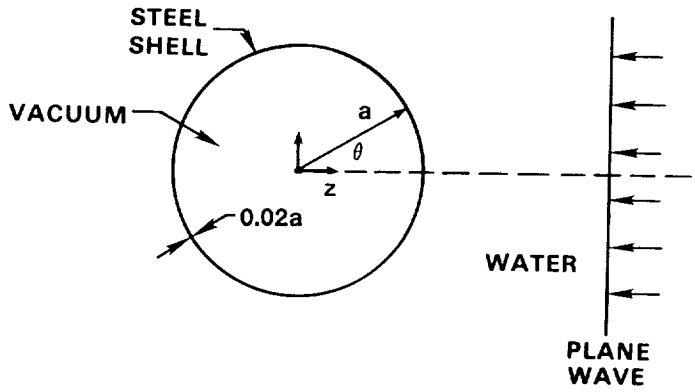

Fig. 2. Scattering from a submerged spherical shell.

The incident free-field pressure $p_i(z,t)$ is given by

$$p_i(x,y,z,t) = \hat{p}_i(t + \frac{z-a}{c}), \tag{23}$$

where (Fig. 3)

$$\hat{p}_i(t) = \begin{cases} p_o\,(1 - \cos\omega t)/2, & 0 \le \omega t \le \pi \\ -p_o \cos\omega t, & \pi \le \omega t \le (n-1)\pi \\ -p_o\,(1 + \cos\omega t)/2, & (n-1)\pi \le \omega t \le n\pi \quad (n \text{ odd}) \\ 0, & \text{otherwise.} \end{cases} \tag{24}$$

For this problem, p_o=1, n=5, and $\omega a/c=\pi$.

Since this problem is axisymmetric, it was modeled for finite element solution using NASTRAN's conical shell elements (CONEAX) for the shell and triangular ring elements (TRIAAX) for the fluid. A typical fluid mesh is shown in Fig. 4, where the shell is coincident with the inner semi-circle of fluid grid points. The actual mesh used to generate the results which follow had the outer fluid boundary located at 8 radii, used 24 elements along the inner radius between the poles and 56 elements in the radial direction, resulting in a total of 25 structural grid points, 6213 fluid grid points, 24 CONEAX elements, 12096 TRIAAX elements, and 6288 independent degrees of freedom. For the direct time integration, 800 nondimensional time steps of size 0.025 were used.

Results are presented for both velocity response of the shell and scattered pressure response in the fluid. Fig. 5 shows plots of time histories of shell velocity in the z direction for the point first

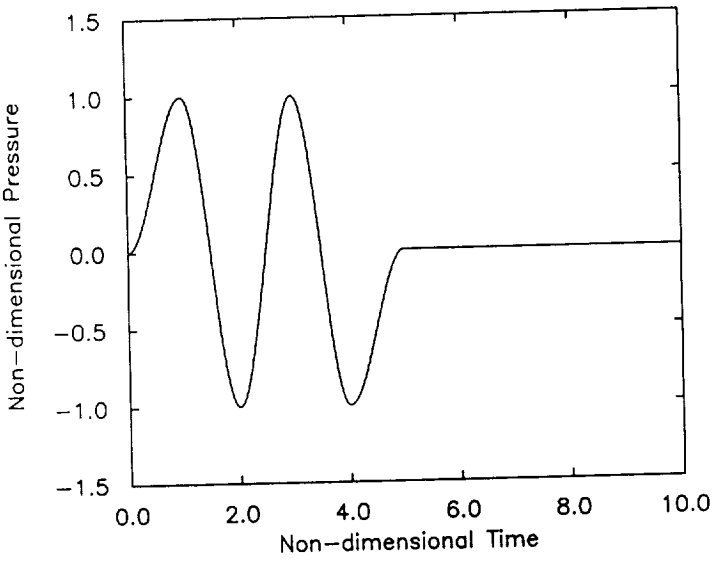

Fig. 3. The incident pressure $\hat{p}_i(t)$ (Eq. 24).

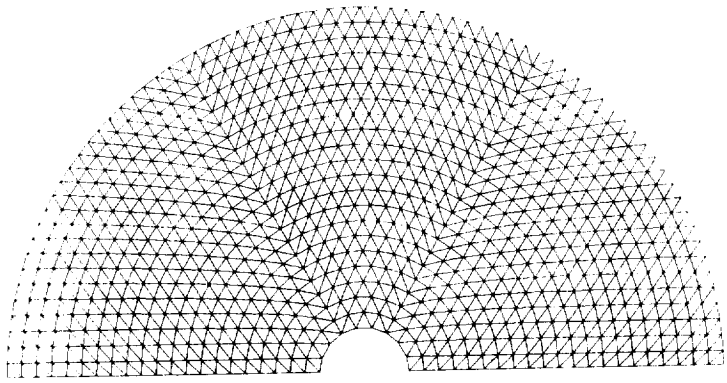

Fig. 4. Typical finite element mesh.

impacted by the pressure wave (θ=0) and the back side pole (θ=180 degrees). We observe from the figure a significant oscillation in the back side of the shell. Back-scattered pressure time histories are displayed in Fig. 6 at 3 and 5 radii from the origin. As expected, the scattered pressure at fluid points is zero until the wave has had time to travel (at unit nondimensional speed) from the spherical shell. Since the two points displayed are located 2 and 4 radii from the shell, the nondimensional time delays for the scattered pressure wave to arrive are 2 and 4, respectively.

DISCUSSION

A practical procedure has been presented, using standard capabilities in NASTRAN, for computing the solution of general time-dependent structural acoustics problems. Although illustrated for the simple geometry of spherical shell scattering, there is no restriction in the approach to particular geometries, so that any structure which can be modeled with NASTRAN can be handled.

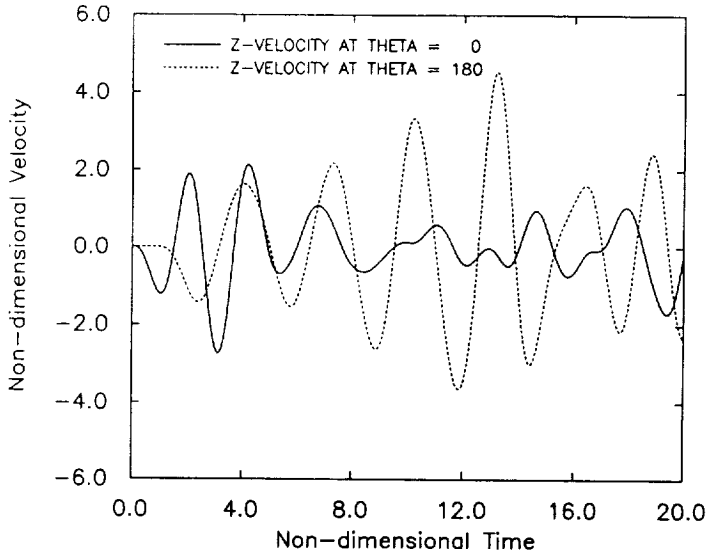

Fig. 5. Time histories of shell velocity in the z direction.

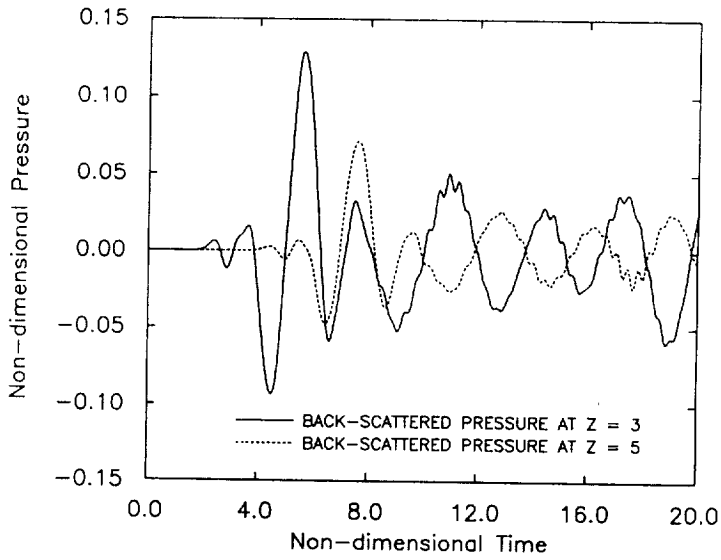

Fig. 6. Time histories of scattered pressure.

One of the major benefits of analyzing transient fluid-structure interaction with a general-purpose code like NASTRAN is the ability to integrate the acoustic analysis of a structure with other dynamic and stability analyses. Thus the same finite element model can often be used for modal analysis, frequency and transient response analysis, linear shock analysis, and underwater acoustic analysis. In addition, many of the pre- and postprocessors developed for use with NASTRAN become available for acoustics as well.

REFERENCES

1. L.H. Chen and D.G. Schweikert, "Sound Radiation from an Arbitrary Body," **J. Acoust. Soc. Amer.**, Vol. 35, No. 10, pp. 1626-1632 (1963).

2. D.T. Wilton, "Acoustic Radiation and Scattering from Elastic Structures," **Int. J. Num. Meth. in Engrg.**, Vol. 13, pp. 123-138 (1978).

3. J.S. Patel, "Radiation and Scattering from an Arbitrary Elastic Structure Using Consistent Fluid Structure Formulation," **Comput. Struct.**, Vol. 9, pp. 287-291 (1978).

4. I.C. Mathews, "Numerical Techniques for Three-Dimensional Steady-State Fluid-Structure Interaction," **J. Acoust. Soc. Amer.**, Vol. 79, pp. 1317-1325 (1986).

5. G.C. Everstine, F.M. Henderson, E.A. Schroeder, and R.R. Lipman, "A General Low Frequency Acoustic Radiation Capability for NASTRAN," **Fourteenth NASTRAN Users' Colloquium**, NASA CP-2419, National Aeronautics and Space Administration, Washington, DC, pp. 293-310 (1986).

6. G.C. Everstine, F.M. Henderson, and L.S. Schuetz, "Coupled NASTRAN/Boundary Element Formulation for Acoustic Scattering," **Fifteenth NASTRAN Users' Colloquium**, NASA CP-2481, National Aeronautics and Space Administration, Washington, DC, pp. 250-265 (1987).

7. A.F. Seybert, T.W. Wu, and X.F. Wu, "Radiation and Scattering of Acoustic Waves from Elastic Solids and Shells Using the Boundary Element Method," **J. Acoust. Soc. Amer.**, Vol. 84, pp. 1906-1912 (1988).

8. G.C. Everstine and F.M. Henderson, "Coupled Finite Element/Boundary Element Approach for Fluid-Structure Interaction," **J. Acoust. Soc. Amer.**, Vol. 87, No. 5, pp. 1938-1947 (1990).

9. O.C. Zienkiewicz and R.E. Newton, "Coupled Vibrations of a Structure Submerged in a Compressible Fluid," **Proc. Internat. Symp. on Finite Element Techniques**, Stuttgart, pp. 359-379 (1969).

10. A. Craggs, "The Transient Response of a Coupled Plate-Acoustic System Using Plate and Acoustic Finite Elements," **J. Sound and Vibration**, Vol. 15, No. 4, pp. 509-528 (1971).

11. A.J. Kalinowski, "Fluid Structure Interaction," **Shock and Vibration Computer Programs: Reviews and Summaries**, SVM-10, ed. by W. Pilkey and B. Pilkey, The Shock and Vibration Information Center, Naval Research Laboratory, Washington, DC, pp. 405-452 (1975).

12. L. Kiefling and G.C. Feng, "Fluid-Structure Finite Element Vibrational Analysis," **AIAA J.**, Vol. 14, No. 2, pp. 199-203 (1976).

13. A.J. Kalinowski, "Transmission of Shock Waves into Submerged Fluid Filled Vessels," **Fluid Structure Interaction Phenomena in Pressure Vessel and Piping Systems**, PVP-PB-026, ed. by M.K. Au-Yang and S.J. Brown, Jr., The American Society of Mechanical Engineers, New York, pp. 83-105 (1977).

14. O.C. Zienkiewicz and P. Bettess, "Fluid-Structure Dynamic Interaction and Wave Forces: An Introduction to Numerical Treatment," **Int. J. Num. Meth. in Engrg.**, Vol. 13, No. 1, pp. 1-6 (1978).

15. M.A. Hamdi and Y. Ousset, "A Displacement Method for the Analysis of Vibrations of Coupled Fluid-Structure Systems," **Int. J. Num. Meth. in Engrg.**, Vol. 13, No. 1, pp. 139-150 (1978).

16. R.E. Newton, "Finite Element Study of Shock Induced Cavitation," Preprint 80-110, American Society of Civil Engineers, New York (1980).

17. A.J. Kalinowski and C.W. Nebelung, "Media-Structure Interaction Computations Employing Frequency-Dependent Mesh Size with the Finite Element Method," **Shock Vib. Bull.**, Vol 51, No. 1, pp. 173-193 (1981).

18. G.C. Everstine, "A Symmetric Potential Formulation for Fluid-Structure Interaction," **J. Sound and Vibration**, Vol. 79, pp. 157-160 (1981).

19. G.C. Everstine, "Structural-Acoustic Finite Element Analysis, with Application to Scattering," in **Proc. 6th Invitational Symposium on the Unification of Finite Elements, Finite Differences, and Calculus of Variations**, edited by H. Kardestuncer, Univ. of Connecticut, Storrs, Connecticut, pp. 101-122 (1982).

20. P.M. Pinsky and N.N. Abboud, "Transient Finite Element Analysis of the Exterior Structural Acoustics Problem," **Numerical Techniques in Acoustic Radiation**, edited by R.J. Bernhard and R.F. Keltie, NCA-Vol. 6, American Society of Mechanical Engineers, New York, pp. 35-47 (1989).

21. J.T. Hunt, M.R. Knittel, and D. Barach, " Finite Element Approach to Acoustic Radiation from Elastic Structures," **J. Acoust. Soc. Amer.**, Vol. 55, pp-269-280 (1974).

22. J.T. Hunt, M.R. Knittel, C.S. Nichols, and D. Barach, "Finite-Element Approach to Acoustic Scattering from Elastic Structures," **J. Acoust. Soc. Amer.**, Vol. 57, pp. 287-299 (1975).

23. J.B. Keller and D. Givoli, "Exact Non-reflecting Boundary Conditions," **J. Comput. Phys.**, Vol. 82, pp. 172-192 (1989).

24. A. Bostrom, "Scattering of Stationary Acoustic Waves by an Elastic Obstacle Immersed in Water," **J. Acoust. Soc. Amer.**, Vol. 67, No. 2, pp. 390-398 (1980).

25. M.F. Werby and L.H. Green, "An Extended Unitary Approach for Acoustical Scattering from Elastic Structures," **J. Acoust. Soc. Amer.**, Vol. 74, pp. 625-630 (1983).

26. M.F. Werby and G.J. Tango, "Application of the Extended Boundary Condition Equations to Scattering from Fluid-Loaded Objects," **Eng. Anal.**, Vol. 5, pp. 12-20 (1988).

27. T.L. Geers, "Doubly Asympototic Approximations for Transient Motions of Submerged Structures," **J. Acoust. Soc. Amer.**, Vol. 64, No. 5, pp. 1500-1508 (1978).

28. H. Huang, G.C. Everstine, and Y.F. Wang, "Retarded Potential Techniques for the Analysis of Submerged Structures Impinged by Weak Shock Waves," **Computational Methods for Fluid-Structure Interaction Problems**, ed. by T. Belytschko and T.L. Geers, AMD-Vol. 26, The American Society of Mechanical Engineers, New York, pp. 83-93 (1977).

29. Y.P. Lu, "The Application of Retarded Potential Techniques to Submerged Dynamic Structural Systems," **Innovative Numerical Analysis for the Engineering Sciences**, edited by R. Shaw, W. Pilkey, B. Pilkey, R. Wilson, A. Lakis, A. Chaudouet, and C. Marino, University Press of Virginia, Charlottesville (1980).

30. M.A. Tamm, "Stabilization of the Coupled Retarded Potential - Finite Element Procedure for Submerged Structural Analysis," Memorandum Report 5902, Naval Research Laboratory, Washington, DC (1986).

31. M.A. Tamm and W.W. Webbon, "Submerged Structural Response to Weak Shock by Coupled Three-Dimensional Retarded Potential Fluid Analysis - Finite Element Structural Analysis," Memorandum Report 5903, Naval Research Laboratory, Washington, DC (1987).

32. G.C. Everstine, "A NASTRAN Implementation of the Doubly Asymptotic Approximation for Underwater Shock Response," **NASTRAN: Users' Experiences**, NASA TM X-3428, National Aeronautics and Space Administration, Washington, DC, pp. 207-228 (1976).

33. D. Ranlet, F.L. DiMaggio, H.H. Bleich, and M.L. Baron, "Elastic Response of Submerged Shells with Internally Attached Structures to Shock Loading," **Comp. Struct.**, Vol. 7, No. 3, pp. 355-364 (1977).

34. H.C. Neilson, G.C. Everstine, and Y.F. Wang, "Transient Response of a Submerged Fluid-Coupled Double-Walled Shell Structure to a Pressure Pulse," **J. Acoust. Soc. Amer.**, Vol. 70, No. 6, pp. 1776-1782 (1981).

35. G.C. Everstine, E.A. Schroeder, and M.S. Marcus, "The Dynamic Analysis of Submerged Structures," **NASTRAN: Users' Experiences**, NASA TM X-3278, National Aeronautics and Space Administration, Washington, DC, pp. 419-429 (1975).

36. G.C. Everstine, "Structural Analogies for Scalar Field Problems," **Int. J. Num. Meth. in Engrg.**, Vol 17, pp. 471-476 (1981).

37. A. Bayliss and E. Turkel, "Radiation Boundary Conditions for Wave-Like Equations," **Comm. Pure and Appl. Math.**, Vol. XXXIII, No. 6, pp. 707-725 (1980).

38. R.H. Cole, **Underwater Explosions**, Princeton University Press, Princeton, NJ (1948).

39. H. Huang, "Transient Interaction of Plane Acoustic Waves With a Spherical Elastic Shell," **J. Acoust. Soc. Amer.**, Vol 45, No. 3, pp. 661-670 (1969).

N91-20518

THE USE OF THE PLANE WAVE FLUID-STRUCTURE INTERACTION LOADING APPROXIMATION IN NASTRAN

R. L. Dawson
David Taylor Research Center
Underwater Explosions Research Division

ABSTRACT

The Plane Wave Approximation (PWA) is widely used in finite element analysis to implement the loading generated by an underwater shockwave. The method required to implement the PWA in NASTRAN is presented along with example problems. A theoretical background is provided and the limitations of the PWA are discussed.

INTRODUCTION

Background

The finite element method is commonly used for analysis of structures exposed to underwater shockwaves. Modeling the structure using the finite element method is of less concern than loading the structure with a shockwave in a fluid medium. The fluid and the structure interact and the loading will be modified by the structure moving in the water. If the structure moves faster than the fluid can respond, then the density of the water near the structure will diminish considerably, causing, in simplified terms, a void in the water. This condition is known as cavitation and will cause the loading from the shockwave to be abated. As the structure slows, the fluid density will return to normal, or the void in the water will collapse due to ambient water pressure. Water closure, sometimes called a water hammer effect, occurs when the cavitation void closes and water slams together causing a momentum transfer. If this happens before the shockwave has passed the structure, then the shockwave loading will continue.

In order to implement the underwater explosion shockwave loading, many finite element codes employ a load function known as the Plane Wave Approximation (PWA). The chief advantage of the PWA is that it is much less complex than other methods which employ modeling the fluid itself. This simplicity translates into faster computer run times with less memory requirements.

Consider a water bounded node of a finite element model. Let:

y = displacement of the node

t = time

$P_i = P_0 e^{-t/\theta}$ be the incident shockwave

$P_r = \phi(t)$ be the reflected pulse off the model

ρ_a = mass per unit area associated with each node

ρ_0 = density of water

θ = time constant of pressure pulse (assumed exponential)

A = water surface area associated with each node

The equation of motion of the node is:

$$\rho_a \ddot{y} = P_0 e^{-\frac{t}{\theta}} + \phi(t) \tag{1}$$

Continuity at the surface of the node stipulates that:

$$\rho_0 c \dot{y} = P_0 e^{-\frac{t}{\theta}} - \phi(t) \tag{2}$$

Eliminating ϕ using equations (1) and (2) results in:

$$\rho_a \ddot{y} + \rho_0 c \dot{y} = 2P_0 e^{-\frac{t}{\theta}} \tag{3}$$

The resulting force applied at the node is given by:

$$F(t) = A\rho_a \ddot{y} = \left[2P_0 e^{-\frac{t}{\theta}} - \rho_0 c \dot{y}\right] A \tag{4}$$

The above equations were originally derived by Taylor in 1941 (reference 1). The solution is exact as long as the water does not cavitate. The water may cavitate at the node or a short distance away from the node. Cavitation at the node will happen when:

$$\rho_0 c \dot{y} \geq 2P_0 e^{-\frac{t}{\theta}} \tag{5}$$

The nodal force derived from the PWA can be stated by combining equations (4) and (5).

$$F(t) = \begin{cases} 0 \; ; \; \rho_0 c \dot{y} \geq 2P_0 e^{-\frac{t}{\theta}} \\ \left[2P_0 e^{-\frac{t}{\theta}} - \rho_0 c \dot{y}\right] A \; ; \; \rho_0 c \dot{y} < 2P_0 e^{-\frac{t}{\theta}} \end{cases} \tag{6}$$

Objective

The objective of this paper is to demonstrate the use of the PWA for underwater shockwave loading in COSMIC NASTRAN for transient analysis problems.

IMPLEMENTATION OF PLANE WAVE APPROXIMATION IN NASTRAN

The PWA can be implemented in COSMIC NASTRAN without the use of the DMAP option. The procedure is facilitated by the use of scalar points and extra points, as these points will add neither mass nor stiffness to the finite element model. Consider a scalar dashpot which is implemented by the CDAMP4 card. The dashpot is constrained to ground by leaving one of the coordinates on the CDAMP4 card blank. This will allow the dashpot to function independently of the structure which is being analyzed. The dashpot is given the value of $\rho_0 c$ and loaded with an exponential shockwave:

$$P(t) = 2P_0 e^{-\frac{t}{\theta}} \tag{7}$$

Equation (7) is best implemented with the TLOAD2 card. NASTRAN will not handle an instantaneous acceleration; therefore, equation (7) must be ramped initially to its peak value. The ramp is established with the TLOAD1 card coupled with the TABLED1 card. A ramp of 10 time steps to peak value was chosen using engineering judgment. The additional 10 time steps increased execution time only marginally while allowing sufficient ramp time to use the TLOAD2 card. Therefore, no attempt was made to fine tune the number of time steps in the ramp further. The TLOAD2 card is made to start on the 10th time step by using the DELAY card. The TLOAD1 and TLOAD2 card are executed together with the DLOAD card as shown in figure 1. From first principles, the velocity of the scalar point is:

$$\dot{u}(t)_{scalar\ pt.} = \frac{2P_0 e^{-\frac{t}{\theta}}}{\rho_0 c} \tag{8}$$

The wet node, extra point, and scalar point are equated using the TF card, as shown in figure 2. Each water bounded node must be assigned its own unique scalar dashpot, extra point and TF card. The TF relation defines the extra point velocity:

$$\dot{u}(t)_{ex.\ pt.} = \dot{u}(t)_{scalar\ pt.} - \dot{y}(t)_{wet\ node} \tag{9}$$

The NONLIN3 card is used to actually load the finite element model. Each wet node must have its own unique NONLIN3 card and corresponding TF card. As shown in figure 2, the NONLIN3 relation is:

$$F(t)_{wet\ node} = \begin{cases} \rho_0 c A[\dot{u}(t)_{ex.\ pt.}] \ ; \ \dot{u}(t)_{ex.\ pt.} > 0 \\ 0 \ ; \ \dot{u}(t)_{ex.\ pt.} \leq 0 \end{cases} \tag{10}$$

By using equations (8), (9), and (10) the PWA will result (see equation (6)).

$$F(t)_{wet\ node} = \begin{cases} A\left[2P_0 e^{-\frac{t}{\theta}} - \rho_0 c \dot{y}(t)\right] \ ; \ \dot{u}(t)_{ex.\ pt.} > 0 \\ 0 \ ; \ \dot{u}(t)_{ex.\ pt.} \leq 0 \end{cases} \tag{11}$$

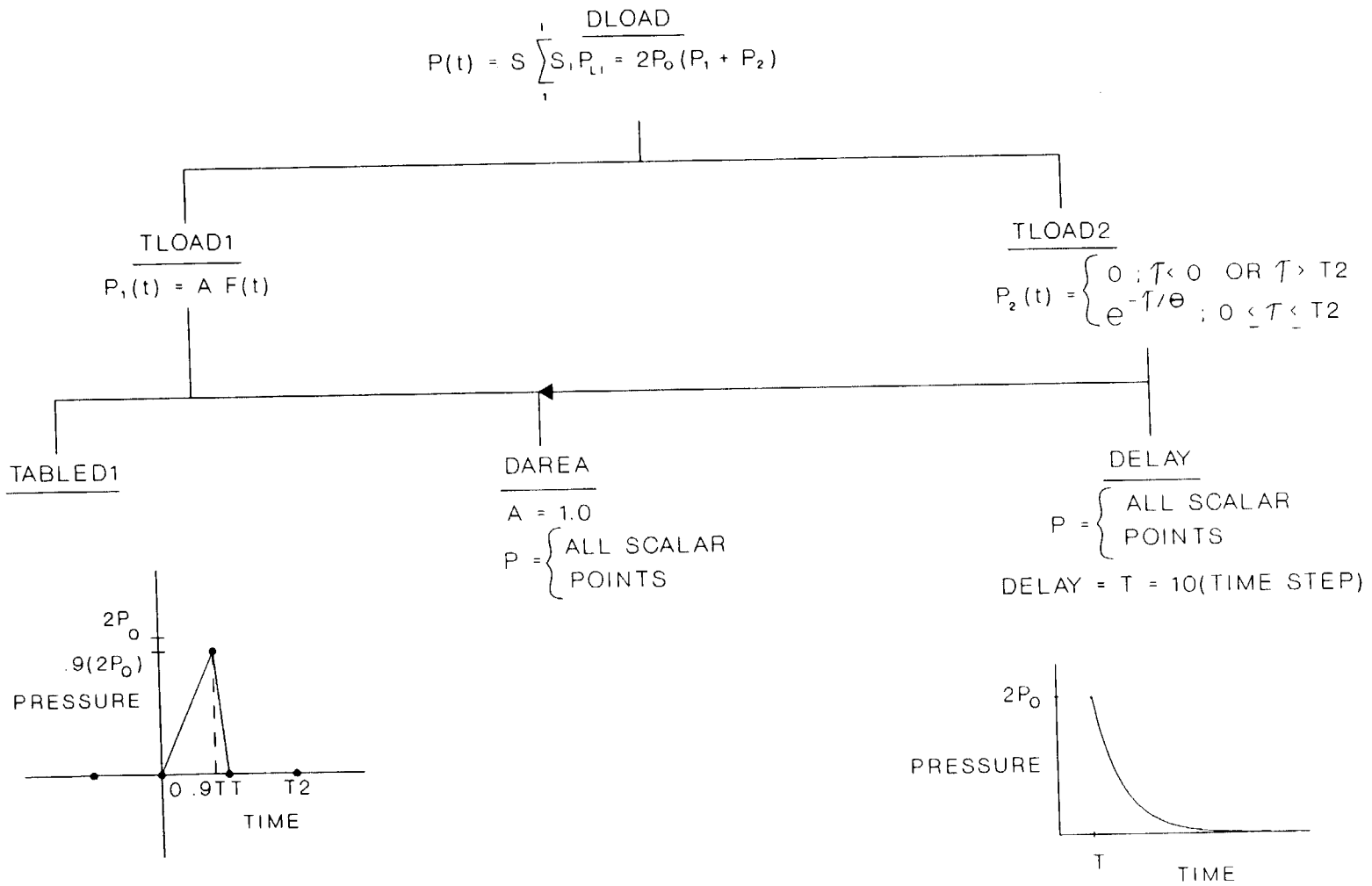

Fig. 1. - Exponential Loading

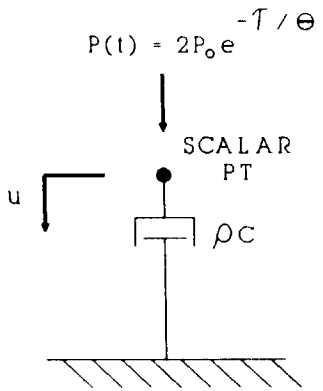

● EXTRA POINT

$$\dot{u}(t)_{EX\ PT} = \dot{u}(t)_{SCALAR\ PT} - \dot{y}(t)_{\substack{WET \\ NODE}}$$

$$P(t)_{\substack{WET \\ NODE}} = \begin{cases} \rho c A(\dot{u}(t)_{EX\ PT}) & ; \dot{u}(t)_{EX\ PT} > 0 \\ 0 & ; \dot{u}(t)_{EX\ PT} \leq 0 \end{cases}$$

CDAMP4	EPOINT	TF	NONLIN3
ONE SCALAR POINT DAMPER FOR EACH WET NODE	ONE EXTRA POINT FOR EACH WET NODE	APPLY CONSTRAINT EQUATION FOR EACH WET NODE	APPLY AT ALL WET NODES

Fig. 2. - Schematic of PWA

ILLUSTRATIVE PROBLEMS

Piston Problem

Consider the one dimensional problem of a rigid piston in a cylinder with a constant pressure on one side and an exponential shockwave in a fluid medium on the other (figure 3). The water can cavitate at the piston or at some distance away from the surface of the piston. The piston problem was solved in closed form by Gordon and Handleton in 1985 (reference 2) and is categorized by the term:

$$\lambda = \frac{\rho_a}{\rho_0 c \theta} \tag{12}$$

The piston can be modeled in NASTRAN with a single plate element constrained to move only in one direction. Four scalar dashpots are used for the four nodes of the plate element, and the dashpots are loaded with an exponential shockwave using the parameters shown in figure 3. The procedure described above is utilized to employ the PWA in NASTRAN. The results are shown in figure 4 in terms of displacement vs. time for varying values of λ. NASTRAN was executed until the point of maximum displacement occurred. For $\lambda = 5.0$ no cavitation occurs, and the PWA solution offers excellent agreement with the closed form solution of Gordon.

When $\lambda = 0.5$ cavitation occurs at the plate, the PWA differs from the closed form solution in terms of maximum displacement by approximately 36%. This difference happens after 15 msec. Prior to this the PWA in NASTRAN has good agreement with the closed form solution. The difference could be attributed to the fact that the closed form solution has the additional impulse due to water closure. The PWA does not model the closure event.

At $\lambda = 0.05$ the PWA in NASTRAN and the closed form solution of Gordon differ by 156% in terms of peak displacement. Cavitation occurs away from the surface of the piston, in the water itself. The PWA in NASTRAN does not indicate any cavitation as it only tracks the water edge at the piston. The PWA and the closed form begin to separate at approximately 4 msec, much earlier than when $\lambda = 0.5$. Again, much of the difference could be attributed to the lack of a water hammer effect in the PWA.

It is apparent that the accuracy of utilizing the PWA for the piston problem is dependent upon the value of λ. Practically speaking, $\rho_0 c$ remains fairly constant and θ can only be varied over a small range. The term which can allow the most deviation is the mass of the piston ρ_a. Thus, the PWA works well for a large mass term which does not allow cavitation. As the mass decreases, the effects of cavitation become more pronounced and the accuracy of the PWA decreases dramatically.

Somewhere between $\lambda = 0.5$ and 5.0 is the crossover value of λ, where no difference exists between the solution of Gordon and the PWA. Assuming a linear relationship exists between λ and the peak displacement difference between Gordon and PWA, the crossover can be found. Accordingly, for

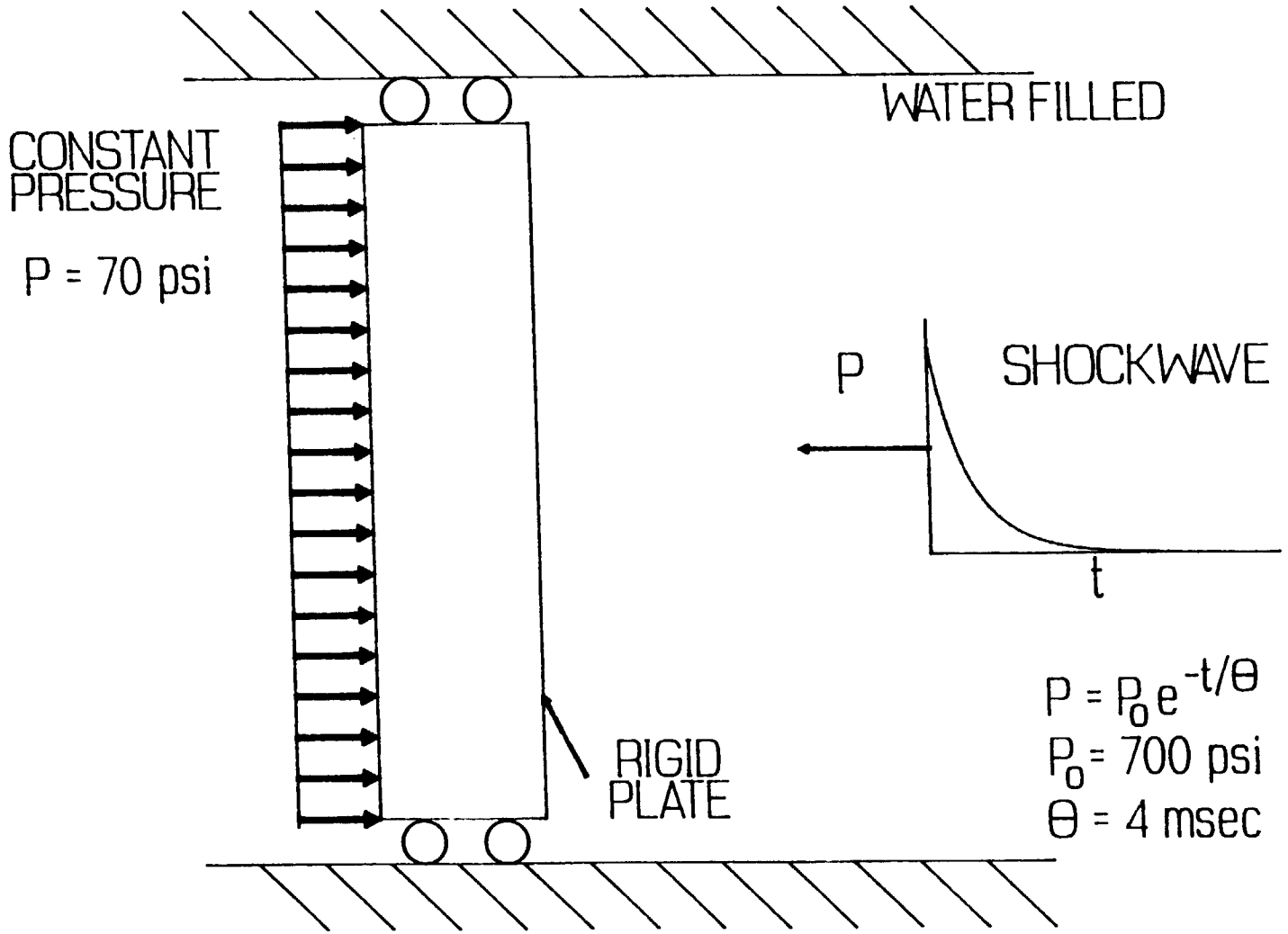

Fig. 3. The Piston Problem

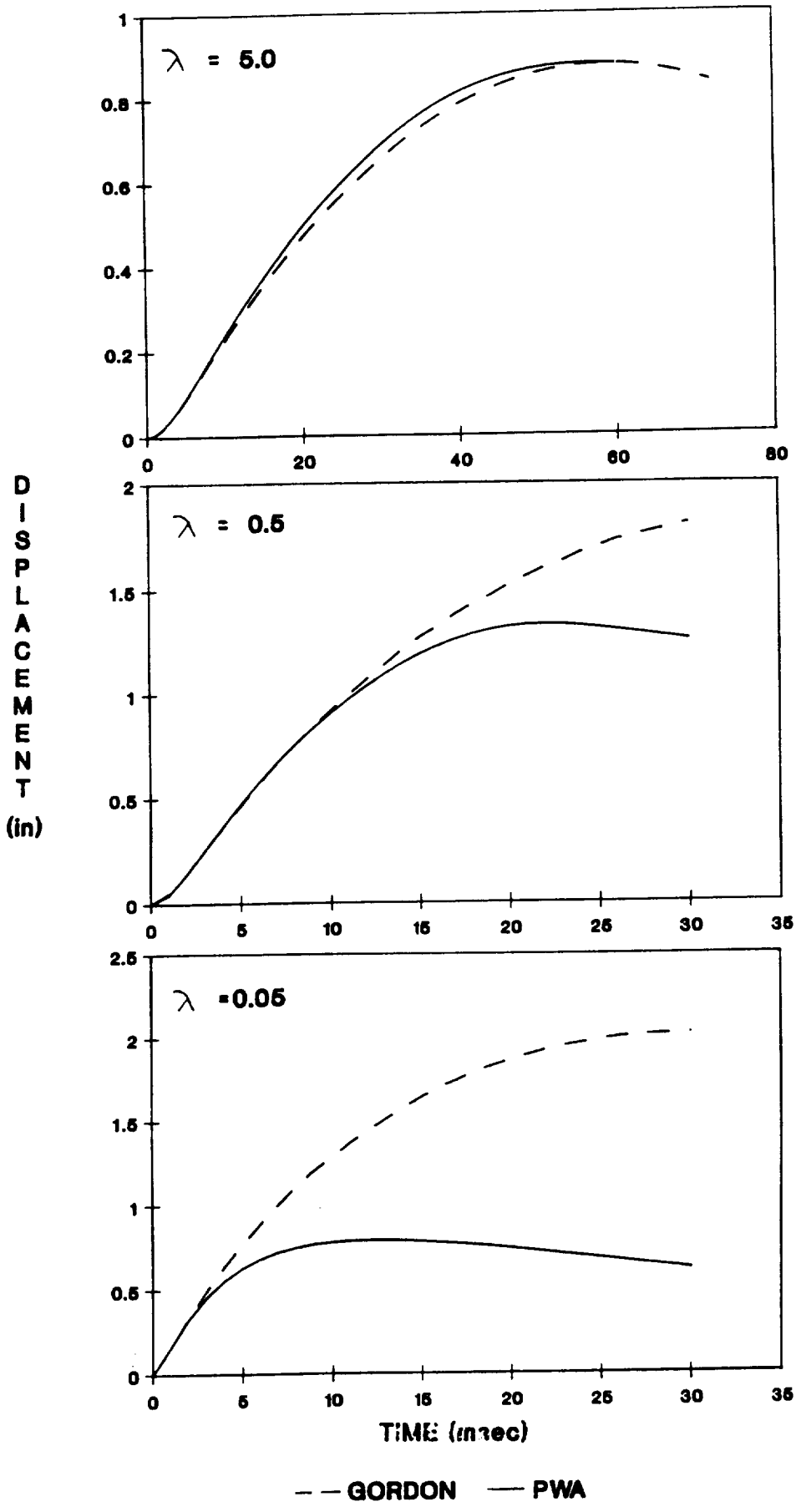

Fig. 4. - Comparison of Results from Piston Problem

λ = 0.64 and greater, no difference in displacement should exist between PWA and the closed form solution of Gordon.

Circular Flat Plate With Mass

In this example a 2-inch thick flat circular plate is welded to a rigid annular backing structure. The backing structure constrains the outside of the plate but allows the inner section of the plate to move. In the center of the plate a dummy mass is welded which weighs approximately the same as the plate. The plate has air on one side, water on the other. A short distance from the plate is an explosive charge which will release an exponential shockwave when detonated.

The experiment was conducted by the Underwater Explosions Research Division of the David Taylor Research Center and is shown schematically in figure 5. Velocity meters were placed on the mass to record the experimental response.

A finite element model was formulated of the plate and mass using COSMIC NASTRAN. Using symmetry, only a quarter of the plate was modeled using plate elements. The mass was formulated using triangular plate elements and the plate with quadrilateral elements. The plate was modeled as pin connected at the edge. The mesh used is shown in figure 6. The PWA as described above was used to load the model.

In this case the lowest value of λ is 0.84. Although this problem is very different than the piston problem, if the problems were analogous we would expect no cavitation and the PWA to be an excellent method in which to employ the underwater shockwave loading. The results from the NASTRAN finite element model are plotted versus the experimental velocity in figure 6. The analytical solution offers good agreement with experimental results in terms of initial average acceleration, average deceleration and peak velocity. These results support the use of the PWA for this application.

CONCLUDING REMARKS

The PWA is a useful engineering method for analyzing the shock response of naval vessels from underwater explosions. The applicability of the method is dependent upon the presence of cavitation in the water.

The PWA can be employed in NASTRAN for transient analysis problems without using the DMAP option. Standard bulk data deck cards can be used.

The method requires the calculation for each wet node of several parameters (A, P_0, θ) as well as an angular correction term if the shockwave and structure are not perpendicular. Additionally, several bulk data deck cards will be needed for each wet node. An accounting system must be set up in order to tie together the correct bulk data deck cards to the proper wet node. If the finite element model is of sufficient size then accomplishing

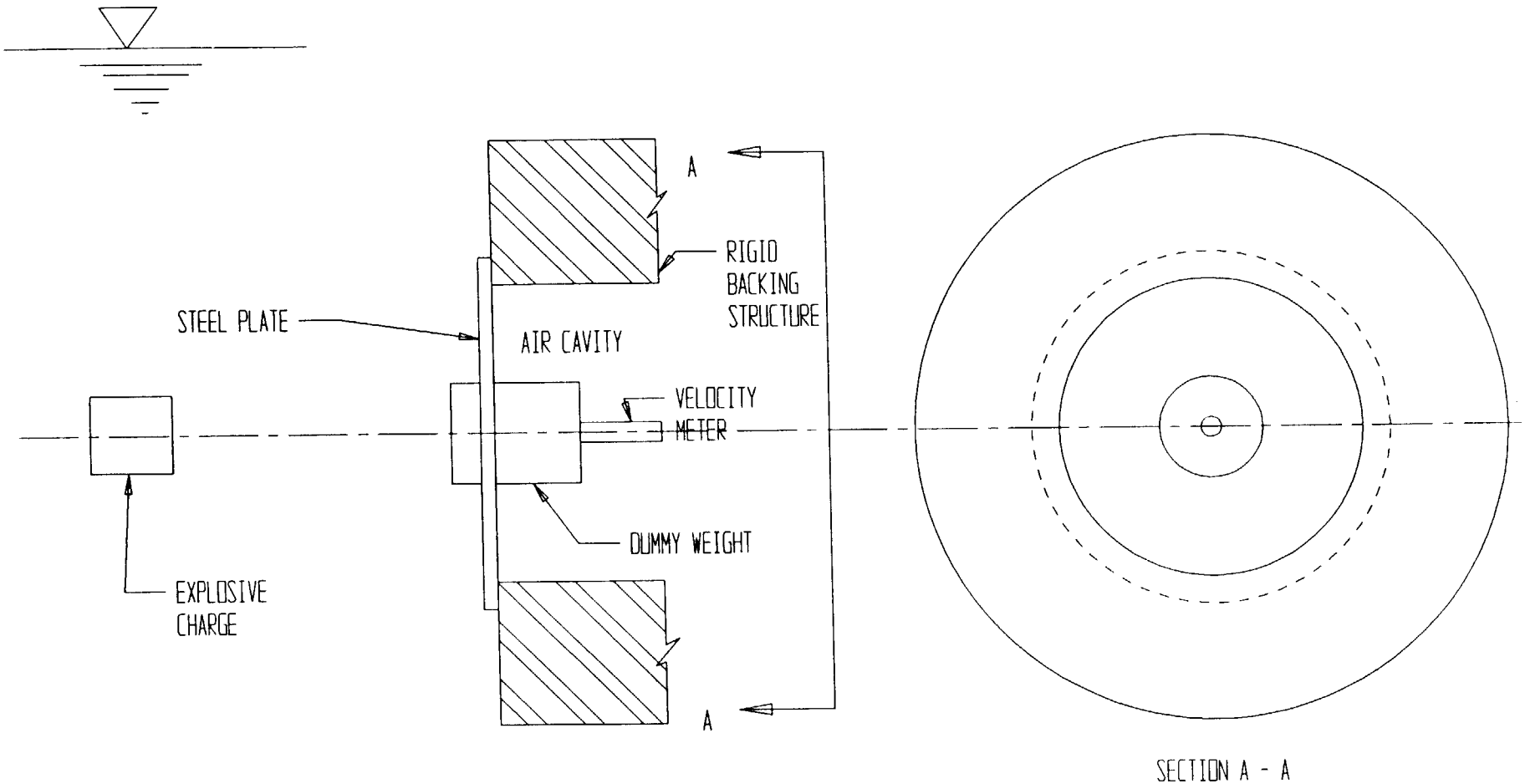

Fig. 5. - Test Arrangement

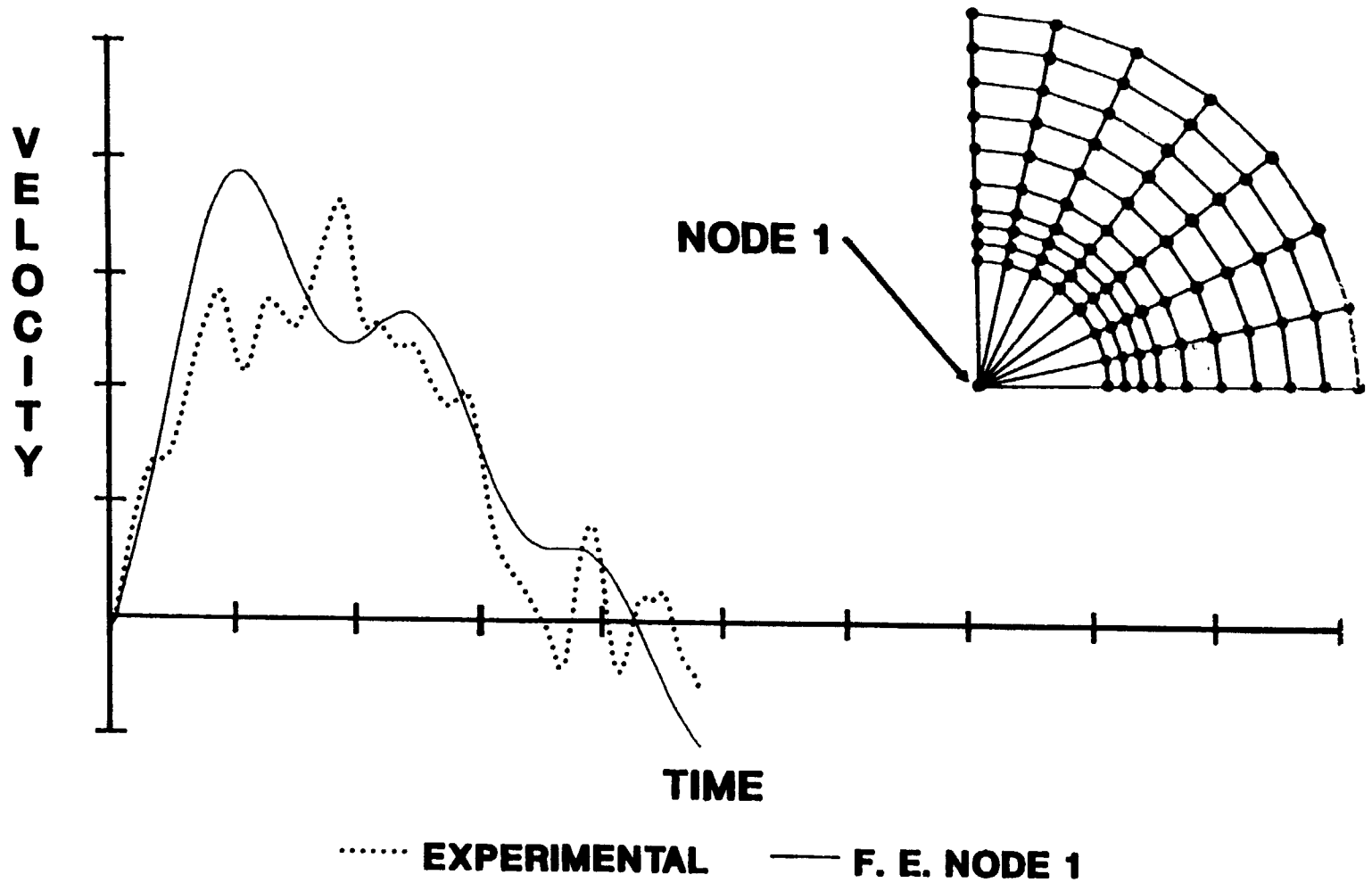

Fig. 6. - Comparison of Results from Experiment and PWA

the above can be quite a labor intensive task. A preprocessor program, which could scan the NASTRAN input deck and output the required bulk data deck cards necessary to implement the PWA, is recommended.

REFERENCES

1. Taylor, G. I., "The Pressure and Impulse of Submarine Explosion Waves on Plates," Underwater Explosion Research, volume 1, Office of Naval Research, 1950.

2. Handleton, R. and Gordon, J., "Energy Absorption at a Restrained Mass," David W. Taylor Naval Ship Research and Development Center report SD-85-24, March 1985.

N91-20519

Sensitivity Analysis and Optimization Issues in NASTRAN

V. A. Tischler and V. B. Venkayya

ABSTRACT

Structural optimization in the context of integrated design is of serious interest in many areas of engineering. In fact most of the commercial finite element analysis software developers around the world are allocating significant resources for implementing optimization in their programs. For example the recent version of MSC/NASTRAN contains an optimization option in addition to the sensitivity analysis which has been available for a number of years. Sensitivity analysis is one of the key elements, and it must precede the implementation of optimization. The purpose of this paper is to develop procedures to extract sensitivity analysis information from COSMIC/NASTRAN and to couple it with a mathematical optimization package. At present the analysis will be limited to stress, displacement and frequency constraints with structures modeled with membrane elements (such as QDMEM1, QDMEM2, and SHEAR), rods and bar elements. Sensitivity analysis with the QUAD4 will be addressed at a later date. The variables in sensitivity analysis are the physical variables such as plate thicknesses, rod areas, etc. The approach for sensitivity analysis is a combination of extracting information from NASTRAN via DMAP and using subroutines written externally to NASTRAN. Two types of sensitivity analysis will be addressed in this discussion. The first is an adjoint variable approach which is most effective when the number of active constraints is significantly less than the number of physical variables. The second approach is based on a first order approximation of a Taylor series. The latter approach is more effective when the number of independent design variables is significantly less than the number of active constraints.

(Paper not available at Press Time)

NASA
National Aeronautics and Space Administration

Report Documentation Page

1. Report No.	2. Government Accession No.	3. Recipient's Catalog No.
NASA CP-3111		

4. Title and Subtitle	5. Report Date
Nineteenth NASTRAN® Users' Colloquium	April 1991
	6. Performing Organization Code
7. Author(s)	8. Performing Organization Report No.
	10. Work Unit No.
9. Performing Organization Name and Address COSMIC, NASA's Computer Software Management and Information Center The University of Georgia Athens, GA 30602	11. Contract or Grant No.
	13. Type of Report and Period Covered Conference Publication
12. Sponsoring Agency Name and Address National Aeronautics and Space Administration Washington, DC 20546	14. Sponsoring Agency Code

15. Supplementary Notes

Also available from COSMIC, Athens, GA 30602

16. Abstract

This publication contains the proceedings of the Nineteenth NASTRAN Users' Colloquium held in Williamsburg, Va., April 22-26, 1991. It provides some comprehensive general papers on the application of finite elements in engineering, comparisons with other approaches, unique applications, pre- and postprocessing or auxiliary programs, and new methods of analysis with NASTRAN.

17. Key Words (Suggested by Author(s))	18. Distribution Statement
NASTRAN, structures, structural analysis, finite element analysis, colloquium	Unclassified - Unlimited Subject Category 39

19. Security Classif. (of this report)	20. Security Classif. (of this page)	21. No. of pages	22. Price
Unclassified	Unclassified	192	A09

NASA FORM 1626 OCT 86 Available from the National Technical Information Service, Springfield, VA 22161

NASA-Langley, 1991